Journal of Chromatography A, 1218 (2011) 1037–1114

Contents lists available at ScienceDirect

Journal of Chromatography A

journal homepage: www.elsevier.com/locate/chroma

Review

Fundamental challenges and opportunities for preparative supercritical fluid chromatography

Georges Guiochon*, Abhijit Tarafder

Department of Chemistry, University of Tennessee, Knoxville, TN 37996-1600, USA

ARTICLE INFO

Article history:
Received 15 July 2010
Received in revised form 8 December 2010
Accepted 13 December 2010
Available online 21 December 2010

Keywords:
Critical state
Enhanced fluidity chromatography
Diffusion coefficients
Equations of state
High pressure chromatography
Preparative chromatography
Supercritical fluid chromatography
Carbon dioxide
Phase diagrams
Peak capacity
Supercritical state behavior
Subcritical state behavior

ABSTRACT

The use of supercritical fluids as mobile phases in chromatography was suggested nearly fifty years ago. In spite of some major potential advantages, this mode of chromatography, generally known as SFC, is only now beginning to be considered by the mainstream community but it still does not yet enjoy a popularity comparable to those of gas or liquid chromatography. This seems to be largely due to a combination of (1) the serious instrumental difficulties that took many years to solve; (2) the complexity of the behavior of supercritical fluids in chromatographic systems when their temperature, pressure, or composition changes; (3) the long-lasting absence of any substantial incentive to use more complex systems, when the simpler and more robust approaches provided by HPLC are available. This situation, however, has begun to significantly change during recent years. The incentive of employing green, sustainable technologies in industrial processes as well as in analyses is increasing. Because mobile phases generally used in SFC tend to be less environmentally harmful and less expensive than those used in HPLC, SFC presents strong economical and regulatory advantages over the latter technique. Added to that, steady advancements in LC techniques in the last three decades has solved many instrumental difficulties related to SFC, which is now taking full advantages of many of these advances. One factor, however, has remained mostly unresolved. A clearer understanding of the physico-chemical behavior of supercritical fluids in preparative chromatographic columns under nonlinear conditions is still needed. This seems to be the main obstacle to the establishment of SFC as a sustainable separation tool. One aim of this review is to highlight these issues in more detail through a survey of the state-of-the-art techniques available for the design and operation of SFC. Another aim is to outline a possible series of investigations, which are necessary to develop a better physical understanding of SFC.

Contents

* Corresponding author at: University of Tennessee, Department of Chemistry, 552 Buehler Hall, Knoxville, TN 37996-1600, USA. Tel.: +1 865 974 0733; fax: +1 865 974 2667.
E-mail addresses: guiochon@utk.edu, guiochon@ion.chem.utk.edu (G. Guiochon).

0021-9673/$ – see front matter © 2010 Elsevier B.V. All rights reserved.
doi:10.1016/j.chroma.2010.12.047

1. Introduction

Our understanding of nonlinear and preparative gas and liquid chromatography is now such that it is possible to calculate the profiles of elution bands obtained under nearly any set of experimental conditions, provided that the competitive multi-component equilibrium isotherms of the sample components and the coefficients of their mass transfer kinetic properties are known [1]. Methods allowing accurate estimates of these coefficients made preparative liquid chromatography a popular separation process in the fine chemicals, pharmaceutical and biotechnological industries where it is now widely used to purify drug intermediates or extract selected proteins from the lyzates of bacterial cells. The design and characteristics of a unit and the experimental conditions under which it is used for a specific application can be modeled, calculated, and optimized with computer assistance. However, the use of this process is still expensive because the ratio of the volume of mobile phase needed to purify a given mass of compound to the volume of the feed purified is large. The solvents used as mobile phases are often expensive to procure, to recycle, and now to destroy. Possible leaks, which can be expected from high pressure operations, could severely pollute the local environment. So, a greener, cheaper alternative is now being seriously considered again, although it has been tried but eventually neglected in the past.

This alternative is preparative SFC, which is the common abbreviation of preparative supercritical fluid chromatography. It should be mentioned at this point that this expression, albeit generally accepted, does not properly represent the process conditions (see later, Section 2.1). Yet, due to its general acceptance, this acronym will be used throughout this review to avoid confusion. Although SFC brings a set of advantages that could make it become more competitive with conventional preparative high performance liquid chromatography, at least for certain applications, it has encountered major roadblocks to a wider applicability. Problems originate mainly from our present lack of knowledge of the fundamentals of SFC. This is combined with our limited understanding of the practical methods needed to apply our knowledge of the physicochemical properties of the subcritical, critical, and/or supercritical fluids, to the development of dedicated separation processes. In spite of these shortcomings, however, the applications of SFC could grow considerably over the years. The situation may be changing progressively in favor of SFC. The procurement and disposal of solvents are becoming increasingly costly, whereas the incentives for operating sustainable, environmentally benign processes are becoming more lucrative. So, a reversal in the economic balance can be expected, which explains why this greener alternative to HPLC is now being seriously considered again.

The primary focus of this review is on the main fundamental issues that need to be studied and understood in order to reach a level of knowledge of SFC similar to the one now achieved in preparative GC [2] and HPLC [1]. Work on these issues should be based on and guided by the detailed understanding of the simpler method of preparative liquid chromatography that has been acquired during the last quarter of century. This work will entail (1) the development of an exact mass balance equation for SFC under the varied conditions encountered in the applications of this method and of appropriate numerical solutions of this equation; (2) the design of suitable models of SFC under nonlinear, nonideal conditions; and (3) the investigation of the influences of the pressure, the temperature, and the mobile phase composition on the parameters of the equilibrium isotherms and of the mass transfer kinetics, parameters which determine the profiles of elution bands and the interferences between the bands of compounds that are closely eluted in preparative SFC. This work essentially depends on developing an accurate understanding of the variation of the mobile phase properties inside SFC systems, which is the prime controller of the equilibrium and of the kinetic behavior. Although the scientific literature contains much useful information on the properties of supercritical fluids, most of it is not directly applicable to preparative SFC. This is because, for practical reasons, SFC is mostly implemented under either subcritical or supercritical conditions, not under conditions that are closely critical. Accurate determinations of the thermodynamic and kinetic parameters of many compounds under a wide range of pressure, temperature, hence mobile phase density, is essential for the design and the operation of this chromatographic process.

The ultimate goal of scientists and engineers in the design of chromatographic separations is to accurately predict the influence of the experimental conditions on the recovery yield, the production rate, and the solvent consumption of a chromatographic separation. This knowledge permits the selection of the best operating conditions that optimize a selected objective function, using appropriate models of the units needed to implement preparative separations and suitable calculation methods. The success of this approach depends on the accuracy of the simulation model, which in turn depends on the understanding of the physical behavior, as described above.

From a fundamental point of view, chromatographic operations consist, while applying for separation purposes, the interactions between three factors, (1) the mobile phase (solvent), (2) the stationary phase, and (3) the sample components. The main difference between SFC and the other two chromatographic methods, LC and GC, is in the different nature of their mobile phase and in the changes that this brings in the thermodynamics of the process and in the physico-chemical interactions between (a) the solute and the mobile phase and (b) the solute and the stationary phase. To understand the physical behavior of SFC and be able to usefully apply it, we need to learn the nature of these changes. This requires, first, that we know the general properties of the fluids used as the mobile phase in SFC and how these properties affect the interactions between the mobile and the stationary phases. Then we discuss the hydrodynamics of the mobile phase in a chromatographic column, which provides an understanding of the nature of changes in the physical properties of the mobile phase along the column. Because the fluids used in SFC are compressible, it is not possible to determine the profiles of the mobile phase velocity, pressure, and density along the column without the knowledge of the equations of state (EOS) of the fluids used in SFC, which is necessary to determine these profiles. The profile of the mobile phase density along the column is of great importance because the fluid density in SFC controls most physico-chemical properties of quasi-critical fluids. The hydrodynamics of the mobile phase in a chromatographic column is important to understand the behavior of the solute zones. Based on a comprehensive understanding of these issues, we can try to comprehend the behavior of solutes in chromatographic columns and their separation, thoroughly investigating retention mechanisms and the mass transfer processes under linear, then nonlinear conditions.

After a brief introduction, we present a short description of the characteristics of supercritical fluids, followed by a brief historical overview of the development of SFC, and a discussion on the advantages and drawbacks of SFC over other chromatographic methods. The issues related to the development of a proper physical understanding of SFC systems are described and discussed first, in Section 2. Sections 3–6 mainly focus on the physical characteristics of the solvents used as mobile phases. Sections 7–9 discuss the effects of changes in the solvent properties on the retention and on the transfer kinetics of solute molecules. Section 10 summarizes the unresolved issues still hampering the development of SFC. Details on the experimental work and on applications are given in Sections 11 and 12.

Table 1
Critical properties of various fluids [6].

Solvent	MW	T_c (K)	P_c (atm)	D_c (g/ml)
Carbon dioxide (CO_2)	44.01	304.12	73.74	0.469
Ammonia (NH_3)†	17	405.4	113.5	0.235
Nitrous oxide (N_2O)†	44	309.6	72.5	0.45
Water (H_2O)	18.015	647.1	220.6	0.322
Methane (CH_4)	16.04	190.6	46.	0.162
Ethane (C_2H_6)	30.07	305.3	48.7	0.203
Propane (C_3H_8)	44.09	369.8	42.5	0.217
Ethylene (C_2H_4)	28.05	282.3	50.4	0.215
Propylene (C_3H_6)	42.08	364.9	46.0	0.232
Methanol (CH_3OH)	32.04	512.6	80.9	0.272
Ethanol (C_2H_5OH)	46.07	513.9	61.5	0.276
Acetone (C_3H_6O)	58.08	508.1	47.0	0.278
Trifluoromethane (CHF_3)	70.01	298.97	48.4	0.526

MW: molecular weight; T_c: critical temperature (°C); P_c: critical pressure (atm); D_c: critical density (g/ml).
† Most dangerous fluids (see Section 11.7 and [9,10]).

2. Supercritical fluids and their application in chromatography

2.1. Definition and characteristics of supercritical fluids

Supercriticality is a state of a fluid which is reached at a temperature higher than its critical temperature and under a pressure higher than its critical pressure (see Section 2.1.1). Although rare, supercriticality exists in nature. The atmosphere of Venus is made of 96.5% carbon dioxide. Its temperature at ground level is 735 K and its pressure 93 bar, conditions that are certainly supercritical (see Table 1). Water in deep oceans, around hot plumes or close to certain submarine volcanos may also be supercritical. This property, however, does not seem to have yet been related to any unusual behavior of sea water in these areas, except possibly to the formation of concretions of salts by dissolution of salts in supercritical water followed by their precipitation when water ceases to be supercritical. Supercritical conditions might exist at the bottom of deep oil wells; water injection could increase yields by enhancing oil solubility and mass transfer kinetics.

Supercriticality was discovered in a laboratory environment by de la Tour [3] in 1822 while the solvent power of supercritical fluid was recognized by Hannay and Hogarth in 1879 [4]. Subsequent investigations clarified some of the physico-chemical properties of critical and supercritical fluids. The definition of the critical state of pure compounds, hence of the conditions under which a compound is supercritical is straightforward as explained below. That of mixtures is more complex.

2.1.1. Critical conditions of pure compounds

The most common definition of supercriticality for pure compounds is based on a characteristic of the vapor–liquid phase equilibrium behavior of these compounds, expressed by their P–T phase diagrams. As illustrated in Fig. 1, which shows the phase diagram of carbon dioxide [5], there is a relationship between the pressure of the vapor in equilibrium with the liquid and the temperature, which is illustrated by a curve, $P = f(T)$. This equilibrium curve exists only between the triple point (T), where three phases, the solid, the liquid and the gas coexist in equilibrium, and the critical point (C). At temperatures below the triple point, the gas phase is in equilibrium with the solid phase and a thermodynamically stable liquid cannot exist. When the temperature of a gas/liquid system in equilibrium increases above the triple point, the density of the liquid phase decreases, which can be more clearly understood from the P–V phase diagram of carbon-dioxide (Fig. 1). On the other hand, the gas density increases under the opposite influences of the increasing temperature (that tends to decrease the gas density) and of the increasing vapor pressure (that tends to increase the gas density). The effect of the increasing pressure is stronger than that of the increasing temperature. At the critical point, the densities of the gas and the liquid become equal and the interface between them disappears. A single fluid, the supercritical fluid, exists under higher pressures, at higher temperatures. Fig. 1[5] shows the pressure/temperature and the pressure/volume phase diagrams of carbon dioxide. Table 1 lists the molecular weight, the critical temperature, the critical pressure, and the critical density of a few solvents used as the main components or possible additives or modifiers of mobile phases currently employed in SFC. Note that ethylene, methane, and all permanent gases available in gas cylinders are under supercritical conditions at room temperature. Other critical data are available in the literature [6,7].

A clear understanding of the consequences of supercriticality is provided by a close look at the $P-V$ phase diagram of carbon dioxide (Fig. 1). Imagine that a mole of a given compound is compressed isothermally, within the range of pressure and temperature in which there is gas–liquid phase equilibria. Between a state of very low density and the condition represented by point B this compression is accompanied by a decrease in its volume and in the product PV, which does not remain constant for real gases; the pressure of the vapor increases. At point B (Fig. 1), a drop of liquid appears and compression from point B to point G is that of a mixture of the gas and the liquid in equilibrium. During this compression, the volume occupied by the mole of sample decreases, but the pressure remains constant and the relative fractions of the compound that are in the liquid and in the gas states changes; progressively a larger sample fraction becomes liquid. At point G, the last bubble of vapor disappears and from G to H and beyond, the pure liquid is compressed. Points B and G represent the molar volumes of the saturated vapor and of the liquid in isothermal equilibrium with it, respectively. Note that it is possible under certain conditions, in the total absence of dust or surface nuclei, to compress a vapor beyond saturation or to expand the liquid below it. All states along these paths are unstable. The critical point is point C where compression of the gas takes place without formation of the liquid and expansion of the liquid takes place without formation of the gas. Point C is the maximum of the bell-shaped curve that is drawn by joining the molar volumes of the saturated vapor and of the liquid in isothermal equilibrium with this vapor with increasing temperature (NB. The critical temperature in this experiment made in 1937 was slightly higher than 31.013 °C, in disagreement with the data in Table 1). In point C, the molar volumes of the liquid and of the gas are the same. Mathematically, in point C, we have

$$\left(\frac{\partial P}{\partial V}\right)_T = 0 \quad (1)$$

and

$$\left(\frac{\partial^2 P}{\partial V^2}\right)_T = 0 \quad (2)$$

All equations of state (i.e., all equations characterizing $f(P, V \cdot T) = 0$ for a compound, see Section 6) must satisfy Eq. (1).

2.1.2. Properties of pure compounds at and beyond their critical point

At the critical point, all thermodynamic and transport properties of a fluid are anomalous. Although the physical properties are continuous, their derivatives are not; often they are infinite and may be of opposite signs below and above this point. This makes the following list often difficult to understand and, apparently self-contradictory. The compressibility, the heat capacities at constant pressure or volume, the velocity of sound propagation, the inten-

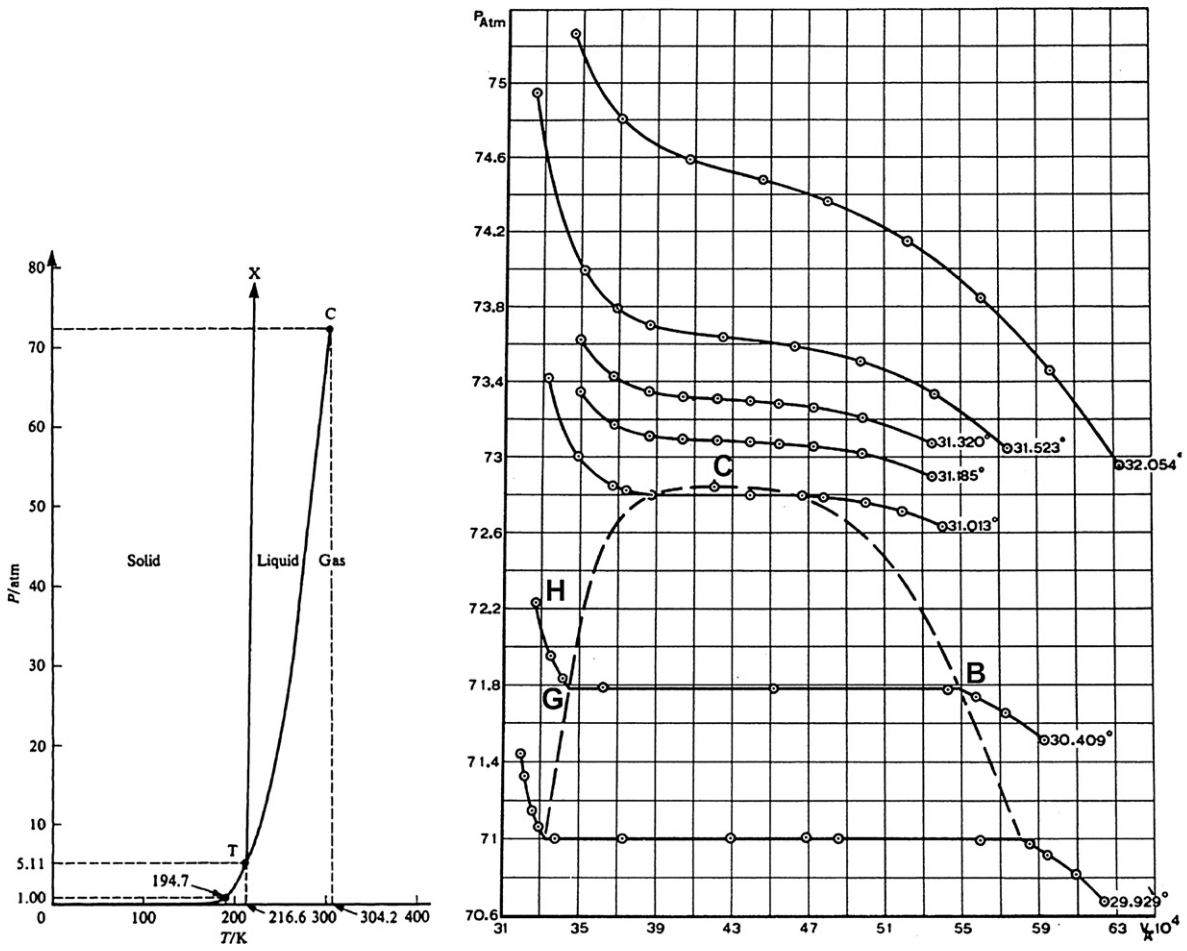

Fig. 1. Left: pressure vs. temperature phase diagram of carbon-dioxide ([8]). The triple point of CO_2 is at $T = 216.6$ K, $P = 5.11$ atm. Right: pressure vs. volume phase diagram of carbon dioxide (Fig. 3 in [5]).

sity of light scattering, the thermal conductivity and the viscosity are infinite [11]. Note, however, that it is practically impossible to perform any measurement at the very critical point. What this statement means is that, around the critical point, all these properties are anomalously large. Correlatively, the diffusion coefficients are nought at the very critical point and tend toward zero in the vicinity of the critical point. This means that analysts should avoid to operate SFC columns under experimental conditions that are close to the critical point of the fluid used as the mobile phase, where they may observe unexpected results.

The supercritical fluid region corresponds to conditions under which the pressure exceeds the critical pressure and the temperature exceeds the critical temperature. Conversely, the subcritical region corresponds to pressures and temperatures below the critical pressure and temperature, respectively. The other two quadrants of the *P*, *T* diagram have no clearly defined name. A liquid under pressures higher than the critical pressure but at temperatures lower than the critical temperature could be called a high density liquid and a fluid under pressures lower than the critical pressure but at a temperature higher than the critical temperature could be a high temperature gas but this nomenclature is not codified. A state of gas-like (i.e., low) density can be turned into one of liquid-like density (i.e., a much larger density) without the formation of an interface, by properly adjusting the temperature and/or the pressure, making the state of the fluid travel along a path around the critical point that does not intersect the gas–liquid equilibrium curve. This transformation becomes easier and more progressive when the initial state is farther removed from the critical state [12]. A wide range of states with intermediate densities can thus be reached that are inaccessible in either the gas or the liquid state.

A particularly important characteristic of the compounds that are under conditions close to critical, either subcritical or supercritical, with reduced pressures between 0.9 and 1.1, is their isothermal compressibility, κ_T:

$$\kappa_T = -\frac{1}{V}\left(\frac{\partial V}{\partial P}\right)_T = \frac{1}{\rho}\left(\frac{\partial \rho}{\partial P}\right)_T \quad (3)$$

The compressibility of fluids is important because it is particularly large in this region [13]. Actually, it is infinite at the critical point and varies very rapidly when either pressure or temperature drifts away from critical values. So, a slight pressure increase in this region will cause a considerable increase in the fluid density. Since the solubility and the retention factor of all compounds are closely related to the fluid density, this behavior is of fundamental importance. Critical data for a large number (618) of compounds are available in Appendix A of the book of Reid et al. [6].

2.1.3. Critical conditions of mixtures

Phase diagrams are far more complex for mixtures than for pure compounds [13–15]. The seminal work in this field was done by van Konynenburg and Scott [14,15]. These authors provided a detailed analysis of the behavior of binary mixtures of compounds having similar or unequal sizes, distinguished and described the different types of diagrams observed and established the nomenclature

still used to identify them. Each pure component of a mixture has its own phase diagram and its own critical point. For mixtures, the relationship between the pressure and the temperature under which the gas and the liquid phases are at equilibrium depends also on the composition of the mixture and the molecular interactions involved. Thus, the critical temperatures and pressures of mixtures depend on their composition. These characteristics are given by the temperature and pressure at which the meniscus separating the gas and the liquid phases of a given sample of the mixture, heated in a closed container, would disappear. A mixture of any composition may be supercritical only at sufficiently high temperatures and under sufficiently high pressures, temperatures and pressures that may be substantially higher than the individual critical temperatures and pressures of the mixture components.

The line that connects the critical points of all the binary mixtures of the two compounds is called the critical curve, $f(T, P, x)$. Each pair of compounds has its own phase diagram and, depending on the specific case, several very different types of diagrams exist [12–17]. Only for mixtures of carbon dioxide and some weakly polar compounds of low molecular weight these diagrams exhibit one simple continuous line connecting the critical points of the two compounds. This line is then monotonous and may have a weak maximum (type 1 diagrams). These compounds include the light alkanes (with 1–11 carbon atoms) and normal light alkenes, cyclohexane, toluene, dimethylether, methanol, ethanol, 1- and 2-propanol, n-butanol, acetic acid, acetaldehyde, acetonitrile, chloromethane, and chlorobenzene [16,18]. Like pure compounds, these mixtures may coexist under atmospheric pressure, at moderate temperatures, as two fluid phases in equilibrium, a gas and a liquid phase. When the temperature and pressure increases, the properties of these two fluids evolve and tend toward each other, until the gas and the liquid phases become one unique phase. Figs. 2 and 3 illustrate the situation of two type-1 binary mixtures of compounds that both have type 1 diagrams. Fig. 2 defines the critical locus or locus of the critical points of simple mixtures. Fig. 3 shows the projections on the P, T plane of the critical loci of mixtures of CO_2 and of various organic compounds as a function of their composition. Many of these compounds are used as modifiers in SFC. The composition of these mixtures is a function of P and T (see left figure).

As shown in Fig. 3, the projections on the P, T plane of the critical loci and of the liquid–vapor equilibria of the two pure compounds separate this plane into two regions, region II in which vapor–liquid separation will never take place, whatever the composition of the system, and region I in which it may, for certain compositions [19]. Based on this observation, Chester et al. [20–22] developed a procedure to determine whether, under certain conditions of pressure and temperature, a mixture of known composition was uni- or di-phasic (see later, in Section 2.1.4). Figs. 3 and 2 are helpful to understand phase behavior in SFC and to select the experimental parameters.

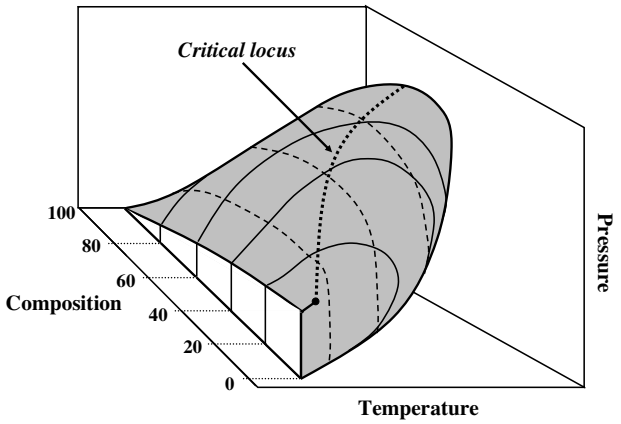

Fig. 2. The two-phase liquid–vapor region of a type I mixture (after Chester [19]). This three-dimensional volume encloses the region where a liquid and a gas phase may coexist in equilibrium. The set of points outside the shaded area corresponds to a continuous one-phase region of the diagram.

In contrast to the simple behavior of these binary mixtures, homogeneous mixtures of CO_2 and more complex and/or polar compounds may separate upon compression and/or heating into two fluid phases in equilibrium, both of which have a finite compressibility. This separation into two different phases lowers the free energy of the system, which otherwise would be materially unstable [12]. The consequence is the existence of most complex phase diagrams for certain types of mixtures. So, instead of the criticality condition in Eq. (1) for a pure compound, the criticality condition for a binary mixture is [12]:

$$\left(\frac{\partial^2 G}{\partial x^2}\right)_{T,P} = 0 \tag{4}$$

and

$$\left(\frac{\partial^3 G}{\partial x^3}\right)_{T,P} = 0 \tag{5}$$

where G is Gibb's free energy and x is the mole fraction.

Most complex diagrams are often observed (currently, there are six types of diagrams identified in the literature [16]), showing two

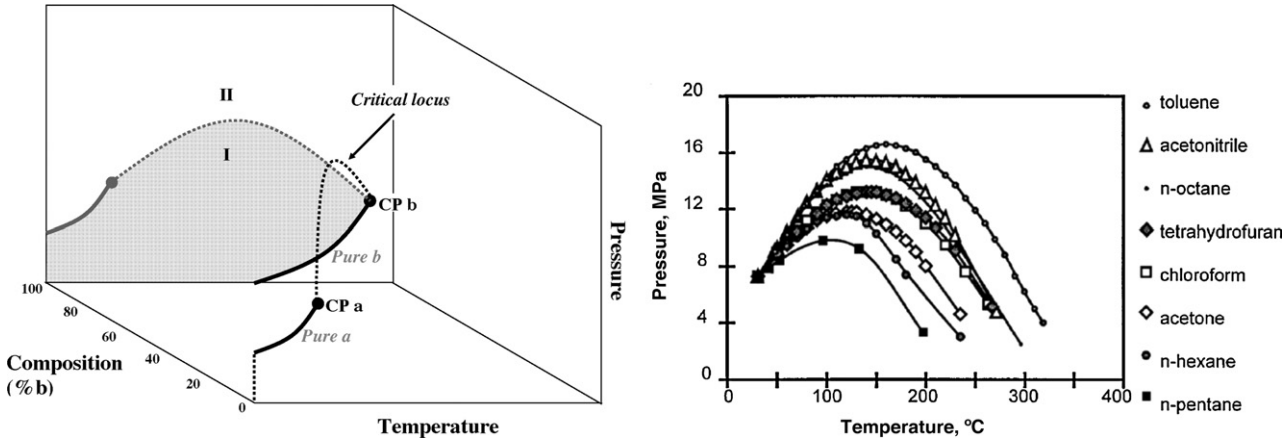

Fig. 3. *Left:* Phase diagram for a binary mixture. Dashed line, position of the critical point as a function of the mixture composition. Solid lines, vapor pressures of the two pure liquids. *Right:* Critical loci in the $P - T$ space for mixtures of carbon dioxide and a few organic solvents [19].

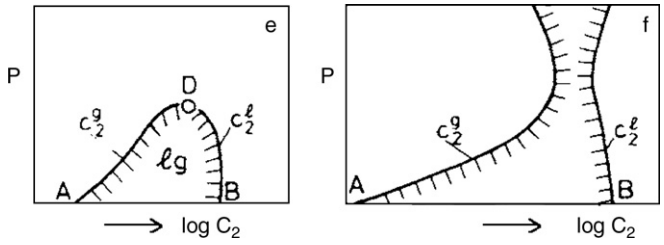

Fig. 4. Phase diagrams of binary mixtures of supercritical fluids [23]. Left, type 1 diagram; right, type 2 diagram.

immiscible liquid phases or even a gas and two liquid phases in equilibrium, with several other critical points where the meniscus between these phases disappears [12,16–18]. Fig. 4 compares the isothermal $P=f(C)$ phase diagrams of two such systems, those of types 1 and 2, respectively. In type 1 diagrams, there are a gas and a liquid phase in equilibrium at low pressures, below the critical curve, ADB. The low concentration branch of this curve (AD) represents the dissolution of the low-volatility liquid component 2 in the supercritical fluid 1, while the high concentration branch (DB) corresponds to the dissolution of the supercritical fluid 1 in the liquid 2. In both cases, the solubility of one fluid into the other one at equilibrium increases with increasing pressure, until the two branches of the curve meet at the critical point of the mixtures of the compounds considered. When temperature increases, the size of the two-phase region shrinks [13]. In the type 2 case, the solubility of either fluid in the other one does not increase constantly with increasing pressure but goes through a maximum for an intermediate pressure, beyond which the miscibility gap increases. The two compounds are never miscible in all proportions but their mutual solubilities are considerably increased by the pressure increase, particularly that of the high molecular weight compound in carbon dioxide.

However, not all possible mixtures should be considered in chromatography. Rarely does the concentration of sample components or that of organic modifiers exceeds ca. 10–15% in preparative chromatography. While in RPLC, the relative concentration of methanol or acetonitrile can span the whole range from 0 to 100%, this does not happen in SFC, where the carbon dioxide concentration should almost always exceed 30–40%, to benefit from the solubility, the viscosity, and the fast mass transfer properties brought by this compound. Yet, in spite of these limitations, it is probable that in many cases the mobile phase composition is such that it is no longer under supercritical conditions because the critical temperature and pressure of pure compounds increase rapidly with increasing molecular weight (for all organic modifiers, T_c exceeds 240 °C, see Table 1). Furthermore, the critical temperature of the sample components will often be very high. Also the phase diagrams of elution bands might be complex and potentially involve several immiscible phases, even at low concentrations.

It has been suggested in the chromatographic literature that the critical point of binary mixtures could be estimated as the arithmetic mean of the critical temperatures and pressures of the two components:

$$T_{c,mix} = x_1 T_{c,1} + x_2 T_{c,2} \quad (6)$$

$$P_{c,mix} = x_1 P_{c,1} + x_2 P_{c,2} \quad (7)$$

This method gives only approximate results, with a somewhat better estimate for the critical temperature than for the critical pressure for compounds giving type 1 diagrams, which tend to give a maximum critical pressure for some intermediate composition but a monotonous variation for the critical temperature. For greater accuracy the critical point should be calculated using the equations of state, when one is available (see Section 6), such as the Lee–Kesler

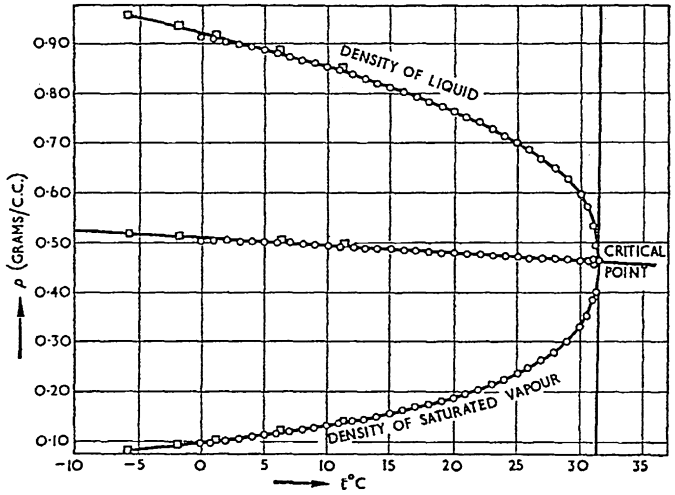

Fig. 5. Diagram of Cailletet and Mathias for the determination of the critical density [5,25].

or the Peng–Robinson equations, or using group contribution methods. Other critical properties, such as the critical density, can also be calculated using the equations of state.

2.1.4. Determination of the critical point

There are many methods used to determine the critical points of pure compounds or binary mixtures [11]. The experimental data found in the literature were measured by different methods, some times with unstated or doubtful precision, at different times, hence with compounds of uncertain purity. This means that, except for a few compounds carefully studied by numerous authors like carbon dioxide, literature data cannot be trusted without reservations. The methods mainly used were reviewed recently [11,24]. They are

1. The visual observation of the meniscus separating the gas and liquid phases in a sealed glass tube, while temperature and pressure are progressively raised by heating the tube. The meniscus must reappear at the same temperature, upon cooling. The fluid must be pure, devoid of gases or dust. The critical pressure could be measured in the same experiment if the tube is connected to a manometer. This method can give a reasonably precise estimate of the critical temperature, provided that it is carried out with a variable volume cell. Since the mass of compound and the volume of a closed tube are constant in the experiment, the point representing the system in Fig. 5 moves along a horizontal line, which will not reach the critical point, unless the cell volume can be adjusted. Thus, this method of determination of the critical pressure and density requires the use of a variable volume pressure vessel with glass windows and a manometer. Used with a sealed glass tube, it is dangerous since, if there is too large a sample mass, the gas phase will disappear and the liquid phase will expand, causing the pressure to raise dangerously when heating continues.
2. The law of rectilinear diameter. This method is based on the observation of Cailletet and Mathias that the average of the densities of the saturated vapor and the liquid in equilibrium with this vapor varies linearly with increasing temperature (see Fig. 5). Extrapolation permits the determination of the critical density, see Fig. 5[5,25]. However, significant deviations from the law take place near the critical temperature and must be taken into account [11]. This method is used to determine the critical density of fluids [25]. Fig. 5 shows the Cailletet and Mathias curve drawn for carbon dioxide, using the data measured by Amagat [26].

3. The *P*, *V*, *T* relationships (see Eq. (1)) provide data regarding the critical temperature and pressure. The *P*(*V*) relationship measured below the critical temperature has a kink at the liquid–gas transition and an inflection point above the critical temperature.
4. The dynamic measurements method is similar to the first one, but use a stream of fluid percolating through a heated cell, the temperature of which can be raised. It permits measurements for fluids that are not thermally stable because the residence time in the cell can be as low as 10 s.
5. The measurements of different properties as a function of isothermal pressurization or isobaric heating provide data on the critical point. The method was used with measurements of the sound velocity, the resistivity, the refractive index, etc.

A large amount of critical data for mixtures of carbon dioxide and of numerous compounds soluble in it are provided by Abdulagatov et al. [11]. Besides values of the critical point characteristics, tables in that review list the method used, the error of measurements estimated, and the concentration range investigated. Phase diagrams are also provided.

Chester and Innis developed an original, simple, accurate method for the determination of the critical loci of binary systems or curves that connect the critical points of two compounds in the *P*, *T*, *x* (*x* composition of the binary mixture) space by joining the critical points of all the binary mixtures. This method consists in determining from series of elution profiles of samples of a mixture of known composition of carbon dioxide and the modifier, which is, at a given temperature, the pressure above which the mixture is uniphasic and under which it separates into a gas and a liquid [27]. Samples of ca. 0.5 μL are injected into a 2–6 m long fused-silica tube, 50 μm i.d.. If the sample is under supercritical conditions when injected, a Gaussian's peak is recorded for the organic compound. If the conditions are subcritical, the sample separates into a gas (mostly CO_2) and a liquid phase (mostly the organic compound). The stream of gas eluted from the open tube contains a constant concentration of the additive, which corresponds to its vapor pressure, hence the eluted peak is a flat top, nearly rectangular [20,21,27]. Operating at constant temperature, the experiment is repeated at increasing pressures, until the peak shape changes drastically from rectangular to Gaussian. Obviously, the connecting tube between the open tubular column and the detector must be kept at a temperature higher than the relevant critical locus. A precision of ca. 1 atm is usually achieved. This method permitted Ziegler et al. [20] to determine the critical loci of mixtures of carbon dioxide and numerous organic solvents, shown in Fig. 6. The CO_2 concentration in the critical mixtures decreases from left to right. This method was later used to determine the critical loci of mixtures of carbon dioxide and numerous other organic solvents [22].

2.2. Application of supercriticality in chromatography—a brief history

SFC was first considered fifty years ago by Klesper et al. [28], as a form of gas chromatography. To separate porphyrin derivatives that cannot be analyzed by GC because they begin decomposing at temperatures where their vapor pressure is too low to allow their elution, these authors used dichlorodifluoromethane (T_c = 114 °C) and monochlorodifluoromethane T_c = 96 °C) under pressures between 70 and 100 atm as the mobile phases. They separated Ni etioporphyrin II and etioporphyrin on columns packed with Chromosorb coated with polyethylene glycol. They were able to recover the purified compounds. Later, Sie et al. used carbon dioxide as the mobile phase and studied its behavior from theoretical and experimental viewpoints [29–32]. Karayannis et al. showed how to control independently the column back pressure and the flow rate and described a UV detector with a cell operating under high pressure [33]. Giddings et al. [34] emphasized the importance of carrying out gas chromatographic separations under extremely high pressures, up to 2000 atm, and suggested a possible convergence with liquid chromatography, due to the very high density of the carrier gas at these pressures. Then, intermolecular forces become very high, allowing the extraction of macromolecules into the gas phase. These authors used helium, nitrogen, carbon dioxide, and ammonia as carrier gases and separated nucleosides, nucleotides, and purines, proteins, peptides and amino acids, sugars, terpenes, and steroids. Unfortunately, this work was not pursued. Giddings shifted toward other interests and other scientists involved in SFC focussed on carbon dioxide, for its great convenience, forgot about organic modifiers, and placed considerable emphasis on the role of the pressure and the mobile phase density, to the point that the molecular interactions between solutes and mobile phases were almost obliterated [35].

Jenthoft and Gouw developed pressure-programmed SFC and applied it to the separation of wide molecular weight range samples of polynuclear aromatic hydrocarbons and of styrene oligomers [36]. They also designed and built an automatic fraction collector [37]. It is remarkable that at that time, instruments for SFC were more sophisticated and advanced than those for HPLC. Yet, the latter took over in the late 1970s while the former remained a niche mode of chromatography to this day. Klesper and Hartmann developed preparative SFC and used it to purify oligomers of styrene, which they also analyzed by mass spectrometry [38,39].

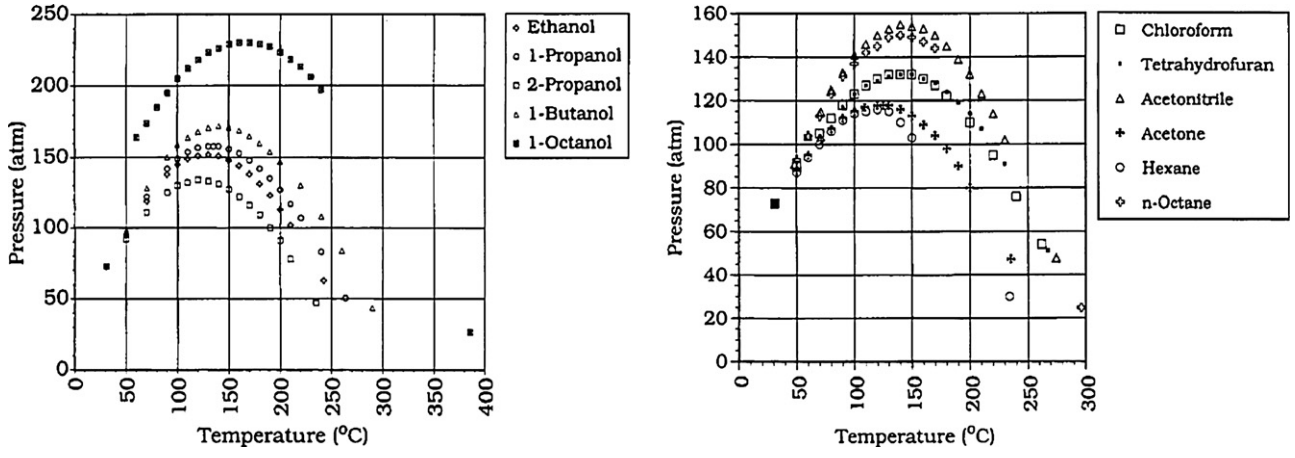

Fig. 6. Left: Critical loci of (from top to bottom) 1-octanol, 1-butanol, 1-propanol, ethanol, and 2-propanol. Right: critical loci of (top to bottom) acetonitrile, n-octane, chloroform, tetrahydrofuran (•), acetone, and hexane [20].

The physico-chemical aspects of the use of carbon dioxide as the mobile phase were studied by Bartmann and Schneider [16], those of the use of light alkanes by Novotny et al. [40]. Later, Randall and Wahrhaftig coupled directly SFC and MS [41]. Van Wasen et al. published an important review of analytical applications that reported also on the physico-chemical properties of critical and supercritical fluids, which are of great importance for the operation of SFC [13].

In the late 1970s, analytical and preparative SFC parted ways. All preparative applications of chromatography require that the columns provide a significant production rate of the purified fractions, hence that they have a sufficiently large cross-section area. So, packed columns have always been used in preparative applications [42,43]. In contrast, most analysts interested in SFC decided that the trend toward the use of columns packed with ever finer particles, which began in HPLC at that time, would be leading to excessive technical difficulties. Packing columns with finer particles certainly provides a higher efficiency than packing them with coarser ones but it was feared that it would give them too low a permeability and, because carbon dioxide is compressible, that a significant pressure drop take place along the column, in spite of the low viscosity of CO_2. This pressure drop would cause a large difference in mobile phase density, hence important variations of the retention factors along the column and a loss in separation power [44]. These results might be explained by the high compressibility of CO_2 in the critical region, where it is highly compressible. Accordingly, packed columns were abandoned in favor of 50 μm i.d. open tubular columns, which became so successful and popular in gas chromatography. The use and advantages of these columns were illustrated by Novotny and Lee [44]. Unfortunately, the flow rates needed in these columns are very low, the column back-pressure could not be controlled independently of the flow rate, and it was most difficult to add a constant concentration of organic modifier, which would also have been inconsistent with the use of a flame ionization detector. Although these groups published an extensive number of applications, the method did not flourish and it is now abandoned.

In the early 1980s, Gere et al. [45,46] demonstrated that a conventional HPLC instrument could be modified to implement SFC using conventional HPLC columns packed with 3, 5, and 10 μm particles. Minimum reduced HETPs of the order of 2–3, comparable to those obtained in HPLC were systematically achieved. The low viscosity of carbon dioxide permits the operation of the HPLC columns packed with fine particles at high velocities with low or moderate inlet pressures, permitting the achievement of high efficiencies and difficult separations [47]. So, longer columns, columns packed with finer particles could easily be used. Finally, because diffusion coefficients are large, the columns should be operated at high velocities. This is why SFC is now conducted with mobile phases containing a significant concentration of an organic modifier, which permits reasonable retention of many moderately polar compounds while the large content in carbon dioxide gives the low mobile phase viscosity required. The pressure profile along the column has a small amplitude but Gere et al. operated their columns under high average pressure where the compressibility of CO_2 is moderate.

Columns do not have to be always operated in the critical region of the mobile phase. Often, in the presence of a significant concentration of modifier, the mobile phase is in its subcritical region. Under such conditions, it can exist as either one of two phases, a low-density one and a high-density one. Although the former could possibly be used in high-density Gas Chromatography, as proposed by Giddings [34], the latter is most commonly used and provides a system in which the density of the mobile phase, hence the retention factors of solutes are less sensitive to changes in the local pressure. Then the column performance in SFC becomes comparable to that achieved in HPLC, although the advantages of a low mobile phase viscosity and a high diffusivity remain. Many fast analyses had been made with 3 and 5 μ particles [43,45,46]. A number of very fast analyses are now being made with columns packed with 1.8–3 μm particles, using mobile phases with ca. 10% methanol or 5% 2-propanol [35]. Now, SFC is considered as a practical implementation of normal phase liquid chromatography (NPLC), with several advantages (see Section 12.1).

Although preparative SFC was pioneered by Sie and Rijnders in the 1960s, by Klesper and Hartmann in the 1970s, and by Novotny and his associates in the 1970s and 1980s, it attracted only little attention, in spite of the significant expansion of supercritical fluid extraction, which became widespread during the same time. Preparative SFC was investigated and assessed by several important research groups in the pharmaceutical industry [42,48,49]. Preparative SFC has now become widely applied to the separation of enantiomers in many pharmaceutical companies where it has been adopted as a general purpose industrial process. This is due to rapidity of the separations performed and to the ease of the recovery of the products from the eluent, in spite of the cost and complexity of preparative SFC instruments and to our lack of understanding of its fundamentals, which makes difficult the optimization of production.

Due to the progressive, albeit slow development of SFC during the last ten years, reliable, leakproof, and safe pumps and valves are now available. New equipment for SFC permits the achievement of excellent separations. This progress combines with the large increase in organic solvent cost, to make SFC attractive (SFC does use organic modifiers, but the popular ones are methanol, 2-propanol, and propane, which are less toxic and greener than acetonitrile. Additionally; the concentrations needed are lower than in HPLC, usually below 7%), making the mobile phase non-flammable. Single-column preparative systems began to be used in the pharmaceutical industry ten years ago, particularly for the separation of enantiomers [50–57]. Simulated moving bed SFC has not taken off yet, due to difficult problems encountered in handling the effects of the pressure swings that each column experiences during the SMB cycle because pressure has a significant effect on the retention and separation factors [58], in spite of elegant work by Di Giovanni et al. [59]. Nevertheless, this issue is actively studied.

2.3. Use of the term SFC

Initially, SFC stood for supercritical fluid chromatography: initially, this method was performed with pure supercritical carbon dioxide as the mobile phase. This does not require extreme experimental conditions, since the critical conditions for CO_2 are $T_c = 31\,^{\circ}$C and $P_c = 73$ bar. However, Sandra [60–65] showed that the actual physical state of the mobile phase, whether supercritical or subcritical and liquid, does not matter much, provided that the compounds of interest have convenient retention factors and that no sample component precipitates and accumulates in the column [64]. It is only important to avoid the boiling of the mobile phase in the column and the detector, for obvious reasons. He named this method *"Simplified Fluid Chromatography"*.

It is obvious that SFC has very often been and still is run under subcritical conditions. Practically, it is almost always carried out under critical conditions when the mobile phase contains a significant concentration of an organic modifier or some other additive, which is most frequent in preparative applications due to the relatively low solubility of polar compounds in pure CO_2. It is certain also that the use of liquid carbon dioxide as the main component of the mobile phase confers to it its unusual viscosity, solubility and mass transfer properties that can be used to advantage by analysts. These properties are essentially related to the low viscosity and the high molecular diffusivity of liquid CO_2.

SFC has a variety of names in the literature, *Supercritical Fluid, Subcritical Fluid, Near-Critical Fluid, High-Temperature Liquid, Super-*

heated Liquid, and Enhanced-Fluidity Liquid Chromatography, names that are used interchangeably and do not lead to major ambiguity as long as the mobile phase used is a liquid or a dense supercritical fluid and provided that the experimental conditions are clearly and completely stated, which often is not the case in the literature. The name *Solvating Gas Chromatography* seems to fit better the implementations of Gas Chromatography using a dense or a high pressure gas but under subcritical conditions (in contrast to Subcritical Liquid Chromatography, which uses a subcritical liquid as the mobile phase). The name *Unified Chromatography* has been proposed by Martire [66] and by Chester [19,66–68] but these authors gave different meanings to this name. For Martire, it means a theory of retention based on statistical thermodynamics, which would apply to GC, HPLC, and SFC, does presuppose the use of any experimental method but emphasized the concept that all chromatographic methods are governed by the same theory. For Chester, this name encompasses all the implementations of chromatography, which seems to be too general. This is why we do not use it.

2.4. Advantages and drawbacks of SFC compared to gas and liquid chromatography

The major differences between GC, HPLC and SFC stems directly from the different nature and properties of the mobile phases used in these methods: gases, liquids or supercritical fluids.

- In GC, the mobile phase is a permanent gas (H_2, He, N_2, and A) that remains under relatively low pressure (below ca. 5 atm). It has a low viscosity (90–200 $\times$ 10^{-6} poise, which increases with increasing temperature), a high diffusivity, a low density and it behaves nearly as an ideal gas. The vapors of all compounds present in the carrier gases have a fugacity that is close to 1, and in which, accordingly, the nature and the pressure of the carrier gas has only a minor influence on the equilibrium constants between the two phases of the chromatographic system and on their retention factors. This influence is seen only with extremely efficient open tubular columns [69] or under unusually high pressures. The retention factors in GC depend first on the vapor pressure of the corresponding compound (hence on temperature) and, second, on its activity in the stationary phase. Ettre noted that, if helium is used as the carrier gas, the first section of a GC column is operated under critical conditions [70].
- In contrast, in HPLC, the mobile phase is a mixture of conventional solvents and the influence of the nature and relative concentrations of these solvents on the retention of sample components depends only on the nature and intensities of the molecular interactions between solutes and solvents. Retention and separation in HPLC is controlled by partitioning between the mobile and the stationary phases and the composition of the mobile phase plays a much more important role in HPLC than in GC. The viscosity of the solvents used as mobile phase components is several hundred times larger than those of common gases (0.3 to 2 $\times$ 10^{-2} poise). The molecular diffusivities are correspondingly lower.
- In SFC, the mobile phase is almost always supercritical carbon dioxide, often modified with some moderate amounts of organic solvents, mainly methanol. The viscosity of supercritical or critical fluids is many times higher than that of the corresponding gases but much lower than that of all solvents [6]. Hence, the molecular diffusivity of a compound is several times lower in these fluids than in gases. However, the viscosity of supercritical fluids is an order of magnitude lower than that of most solvents and the diffusion coefficients of solutes in these fluids an order of magnitude larger than in common solvents.

This suggests that the maximum efficiency of columns should be comparable in these three methods and that is inversely proportional to the square of the particle diameter. The optimum flow velocity is inversely proportional to the particle size and proportional to the diffusion coefficient of the compound considered. In all cases, high pressure gradients will be required to achieve the needed flow rates and difficulties will arise from the mobile phase compressibility that tends to considerably decrease from gases to critical fluids, to supercritical fluids, and to liquids, for which it is very low. The compressibility of fluids (see Eq. (3)) is high in the critical region and becomes infinite at the critical point (the isochore compressibility of all gas–liquid diphasic mixtures is infinite at the critical point, which is the last point in the two-phase region where the compressibility of the system is infinite, as indicated by its horizontal inflection point [12]). Depending on the experimental conditions, the variation of the mobile phase density along the column, hence of the retention factors, may be negligible (HPLC), have negligible effects on retention (GC), or be significant to a degree depending on the experimental conditions (SFC).

Preparative chromatography requires large volumes of mobile phase. This was already the major objection that Willstater made to Tswett and to liquid chromatography [71]. This will never change and is valid for SFC as for HPLC. The reason is that chromatography can separate compounds well only if they are relatively dilute in the mobile phase. The equilibrium isotherms of the sample components between the two phases of the system are nonlinear. So, when their concentrations increase, their elution profiles become broader and the elution bands of closely retained components interfere, preventing efficient separation (see Section 9). Therefore, in practice, the separated products obtained are dilute and the collected fractions must be concentrated without loss. Recovery of pure products from the effluent of GC preparative columns is one of the technically most difficult step in preparative SFC [72]. It requires the cooling of the mobile phase. This cooling must be progressive to avoid the formation of stable aerosols, a difficulty similar to the one encountered in preparative GC. Recovery of pure products from the effluents of SFC columns requires the progressive decompression of the mobile phase, to avoid the formation of a mist and the loss of part of the purified products. The traps must be designed so that the condensation of the fractions is like the formation of a rain rather than a fog. Carbon dioxide vaporizes and leaves products concentrated in the organic modifier, from which they must be recovered. In both these two cases, the recovery is relatively inexpensive (see Section 11.5). In HPLC, in contrast, recovery of the pure products is made at important evaporation costs [42].

Compared to preparative GC, SFC shares the advantages of HPLC, the flexibility given by the use as the mobile phase of a solvent or a mixture of solvents that dissolve all the sample components, allow operation at moderate temperatures, and afford the choice of a wide range of eluent compositions that can be modulated to moderate or enhance the interactions of the sample components and the stationary phase and maximize the resolution between the compound of interest and those that must be eliminated from the final product.

Preparative SFC presents significant advantages over HPLC:

1. Normal phase chromatography is easier to implement in SFC because the retention factors are less affected by the presence of small amounts of water in the mobile phase [35]. This may be due to the higher solubility of water in CO_2 than in the organic solvents used in NPLC and to the insulation of liquid carbon dioxide from the laboratory atmosphere being better because easier than that of solvents.
2. Most conventional active pharmaceutical ingredients and the compounds used for their synthesis are as soluble or more soluble in mixtures of supercritical fluids and organic modifiers than in organic solvents.

3. The equilibrium isotherms of pharmaceutical ingredients between supercritical fluids and the adsorbents used to pack preparative columns are often less curved, so column loadability, hence productivity and throughput of preparative SFC are 5–10 times larger than those of preparative HPLC [42].
4. Recovery of purified products from collected fractions is easier and less costly because solubilities in supercritical fluids decrease rapidly with decreasing pressure near the critical pressure; controlled expansion of the supercritical fluid solution gives a product with a high recovery yield [42].
5. The main component of supercritical fluid phases, CO_2, is cheaper, greener and safer than organic solvents.

On the other hand, HPLC retains some critical advantages over SFC

1. The rapid development of GC created a considerable support system, which was well established long before SFC ever began. Combined with more difficult technical requirements, this stifled the development of SFC.
2. The extraordinary development of HPLC in the last forty years has indirectly created a huge support system and much scientific and technical expertise, which is not available to SFC.
3. Instrumentation is more simple and less expensive in HPLC than in SFC.
4. The effect of operational parameters on the elution profiles are different and more complex in SFC than in HPLC or GC.
5. Advanced knowledge in the physical chemistry of liquid/solid adsorption is nearly ubiquitous while it is still lacking for supercritical fluid/solid adsorption. A profound knowledge of the theoretical and experimental principles of SFC is necessary for the pioneers.
6. Manpower with the necessary experimental skills is available in nearly any laboratory in the world in HPLC, not yet in SFC.
7. Massive leaks of carbon dioxide are a constant risk for the operators of an instrument or a unit. This risk is difficult to assess properly and can too easily be neglected or overestimated because there are few comparable chemicals.
8. RPLC is more difficult to use in SFC than in HPLC for the lack of a suitable polar supercritical fluid. The only possible other fluids would be ammonia, sulfur dioxide, and water. The first two are toxic, their critical properties are poorly known, and their use would raise too great difficulties. The critical temperature and pressure of water are high, making it difficult to use; however, subcritical water extraction is an attractive technique and subcritical water chromatography might prove to be quite useful.

There has been a significant number of attempts made by reputed chromatographers and by fledging companies to launch SFC to orbit as a full-fledged chromatographic method of analysis or of production. The latter applications have been somewhat more successful than the former but SFC still remains today a niche method. The essential obstacle is that it has never found its "killer application" [73], the one application of major importance that it can perform so well that no other separation method can even dream of competing with it. For GC, it was the separation of petroleum products, for HPLC, the analysis of low molecular weight pharmaceuticals, their metabolites and their other relatives. So far, more complex to understand and use, more expensive to practice, performing as well as GC or HPLC in many cases but rarely much better, SFC has remained the Cinderella of separation methods.

The landscape may now be on the verge of changing. Significant progress was recently made in the design, the performance and the reliability of instruments, in spite of a narrow market. More importantly, economic and regulatory issues are favoring SFC over HPLC. The latter method utilizes organic solvents that are toxic, hazardous, and expensive. SFC uses mostly carbon dioxide which is considered as CO_2 neutral, since the process itself does not produce it. Admittedly, SFC uses also, besides carbon dioxide, significant amounts of organic solvents but far less than HPLC. Finally, while small residual concentrations of many organic solvents in drugs or food additives should be carefully controlled and must often be entirely eliminated, there is no such problem with carbon dioxide which is toxic only at high concentrations and is not chronically toxic at low concentrations.

This suggests that the interest of separation scientists and engineers for SFC should increase in the next few years, provided that significant progress is made in a number of fundamental issues that are not yet fully understood. This purification method could become more important than it is at present, under the combined pressure of economic considerations (the price of conventional solvents, except methanol, is closely linked to that of crude oil and might increase considerably in the next few years) and of environmental regulations regarding the use of these solvents. This does not mean that we suggest that SFC will ever replace GC and/or HPLC. We rather think that it should take a significant share of the attention, interest and market of the separation sciences but a relatively modest, certainly not an overwhelming one.

3. Physico-chemical properties of high temperature, high pressure fluids

Accurate estimates of the physico-chemical properties of mobile phases used in chromatography are crucial for developing further understanding on its role in solute retention and transport. In this review, only the properties that are relevant to SFC are discussed. The particular physico-chemical properties of carbon dioxide and methanol will be discussed in Sections 4.1 and 4.3. The phase diagrams of mixtures of the eluents used in SFC and of the components of the bolus of feedstock to be processed in preparative SFC cannot be predicted because the critical conditions of SFC eluents mixed with unknown compounds having large complex molecules of complex structures are not yet well understood. The viscosity, the compressibility, and the thermal properties (thermal conductivity and thermal expansion) of supercritical fluids are properties of fluids that are so important that they are discussed in separate sections, respectively, Sections 5.3, 6, and 5.8.

3.1. Solubility equilibria in supercritical fluids

Supercritical fluids are "adjustable" solvents, with a continuous transition between being excellent solvents under the supercritical state, mediocre solvents in the subcritical region, and poor solvents as merely compressed gases, at pressures well below the critical pressure. The rapid separation of the purified compounds from the SFC eluent after fraction collection by changing the pressure and the temperature of the fluid is most useful as it permits considerable savings in time and energy. However, phase diagrams are very complex [12,16,18], which may be a serious source of difficulties in (1) the selection of suitable organic modifiers; and (2) in preparative chromatography, where operating at high sample concentration is an economic necessity. Brennecke and Eckert have reviewed experimental data and analytical methods and attempted to delineate the advantages, potentials, and limitations of SFC in extraction [74].

The measurements of the solubility of solid or liquid compounds in supercritical fluids or in fluids in their near critical region are fraught by several poorly known phenomena which seem to have been ignored by many chromatographers. In the presence of high-pressure fluids, solids may experience significant freezing point depression. The selective dissolution of the fluid phase compo-

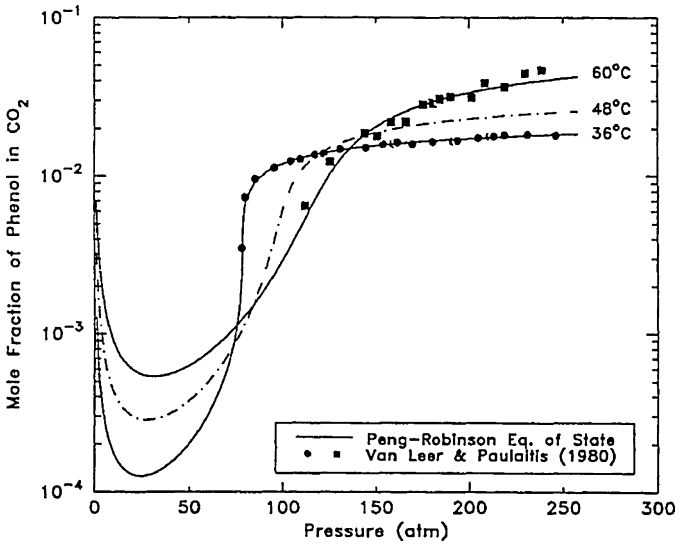

Fig. 7. Solubility of phenol in supercritical dioxide as a function of the pressure at different temperatures [77].

nents in the molten sample may affect the composition of the two phases. Also the solubility of the high-pressure fluid in liquid samples is often very high [75] and the compositions of the two fluids at equilibrium tends toward the same limit, reached at the upper critical endpoint, where the composition of the liquid phase becomes identical to that of the gas phase [74]. The solubility versus pressure equilibrium isotherms of liquids in supercritical fluids does not fall as precipitously with decreasing pressure as that of solids [76]. Akman and Sunol [77] calculated the solubility of phenol in carbon dioxide at 36, 48, and 60 ° C under pressures between 100 and 150 atm, using the Peng and Robinson equation of state (see Section 6.5). The calculated values agree well with the experimental data of van Leer and Paulaitis [76], as illustrated in Fig. 7.

Schneider has shown that the critical $P(T)$ curves in phase diagrams of carbon dioxide and alkanes vary progressively with increasing number of carbon atoms in the alkyl chain. Similar behavior was observed for systems of a component 1 of high volatility (e.g., CO_2, C_2H_6, and CF_4) mixed with a component 2 of low volatility (e.g., alkanes, alkanols, and carboxylic acids) differing considerably from 1 in terms of molecular mass, shape, structure or polarity. Complex diagrams of different types can be obtained [78]. Frequently, a mixture of two components, B and C is more soluble in a critical fluid than each one of these two components alone. The study of mixtures (e.g., 1-butanol and 2-methyl-2-propanol) under very high pressures (above 300 MPa and up to 2 GPa, respectively) shows that homogeneous solutions separate into several solutions in equilibrium. Increasing the pressure of a multicomponent mixture (e.g., 1-butanol, 2-methyl-2-propanol, and water) at constant temperature may lead to heterogeneous states. This behavior is named *high pressure immiscibility* [79].

Jha and Madras measured the solubility of naphthalene in supercritical carbon dioxide at 308 K, for pressures up to 250 bar [80] and compared their experimental results to values calculated using the Peng–Robinson equation of state with two-parameter mixing rules [81] and fundamental thermodynamic equations (see later in this paper, Eqs. (124)) and (125) and Section 6.5). They found an excellent agreement, with an average absolute relative deviation of 5%.

Numerous authors measured the solubility of a wide variety of compounds in supercritical fluids. Mishima et al. measured the solubilities of undecanolide and pentadecanolactone in supercritical carbon dioxide at two temperatures, under different pressures between 12.2 and 25.3 MPa [82]. Tuma et al. measured the solubilities of a series of anthraquinone dyes [83]; Roth et al. measured that of 11 n-alkanes between C_{21} and C_{40} and that of two fullerenes, C_{60} and C_{70}[84]. These data permitted the derivation of the partial molar volumes, dissolution enthalpies and measures of the short-range interactions between the molecules of these compounds and those of carbon dioxide. Later, they determined the second virial coefficients for a series of n-alkanes and carbon dioxide and the Krichevskii parameters of several n-alkanes in CO_2, noting the linear variations of these parameters with the number of carbon atoms [85].

3.1.1. Solubility in ternary systems with carbon dioxide

Francis reported the mutual solubility of carbon dioxide and 261 other substances and the phase diagrams of 464 ternary systems at or near room temperature [86]. Most possible types of such diagrams were found, including those with several binodal curves. Carbon dioxide has two unusual properties, which make these diagrams possible. They are probably related to the closeness of the critical temperature and the temperature at which measurements were made (25 °C). At moderate concentrations, up to ca. 40% (w/w), carbon dioxide acts as a dissolved gas and enhance the miscibility of the other two substances. Most pairs of immiscible liquids become an homogeneous solution upon mixing with a sufficient amount of carbon dioxide [86]. In contrast, at higher concentrations and especially above 60–90%, carbon dioxide is a rather poor solvent for many of these same substances and may be a strong demixing or precipitating agent [86].

In all this work, carbon dioxide was subcritical. The temperature had little influence on the solubility due to a compensation effect between the increase of solubility with increasing temperature and its decrease with decreasing density of the fluid. Carbon dioxide has a selectivity different from those of many other solvents. It is completely miscible with aliphatic and monocyclic hydrocarbons but incompletely miscible with dicyclic hydrocarbons, whether naphthenic or aromatic in the same range of boiling points. It is weakly acidic and does exhibit a strong affinity for weak bases like aniline and pyridine. Some details were given in Section 4.1.

3.2. Solubility parameter

[1] One of the most serious difficulties encountered in chromatography and particularly in preparative chromatography is the solubility of the sample components in the mobile phase. This parameter controls the amount of sample that can be injected into the column, hence the production rate of any unit. This issue is most important in SFC because carbon dioxide is a good solvent for nonpolar compounds but not for polar compounds and the latter account for most pharmaceutical products. So, it is important to be aware of the recent work done on solubility, the parameters that control solubility and to understand how these parameters relate the retention.

Hildebrand and Scott [87] defined the solubility parameter as

$$\delta = \sqrt{\frac{\Delta E_v}{V}} = \sqrt{\frac{\Delta H_v - RT}{V}} \tag{8}$$

where ΔE_v is the energy needed to vaporize the molecules of a compound contained in the volume V of liquid. The ratio $\Delta E_v/V$ is the density of cohesive energy of the compound. It is related to the intensity of the intermolecular interactions, which increases with polarity and δ correlates strongly with the polarity. The solubility parameter is an important quantity that helps to understand the solubility of two compounds. The Hildebrand solubility parameter

[1] See the definition of the parameters later, in the nomenclature section.

provides a quantitative estimate of the possible degree of interaction between materials, which is a good indication of solubility, particularly for non-polar materials. Materials with similar values of δ are likely to be miscible.

Regular solutions are solutions in which the solute molecules disperse randomly among the solvent molecules and both solute and solvent molecules have similar sizes [87]. Then, the mixing entropy is negligible. The enthalpy change associated with the transfer of the pure nonpolar solute into the nonpolar solvent 1 at infinite dilution is approximately [87]

$$\Delta\bar{H}^{o}_{i,1} = \bar{V}_i(\delta_i - \delta_1)^2 \tag{9}$$

assuming that the molecular interactions in both solute and solvent are controlled by London dispersion forces. A similar equation could be written for the enthalpy of dilution of the solute i into a similar solvent 2. Then, the transfer of a mole of solute from solvent 1 to solvent 2 entails an enthalpy change

$$\Delta\bar{H}^{o}_{i} = \Delta\bar{H}^{o}_{i,2} - \Delta\bar{H}^{o}_{i,1} = \bar{V}_i[(\delta_i - \delta_2)^2 - (\delta_i - \delta_1)^2] \tag{10}$$

Since the mixing entropy is negligible, $\Delta\bar{S}^{o}_{i} = 0$ and the change in chemical potential of the solute is

$$\Delta\mu^{o}_{i} = \bar{V}_i[(\delta_i - \delta_2)^2 - (\delta_i - \delta_1)^2] \tag{11}$$

which gives the distribution coefficient of the compound between the two solvents

$$\ln K = \frac{-\bar{V}_i}{RT}[(\delta_i - \delta_2)^2 - (\delta_i - \delta_1)^2] \tag{12}$$

Although this equation is approximate, it provides useful relationships between the properties of pure compounds, the solutes and solvents, their molecular interactions, and the physico-chemical properties of their solutions. It is important to note that this equation provides help in the selection of the solvents needed to dissolve a solute, even when solute and solvent have somewhat different molecular volume and a moderate polarity. Eqs. (11) and (12) show that the dissolution of a solute takes place preferentially in the solvent having the solubility parameter closest to that of the solute considered.

Later, Hansen [88] developed the Hansen Solubility Parameters that provide a more reliable estimate of the solubility of one compound into another one. In this approach, each molecule is given three Hansen parameters, related to the energies from (a) the dispersion bonds δ_d, (b) the polar bonds δ_p, and (c) the hydrogen bonds δ_h, formed between its molecules. These parameters are treated as coordinates for a point in a Hansen space. The possibility of two compounds dissolving in each other increases with the proximity of the two molecules in this three dimensional space. The Hansen solubility parameter has found wider applicability in predicting solubility in different kind of solvents, unlike the Hildebrand solubility parameter which is reported to be more useful with non-polar solvents.

3.2.1. Solubility parameters of supercritical fluids

Although designed and developed for liquids, the concept of solubility parameter was readily extended to dense gases and supercritical fluids [89]. The solubility parameter of a dense gas can be estimated by one of the two equations

$$\delta = 1.25\sqrt{P_c}\frac{\rho}{\rho_{liq}} \tag{13}$$

$$\delta = \delta_{liq}\frac{\rho}{\rho_{liq}} \tag{14}$$

where ρ/ρ_{liq} is the ratio of the density of the dense gas to that of the liquid at its boiling point.

Eq. (13) shows that the solvent power of a critical or subcritical fluid depends on two different factors, its personality and its density [89]. The former reflects the structure of the solvent molecule and its polarity. Water (δ = 23.4), ammonia (δ = 16.3), methanol (δ = 14.5), being highly polar have a high solubility parameter and dissolve polar compounds. Nonpolarizable compounds like argon (δ = 6.8) or light hydrocarbons have negligible or nearly negligible solvent effect. Carbon dioxide (δ = 8.9 at T_c = 31 °C) is an excellent solvent for molecules of moderate polarity, but dissolves poorly polar compounds. It should be noted that the critical temperature, like the boiling point of molecules increases with increasing polarity, making inconvenient the use of polar compounds as mobile phases in SFC. The second factor controlling the solvent power of dense gases or supercritical fluids is their density, which has the advantage of being easily tuned [90].

Tijssen et al. [91] showed that the solubility parameter can readily be derived from an equation of state, using the relationship:

$$\delta^2 = -\frac{RT_c}{v}\left[\frac{H - H^*}{RT_c} + T_r\right] + \frac{3}{2}\frac{RT}{v} \tag{15}$$

where the term $(H - H^*)/RT_c$, called the residual enthalpy function or enthalpy departure, can be estimated from tables given by Lee and Kesler [92]. The second term, $3RT/2v$, accounts for the change in the number of degrees of freedom of the molecules compared to those of an ideal gas, a change which under SFC conditions in which the fluid density, hence its molar volume, depends considerably on the pressure, so the second term may be substantial.

The enthalpy departure in Eq. 15 is given by

$$\frac{H - H^*}{RT_c} = T_r\left(Z - 1 - \frac{b_2 + 2b_3/T_r + 3b_4/T_r^2}{T_r V_r} - \frac{c_2 - 3c_3/T_r^2}{2T_r V_r^2} + \frac{d_2}{5T_r V_r^5} + 3E\right) \tag{16}$$

with

$$E = \frac{c_4}{2T_r^3\gamma}\left(\beta + 1 - \left(\beta + 1 + \frac{\gamma}{V_r^2}\right)e^{-\frac{\gamma}{V_r^2}}\right) \tag{17}$$

3.2.2. Crossover pressures in solid-SFC equilibria

The solubility of a solid in a supercritical fluid is not a well-behaved function of pressure [93]. Solubility initially decreases with increasing pressure, reaches a minimum, then rises rapidly in the critical region. The solubility increases with increasing temperature at low pressures and at high pressures, as does the vapor pressure of the solid. However, in an intermediate range of pressures, the solubility decreases with increasing temperature (see earlier, Fig. 7). This is a consequence of the rapid decrease in the density of the solvent in that range. There are two crossover pressures, at a low and a high pressures ones, at which the plot of the solubility versus temperature changes sign. The criteria is

$$\left(\frac{\partial x_2}{\partial T}\right)_P = 0 \tag{18}$$

For ternary systems, the crossover regions may be sufficiently different for the two solids to allow for their separation.

3.3. Fugacity in SFC phases

An equation for the fugacity coefficient of a pure compound can be derived from the Lee–Kesler equation of state (see Section 6.4.1). This equation was derived by Schoenmakers [7] and it is written

$$\ln\phi = \ln\frac{f}{P} = Z - 1 - \ln Z + \frac{B}{V_r} + \frac{C}{2V_r^2} + \frac{D}{5V_r^5} + E \tag{19}$$

where f is the fugacity, ϕ the fugacity coefficient, and V_r the reduced volume (see Eq. (77)). Z is the compressibility factor, the definition of which is also discussed in Eq. (81) while a method for its determination is given in Eq. (100). The coefficients B, C, D, and E can

Table 2
Coefficients of the Lee and Kesler equation of state [92].

Coefficient	Simple fluid (°)	Reference fluid ^{r}
b_1	0.1181193	0.2026579
b_2	0.265728	0.331511
b_3	0.154790	0.027655
b_4	0.030323	0.203488
c_1	0.0236744	0.0313385
c_2	0.0186984	0.0503618
c_3	0.0	0.016901
c_4	0.042724	0.0415779
d_1	0.155488×10^{-4}	0.48736×10^{-4}
d_2	0.623689×10^{-4}	0.0740336×10^{-4}
β	0.65392	1.226
γ	0.060167	0.03754
ω^r		0.3978

be calculated following Eqs. (78) and (17). The coefficients b_1, b_2, b_3, b_4, c_1, c_2, c_3, d_1, d_2, β, and γ in these equations have numerical values that are independent of the compound considered (see Table 2).

The fugacity coefficient of compound 2 in a binary mixture is given by [94]

$$\ln \phi_2 = \ln \phi_m + (1 - x_2)\left(\frac{\partial \phi_m}{\partial x_2}\right)_{P,T} \quad (20)$$

where ϕ_m is the fugacity coefficient of the mixture and x_2 is the molar fraction of component 2. In chromatography, the important parameter is the fugacity coefficient at infinite dilution or limit of $\ln \phi_2$ when x_2 tends toward 0.

3.4. Partial molar volumes in supercritical solvents

The partial molar volume of the solute in a solvent is an important property that permits investigation of molecular interactions between solute and solvent [95]. It is important in determining the retention dependence on the mobile phase density [96]. Wheeler had shown that the partial molar volume of solutes at infinite dilution should diverge toward infinity at the solvent critical point, the values becoming negative if there are attractive interactions between solute and solvent molecules, positive if these interactions are repulsive [97]. However, the limiting values depend on the path of approach [74]. Experimental values support this fundamental result and suggest that clustering of a large number of solvent molecules takes place around each solute molecule. The knowledge and understanding of molecular interactions is thus, more than in HPLC, most critical to understand the behavior of retention in SFC.

On theoretical grounds and on the basis of a lattice-gas model, Wheeler predicted that the partial molar volume of solutes in the critical region should be dominated by the compressibility of the fluid [97]. Accordingly, it should tend toward a negatively infinite value at the critical point. This prediction was confirmed by experimental results of van Wasen and Schneider [23]. Using SFC, these authors measured the partial molar volumes of naphthalene and fluorene in carbon dioxide at 35, 40 and 50 °C, for pressures between 50 and 130 bar. They assumed the partial molar volume of the solute to be constant in the adsorbed phase and measured the variation of the partial differential of the retention factor of the solute $\partial k/\partial P$ with the pressure. The influence of the pressure on the retention factor of naphthalene, at different temperature is illustrated in Fig. 8[7], which is very similar to that shown by van Wasen and Schneider, and the partial molar volumes of the two solutes in Fig. 9. The solid line shows the isothermal compressibility of pure CO_2. The partial molar volumes of solutes were also studied by Eckert et al. [98].

Solubility data measured by Roth [84] were used to derive the partial molar volumes of the C_{60} and C_{70} fullerenes and of the

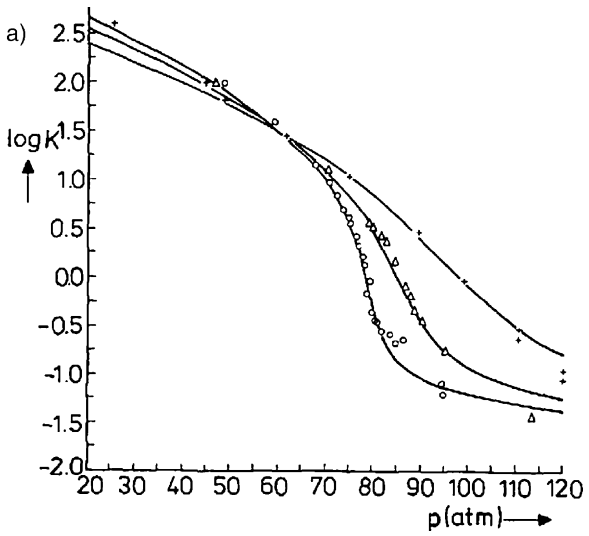

Fig. 8. Retention factor of naphthalene in carbon dioxide as a function of the pressure at different temperatures, ◯ 35 °C; △, 40 °C; + 50 ° C [7].

C_{21} to C_{40} n-alkanes at infinite dilution in carbon dioxide (see Section 3.1). These data were used to derive quantities characterizing short-range solute-CO_2 interactions. Differences between these interactions for fullerenes and n-alkanes are significant and were discussed. They suggest that the interactions between carbon dioxide and fullerene molecules are less than those between CO_2 and n-alkanes.

3.5. Linear solvation energy relationships in supercritical systems

A cogent review on linear solvation energy relationships (LSER), their interpretation and use was recently published by Vitha and Carr [99]. The currently accepted symbolic representation of LSER was provided by Abraham et al. [100].

$$SP = c + eE + sS + aA + bB + vV \quad (21)$$

where SP is a property related to free energy (e.g., the logarithm of the retention factor of a compound, $\log k$), and the letters E, S, A, B, and V denote solute dependent input parameters that are related to measures of the polarizability of the solute in excess of that of an n-alkane of comparable size, of its dipolarity (with some contribution from its polarizability), its hydrogen bond acidity (or donating

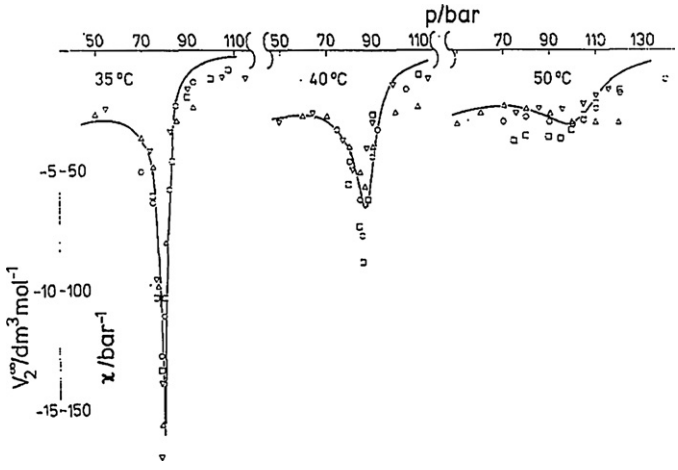

Fig. 9. The partial molar volumes of naphthalene and fluorene in carbon dioxide at different temperatures. Experimental data [23] and calculated curve [97]. ▼, naphthalene on PerisorbA; ▲, naphthalene on PerisorbRP-8; □, fluorene on PerisorbA; ◯, fluorene on Perisorb RP-8.

ability), its hydrogen bond basicity (or accepting ability), and its molecular volume. These parameters are included to account for the contribution of a specific type of intermolecular interactions. The coefficients e, s, a, b, and v and the constant, c, are characteristics of the specific system involved, the system of two phases between which the free energy difference of the compound must be calculated. These coefficients are actually determined via multiparameter linear least-squares regression analysis of a data set comprised of solutes with known E, S, A, B, and V values and which span a reasonably wide range in interaction abilities [99]. Considerable energy has been spent by numerous scientists to investigate these relationships. It is unfortunate that most of them ignore the important work of Krug et al. who identified a major pitfall of overambitious linear free energy relationships and provided tests to avoid them [101–103]. A typical LSER is the relationship between the Kovats retention indices of alkanes and their van der Waals volumes [104]. LSER have been used to interpret retention mechanisms and to predict retention data [99].

3.5.1. Solvatochromic effects in supercritical systems

The set of solvent parameters or solvent descriptors are related to their solvent strengths in the various scales available and, particularly to the solvatochromic scale of solvent dipolarity/polarisability of Kamlet, Taft and Abboud [105–110]. Numerous gas–hexadecane, gas–octanol, gas–water LSER have been developed and used to characterize stationary phases and predict their selectivity, facilitating the selection of the best phase for a given separation [99]. A similar, larger effort was made in HPLC, particularly for RPLC phases. Difficulties were encountered, however, in accounting for the molecular size of the solid. In the liquid phase, a cavity must be made to accommodate the solute, which is not the case in the gas phase. Diffusive interactions are the dominant intermolecular interactions in gas–liquid transfers but, although they correlate strongly with molecular size, are not well represented by a simple volume term. For this reason, Abraham suggested using the logarithm of the gas-to-hexadecane partition coefficient, L[16] as a combined measure of the influence of the energies of dispersive interactions and cavity formation on the free energy of the solute in GC correlations, with l being the associated parameter of the system studied [111].

Schneider reported that the Kamlet–Abboud–Taft scale could be extended by spectroscopic measurements on five probe compounds (nitrobenzene derivatives) dissolved in supercritical fluids in a large range of temperatures and pressures, which permits a comparison with conventional solvents [78]. All non-selective interactions can be described by a polarity parameter, π^*, defined by

$$\bar{\nu} = \bar{\nu}_0 + \pi^* s \tag{22}$$

where $\bar{\nu}$ and $\bar{\nu}_0$ are the wavenumbers of the absorbance maxima in the fluid studied and in a reference fluid (e.g., cyclohexane), respectively and s is a parameter characteristic of the probe compound, which is found in the literature. The polarity parameter increases with increasing reduced density of fluids. For carbon dioxide, the increase is nearly linear in the reduced velocity range between 0.7 and 1.8.

3.6. Dielectric constant

This constant provides a measure of the efficiency of a solvent at promoting the dissociation of the solutes, which are electrolytes, into their ions. In solvents with a high dielectric constant (e.g., water), electrolytes dissociate readily while in solvents with a low dielectric constant considerable ion-pairing occur (e.g., ethers). The dielectric constants of most solvents used in SFC are known but those of mixtures of these solvents are not. They are needed, however, to predict the solubility of chemicals in mixed solvents that are commonly used in chromatography or in other separation techniques. The common method of calculating the values of this constant for mixed solvents consist in assuming a simple additivity rule and in deriving the constant as the weighted average of the mixture components. This would be valid for ideal solvent mixtures but is highly imprecise for mixtures of solvents exhibiting strong intermolecular interactions.

Jouyban et al. [112] suggested that the dielectric constant of a binary mixture of known composition is given by the equation

$$\ln \epsilon_{m,T} = \ln \phi_1 \epsilon_{1,T} + \ln \phi_2 \epsilon_{2,T} + \phi_1 \phi_2 \sum_{j=0}^{2} \frac{A_j(\phi_1 - \phi_2)}{T} \tag{23}$$

where $\epsilon_{i,T}$ is the dielectric constant of component i at temperature T, $\epsilon_{m,T}$ that of the mixture, ϕ_i the volume fraction of the solvent i, and A_i an empirical constant. The average deviation between calculated and measured values is generally of the order of one percent. The major difficulty in the application of this method lies in the lack of tables of empirical constants.

4. Particular physico-chemical properties of some common sfc solvents

The state of fluids in SFC is profoundly different from that of gases in conventional gas chromatography, where pressures are less than ca. 10 bar. The fluids used in SFC have a density markedly higher than that of these gases, by at least an order of magnitude. We describe here the physico-chemical properties of fluids commonly used as the main component or as additives of mobile phases for SFC, carbon dioxide, water, methanol, propanol. If it were not for some technical difficulties that would obviously be encountered, several common gases (which actually are supercritical fluids in their conventional tanks) could also be used, such as nitrogen, argon, xenon, or sulfur hexafluoride.

4.1. Carbon dioxide

This is by far the fluid most useful in SFC. This is due to a rare combination of characteristics. Its critical point makes it easy to handle under the supercritical state, with a critical temperature of 304.1282 ± 0.01 K (ca. 31 °C), a critical pressure of 7.3773 ± 0.0030 MPa (ca. 74 atm), at a critical density of 0.4676 ± 0.0006 g cm^{-3}[113]. So, it can be used at temperatures barely higher than room temperature, at pressures between 50 and 200 atm. The relationships between the density, the viscosity (η), and the diffusivity of carbon dioxide ($D_{1,1}$) and the pressure at a temperature of 40 °C, ca. 9° C above the critical temperature are illustrated in Fig. 10. The viscosity is remarkably constant up to reduced pressure of nearly 0.95 but continue increasing rapidly with increasing pressure until a reduced pressure of ca. 3 before tapering off. The product $\eta D_{1,1}$ remains nearly constant. Thus, in a significantly wide region, carbon dioxide has a density and a solvent power comparable to those of poorly polar organic solvents but a viscosity and a diffusivity intermediate between those of gases and of conventional solvents [13]. A graph showing the viscosity of carbon dioxide as a function of temperature and pressure is shown later, in Fig. 12

The permittivity of carbon dioxide increases rapidly from ca. 1.1 to 1.5 for pressures between 5 and 25 atm and remains lower than 1.8 at the highest pressures, corresponding to liquid density [12]. Carbon dioxide does not have a dipole moment and its polarizability is low. So, solvation effects are unimportant and intermolecular interactions are essentially of the van der Waals type. Consequently, carbon dioxide is a good solvent for the components of

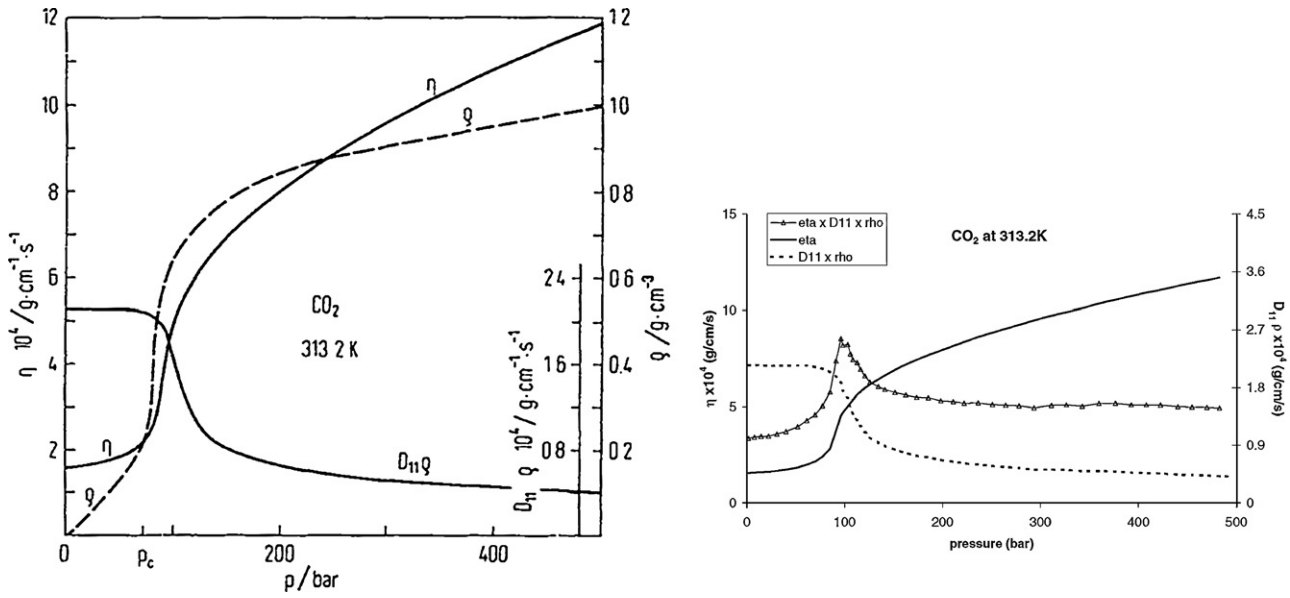

Fig. 10. Left: Relationship between the density, the viscosity, and the diffusivity of supercritical carbon dioxide at 40 ° C with its pressure [13]. Right: Plot of the product of the density, the viscosity, and the diffusivity of supercritical carbon dioxide as a function of its pressure.

low polarity and moderate molecular mass found in products of the food, pharmaceutical, and cosmetic industries. Because it can be used at temperatures barely above ambient, and it is not reactive, thermal or chemical degradations are avoided. However, it has been reported to react with amines and form carbamides. It is also not combustible, not hazardous (except at high concentrations) and nontoxic and it is a natural product. Although it exhibits an acute toxicity at high concentration because its presence switches off breathing, it is not toxic at low concentrations, with no chronic effects. Any residual trace of it in any product would be harmless.

The viscosity of supercritical carbon dioxide is low [114] and its self-diffusion coefficient is high [115]. When carbon dioxide is used as a supercritical cosolvent in subcritical solvents, it decreases considerably the viscosity of solutions and enhances the mass transfer kinetics, which is particularly important in SFC.

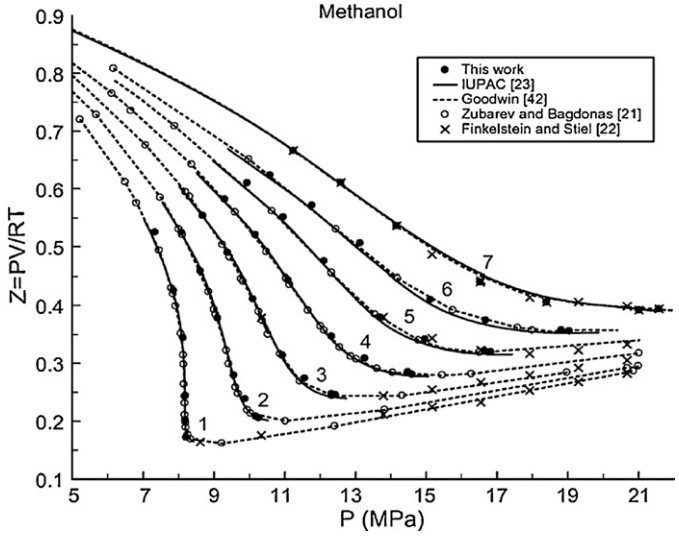

Fig. 11. Compressibility factor of methanol as a function of pressure along supercritical isotherms, •. Comparison with data of other authors (○, [125], **x**[126]) and with curves calculated from equations of state not reported in this review. [124].

4.2. Water

The critical temperature and pressure of water are $T_c = 373$ ° C and $P_c = 217$ atm. This combination of physical conditions is difficult to achieve. However, the physico-chemical properties of water change rapidly with increasing temperature and pressure and one can consider that the subcritical range of water begins around $T = 100$ ° C and $P = 10$ atm. This fluid is used in numerous applications of subcritical water extraction (SWE), a process that is now wide spread [116,117]. It is based on the observation that the dielectric constant (80.1 at 20 °C) and the surface tension of water decrease with increasing temperature and become close to those of methanol. This effect is explained by the progressive breaking down of the hydrogen bonding between water molecules. As a consequence, compounds such as polycyclic aromatic hydrocarbons (PAH) and polychlorinated biphenyls (PCB) become soluble in water. Obviously, as the temperature rises, so does the vapor pressure, which for water is approximately given by $P(\text{atm}) = (T/100)^4$ ° C)/100, meaning that it is still less than 40 atm at 250 °C.

Pure, hot subcritical water has attracted much interest as a mobile phase in chromatography. This field was reviewed by Greibrokk and Andersen [118] and Teutenberg [119]. Its use as a mobile phase allows replacing the UV–vis spectrophotometric detector with a flame ionization detector, as shown by Guillemin et al. [120,121], by Hawthorne et al. [117], and later by Yang et al. [122], who could separate carbohydrates, carboxylic acids and amino acids. The viscosity of water decreases rapidly with increasing temperature, which allows the use of columns packed with 3 μm particles at temperatures above 100 °C. Numerous other separations were made with subcritical water [119–121,123].

Finally, practitioners should note that the solubility of silica in water increases with increasing temperature and supercritical water is very corrosive to silica.

4.3. Methanol and ethanol

The critical temperature of methanol is 512.75 ± 0.1 K, its critical pressure 8.120 ± 0.02 MPa and its critical densities 271.6 ± 3 kg/m^3 [124]. These values are important because they show that mixtures of methanol and carbon dioxide can rarely be

supercritical, unless the methanol concentration is low. Besides the recent work of Bazaev et al. [124], there are few determinations of the PVT data for methanol in the sub- and supercritical regions [125–128].

Fig. 11 shows plots of the compressibility factor, $Z = PV/RT$, of methanol at pressures between 50 and 210 bar, at different temperatures and compare the data measured by Bazaev et al. [124] with the data of Zubarev and Bagdonas [125] and of Finkelstein and Stiel [126] and with the curves calculated using the equations of state of IUPAC and of Goodwin. The agreement is more than satisfactory, with deviations less than 1%.

To perform separations previously made in HPLC, using aqueous solutions of acetonitrile in the HILIC mode, the group of Sandra [64,129] recommends the use of ethanol as a modifier of carbon dioxide, but with higher ethanol concentrations (25–50% of the eluent) than normally used in SFC. This is an application of enhanced fluidity chromatography of Sandra [64] or unified chromatography of Chester [68].

4.4. Mixture properties

Helium has been used to pressurize carbon dioxide cylinders and its presence in head-spaces may cause problems. A liquid–vapor separation may take place, resulting in the coating of capillary tubings by a carbon dioxide-rich liquid film with the possible partitioning of components between this film and a helium-rich gas phase. Similar phenomena may take place with other mobile phase additives [130–132].

Nazmutdinov et al. have measured the critical temperatures of ten binary mixtures as a function of their composition, using the classical ampule method [133]. The components of the eleven mixtures studied included all aliphatic alcohols having one to five carbon atoms, the n-alkanes with five to ten, twelve, and fourteen carbon atoms, benzene, toluene, and methyl ethyl ketone [133]. Data from the literature including fifty other mixtures were collected. The measurements of the critical temperatures were made for three to eight different concentrations. The relationship between the critical temperatures, $T_{c,m}$, of a binary mixture, those of its components and the mixture composition was approximated with the Redlich–Kister empirical equation

$$T_{c,m} = x_1 T_{c,1} + x_2 T_{c,2} + x_1 x_2 \left(A_1 + A_2[(x_1 - x_2)] + A_3(x_1 - x_2)^2\right) \quad (24)$$

In most cases, the difference between the experimental results and the values calculated using the Lee and Kesler equation of state for mixtures (see Section 6.4) is less than one degree. In almost all cases when this difference is more than a degree, it involves n-decane [133].

Abdulagatov et al. published a large compilation of data regarding the critical properties of binary mixtures of carbon dioxide and numerous compounds, including n-alkanes and other hydrocarbons, light alkyl alcohols, aromatic hydrocarbons, and a variety of low molecular weight compounds, organic or inorganic [11]. The critical temperatures and pressures are given as functions of the composition of the binary mixtures, as reported by numerous authors. Although the results found in the literature are often in agreement, occasional important differences were observed, illustrating the difficulties encountered in the measurement of critical data and the different precision of the methods used for these determinations.

4.5. Organic modifiers

Unfortunately, carbon dioxide is not a good solvent for polar compounds [134,135]. The solubility of the components of most mixtures to analyze, separate, or purify is generally poor, their retention high, and the selectivity of the phase systems for compounds of similar structure or molecular weights is insufficient. Much work has been done and is still done to modify this solvent and to increase the solubility and the selectivity of the eluent [74]. Polar modifier, such as methanol and ethanol, have been successfully used to enhance solubility and selectivity toward molecules than may interact with the modifier through dipole–dipole interactions or hydrogen bonding [135]. The addition of water, which is not very soluble in carbon dioxide but adsorbs easily and strongly on the surface of most packing materials used in chromatography, may considerably modify the retention and the selectivity of polar compounds, having the same effect in SFC as water has in normal phase liquid chromatography. However, carbon dioxide is highly soluble in water under pressure and using their mixture under experimental conditions that are supercritical for carbon dioxide but subcritical for water may considerably affect separations made in a variety of chromatographic modes (e.g., HILIC and RPLC), although low water concentrations are generally used. The use of additives, including salts, soluble in the organic modifiers has also been heavily promoted [134].

Light hydrocarbons have been used to increase the solubility of high-molecular weight compounds of low polarity such as triglycerides. The use of these modifiers permit adjustment of the retention times and of the separation factors. In preparative chromatography, increasing the solubility leads to improved productivity and better peak shapes.

The major problem with the use of organic modifiers in carbon dioxide is the extreme potential complexity of the phase diagrams [19,135]. This makes their use difficult to control in numerous cases (see Section 2.1.3 and Fig. 3). It may lead to spectacular failures when the mobile phase splits into two different fluids, a gas and a liquid, which are in equilibrium with each other, percolate simultaneously through the column bed, each of them being equilibrium with the stationary phase. Furthermore, for the lack of sufficient information on the relevant phase diagrams, the behavior of such chromatographic systems may be impossible to model [135]. Vincent et al. [136] and West et al. [137] studied the behavior of systems made of methanol, propanol or acetone dissolved in carbon dioxide as the mobile phase and cross-linked poly(dimethylsiloxane) coated on silica as the stationary phase. Considerable changes of the volume of the polymer layer take place with changes in the pressure and in the organic modifier concentration. Yuan and Olesik measured the phase diagram of carbon dioxide and THF between 10 and 90 mole% CO_2, and between 25 and 100 °C [138]. They found the system to be monophasic for pressures above 110 atm and temperatures below 100 °C. They used eluent made of these mixtures for separations of polystyrene by size exclusion chromatography. Zhao and Olesik [139] measured the phase diagrams of methanol/trifluoromethane and of methanol/water/trifluoromethane between 25 and 100 °C and between 1 and 340 atm. Fluoroform (CF_3H) is highly polar, has a low viscosity and more miscible with methanol and water than carbon dioxide.

Wells et al. drew an approximate phase diagram of carbon dioxide and methanol [135], which seems to be less correct, at least around the critical point, than the schematic diagram in Fig. 2. Francis determined the ternary phase diagrams of carbon dioxide, water, and methanol, ethanol, 2-propanol, 2-butanol, phenol, acetone, 2-butanone, furfural, acetic acid, or succinonitrile [86]. All these diagrams show regions in which two phases coexist. For example, although methanol is miscible in all proportions with either carbon dioxide or water, a large fraction of the surface area of the ternary diagram is occupied by a region corresponding to two different liquid phases, a water-rich aqueous solution of methanol and carbon dioxide and a CO_2-rich solution of water and methanol. In all cases also, the solubility of carbon dioxide in the other two

liquids is markedly higher than the solubility of these other liquids in carbon dioxide. Light hydrocarbons and their derivatives substituted with halogen atoms or carrying carbonyl groups are miscible with carbon dioxide. The addition of carbon dioxide to a binary mixture tends to increase the solubility of each one of the two compounds in the other one.

Recently, Cox et al. [140] showed that the use of methylene chloride, chloroform, methyl and ethyl acetate, THF, acetonitrile, and methyl*t*-butylether (MTBE) as additives combined or not with methanol improves, some times considerably the selectivity of chiral selective stationary phases, such as Chiralpak IA, IB, and IC (Daicel Inc., Osaka, Japan; Fort Lee, NJ, USA). The concentration of these modifiers may positively affect the solubility, the retention, the enantiomeric selectivity, and the parameters of the isotherms (particularly the saturation capacity) of pairs of enantiomers, hence the production rates of their separation. The use of these non-alcohol modifiers often improves production rates and recoveries more than that of methanol or ethanol.

Organic modifiers have 10–100 times higher viscosity and provide sample components with 10–100 times lower diffusion coefficients than CO_2. The solution obtained by mixing organic modifiers and CO_2 has intermediate properties. The variation of these properties with the concentration is not linear. For example, the viscosity of a 40/60 molar solution of methanol in CO_2 has a viscosity equal to one third the viscosity of methanol [141].

5. Hydrodynamics of supercritical fluids in porous media

The laws governing the flow of fluids through porous media like chromatographic beds are fundamentally the same in GC, HPLC, and SFC but each method has its own specific peculiarities that are essentially related to the consequences of the compressibility of the mobile phase, which is different for gases, liquids, and fluids near or above the critical point. In SFC, these problems derive directly from the important influence of the pressure on the density, the viscosity and a few other properties of supercritical fluids. So, for the development of a clear understanding of the fluid behavior inside the column, efforts are required to determine:

1. the hydrodynamics of the mobile phase stream or the relationship between its flow rate, the inlet and the outlet pressures, and the characteristics of the mobile phase,
2. the profiles of the mobile phase density and pressure along the column, which are also a function of the temperature,
3. the average flow rate, and the hold-up time.

5.1. Nature of the flow in supercritical and subcritical fluid chromatography

The flow rate always remains laminar in SFC because (1) even for columns packed with fine particles, the efficiency is high only at relatively low or moderate flow velocities (although these velocities are several times larger than in HPLC); and (2) the pressure gradient along the column must be kept moderate to avoid that a high pressure drop resulting in a large, even possibly an excessive variation of the mobile phase density, hence variations of the viscosity and the retention factors. The Reynolds number, *Re*, characterizes the flow, with

$$Re = \frac{ud_p\rho}{(1-\epsilon_e)\eta} \tag{25}$$

where u is the interstitial velocity of the stream, ρ its density, η its viscosity, d_p the average particle size, and ϵ_e the external porosity of the bed. This number is always lesser than 1 under the experimental conditions which are used to implement SFC (typical values are [45] ca. $u = 1$ cm/s, $\rho = 0.5$ g/ml, $\eta = 0.1$ cP, $d_p = 10$ μm and $\epsilon_e = 0.4$, giving $Re = 0.10$). In open tubes, flows become turbulent at Reynolds numbers of the order of 2000. However, Darcy's law remains valid only up to lower values of the Reynolds number because the fundamental characteristic of the beds of packed particles is not the existence of bundles of parallel capillary tubes, as postulated in applications of Darcy's equation to these beds, but the interconnection of the channels at all levels and the continuous and often rapid variation of their cross-sections. The flow conditions therefore differ considerably from those prevailing in an empty tube; the fluid is being subjected to a sequence of violent accelerations and decelerations under conditions far removed from thermodynamic reversibility. Some of the energy, in proportions increasing with the flow rate, is given up to the surrounding medium as heat, a phenomenon which may be interpreted as a progressive decrease in the permeability coefficient. A more complex model due to Ergun relates the column pressure drop and the flow velocity through a quadratic equation, but the second order coefficient is negligible under any possible chromatographic conditions, with deviations from linear behavior possible only for $Re > 1$ [142].

5.2. Column permeability

To sustain the percolation at a constant flow rate of a stream of mobile phase along a column, a certain pressure must be maintained at the column inlet. Without any loss of generality, we may assume that the fluid is Newtonian and that the flow of this stream is laminar (see above). Then, this pressure, P, is related to the flow velocity and the characteristics of the column and of the mobile phase through the Darcy equation [1,42,143]

$$\frac{\Delta P}{L} = \frac{\eta u}{K} \tag{26}$$

where K is the column permeability. However, the density and the viscosity of the mobile phase significantly depend on the pressure and vary along the column. So, the velocity in SFC is not practically constant as it is in HPLC and the pressure drop must be calculated by numerical integration of the differential form of Eq. (26) which is

$$\frac{dP}{dz} = -\frac{\eta u}{K} \tag{27}$$

combined with the mass conservation of the eluent ($u = Q/(\rho S)$, with Q the mass flow rate of the mobile phase and S the cross-section area of the column), the relationship between the mobile phase viscosity, the pressure and the temperature [6], and the equation of state, $\rho = f(P, T)$ (see Section 6). Obviously, under steady-state conditions, the mass flow rate is constant along a column: obviously, what enters the column in a given time must leave it at the same rate. This means that, if the mobile phase expands along the column due to the decompression of the compressible mobile phase, the linear velocity of the mobile phase increases, the local flow velocity being inversely proportional to the local eluent density. While integrating Eq. (27) from $z = 0$ to $z = L$ gives the pressure drop, integrating it from $z = 0$ to z gives the pressure profile, hence the density profile along the column, knowing the equation of state.

The permeability is a characteristic of the column bed itself and is independent of the properties of the fluid percolating through that bed. There seems to be few reports in the literature comparing the permeability of any given column measured with streams of gases, liquids or fluids in their critical region. However, it should, at least in principle, be possible to measure the permeability and the hold-up volume of a column using the classical, proven methods of HPLC and use this data in SFC. This would provide independent estimates of important column parameters.

A considerable body of evidence shows that, in the range of velocity used in chromatography whether GC, SFC, or HPLC, the

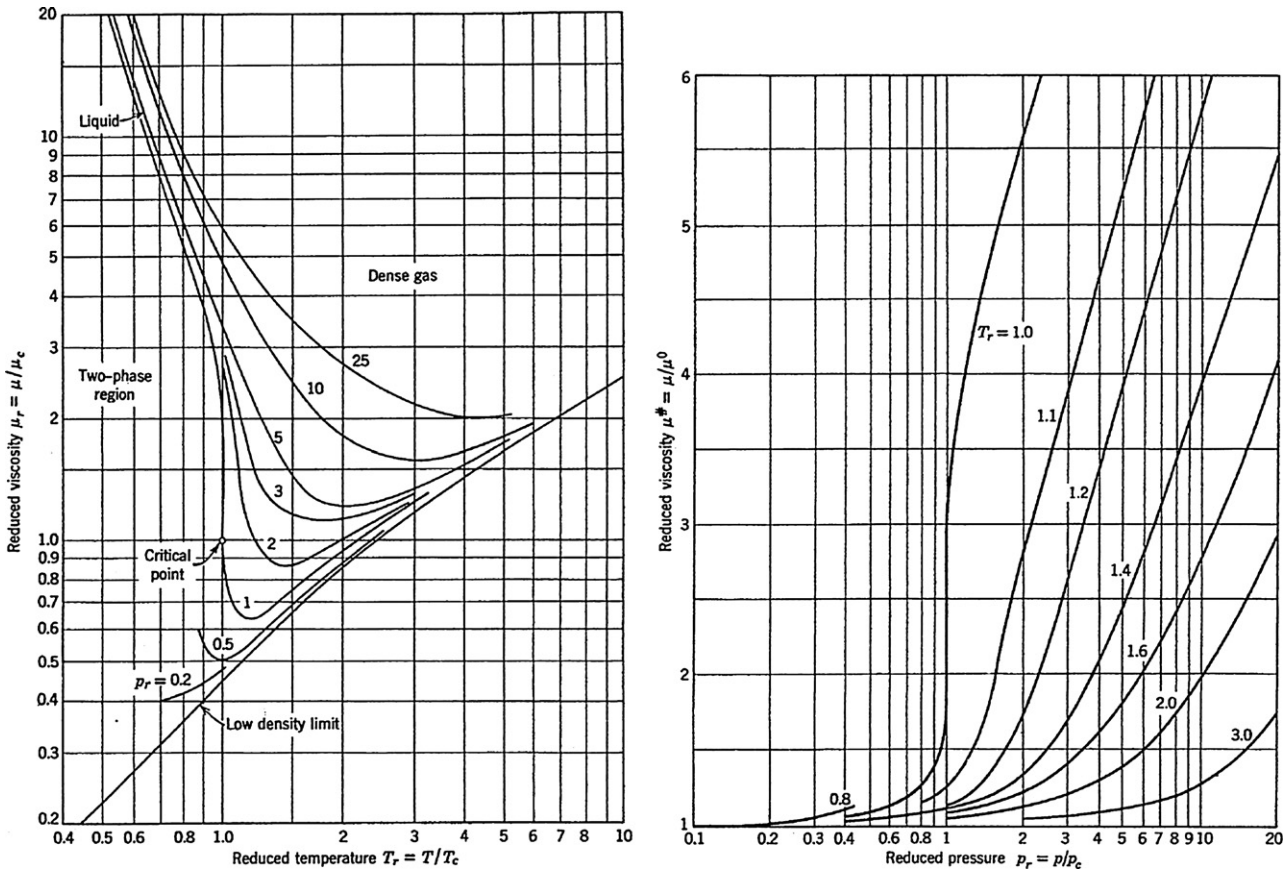

Fig. 12. Viscosity of fluids in the critical region. (a) Plot of the reduced viscosity, μ/μ_c (actually η/η_c) vs. the reduced temperature, at different reduced pressures [156]. (b) Plot of the second reduced viscosity, $\mu_\# = \eta/\eta_0$ (with η_0 viscosity under the atmospheric pressure) vs. the reduced pressure, at different reduced temperatures, T_c [157].

permeability of a bed is proportional to the square of the diameter of the particles with which the bed is packed. Therefore

$$K = k_0 d_p^2 \tag{28}$$

where k_0 is the specific column permeability, and d_p the average size of the particles packed into the column bed. The specific permeability of the packed beds used in liquid chromatography is of the order of 1×10^{-3} [1,144,145]. For no apparently good reason, chromatographers tend to prefer the use of $\phi = 1/k_0$ to characterize the specific permeability [1,146–148]. This is another deviance from the traditional definitions used in chemical engineering, which both illustrates and reinforces the estrangement between the two communities that still have much to learn from each other.

The specific column permeability is related to the column porosity through the Kozeny–Carman equation [142]

$$k_0 = \frac{\epsilon_e^3}{180(1-\epsilon_e)^2} \tag{29}$$

There is some uncertainty on the value of the numerical coefficient but since few authors report column permeability data, a systematic study has not been made yet. Note that the data of Neue [145] (see Table 4.2, p. 84) show that the particle size distribution has a significant influence on the column permeability, beside its influence on the column external porosity. This is further confirmed by recent data from the same author [149].

The microstructural details of the packing of chromatographic columns were studied by Tallarek et al. [150]. These authors studied the influence of the morphology of different types of packings of spherical particles and the corresponding flow patterns on the velocity profiles in these beds. Schure et al. used a complex 3-D calculation method to derive flow, dispersion, and the HETP in chromatographic columns [151]. Their method allows the study of the influence of varying the external porosity while keeping the packing random or of introducing defects in this random packing. Schure's study showed that the external porosity has little effect on the column efficiency as long as the defects are randomly distributed but that the systematic association of small defects (e.g., defects aligned in a direction parallel to the column axis) may cause major efficiency losses [152,153].

5.3. Viscosity of fluids

We need to distinguish between the viscosity of the mobile phase in the conventional low pressure range for gases, in the low or high pressure ranges for liquids and the viscosity of fluids in the subcritical, critical, and supercritical ranges. Under moderate pressures as those used in conventional HPLC, the viscosity of the mobile phase remains nearly constant. However, when the pressure exceeds ca. 300–400 atm, the viscosity of conventional liquids increases by a few percent (some times up to 5%) per hundred atm. In the critical region, however, the viscosity of fluids varies widely (see Figs. 10 and 12).

5.3.1. Viscosity of fluids around their critical point

A large amount of data regarding the viscosity of gases and liquids in a wide range of temperatures and pressures is available in the literature [6,154]. Two correlations based on the analysis of these data are available [142]. They are based on the corresponding-states approach [155]. Fig. 12 gives plots of the reduced viscosity, $\eta_r = \eta/\eta_c$ (note that the authors used μ as the symbol for the viscosity instead of η), as a function of the reduced temperature at constant reduced pressures (between 0.2 and 25) and of the

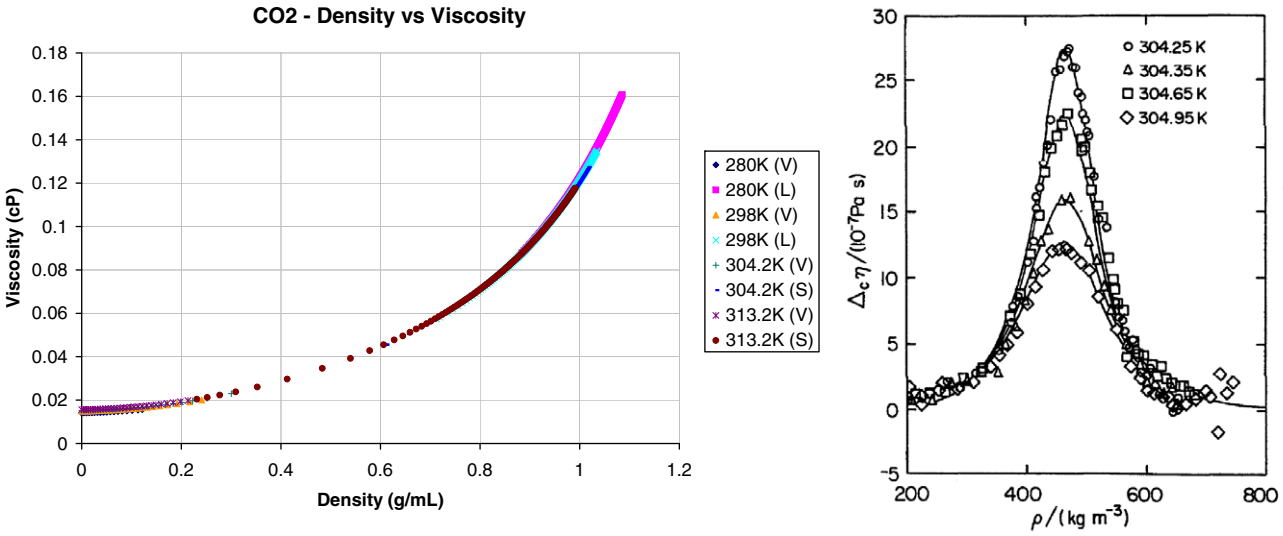

Fig. 13. Left: viscosity of carbon dioxide as a function of its density at different temperatures [162]. Experimental data [163] and curves calculated with Eqs. (37)[159]. The letters V, L and S in the brackets represent vapor, liquid and supercritical conditions achieved at different temperatures by varying the pressure. Right: the critical viscosity enhancement is significant but only in the critical region.

reduced pressure at constant reduced temperatures (between 0.8 and 3.0 [156]. It shows that the viscosity of a gas tends toward a limit when the pressure tends toward 0 at constant temperature. This limit is called the low-density limit of the viscosity. For most gases, the viscosity below pressures of a few atmospheres is equal to this limit. The viscosity of gases increases with increasing temperature while that of liquids decreases. For most vapors, experimental values of the viscosity, let alone the reduced viscosity are seldom available. They may be estimated using one of the following two correlations.

If the critical temperature, the critical pressure, and the critical density are known, the critical viscosity, η_c can be calculated from either one of the following two equations.

$$\eta_c = 61.6\sqrt{MT_c}(V_c)^{-2/3} \tag{30}$$

$$\eta_c = 7.70\sqrt{M}P_c^{2/3}T_c^{-1/6} \tag{31}$$

where η_c is in micropoise, P_c in atm, T_c in K, and V_c in ml/mole.

Fig. 12 shows a plot of the ratio $\eta^{\#} = \eta/\eta_0$ as a function of the reduced pressure and temperature, where η is the viscosity of the fluid at a certain temperature and pressure and η_0 is the viscosity under atmospheric pressure and at the same temperature [157]. Knowing the critical temperature and pressure of a fluid it is possible to derive an estimate of $\eta^{\#}$ for a fluid from this figure. Since the determination of the viscosity of a fluid under atmospheric pressure is usually possible [158], η can be calculated from $\eta^{\#}$. The prediction of the viscosity of gases under low pressures has been thoroughly discussed [6,142]. Reasonable results are achieved for those gases, the molecules of which are neither elongated nor strongly polar.

One way of expressing the fluid viscosity in the dense phase region as a function of its states can be [159]:

$$\eta(P,T) = \eta_0(T) + \Delta\eta(P,T) + \Delta_c\eta(P,T) \tag{32}$$

where $\eta_0(T)$ is the low density limit of viscosity (see above) at temperature T, $\Delta_c\eta(P,T)$ is the contribution of the critical phenomenon on the viscosity, and $\Delta\eta(P,T)$, which is called the excess viscosity [159] or, sometimes, the residual viscosity [160], represents all the other molecular interactions in the dense phase. As the critical enhancement of viscosity is quite weak and restricted only to a limited region around the critical point [159], its contribution is often neglected. A convenient way of formulating viscosity equations is to write them in terms of the residual viscosity, $\Delta\eta(P,T)$, which suggests that the difference, between the viscosities of the dense phase and the dilute gas is approximately independent of temperature and can be expressed as a function of the density only [159,161], as:

$$\Delta\eta(P,T) = \eta(P,T) - \eta_0(T) = F(\rho_r) \tag{33}$$

where $\rho_r = \rho/\rho_c$ is the reduced density and η_0 the viscosity of the gaseous eluent under low pressure and at temperature T.

Fig. 13 confirms that the viscosity of a fluid, subcritical, critical or supercritical depends essentially on its density (which is admittedly a function of the pressure and the temperature), but depends little on the temperature alone. The experimental data of NIST [162], Iwasaki [163], and Pensado et al. [164] all lead to this same conclusion. Only minor fluctuations in the regularity of the plot are observed around the critical point (see Fig. 13, right). These fluctuations represent rather small variations of 3–7% that take place only near 304 K and quickly tend to zero beyond 305 K.

Another form of writing Eq. (33) is [6]:

$$\eta(P,T) = \eta_0(T) + \xi^{-1}F(\rho_r) = \eta_0(T) + f(\rho_r)\sqrt{M}P_c^{2/3}T_c^{-1/6} \tag{34}$$

The function $Ff(\rho_r)$ in Eqs. (33) and (34) can be derived using one of several correlations available in the literature. Those recommended by Reid et al. [6] are

- For a nonpolar eluent, the correlation of Jossi et al. [160]:

$$[(\eta-\eta_0)\xi+1]^{0.25} = 1.0230 + 0.233364\rho_r + 0.58533\rho_r^2 - 0.40758\rho_r^3 + 0.093324\rho_r^4 \tag{35}$$

  which is valid for $0.1 \le \rho_r \le 3.0$.
- For a polar eluent, the correlation of Stiel and Thodos [165]:

$$\log\{-\log\left[(\eta-\eta_0)\xi\right]\} = 0.6439 - 0.1005\rho_r \tag{36}$$

  which is valid for $0.9 \le \rho_r \le 2.2$.

The term ξ is expressed as $\xi = T_c^{1/6}M^{-1/2}P_c^{-2/3}$.

5.3.2. Viscosity of carbon dioxide

Vesovic et al. [159] have reviewed the literature for data regarding the viscosity and the thermal conductivity of carbon dioxide in

the gas and the liquid state and in the critical region. They showed that the excess viscosity in the critical region is given by

$$\eta^o(\rho, T) = \eta_o(\rho, T) + \Delta_c\eta(\rho, T) \tag{37}$$

with

$$\Delta\eta(\rho, T) = 5.5934 \times 10^{-3}\rho + 6.1757 \times 10^{-5}\rho^2 + 2.6430 \times 10^{-11}\rho^4 \tag{38}$$

There is only a slight enhancement of the viscosity around the critical point, as illustrated in Fig. 13[163]. This increase is less than 1% in the critical region [159].

5.3.3. Viscosity of fluids under low pressures

The viscosity of common gases under low pressures can be calculated with an excellent precision from the parameters σ and ϵ/k of the Lennard–Jones potential, using an equation derived by Kim and Ross [166]

$$\eta = \frac{16.64\sqrt{MT}}{\sqrt{\epsilon/k}\sigma^2} \tag{39}$$

where the energy ϵ is the characteristic energy or minimum of the $\psi(r)$ function of the potential energy of interaction between two molecules separated by the distance r. This equation leads to the following equation [6]:

$$\eta_0 = 26.69\frac{\sqrt{MT}}{\sigma^2\Omega_V} \tag{40}$$

where σ is the collision diameter or distance at which $\psi(r) = 0$.

$$\Omega_V = \frac{A}{T^B} + Ce^{-DT^*} + \frac{E}{FT^*} \tag{41}$$

with $T^* = kT/\epsilon$, k is Boltzmann's constant, and the numerical coefficients are $A = 1.16145$, $B = 1.14874$, $C = 0.52487$, $D = 0.77320$, $E = 2.16178$, and $F = 2.43787$. Sets of values of σ and ϵ^* for different compounds are found in the literature [6].

Vesovic et al. reviewed a large volume of literature and proposed the following equation for the low density viscosity of carbon dioxide (see Table 1 and Eqs. 3 and 4 in Ref. [159]):

$$\eta_0 = \frac{1.00697T^{1/2}}{f(T)} \tag{42}$$

where

$$f(T) = 0.235156 - 0.491266\ln\frac{kT}{\epsilon} + 5.211155 \times 10^{-2}\left(\ln\frac{kT}{\epsilon}\right)^2 + 5.347906 \times 10^{-2}\left(\ln\frac{kT}{\epsilon}\right)^3 - 1.537102 \times 10^{-2}\left(\ln\frac{kT}{\epsilon}\right)^4 \tag{43}$$

with $\epsilon/k = 251.196$ K. The deviations of the experimental data from the values calculated with this equation is less than 1% in 97 cases out of 100 [159].

For less usual gases, methods based on the combination of contributions from the different groups in a molecule are available, but less accurate [6,42]. Numerical values for the parameters of CO_2, N_2O, CHF_3, CF_3Br, and SF_6 are in the literature [6,42]. The pressure dependency of the viscosity of carbon dioxide is illustrated in Fig. 10.

As shown by Perrut, who listed them, the viscosities of the supercritical fluids used in SFC are of the order of 0.01 cP under critical conditions and of about 0.03 cP at the critical temperature but under a pressure four times the critical pressure [42] These values seem, however, to be somewhat underestimated, as can be noted in the graph of the viscosity of carbon dioxide as a function of temperature and pressure given in Fig. 12 or in the similar figure published by Lucas [167].

5.3.4. Viscosity of liquids

Considerable information is available on the viscosity of liquids in general [6] and on that of solvents used in liquid chromatography [1].

5.3.4.1. Influence of temperature on the viscosity. The viscosity of liquids decreases with increasing temperature. The phenomenon has an exponential character, with a relatively low activation energy, of the order of a few kcal/mole. For examples, the viscosity of benzene decreases by one-half when the temperature is increased by 120 °C; in contrast, a temperature increase of only ca. 45 ° C (from ca. 20 to 65 °C) is sufficient to decrease the water viscosity of water by one-half.

5.3.4.2. Influence of the pressure on the viscosity. The viscosity of liquids increases slowly with increasing pressure (water is an exception below about 20 °C). For pressures below about 2000 atm, and for temperatures below $0.85T_c$, the increase is practically linear [6,168] and can be expressed as:

$$\eta = \eta_0[1 + \alpha\Delta P] \tag{44}$$

where η_0 is the viscosity under atmospheric pressure. Values of the coefficient α are of the order of 1×10^{-3} at room temperature. The deviation from linear behavior is less than 5% below 1000 atm. When the pressure increases from 0 to 200 atm, the viscosity increases by 10% for methanol and 25% for benzene. These changes cannot always be neglected in the computation of chromatographic dynamics [169]. An increase in the pressure, hence in the viscosity, results in an increase of the retention times compared to the times predicted for a mobile phase with a constant viscosity [170]. However, there is no change in the retention volumes. In situations in which more accurate values are needed for the pressure dependence of viscosity, Reid et al. provide a more complex expression [6].

5.3.4.3. Influence of the mobile phase composition on the viscosity. The viscosity of solutions depends markedly on their composition. In preparative chromatography, the viscosity of concentrated sample solutions may be quite different from that of the pure mobile phase. Numerous models have been proposed to calculate the viscosity of liquid mixtures from the viscosity of their pure components. These models rely on interpolation. As is often the case, mixtures of components which can exhibit intermolecular hydrogen bonding, especially aqueous solutions must be considered separately.

The most recommended method for the calculation of the viscosity of mixtures is the Grunberg–Nissan equation [171]. Although it has only one constant, this equation is accurate for nonaqueous solutions. It gives the viscosity of low-temperature liquid mixtures as

$$\ln\eta_m = \sum_i x_i\ln\eta_i + \sum_i\sum_j x_ix_jG_{ij} \tag{45}$$

where η_i and η_m are the viscosities of the pure compounds i and of the mixture, respectively, and x_i is the mole fraction of component i. The interaction parameter, G_{ij}, is a mild function of temperature (i.e., a linear, not an exponential, function of T). It depends on the nature of the pure components i and j ($G_{ii} = 0$). The constant G_{ij} can be determined from experimental data. In the case of binary mixtures, it can be calculated using a group contribution method [6]. In many cases, however, the excess term in Eq. (45) is ignored, and this equation becomes identical to the one proposed by Arrhenius in 1887 for binary mixtures:

$$\ln\eta_m = x_1\ln\eta_1 + x_2\ln\eta_2 \tag{46}$$

The results obtained with this equation might not account exactly for the behavior of a particular mixture, but they seem to give an excellent approximation of the dependence of the mobile phase viscosity on its composition, provided the reduced temperature (T/T_c) is below about 0.7 [6]. Li and Carr [172] have shown that the viscosity data of mixtures of water and methanol or acetonitrile [158] are not well accounted for by the Grunberg–Nissan equation [171]. Far better results were obtained with the following empirical equation where ϕ is the volume fraction of the corresponding component

$$\eta_m = \phi_{org}\eta_{org}\exp(\phi_{H_2O}\alpha_{H_2O}) + \phi_{H_2O}\eta_{H_2O}\exp(\phi_{org}\alpha_{org}) \quad (47)$$

In this equation, α_{org} and α_{H_2O} are two empirical constants. Both are functions of the temperature and are determined by fitting experimental data to this equation. Using this empirical equation, Li and Carr [172] obtained relative errors less than 10%. Note that the progressive changes in the profiles of the $\eta(T)$ curves with decreasing temperature for acetonitrile/water mixtures is probably explained by the formation of water-rich and ACN-rich clusters of increasingly large size with decreasing temperature [173].

5.4. Pressure drop along the column

The pressure drop along the column can be calculated numerically by integrating Eq. (27) between the column inlet and outlet, using the equations derived in Sections 6 and 5.3.1. The application of these equations requires knowledge of the physico-chemical characteristics of the eluent. These include the critical temperature, pressure and density, and its viscosity in the gas phase at low pressure. Many of these parameters are available in the literature, particularly for the most common eluents [6]. However, the data provided by different authors for the same compounds may sometimes be inconsistent. Furthermore, while abundant data are available for pure eluents, the determination of these important parameters for mixtures of solvents, such as those used in most actual applications of SFC, is not straightforward.

The local pressure gradient in an SFC column can also be expressed by [174]:

$$\frac{dP}{dz} = -\beta\frac{(\rho u)\eta}{\rho} \quad (48)$$

with ρ the local density of the mobile phase, u its interstitial velocity (with the continuity equation expressed as $d(\rho u)/dz = 0$), η its viscosity, and β an empirical parameter depending on the characteristics of the column used. Since the product ρu is constant along the column, this equation is equivalent to Eq. (27). Eq. (48) and the continuity equation must be closed with a suitable equation of state.

Rajendran et al. used the Span and Wagner equation of state [175] to calculate the density profile along the column, while the viscosity was derived from the correlation of Fenghour et al. [176]. Actually, the accessible data are sets of mass flow rates of the eluent versus the inlet and the outlet pressure of the column. Rajendran et al. corrected for the pressure drops in the extra column volumes using the Blasius equation [174]:

$$\frac{dP}{dz} = -\alpha\frac{G^{7/4}\eta^{1/4}}{\rho} \quad (49)$$

where G is the mass flow rate of eluent and α is a numerical coefficient, which is constant for a given column and is independent of the operating conditions. It is obtained by fitting the pressure and mass flow rate data to this equation in the same way as the coefficient β in Eq. (48) was determined, and by conducting the same measurements with and without column. Rajendran et al. calculated the pressure drop across the column by subtracting the calculated pressure drops across the extra-column volume (using Blasius equation) from the measured values of pressure drop across the entire system. At 55 °C, the pressure drop along a 125 × 4 mm LiChrospher RP-18 (Merck, Darmstadt, Germany) column packed with 5 μm silica particles did not significantly vary when the outlet pressure was raised from 130 to 210 bar at constant mass flow rate. For a flow rate increasing from 0.3 to 1, to 5 cm^3/min, the pressure drop, $\Delta P = P_i - P_0$, increased from 0.1 to 4.5, to 32 bar. As expected, ΔP is much lower than what is typically reported in HPLC. The pressure drop contributions across the extra column volumes, which were quite significant, were corrected for and the maximum pressure drops reported were 12 and 21 bar for the inlet and outlet volumes [174].

5.5. Pressure and density profiles along the column

The pressure profile along the column can also be calculated following the same approach as for the calculation of the pressure drop, but by integrating Eq. (27) from the column inlet, where the pressure is known, till the distance z along the column. This provides the profile $P(z)$. The density profile can then be derived from the local pressure, using Eq. (66), itself derived from the numerical solution of Eq. (100) or, more generally, from any appropriate equation of state. All pressures must be corrected for the contributions of the extra-column volumes, using Eq. (49).

Baker et al. [177,178] have measured the profile of density of carbon dioxide in packed capillary columns by Raman spectrometry while elution of the analytes was monitored by laser-induced fluorescence. They found that initially the linear velocity of the mobile phase increases gradually to rapidly rise near the column outlet. However, the influence of this rapid velocity of the eluent on the retention of analytes is offset by the important loss of the solvating power of the mobile phase due to the pressure drop. This ultimately limits the speed of separation [177].

5.6. Hold-up time and volume

The hold-up time that is measured for a column is the sum of two terms, the true column hold-up time and the contributions of the extra column volume of the instrument, i.e., the residence time of compounds in the extra-column volumes of the instrument. The latter is due to the time taken by a band to transit through the injection device, and the connecting tube to the column, and the connecting tube from the column exit to the detector and the detector cell. Each of these devices is connected through union connectors that add volume and contribute to additional band spreading. For all the fundamental studies, these contributions must be accounted for and subtracted from the value measured for the hold-up time. In most applications, these contributions are often neglected, with little practical consequences.

The extra-column volume is typically measured by replacing the column with a zero-volume connector. The true hold-up time of the column is obtained subtracting the hold-up time measured without the column from the one measured with the column. In HPLC these measurements are simple. In SFC, they may be more complex if the pressure drop along the column is large enough for the mobile phase density to vary along the column and cause a significant influence of the pressure on the apparent hold-up volume. To avoid this source of error in the determination of the extra-column volume of the instrument, or at least to mitigate it, the zero-volume connector used should have a permeability comparable to that of the column so that the average pressure in the extra-column volumes that are upstream and those that are downstream the column be the same when the column is replaced by the connector are fitted to the instrument. This requirement is far more difficult to meet satisfactorily in SFC than it would be in HPLC.

When the density along the column does not vary significantly, the true hold-up time is calculated as

$$t_0 = \frac{\epsilon_T S}{Q} \tag{50}$$

where ϵ_T is the total bed porosity, S the column cross-section area and Q the volumetric flow rate. For SFC, however, as the density may significantly vary along the column if the pressure varies, the hold-up time is calculated by integrating the corresponding differential equation from $z = 0$ to $z = L$ [174]

$$t_0 = \int_0^L \frac{dz}{u(z)} \tag{51}$$

with $u(z) = G/(\epsilon_T S \rho(z))$, where G is the mass flow rate of the mobile phase, which is constant. The value of the mobile phase density in the equation, ρ, can be obtained from the equations discussed earlier. Because ρ depends on the local pressure, it varies along the column. So, unless the pressure drop along the column is small, the hold-up volume of the column depends indirectly on the flow rate, through the density hence the pressure gradient along the column. A similar effect was observed, measured, and corrected for in HPLC [168,179], a case in which the mobile phase compressibility is lower than in SFC, but the column pressure drop is much higher. Lübbert et al. reported a negligible pressure dependence of the hold-up time corrected for mobile phase compressibility for Nucleosil and a small but significant one for Kromasil [180].

If the pressure drop is small, an approximation is

$$t_0 = \frac{L}{u(\bar{\rho})} \tag{52}$$

where $\bar{\rho}$ is the average density between the inlet and the outlet of the column. In these calculations, it is generally assumed that the column is isothermal, which is not always the case. While calculations suggest that the pressure drops and the flow rates typical of SFC may often be insufficient to generate significant frictional heat in the column, the rapid expansion of the mobile phase during its migration through the column is endothermic and, at least under experimental conditions close to the critical region, cools the column sufficiently to warrant attention [181–183]. Therefore, a study of this effect using the same methods as those used in HPLC [184–193] is warranted. However, relevant data are still missing regarding the performance of columns packed with fine particles (sub 2 μm particles) in SFC.

Measurements of the hold-up volume provide a convenient method to investigate the swelling of the stationary phase (polymeric particles, bonded polymeric films) in a supercritical fluid [194]. Figs. 14 compare measured values of the hold-up times and those calculated with the Lee and Kesler EOS 6.4.

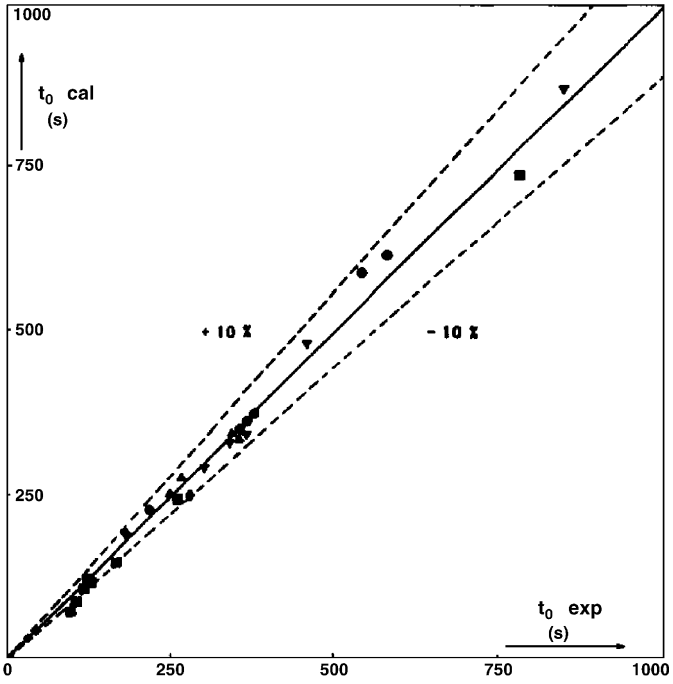

Fig. 14. Comparison between calculated and experimental column hold-up times. Eluent, CO_2. Column Hypersil 235 × 4.6 mm, tracer CF_3Br. Temperature • 40; △ 45; ▽. 50; ◊ 55; ■ 60 °C. [42].

5.7. Thermal effects in SFC columns

Efforts to improve the efficiency of modern columns and to perform faster analyses have lead manufacturers to develop the production of fine, now sub-2 μm, particles and to the production of columns packed with these particles. The columns packed with these particles exhibit a high efficiency and have a high optimum velocity for maximum efficiency. Columns packed with 1.7 μm particles are nearly twice more efficient than those packed with conventional 5 μm particles for a given length and deliver this efficiency almost three times faster, which provides another important gain. Furthermore, to achieve the same efficiency, a column one-third of the length is needed, which reduces the analysis time in a comparable ratio (in the same ratio in HPLC; in SFC, changing the column length at constant mass flow rate affects the density profile along the column, hence the local properties and their integrals along the column). A gain of nearly an order of magnitude in the analysis time at constant separation power is thus possible. Unfortunately, these gains are achieved only when the pressure gradient along the column remains moderate and the band broadening contribution of the instrument is small.

The cost of replacing particles by finer ones is the rapid decrease in the column permeability, because this permeability is proportional to the square of the particle size. If two columns of the same length are packed one with particles one-third the size of the other, the inlet pressure required to operate them at the same reduced velocity is 27 times larger for the first than for the second column (a factor 9 due to the smaller permeability and 3 due to the increased required velocity). This increase is considerable. If we keep the column efficiency constant, then the increase in inlet pressure is still an order of magnitude, corresponding to a threefold decrease in the analysis time (three times shorter column). Because tubes, valves, connectors that can operate under very high pressures must be made of high tensile strength alloys and carefully designed and manufactured, they are expensive. There are practical limits to the pressure that can be reached with instruments, somewhere between 1200 and 1500 atm, which is the range of pressures at which very high pressure liquid chromatography is currently performed for the analysis of low molecular weight compounds. The only possible escape to this pressure limitations would come from (1) the use of low viscosity eluents, which might render SFC more attractive than HPLC; and (2) the analysis of high molecular weight compounds, particularly that of biopolymers like proteins, in which case the column must be operated at lower actual flow rates, to compensate for the slower diffusion rate of these compounds.

The need to operate low permeability columns at high flow rates, under high pressure gradients causes unexpected, serious difficulties in both HPLC and SFC. The friction of the mobile phase against the bed through which it percolates generates heat, the power generated being proportional to the product of the pressure gradient and the mobile phase velocity. When this power exceeds a few W/mL, the loss of heat through the column wall causes a radial temperature gradient, itself a cause of radial gradients of viscosity,

velocity, and retention factors. These gradients combine to cause important loss of column efficiency [195–198]. Another source of thermal effects is the endothermic expansion of the mobile phase when its compressibility is important. This effect is negligible in HPLC, because the solvents used in this technique have a low compressibility, but it is important in SFC.

5.7.1. Expansion of the mobile phase along the column

Schoenmakers et al. [199] observed that the temperature along SFC columns is often not constant but decreases from the inlet to the outlet, due to the endothermal nature of adiabatic expansion [199]. The effect is more important for longer columns, for columns packed with smaller particles, for columns operated under experimental conditions closer to the critical state, and when the flow rate increases. They modeled the phenomenon by integrating numerically the heat balance equation, which provides pressure, density, and temperature profiles along the columns. The thermal effects were found to be small, particularly when 2 mm i.d. packed columns were used.

Rajendran et al. have shown that large efficiency losses take place when SFC columns are operated under significant pressure gradients, under such conditions that the compressibility of the mobile phase is important [200,201]. Good efficiencies were observed when the outlet pressure exceeded ca. 130 bar, meaning that the mobile phase was under clearly supercritical conditions, and the compressibility of carbon dioxide moderate. For lower values of the outlet pressure, poorly shaped peaks were recorded, low efficiencies observed, and the column performance drifted away from theoretical predictions [202].

Poe et al. [181,183,203] have demonstrated the importance of the thermal effects due to the cooling associated with the expansion of the mobile phase when columns packed with fine particles are operated in the critical region. since the compressibility of the mobile phase becomes very important in this region, its expansion is rapid when the mobile phase flow rate is large and the cooling causes the central region of the column to cool; heat diffuses from the column wall to its center, causing a radial temperature gradient and affecting the band migration (top chromatogram, critical density 1). Far from critical conditions, the compressibility of CO_2 is moderate, the cooling effect is small and the peaks are not considerably deformed (bottom chromatogram, critical density, 1.5). If the column is thermostated, the thermal gradient due to the cooling of the central region of the column causes a radial gradient of mobile phase viscosity, hence a radial gradient of mobile phase velocity and a radial gradient of the retention factor. The mobile phase velocity is higher along the column wall where the retention is also lower. This causes a significant broadening or even deformation of the elution peaks (see Fig. 15, top) and a rapid loss of efficiency (see Fig. 17 and, later, Section 8.4 and). The variation of the apparent retention factor is more complex to explain, as it results from the variations of both the pressure and the temperature (see Fig. 16 that illustrates the influence of the combination of these effects in the presence of heat effects due to viscous friction). If the column is thermally insulated (middle chromatogram), the loss of column efficiency disappears. However, the temperature decreases markedly from the inlet to the outlet of the column. The retention factors increase rapidly with decreasing temperature and with decreasing pressure. However, the concurrent cooling and expansion of the mobile phase tend to minimize its density change and to yield smaller change in the retention factor. Therefore, the temperature drop results in a decrease in k relative to the isothermal condition.

Far worse chromatograms than those in Fig. 15 were recorded with a similar column packed with the same stationary phase but with an average particle size of 3 μm. The peaks of the four alkanes were not completely separated due to a very long tailing. In contrast, the chromatograms eluted from a similar column packed

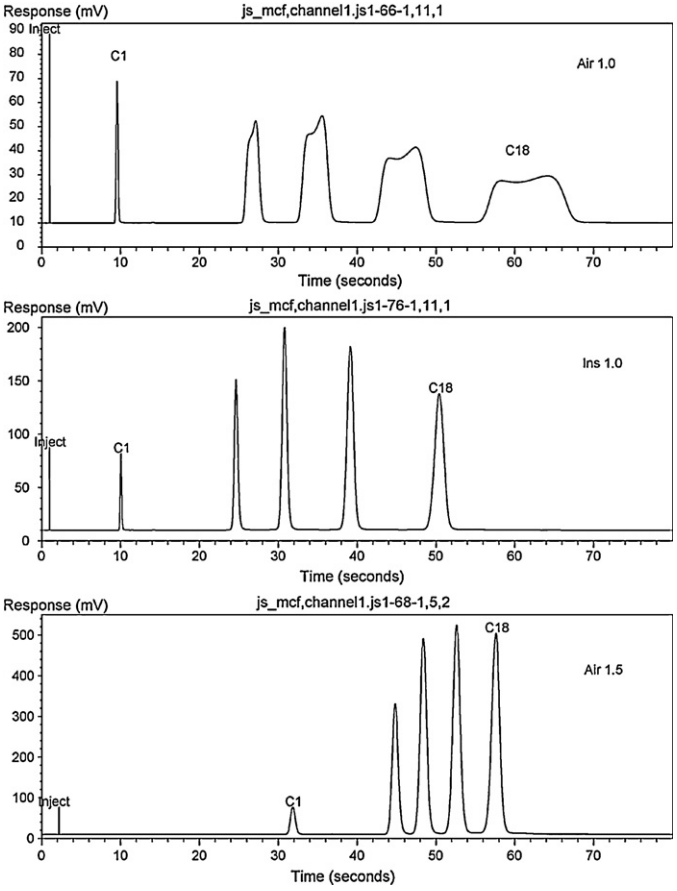

Fig. 15. Chromatograms of n-dodecane, n-tetradecane, n-hexadecane, and n-octadecane on a 2 × 150 mm column packed with 5 μm particles of Spherisorb C8 (Waters, Milford, MA, USA), eluted with CO_2 at 50 °C (T_c=1.07. Conditions, P_i bar, P_0 bar, F_v ml/min, ρ g/ml, ρ_c: top: 118.4, 93.5, 1.265, 0.47, 1; middle: 118.5, 93.5, 1.265, 0.47, 1; bottom: 155.9, 144.9, 0.492, 0.71, 1.50. Top, column in an air bath, significant radial heat loss, reduced density, 1.0. Middle, thermally insulated column, no radial heat loss, reduced density, 1.0. Bottom, column in an air bath, significant radial heat loss, reduced density, 1.5. [183] (Figs. 2.

with 10 μm particles exhibited good shapes and efficiency. Insulating the 5μm particle column provided a reduced HETP that was significantly higher than that of the 10 μm particle column (h_{min} ca. 2.0 and 2.5, respectively).

Poe and Schroden [183] measured the exit temperature of the column and showed that the column outlet can be more than 10 °C colder than its inlet when a column packed with fine particles is operated in the critical region (see Fig. 18). These authors wrote the energy balance for the column and qualitatively discussed its solution but did not provide numerical solutions. The approach followed is similar to the one used to handle the effects of viscous friction in VHPLC [197,198]. It provides similar results [204].

Considerable improvements in the column performance was achieved by insulating it [183]. This result confirms previous observations [181,182].

These thermal effects might have a significance in preparative SFC. Due to the low viscosity of carbon dioxide, fast mobile phase flow rates are used and the packing material tends to be made of finer particles than in preparative HPLC. Accordingly, a significant amount of energy is absorbed by decompression of the eluent. Although the density of energy absorbed per unit volume of column will most probably be markedly less than in the experiments of Poe and Schroden, the diameter of preparative columns is much larger than that of analytical columns, making heat transfer from the column wall to its center slower and increasing the radial thermal

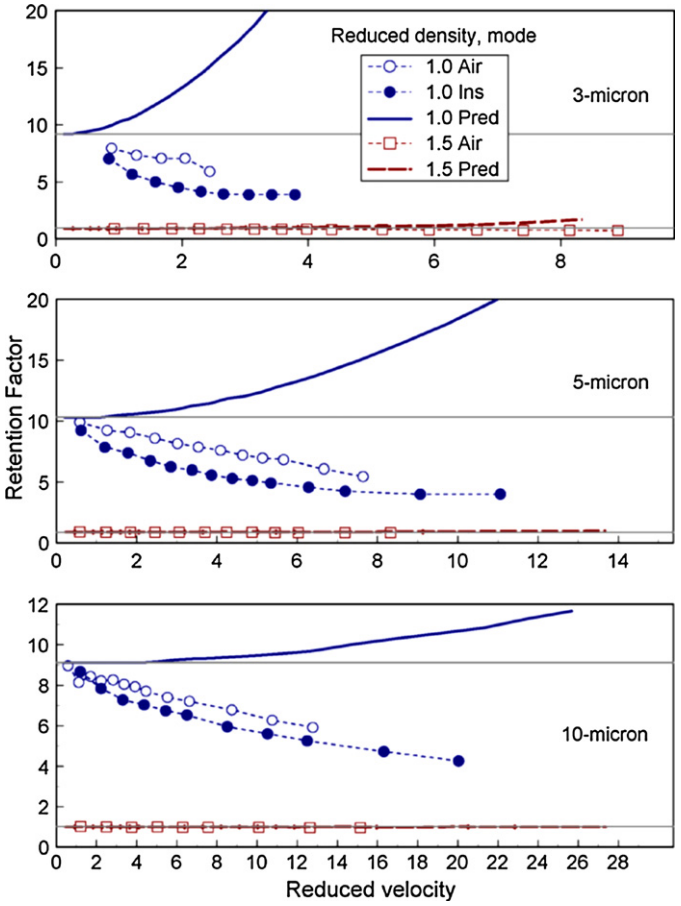

Fig. 16. Retention factor of n-octadecane on 2 × 150 mm columns packed with 3, 5, and 10 μm particles of Spherisorb C8 (Waters, Milford, MA, USA), eluted with CO_2 at 50 ° C (T_c = 1.07). Isopycnic elution (constant mobile phase density). [183] (Fig. 4).

gradient. It might even be possible that, under certain conditions (e.g., with a major leak of the mobile phase at the column exit), adiabatic cooling results in the freezing of carbon dioxide in the column, blocking the flow. These phenomena will make an interesting topics of investigations.

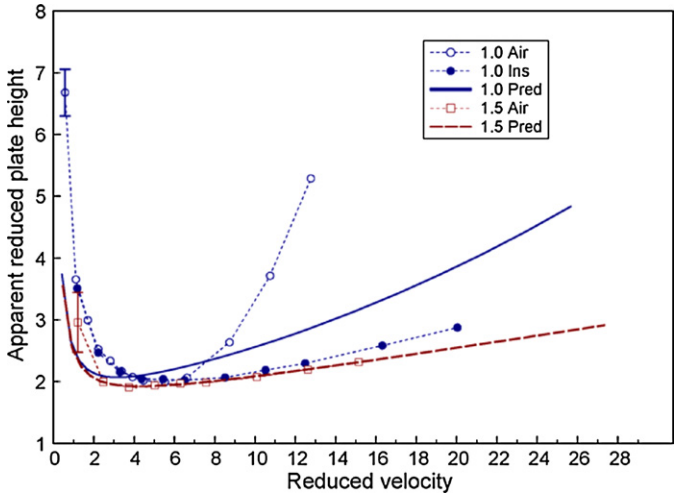

Fig. 17. Efficiency of n-octadecane on a 2 × 150 mm column packed with 10 μm particles of Spherisorb C8 (Waters, Milford, MA, USA), eluted with CO_2 at 50 ° C (T_r=1.07, ρ_r=1.0 and 1.50). Air: column in an air bath; ins: thermally insulated column; pred: calculated. [183] (Fig. 6).

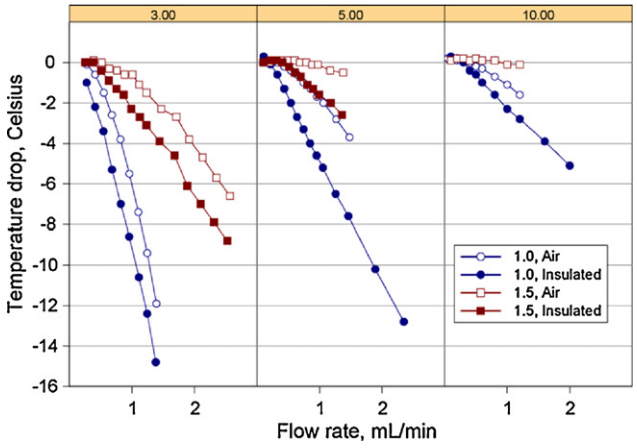

Fig. 18. Temperature drop along a column as a function of the flow rate. The data points along each curve report the temperatures of the approximately equidistant sensors glued along the column. Particle size (μm) at the top of each panel. Spherisorb C8 (Waters, Milford, MA, USA), eluted with CO_2 at 50 ° C (T_c = 1.07). Isopycnic elution (constant mobile phase density, with ρ = 1.0 and 1.5). [183] (Fig. 9).

5.7.2. Friction of the mobile phase against the packed bed

Thermal effects have become considerable in modern HPLC columns [195,198]. A major source of limitations in the use of long columns packed of fine particles and operated at high flow rates is in the large amount of heat generated by the friction of a stream of mobile phase percolating at high velocity, under a high pressure gradient, through a bed. Once generated everywhere in the column bed, this heat must escape. It does so by convection, the eluent exiting the column at the temperature higher than its temperature at column inlet, and by radial and axial conduction. Once steady-state condition has been reached, a radial and an axial temperature gradient are established across and along the column. As a consequence, the mobile phase viscosity and the solute retention factors are different everywhere in the column [205]. This has serious consequences for the overall retention times, the overall column efficiency and the shapes and resolution of the eluted peaks. The larger the amplitude of the axial gradient, the smaller the apparent retention factors and the time spent by a compound in the stationary phase. This only moderately affects the band profiles and reduces the resolution only insofar as the retention is decreased. The consequences of the radial temperature gradient are more harmful [206]. The band no longer migrates as if carried by piston flow. The part of the band in the center of the column, which is warmer than the wall region, moves faster because both the mobile phase viscosity and the retention factors are lower there than close to the wall. Kaczmarski et al. [197,198] and Gritti et al. [195,207] determined the origin and the fate of the heat generated in a RPLC column packed with 5 [197,198] and 1.7 [195,207] μm particles, calculated the temperature distribution along and across the column and its tube (see example in Ref. [208], Fig. 3), and the influence of the temperature heterogeneity on the column properties (see HETP plots in Ref. [209], Fig. 4).

Relatively small thermal gradients along and across the column were observed with conventional columns, at high flow rates, [196,205], leading us to predict a significant loss of column efficiency at high linear velocities, assuming no radial dispersion across the column [206]. In fact analyte molecules disperse radially through molecular and eddy diffusion, which limits the efficiency loss. We used the general dispersion theory of Aris [191] to assess the true column HETP by taking into account the trans-column heterogeneity due to the strong radial thermal gradients [195,196]. The calculated HETP curve is in fair agreement with experimental data [195]. This shows that the definitive solution of this problem requires the numerical solution of the coupling of the energy

balance and the mass balance equations for a chromatographic column [197,198]. When the column is insulated to reduce the radial heat loss and minimize the radial temperature gradient, its efficiency is close to that predicted by the HETP equation [195,210], but a strong axial temperature gradient occurs, meaning that the retention factor varies along the column. New equations relate the apparent retention factor derived from the experimental retention time to the equilibrium constant and the enthalpy of the retention process [211,212]. When the column is placed in a stream of fluid kept at a constant temperature, the axial temperature gradient is constant and so should be the retention factors. However, a radial temperature gradient is formed, with an amplitude that increases with increasing flow rate. Then there is a parabolic radial distribution of the eluent viscosity and a similar distribution of the solute retention factors and bands deform markedly during their migration [195,198].

Similar phenomena have rarely been reported in SFC. Most authors seem to consider that columns remain isothermal during their operation in nearly all practical cases. However, Rajendran et al. [201] reported a significant, systematic difference between the column efficiency measured with a back pressure of 130 bar and the average of those obtained at 150, 180, and 210 bar, particularly at low organic modifier concentrations (see Fig. 38a). This trend is similar to the one observed earlier with pure carbon dioxide as the mobile phase [174] and could be explained by the high compressibility of the supercritical mobile phase at moderate pressures (see Fig. 39). The expansion of the mobile phase along the column causes its cooling, resulting in axial and radial temperature gradients that may affect negatively the column efficiency [169,213]. This explanation is consistent with the behavior of the curve at a back pressure of 130 bar with 7% ethanol, since the compressibility of the mobile phase decreases with increasing organic modifier concentration and is much reduced with 7% ethanol. As the back pressure increases beyond 130 bar, the influence of the expansion of the mobile phase on the column efficiency decreases rapidly [201]. Recently, Poe demonstrated that, under certain experimental conditions, the cooling of the mobile phase resulting from its expansion causes most distorted elution profiles [183]. The importance of this phenomenon could become more serious if finer particles are used in SFC. Then, the combined influence of the heat friction and the eluent decompression may have to be understood.

5.8. Thermal conductivity of fluids

Thermal conductivity is a property that plays in the transport of heat a role equivalent to that played by viscosity and diffusion in the transports of momentum and mass, respectively [142]. In the context of HPLC, the role of thermal conductivity is significant only when the mobile phase and the column are at different temperatures, when the air around the column changes temperature rapidly [214] or when columns is packed with very fine particles are operated under high pressure gradients, exceeding ca. 100 bar/cm [169,195–198,213]. This is because standard HPLC operations can be considered as approximately isothermal, the heat of adsorption being small and practically negligible even under nonlinear conditions. This approximation served well in the development of theoretical studies of preparative chromatography [1]. In SFC, the temperature distribution can be quite heterogeneous along and across the column for two reasons. First, as in HPLC there can be heat generated by friction against the particles in the bed, when the mobile phase density is high and the column permeability low. Second, the adiabatic expansion of the mobile phase, as discussed in the previous two sections, absorbs heat and cools the column, sometimes considerably [182,183]. This obviously calls for a quantitative investigation of the influence of heat effects on column efficiency,

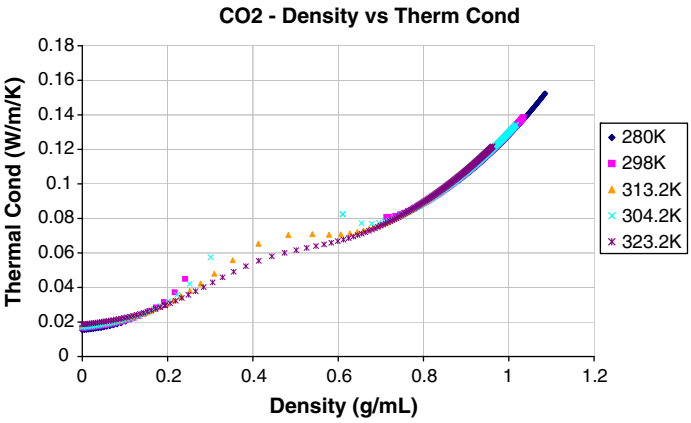

Fig. 19. Plot of the thermal conductivity of carbon dioxide as a function of the density, at different temperatures [162].

which requires the knowledge of the thermal conductivity of the mobile phase.

Fig. 19 shows that, like the viscosity, the thermal conductivity of carbon dioxide depends essentially on its density, rather than separately on the pressure and the temperature, except in the critical region, where a relatively high influence of the temperature is observed. At low and high densities, the curve is smooth, and the separate influence on the temperature is negligible. The comparison with the viscosity is impressive (see Fig. 13).

5.8.1. Thermal conductivity of gas mixtures

A fair estimation of the thermal conductivity, λ, can be made by using the corresponding states chart, shown in Fig. 20 (λ is shown as k in the figure). This chart, similar to the chart of viscosity shown in Fig. 12, provides estimates of the value of the thermal conductivity at a certain pressure and temperature, provided the critical properties, including the critical thermal conductivity, λ_c, of the compound of interest are known. Although this chart has been plotted based on experimental results for monoatomic substances, it can be used to generate approximate estimates for polyatomic compounds as well [142].

For more accurate estimation for the thermal conductivity of polyatomic gases, Eucken's equation [6] can be used.

$$\frac{\lambda M}{\eta C_v} = \frac{15R}{4C_v} + f_{int}\left(1 - \frac{3R}{2C_v}\right) \tag{53}$$

where M is the molecular weight, η the viscosity, C_v and $C_p = C_v + R$ the heat capacities at constant volume and pressure, respectively, and R the ideal gas constant. The Eucken equation decouples the contributions of the translational and internal energies, and assumes the coefficient for the translational energy contribution to be equal to 2.5 for the sake of consistency with the value for monoatomic gases. Eucken suggested to take $f_{int} = 1$ and the equation reduces to

$$\frac{\lambda M}{\eta C_v} = 1 + \frac{9R}{4C_v} \tag{54}$$

This assumption was challenged and other suggestions were made for the proper value of f_{int} [6]. The Eucken factor is nearly constant when temperature increases or rises slowly.

The thermal conductivity of gases depends on their pressure. Below ca. 10 bar it does not vary significantly, at most by 1% for each 1 atm increase in the pressure. This effect, which is often ignored [6], can be calculated by Eucken's and/or other related methods. At higher pressures, however, the thermal conductivity increases and is quite sensitive to pressure or temperature changes in the critical region. An excess or residual property approach, as adopted for the

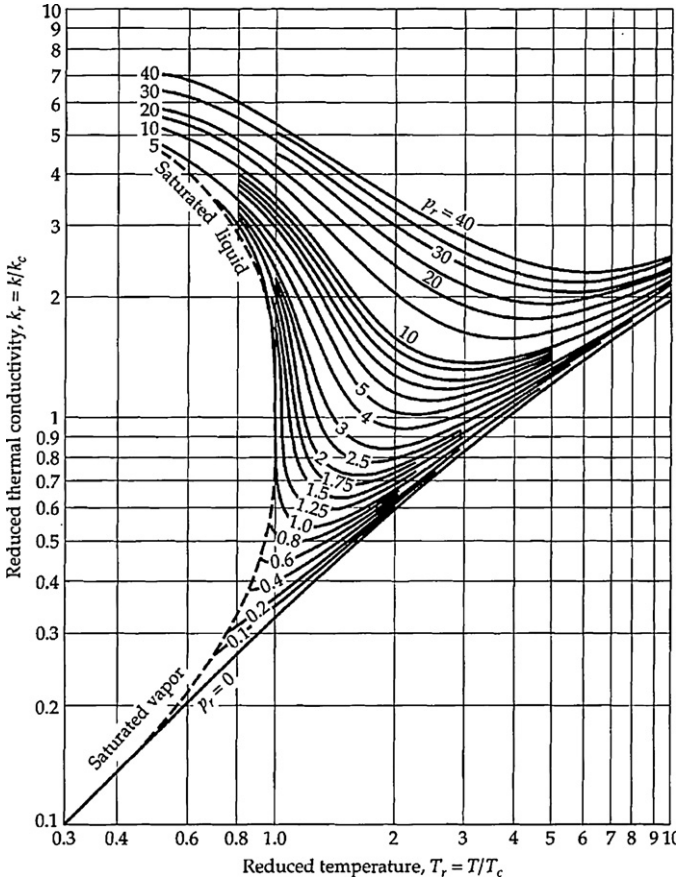

Fig. 20. Reduced thermal conductivity as a function of the reduced pressure and temperature.

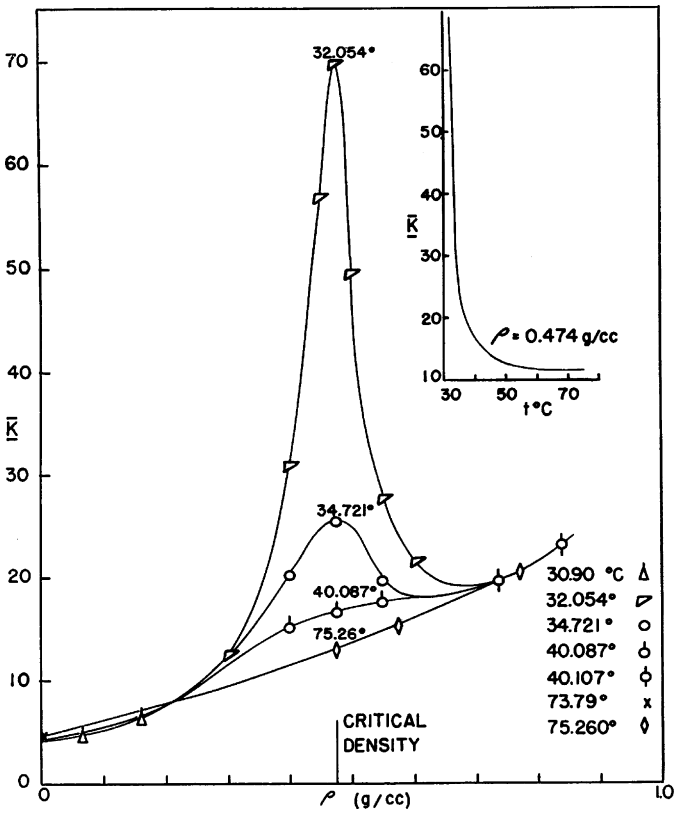

Fig. 21. Thermal conductivity of carbon dioxide near the critical point. *Reproduced with permission from L.A. Guildner, Proc. Natl. Acad. Sci.* 44 (1958) 1149–1289 © 2008 Wiley VCH.

viscosity estimation, can be employed for the thermal conductivity as well. It is expressed as [159]:

$$\lambda(P,T) = \lambda_0(T) + \Delta\lambda(P,T) + \Delta_c\lambda(P,T) \tag{55}$$

where $\lambda_0(T)$ is the thermal conductivity at low pressure but at the same temperature, $\Delta\lambda(P,T)$ is the residual or excess thermal conductivity and $\Delta_c\lambda(P,T)$ is the additional variation of λ near the critical region. Like in viscosity, there are some correlations that relate the excess thermal conductivity contribution as a function of the reduced pressure, ρ_r.

For polar substances Stiel and Thodos proposed the following correlation:

$$(\lambda - \lambda_0)\Gamma Z_c^5 = 1.14 \times 10^{-2}[\exp(0.67\rho_r) - 1.069] \tag{56}$$

valid for $0.5 < \rho_r < 2.0$. In this equation, the term $\lambda - \lambda_0$ is the excess thermal conductivity, while Z_c is the critical compressibility factor. The term Γ comes from the dimensionless analysis of thermal conductivity, similar to the way it was done for ξ and is expressed as $\Gamma = 210(T_c^{1/6}M^{1/2}P_c^{-2/3})$.

The accuracy of this approach, however, is doubtful and errors of ±10 to 20 percent are possible [6]. They may be due to the variation of the thermal conductivity, which, unlike that of viscosity, is quite significant in the vicinity of the critical region [215] and can be noted from Fig. 21. A more specific approach to address this issue was reported by Vesovic et al. [159], for the particular case of CO_2. Correlating a vast volume of thermal conductivity data on CO_2, he proposed the following functions:

$$\lambda_0(T) = \frac{0.475598T^{1/2}(1+r^2)}{F_\lambda(kT/\epsilon)} \tag{57}$$

with

$$F_\lambda\left(\frac{kT}{\epsilon}\right) = 0.4226 + 0.628\left(\frac{kT}{\epsilon}\right)^{-1} - 0.5387\left(\frac{kT}{\epsilon}\right)^{-2} + 0.6735\left(\frac{kT}{\epsilon}\right)^{-3} \tag{58}$$

$$-0.4362\left(\frac{kT}{\epsilon}\right)^{-6} + 0.2255\left(\frac{kT}{\epsilon}\right)^{-7} \tag{59}$$

and

$$\Delta\lambda(P,T) = 2.447 \times 10^{-2}\rho + 8.705 \times 10^{-5}\rho^2 - 6.548 \times 10^{-8}\rho^3 + 6.595 \times 10^{-11}\rho^4 \tag{60}$$

The expressions that are required for the derivation of $\Delta_c\lambda(P,T)$ are rather long. The reader is referred to their original source [159]. The above two equations are still useful for highly supercritical conditions. In the supercritical region, the thermal conductivity increases with increasing temperature at low pressure but decreases at high pressures, which is illustrated in Fig. 20.

5.8.2. Thermal conductivity of mixtures

There are methods to estimate the thermal conductivity of mixtures of gases under low pressures [6]. The recommended approach is the equation of Wassiljewa

$$\lambda_m = \sum_{i=1}^{n} \frac{x_i\lambda_i}{\sum_{j=1}^{n} x_j A_{i,j}} \tag{61}$$

where λ_m is the thermal conductivity of the mixture, x_i the mole fraction of component i, and $A_{i,j}$ a function given as

$$A_{i,j} = \frac{\left[1 + \left(\lambda_{tr,i}/\lambda_{tr,j}\right)^2 \left(M_i/M_j\right)^{1/4}\right]^2}{[8(1 + M_i/M_j)]^{(1/2)}} \quad (62)$$

where M_i is the molecular weight of compound i and $\lambda_{te,i}$ the monoatomic value of the thermal conductivity. However, it was shown that

$$\frac{\lambda_{tr,i}}{\lambda_{tr,j}} = \frac{\eta_i}{\eta_j}\frac{M_j}{M_i} \quad (63)$$

So, $A_{i,j}$ is the interaction parameter for gas mixture viscosity [6].

Estimation of the thermal conductivity of gas mixtures at high pressures can be done through the same correlation proposed by Stiel and Thodos (Eq. (56)) for pure compounds under high pressure conditions. For estimation of mixture properties, however, the terms in the equation should be converted to equivalent mixture terms from appropriate correlations [6].

5.8.3. Thermal conductivity of liquids

Like their viscosities, the thermal conductivities of gases are between 10 and 100 times lower than those of the corresponding liquids. However, their temperature dependence is much lower and is nearly linear, not exponential. For most organic solvents below their boiling point, λ is between 0.10 and 0.17 W/(m K) and the dimensionless number $M\lambda/R\eta$ is nearly constant and between 2 and 3 [6]. So, viscous liquids have a higher thermal conductivity than others. These comments do not apply to metals and highly polar liquids. The thermal conductivities of mixtures tend to be somewhat less than the mole or weight fraction average of those of their components [6].

5.8.4. Thermal conductivity of the chromatographic bed

The thermal conductivity of a porous medium impregnated with a liquid depends on its geometry, on its porosity, and on the thermal properties of the different components of the bed [142]. The mechanism of thermal conductivity is still poorly understood, which is why the thermal conductivity of heterogeneous systems is difficult to predict from the conductivities of its components. If the thermal conductivities in the solid and in the fluid phases take place in parallel, the effective conductivity should be the weighted arithmetic mean of the heat conductivities of the phases involved. In RPLC, there are three phases, the eluent (1) the alkyl ligands (2) and the silica skeleton of the particles (3):

$$\lambda_m = \epsilon_1\lambda_1 + \epsilon_2\lambda_2 + \epsilon_3\lambda_3 \quad (64)$$

where ϵ_i represent the volume fractions of the respective phases wrt the total column volume, and λ_i represent the thermal conductivity through these phases.

If the thermal conductivities take place in series, the thermal conductivity would be the weighted harmonic mean. Zarichnyak and Novikov [216] proposed for the thermal conductivity of a two-component heterogeneous system having a chaotic structure

$$\lambda_m = \epsilon_1^2\lambda_1 + \epsilon_2^2\lambda_2 + 4\epsilon_1\epsilon_2\frac{\lambda_1\lambda_2}{\lambda_1 + \lambda_2} \quad (65)$$

where indices 1 and 2 represent the mobile and the stationary phases respectively. This equation was used first to calculate the effective conductivity of the particles made of silica and of the C_{18} ligands, then the effective conductivity of the bed was obtained from the conductivities of the particles and of the eluent [198].

The thermal conductivity of the chromatographic bed is an important parameter in preparative chromatography due to the potential importance of heat transfer when the column temperature and the mobile phase or the sample are at different temperatures [214]. This is of particular importance if the column temperature must be set above ambient temperature, which is the normal case in SFC, if the mobile phase is not stored in the room where the column is operated, or when the expansion of the mobile phase is sufficient to decrease appreciably its temperature. In all these cases, knowledge of the thermal conductivity of the bed will be useful to estimate the consequences of the thermal effects and determine possible remediation.

6. Thermodynamics and the equations of state

Equations of state (EOS) are relationships that connect the pressure, the volume and the temperature of a given mass of a fluid. Depending on the accuracy of the measurements performed near the critical state, an accuracy that has markedly increased in recent times, the complexity of EOSs varies considerably. A sufficiently accurate EOS that relates the pressure and the volume of a mass of a dense gas at a constant temperature, may need five constants. Due to the great intricacy of the behavior of critical and supercritical fluids, these equations are complicated. To relate the pressure and the volume of a mass of a dense gas, a critical or a supercritical fluid at a constant temperature may need five constants. The temperature dependence of each of these constants may require three further further constants. There are several equations, however, which include only three or four constants and may account for the experimental results within ±1 to 2% of the observed values within a sufficiently wide range for the purpose of SFC. They make up in compactness what they lose in accuracy [217]. Obviously, scientists who pioneered in the study of the behavior of of gases throughout the critical region and under higher pressures, searched for simple but reasonably accurate equations because they had little calculation power. Now the use of complex equations with a large number of parameters and the identification of these parameters are easier.

Because the compressibility of liquids is generally so small, its consequences are negligible in HPLC, unless very high pressures are used [218]. The only major problem arose when some instrument companies attempted to develop syringe pumps at a time when suitable sensors, computers, and software were not available and they failed. Simple syringe pumps could not deliver constant flow rates [219–221]. Even when compressibility is not negligible, however, a simple two term expansion can account accurately for the behavior of the eluents. So, EOS are practically unknown in HPLC. In GC, a simple EOS is used but it is so common that its use is instinctive, it is the Boyle Mariotte law, which applies practically always because in the pressure range used in GC ($P < 5$ atm), common carrier gases behave as ideal gases.

In SFC, however, the fluids used as eluents are compressible and we need an equation to relate the pressure, the temperature, and the volume of a constant mass of gas, its EOS. The selection of the EOS used in SFC is most important because retention behavior is strongly related to the density of the mobile phase, which is provided by the EOS as a function of the directly measurable temperature and pressure. For practical reasons, the density of fluids in the critical region is often expressed as

$$\rho = \frac{MP}{ZRT} \quad (66)$$

with M the molecular weight, R the universal gas constant, and Z the compressibility factor, $Z = Z(P, T)$, which is given by the equation of state.

Many EOSs with varying degrees of accuracy and ranges of application have been proposed in the literature [222]. In this review, we note mostly the EOS of Peng and Robinson [81], of Lee and Kesler [92], and of Span and Wagner [175] which have been used in SFC [7,42,201,223–225] and the recent equation of Saeki [226]. Many early equations were reviewed and compared long ago [217,227].

The closer to the critical point of CO_2 are the experimental conditions and/or the larger the differences between the sizes and the molecular interactions of CO_2 and of the compounds to be separated are [227], the more complex the EOS needed in SFC. The complexity of the appropriate equations further increases when the use of mixtures of CO_2 and e.g., CH_3OH, 2-C_3H_7OH, or C_3H_8 as mobile phase modifiers is required, instead of a pure supercritical solvents such as CO_2. The critical temperatures and pressures of these fluids being quite different, the criticality of their mixtures is not always ensured under the chosen experimental conditions. This criticality is also most difficult to check, which is why users often neglect to do it. An assessment of the relative value of the equations of state based on experimental data corresponding to systems of importance in SFC appears to be very much needed.

6.1. The van der Waals equation of state

The basic assumption of this EOS is that fluid systems are made of incompressible spheres which attract each other with a force that is inversely proportional to the fourth power of their distance apart. This causes an attractive pressure which varies directly as the square of the concentration. The spheres having a finite volume, the gas may only occupy a volume smaller than the real volume available, as the centers of two molecules cannot come nearer than their common diameter. For one mole of fluid, it is written as

$$P = \frac{RT}{V-b} - \frac{a}{V^2} \tag{67}$$

The equation has only two constants, the parameters a and b, which can be directly calculated from the critical temperatures and pressures. Although it accounts sufficiently well in certain situations, the agreement between experimental data and Eq. 67 is not satisfactory at the high pressures considered in SFC. This is because it approximates the complex intermolecular interactions that take place under such conditions with an average effective field that is the same for all the molecules of the mixture considered [222].

6.1.1. The van der Waals compressibility factor

Efforts have been made to correct the shortcomings of the van der Waals model. Dou et al. pointed out that the parameter b in the van der Waals equation is a constant, which is independent of the fluid density, derived from results of the study of pair collisions [228]. However, when the pressure and the fluid density increase, so do the probabilities of simultaneous collisions of three or more molecules. Thus, the parameter b should decrease with increasing density. They suggested to write the equation as

$$P = \frac{RT}{V\left(1-\frac{b}{V}+0.2610\left(\frac{b}{V}\right)^2\right)} - \frac{a}{T^{1/2}V^2\left(1+\frac{b}{V}\right)} \tag{68}$$

where a and b are the van der Waals constants and V the molar volume. The equation obtained provides values of PV/NkT that are in good agreement with experimental results for ten compounds, water, ammonia, carbon dioxide, methane, ethene, ethane, propene, propane, benzene, and chlorotrifluoromethane, in a range of reduced pressures from 1 to 18 and reduced temperature from 1 to 7 for carbon dioxide.

6.2. The Reichsanstalt and the Leiden equations of state

Limited developments of the product PV in terms of P^n or ρ^n have been widely used in the past

$$PV = A + BP + CP^2 + DP^3 + EP^4 \tag{69}$$

$$PV = A + B\rho + C\rho^2 + D\rho^3 + E\rho^4 \tag{70}$$

The coefficients A, B, C, etc. are independent of the pressure in Eq. 69 and of the density in Eq. (70), with $A = nRT$ (n being the number of moles in the system) and B the second virial coefficient in Eq. (69). These equations are less used since Michels et al. demonstrated that these series do not converge at high pressures when the number of their terms is increased [5,229,230].

Values of the virial coefficients and their temperature dependence for over a hundred inorganic and organic gases, many of which could be used as critical fluids, are listed in the CRC Press Handbook of Chemistry and Physics [231]. Values of the van der Waals constants for many gases and vapors can also be found in the same handbook and in ref. [6].

6.3. The Dieterici equation of state

This equation seems to be more successful than other simple equations[232].

$$P = \frac{RT}{V-b} e^{-\frac{A}{RT^{3/2}V}} \tag{71}$$

where b has the same meaning as in van der Waals equation and A is an empirical constant. It can be shown that the critical parameters are

$$T_c = \left(\frac{A}{4bR}\right)^{2/3} \tag{72}$$

$$P_c = \frac{R}{b}\left(\frac{A}{4bR}\right)^{2/3} e^{-2} \tag{73}$$

$$\frac{RT_c}{P_cV_c} = \frac{e^2}{2} = 3.695 \tag{74}$$

The experimental value of R_cT_c/P_cV_c hovers around 3.98 [217]. With only two parameters, this equation accounts reasonably well for many experimental results. However, SFC needs a more accurate equation.

6.4. The Lee–Kesler equation of state

This three-parameter equation is quite complex but offers the following attractive features [7,92].

1. It covers a wide range of reduced temperatures ($0.3 < T_r < 4$) and pressures ($0 < P_r < 10$) ($T_r = T/T_c$, $P_r = P/P_c$ are the reduced temperature and pressure).
2. It applies to mixtures as well as to pure compounds.
3. All the coefficients of this equation are independent of the substances considered, whether those are pure compounds or multi-component mixtures (see Table 2).
4. It gives accurate results for a wide variety of compounds.

The Lee–Kesler equation is written

$$Z = \frac{pv}{RT} = \frac{P_rV_r}{T_r} \tag{75}$$

$$= 1 + \frac{B}{V_r} + \frac{C}{V_r^2} + \frac{D}{V_r^5} + \frac{c_4}{T_r^3V_r^2}\left(\beta + \frac{\gamma}{V_r^2}\right) e^{\frac{-\gamma}{V_r^2}} \tag{76}$$

where v is the molar volume and V_r is a reduced volume defined by

$$V_r = \frac{P_cv}{RT_c} \tag{77}$$

Note that $V_r \neq vV_c$, just because the fluid is not an ideal gas. In Eq. (75), the constants B, C, and D are given by:

$$B = b_1 - \frac{b_2}{T_r} - \frac{b_3}{T_r^2} - \frac{b_4}{T_r^3} \tag{78}$$

$$C = c_1 - \frac{c_2}{T_r} + \frac{c_3}{T_r^3} \tag{79}$$

$$D = d_1 + \frac{d_2}{T_r} \tag{80}$$

The parameters b_1, b_2, b_3, b_4, c_1, c_2, c_3, d_1, d_2, β, and γ have numerical values that are independent of the compound considered (see Table 2). However, there are two different sets of these constants, one for the "simple" fluids and the other one for the "reference" fluid. Eq. (75) is solved numerically with both sets and the actual compressibility factor of a real fluid is then expressed by

$$Z = Z^o + \frac{\omega}{\omega^r}(Z^r - Z^o) \tag{81}$$

where ω^r is the acentric factor, another numerical constant. For the reference fluid, it is given in Table 2. For simple fluids, it must be found in the appropriate literature.

6.4.1. The Lee–Kesler equation of state for mixtures

The pseudo-critical method of Prausnitz [94] was used to calculate the properties of mixtures using the Lee–Kesler equation of state [7]. This method has the great advantage that the mixture is treated as a pure compound in order to estimate a set of critical parameters (i.e., T_c, P_c, and ω). The numerical values of the constants in Table 2 remain valid and no new parameter is needed to account for molecular interactions. Although this method is empirical, it is justified by the excellent agreement observed between the values calculated and measured for numerous mixtures [7,233,234].

The main difficulty of this model is in relating the critical parameters of the mixture to those of its components. Several sets of rules were tested by Schoenmakers [7] who recommends the rules of Plöckner et al. [235] developed specially for the Lee–Kesler equation [92]. To apply these rules, the critical properties of the mixture components must be known. A binary interaction parameter, $\kappa_{1,2}$, is also necessary. This parameter depends on the components involved, which is the main inconvenience of the method. However, for ternary or more complex mixtures, only the set of binary parameters is needed.

Plöckner et al. suggested a correlation for different kinds of mixtures between $\kappa_{1,2}$ and the dimensionless parameter r defined as

$$r = \frac{T_{c,2}\nu_{c,2}}{T_{c,1}\nu_{c,1}} \tag{82}$$

with $\nu_{c,i} = Z_{c,i}RT_{c,i}/P_{c,i}$. For hydrocarbon mixtures, the correlation is

$$\kappa_{1,2} = -6 \times 10^{-4} r^2 + 0.042r + 0.94 \tag{83}$$

For the mixtures of carbon dioxide and hydrocarbons that are useful in SFC, an estimate would be given by

$$\kappa_{1,2} = 0.9 + 0.02r \tag{84}$$

When the temperature is remote from the critical temperature, the value of $\kappa_{1,2}$ has an important influence on the results of the calculations made with the Lee–Kesler equation, which suggests that it might be better to use an approximate estimate of $\kappa_{1,2}$ than to assume that $\kappa_{1,2}$ is close to unity [7]. However, when the temperature increases toward the critical temperature, the influence of $\kappa_{1,2}$ decreases.

The critical parameters of a mixture are calculated using the following equations

$$Z_{c,i} = 0.905 - 0.085\omega_i \tag{85}$$

$$\nu_{c,i} = \frac{Z_{c,i}RT_{c,i}}{P_{c,i}} \tag{86}$$

$$\nu_{c,1,2} = \frac{\nu_{c,1}^{1/3} + \nu_{c,2}^{1/3}}{8} \tag{87}$$

$$\nu_{c,m} = x_1^2\nu_{c,1} + 2x_1x_2\nu_{c,1,2} + x_2^2\nu_{c,2} \tag{88}$$

$$T_{c,1,2} = \kappa_{1,2}\sqrt{T_{c,1}T_{c,2}} \tag{89}$$

$$T_{c,m} = \frac{1}{\nu_{c,m}^{\eta}}\left(x_1^2\nu_{c,1}^{\eta}T_{c,1} + 2x_1x_2\nu_{c,1,2}^{\eta}T_{c,1,2} + x_2^2\nu_{c,2}^{\eta}T_{c,2}\right) \tag{90}$$

$$\omega_m = x_1\omega_1 + x_2\omega_2 \tag{91}$$

$$P_{c,m} = \frac{Z_{c,m}RT_{c,m}}{\nu_{c,m}} \tag{92}$$

where a value of 0.25 is recommended for the empirical constant η. Equations for the calculation of the critical parameters of the higher alkanes were given by Schoenmakers [7].

6.4.2. Conclusion on the Lee–Kesler equation of state

This equation was extensively used and studied by Schoenmakers [7]. The conclusions of this work can be summarized as follows

1. The Lee–Kesler equation is purely empirical. It accounts fairly well for a large number of experimental results. However, there is no guarantee of accuracy when this equation is applied to data obtained with a different solvent or families of solutes. Large errors always remain possible and careful investigation of the validity of the equation for any new system remains necessary.
2. Numerous values of the critical parameters and the acentric factors of chemicals are tabulated. When such values are not available, they should be measured or estimates derived.
3. The application of the equation to mixtures, the derivation of pseudo-critical parameters for mixtures, and the method of handling them are empirical and can give only approximate results of uncertain accuracy.
4. In all applications of the Lee–Kesler equation of state as in the applications of many other equations of state, the stationary phase is supposed to be incompressible and not to dissolve nor absorb the mobile phase, which might very well be quite approximate.
5. The vapor pressure of all solutes is considered to be negligible compared to the local pressure applied to the mobile phase.
6. The pressure applied to the system is constant and homogeneous. In chromatography, the pressure decreases along the column. The physico-chemical parameters of the eluent and the mobile phase being a function of the local pressure, the recorded results, retention time, column efficiency, are averages to be determined.

6.5. The Peng–Robinson equation of state

This equation was recommended by many authors [7,42,236]. It is written:

$$P = \frac{RT}{V-b} - \frac{a}{V(V+b)+b(V-b)} \tag{93}$$

with : (94)

$$a = 0.45724\frac{R^2T_c^2}{P_c}[1 + K_i(1 - \sqrt{T_r})]^2 \tag{95}$$

$$b = 0.0778\frac{RT_c}{P_c} \tag{96}$$

$$T_r = \frac{T}{T_c} \tag{97}$$

$$K_i = 0.37464 + 1.54226\omega - 0.26992\omega^2 \tag{98}$$

where ω is the acentric factor, which can be found in tables or may be calculated from

$$\omega = -\log P_{V_R} - 1 \tag{99}$$

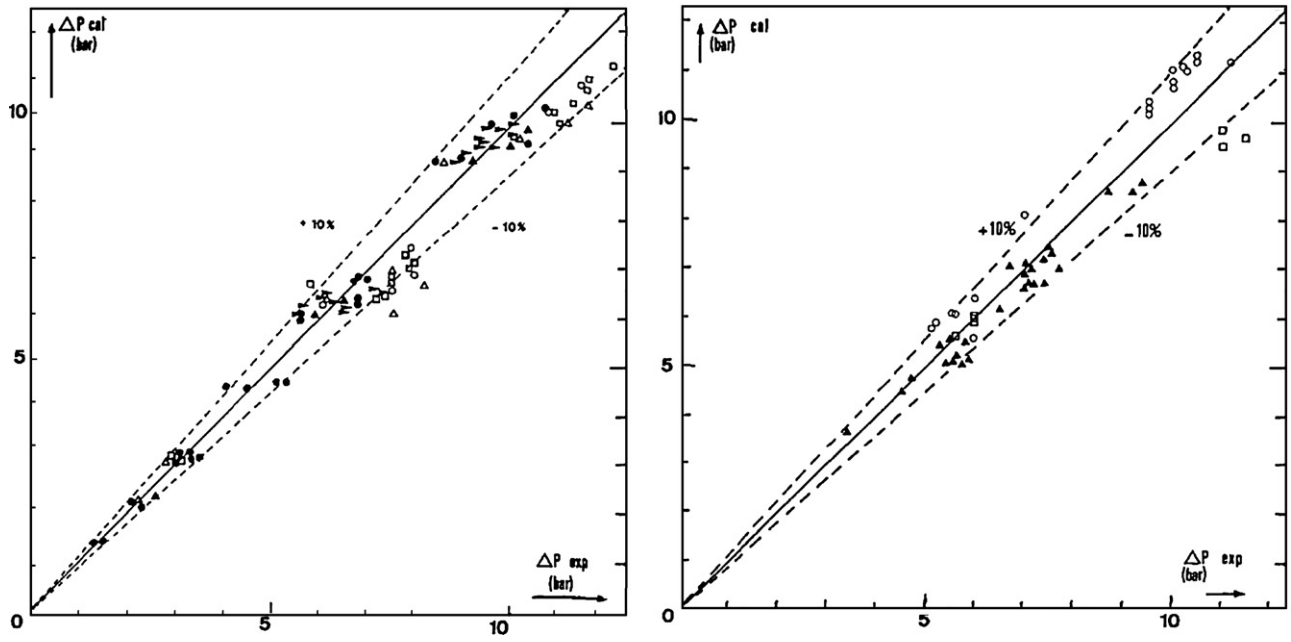

Fig. 22. Comparison between experimental pressure drops and those calculated with the Peng–Robinson equation of state [42,236]. (a) Eluent, carbon dioxide, two RPLC 300 × 4 mm columns packed with 10 μm particles of C_{18} silica. Temperature □ 20; ○, 25; △ 30; *, 35; ▷, 40; ◁, 45 °C. (b) ○, Eluent: CO_2; ▲, CHF_3; □, N_2O. *Reproduced with permission from M. Perrut, J. Chromatogr. A*, 658 (1994) 293–313, Fig. 3.

where P_{V_R} is the reduced vapor pressure ($P_{V_R} = P_v/P_c$) at a reduced temperature of 0.7 (i.e., at $T = 0.7T_c$.

The Peng–Robinson equation of state does not give an analytical expression for the volumetric mass, which must be calculated numerically. The easiest route is to derive Z as a numerical solution of the equation

$$Z^3 - (1 - B)Z^2 + (1 - 3B^2 - 21B)Z - (AB - B^2 - B^3) = 0 \qquad (100)$$

with

$$A = \frac{aP}{R^2T^2} \qquad B = \frac{bP}{RT} \qquad (101)$$

The density of the mobile phase is derived from Z and from its definition (see Eq. (66)). It should be noted that, like for many other equations of state, the results given by this equation are approximate and generally are more precise for supercritical than for subcritical fluids, even though the subcritical fluids used in SFC are liquids rather than gases. Fig. 22 compares the pressure drops calculated with the Peng–Robinson equation of state and the experimental results obtained. There is a general agreement but errors up to 10% are observed [42,236].

6.6. Empirical equations of state

6.6.1. The Span and Wagner equation of state

Besides the general equations of state listed above, a dozen specific empirical equations have been derived for carbon dioxide [175]. These equations are based on most of the experimental data regarding the behavior of CO_2 available at the time of their derivation. These equations suffer also from a number of drawbacks

1. Most state of the art data for the relationship between P, ρ, and V are not accounted for within their experimental uncertainty.
2. State of the art data on the liquid–vapor equilibria are not accounted for within their precision.
3. The calculation of thermal properties within the critical region yields unreasonable values.
4. Interpolation through regions in which data are limited or insufficient give unsatisfactory results.
5. Extrapolation of the equations to temperatures and pressures outside the ranges of available data often yields unsatisfactory values.

In an attempt to remediate this situation, Span and Wagner developed an equation of state which is explicit in the Helmholtz free energy [175].The consistent use of sophisticated fitting and optimization procedures allows the representation of the most accurate data within their level of accuracy.

The Helmholtz energy A is a function of the density, ρ, and the temperature. It is commonly given as the sum of two terms, one accounting for the behavior of an ideal gas, the other for the residual behavior of the fluid, with:

$$\phi = \frac{A}{RT} = \phi^o(\delta, \tau) + \phi^r(\delta, \tau) \qquad (102)$$

where $\delta = \rho/\rho_c$ is the reduced density and $\tau = T_c/T$ is the inverse of the reduced temperature. Since the Helmholtz energy is a fundamental thermodynamic property, it can be obtained by combining the derivatives of Eq. (102).

The Helmholtz energy of an ideal gas is given by the equation

$$A^o(\rho, T) = h^o(T) - RT - Ts^o(\rho, T) \qquad (103)$$

where h^o is a function of the temperature and s^o a function of the temperature and the gas density. Both functions can be derived from an equation for the heat capacity of the ideal gas. In contrast, there is no general equation for the residual part of the equation. A general procedure was developed to derive an empirical equation by using different series of data for different properties of the fluid [175]. This needed the use of a large bank of terms. Their coefficients were derived from a nonlinear fit of the experimental data. The final equation and its 42 numerical parameters are given in Ref. [175]. They are not reported here.

This equation was selected by Ottiger et al. [223]. It is valid for temperatures up to 1100 K and pressures up to 800 MPa. It accounts for all numerical series of measurements of data related to the equation of states within their level of accuracy.

Later, Span and Wagner [237–239] published an expansion of their early work [175]. Their work on CO_2 predictions numerous

properties of that fluid quite accurately because the functional form of the equations along with their coefficients were optimized to best fit only the set of experimental data available for CO_2 and because this set consists of an abundance of accurate data. In the extended work, they focused on the development of optimized functional forms that would be specific to certain groups of fluids (e.g., polar, weakly polar, or non-polar) rather than to any particular fluid like CO_2. They used simultaneously numerous data sets of different fluids, which enabled them to derive equations of state valid for a particular group. Now, such group-specific functional forms do not provide the best fit to the data for a particular fluid, but the best fit for the data for a particular group of fluids. The real advantage, as these authors pointed out, of having such group-specific optimized equations is that reliable EOS can then be developed easily for any fluid representing that group, even when sufficiently broad and detailed sets of experimental data are not available. Their simultaneously optimized EOS have characteristic features that are described in detail, which avoid the shortcomings of prior multiparameter EOS [237]. Substance specific parameters for nonpolar [238] and polar [239] fluids and comparisons with other results are also provided. A variety of alkanes, halogenated alkanes, ammonia and carbon dioxide are included. Span and Wagner discussed in detail the fitting strategy they developed to ensure applicability of these equations to a wide range of temperatures and pressures. The fitted equations have 12 terms, which are still fewer than contained in some other EOS, but they provide an increased accuracy. Understandably, if one wants to have an EOS for another fluid, e.g. methanol, although polar, a new set of coefficients is required, which was not reported. So although the new approach addresses a group of fluids, rather than a particular one, its applicability is still not as general as the Lee–Kesler one. Additionally, their approach does not mention anything regarding the properties of mixtures. Given their approach to develop different functional forms for polar and non-polar fluids, any effort to (equally) accurately estimate the non-polar–polar mixture properties through this approach, would be more than challenging. These limitations are most serious in SFC since this method uses frequently a wide range of modifier compositions.

Span and Wagner reported the coefficients for (a) non or weakly polar compounds, methane, ethane, propane, isobutane, n-butane, n-pentane, n-hexane, n-heptane, n-octane, argon, oxygen, nitrogen, ethylene, cyclohexane, and sulfur hexafluoride [238], and (b) compounds, (trichlorofluoromethane (CFC-11), dichlorodifluoromethane (CFC-12), chlorodifluoromethane (HCFC-22), difluoromethane (HFC-32), 1,1,2-trichlorotrifluoroethane (CFC-113), 2,2-dichloro- 1,1,1-trifluoroethane (HCFC-123), pentafluoroethane (HFC-125),1,1,1,2-tetrafluoroethane (HFC-134a), 1,1,1-trifluoroethane (HFC-143a), 1,1-difluoroethane (HFC-152a), carbon dioxide, and ammonia [239].

6.6.2. Saeki equation of state

Saeki derived an empirical equation of state from the fundamental equation of thermodynamics [226]:

$$G = U - TS \tag{104}$$

with respect to the volume, V, at constant temperature. This gives

$$P = -\left(\frac{\partial G}{\partial V}\right)_T = T\left(\frac{\partial S}{\partial V}\right)_T - \left(\frac{\partial U}{\partial V}\right)_T \tag{105}$$

Complex mathematical manipulations combined with thermodynamic relationships and some assumptions lead to the following equation

$$P = P^*(T) - a_k(T)Xe^{-X} - b_k(T)[X + c_k(T)]^4X \tag{106}$$

where P^* is the pressure under which $V = V_c$ at temperature T (pressure–temperature relationship along the critical isochore), $a_k(T) = 0$ at the critical point, and either $b_k(T) = 0$ or $c_k(T) = 0$, or $b_k(T) = c_k(T) = 0$ at the critical point; in this equation, $X = (V - V_c)/V$, and the subscript k indicates the gas phase when $V > V_c$ or the gas phase when $V < V_c$ and the temperature is below the critical temperature ($T < T_c$).

Calculations showed that the Saeki equation gives $P - V$ isotherms that are in very good agreement with the experimental data, with an accuracy that is comparable to those of the Benedict–Webb–Rubin and the Beattie–Bridgeman equations.

6.7. The elementary physical models

Elementary physical models (EPM) were proposed [240] and refined [241] to calculate thermodynamic properties of carbon dioxide and the density dependence of its dielectric constant and its structure. The EPM was initially proposed as a site-based intermolecular potential model for CO_2, using point charges and Lennard–Jones intermolecular interactions centered at each atom. This model predicts satisfactory values for the critical properties and the liquid–vapor coexistence curve. Simple corrections to the parameters of this first EPM model give a second model predicting the correct critical properties and curve [240].

The EPM approach requires a potential model of which there are two kinds, empirical models and models based on ab initio quantum mechanical calculations. The latter models suggest that the molecule of carbon dioxide is flexible and marginally nonlinear. Supercritical carbon dioxide would thus have a small dipole moment, a large quadrupole moment, and its dielectric constant would no longer be equal to unity. This nonlinearity concept was introduced in the EPM by Zhang et al. [241]. Numerical calculations using standard Monte Carlo simulations in the canonical ensemble demonstrated an excellent agreement between the experimental data for the pressure dependence of the density and the dielectric constant at 313, 333, and 353 K, particularly with the values derived from the model assuming a flexible carbon dioxide molecule.

Calculations show the formation of large molecular clusters under moderate pressures and a large inhomogeneity of the local density while the fluid is more homogeneous under high pressures. This suggests that the fluid structure at low density is controlled by attractive forces while at high density it is determined by repulsive forces. The T-shaped relative orientation of next neighbor molecules is dominant in the range of densities studied. This structure, the finite but small dipole moment, and the large quadrupole moment have a strong effect on the solubility of components in carbon dioxide.

Moelwyn–Hughes showed that the mean free path of a molecule is commensurate with its radius at the critical point. In contrast, the mean free path of a molecule is larger than its radius in the gas phase and it is smaller than its radius in the liquid phase [217]. This suggests that there should be a relationship between the critical point and the energy of interaction between two molecules. The relationship between the properties of critical fluids and this interaction energy is complex and still incompletely understood, which explains why there are so many equations of state, why they are so complicated, and why these equations have so many parameters.

6.8. EOS for mixtures

Several EOS, particularly the Lee and Kesler EOS provides good predictions of the P, V, T behavior of mixtures of similar compounds, and particularly of CO_2 and nonpolar compounds. Unfortunately, SFC uses mixtures of nonpolar (essentially carbon dioxide) and an organic modifier, which is polar (e.g., methanol, ethanol. acetonitrile). The Lee and Kesler EOS gives only approximate results

that are often too inaccurate for the needs of SFC. Because the molecules of polar compounds tend to associate easily, large statistical fluctuations of these mixtures form in the vicinity of the critical point, making accurate predictions difficult [242,243]. New equations based on the SAFT equation of state of Kiselev et al. [243] seem to be promising for binary mixtures involving CO_2.

6.9. Choice of an equation of state

There is no consensus yet on the best equation of state to use in SFC. Schoenmakers chose the Lee and Kesler equation [7]. Perrut chose the Peng and Robinson equation [42]. Brunner, Mazzotti and Rajendran [223], and Rajendran [201,224,225] preferred the Span and Wagner equation [175,180]. Unfortunately, there are few, if any, detailed comparisons made between these different equations, which makes a rational choice difficult. The Span and Wagner equation is certainly the most accurate but it is also much more complex. More importantly, this equation is applicable only for pure CO_2; it does not have any explicit mechanism to handle the EOS of a mixture. It is probable that the simpler Lee and Kesler and Peng and Robinson equations can often yield results that are sufficiently accurate for the needs of most SFC applications. Zhao and Olesik [139] were able to model the data that they had measured for the system methanol/trifluoromethane between 25 and 100 °C and between 1 and 340 atm, by using the Peng–Robinson EOS, with two temperature-independent binary parameters. The average relative standard deviation was 6% over the entire range of experimental conditions.

7. Retention mechanism in SFC

Fundamentally, the retention mechanisms are similar in SFC compared to GC and LC. There have been, however, numerous studies undertaken to develop an insight into the specific interactions of the solutes and the stationary phases, with the mobile phases, in the critical and supercritical regions [244]. Sie et al. [29] demonstrated that supercritical carbon dioxide is soluble in a coated liquid stationary phase. Janssen et al. [245] studied adsorption behavior of various compounds, typically used as modifiers in SFC, on octadecyl-modified silica. The mass isotope tracer pulse chromatography was used by Selim and Strubinger to investigate the adsorption of pure n-pentane in its critical region on SE-30 and SE-54, then its adsorption on the same polymers in the presence of methanol [246,247]. The excess amount adsorbed at equilibrium, increases with increasing pressure until a maximum is reached, beyond which it decreases [244].

This is a general result with excess isotherms of pure compounds, the excess isotherm or difference in concentrations between the adsorbed layer and the bulk fluid tends toward zero when the pressure increases indefinitely [248] Similar results were obtained by Yonker and Smith in the study of the adsorption of 2-propanol [244,249] and by Parcher and coworkers [250,251]. In SFC, the adsorbed phase is usually a layer of various organic materials (ligands, adsorbed organic modifier, or polymer chains) and adsorption of the solutes in the presence of the supercritical mobile phase is usually a competitive process. Additionally, some polymeric stationary phases shows significant volume change with sorption [252], which further complicates the problem. Mink et al. [253] demonstrated that certain solutes compete with methanol, used as a modifier with carbon dioxide, to access the active adsorption sites on silica in packed-column SFC. Springston et al. [254] used supercritical butane and carbon dioxide to study the swelling of the polymeric stationary phase, SE-30, in capillary SFC. They found that the expansion of the stationary phase with butane was much higher than that with carbon dioxide. Rajendran et al [252] developed a novel method to simultaneously measure the sorption of carbon dioxide on a polymer (poly-methyl-methacrylate) and the swelling of the polymer due to this sorption. Such interactions between the mobile phase and the stationary phase can substantially alter the chromatographic retention mechanism for SFC.

While modeling the retention behavior in SFC, however, all the specificity of such interactions can be lumped into the equilibrium isotherms, as is done for HPLC. The problems specific to SFC are essentially related to the consequences of the compressibility of the mobile phase under conditions near, below or above the critical point and how the pressure or density of the fluid affects the equilibrium constant of adsorption, or the partitioning coefficients. More precisely, these problems can be related to

1. The influence of the mobile phase density on the parameters of the equilibrium isotherms and particularly on the retention times and factors of analytes under linear conditions (Henry constant) and nonlinear conditions (saturation capacity).
2. The influence of the mobile phase density profile along the column on the mass balance equation of the sample components.
3. The competition for access to the adsorbent surface between the components of the sample and those of the mobile phase, mainly carbon dioxide and the organic modifier, generally methanol.
4. Effect of stationary phase swelling on the void volumes inside the packed columns.

7.1. The retention factor

The retention factor, k', which is generally used in linear chromatography to quantify the retention behavior, is the ratio of the number of moles of the solute attached to the stationary phase, to the number of moles in the mobile phase, at equilibrium. It is proportional to the initial slope of the isotherm or Henry constant, i.e., to the equilibrium constant of the compound at infinite dilution. In chromatography, the retention factor is often given by

$$k = \frac{t_R - t_0}{t_0} \tag{107}$$

where t_R and t_0 are the retention times of the compound considered and the hold-up time of the column, respectively. While this equation is straightforward, its interpretation raises different problems in GC, HPLC, and SFC. In HPLC, the mobile is practically incompressible, the retention factor is constant all along the column, and it is proportional to the equilibrium constant of the compound between the two phases of the chromatographic system. In GC and SFC, the mobile phase is compressible. So, the relationship is more complex. The value provided by Eq. (107) depends on the flow rate and the column length, so it is an empirical parameter of limited value. Most of the relationships used in HPLC that relate the retention factor to various thermodynamic properties no longer apply. The same situation arises in GC but the simplicity of the EOS used in GC permits a correction which has no equivalent in SFC.

Substantial work has been done to understand the retention behavior in SFC systems, where the main effort was to correlate the retention factor with state conditions like pressure and temperature, or to specific properties of the mobile phase e.g. density or fugacity, or the solubility of the solute compounds in the mobile phase. In the following paragraphs some of these studies have been discussed. Retention in SFC, however, is most easily understood as depending on the density of the mobile phase: the higher the density, the more soluble the solute in the mobile phase, the lower its retention. Increasing the pressure at constant temperature increases the mobile phase density hence decreases retention; increasing the temperature at constant pressure decreases the mobile phase density, hence increases retention. Increasing the

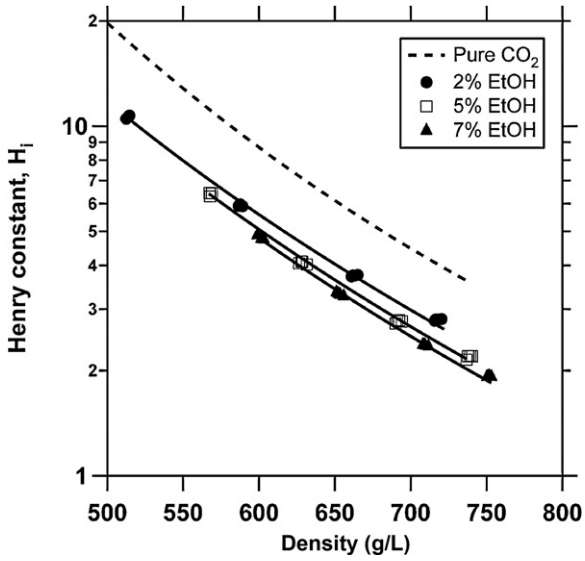

Fig. 23. Experimental points (symbols) and best calculated values (lines) of the Henry constant of phenantherene as a function of the CO_2 density [201], Fig. 3.

temperature at constant density affects retention slightly in most cases but the effect is not always negligible [199].

7.1.1. Influence of pressure and temperature on the retention factor

The retention factor of SFC not only depends on the temperature and the mobile phase composition, as in HPLC, but also on the pressure. The pressure dependence of SFC is through the influence of pressure on the density of the mobile phase and on the partial molar volumes of the solutes in the fluid and in the adsorbed phases. Reports on these influences are quite different and could appear at first glance as contradictory. Actually the opposite effects of the temperature and the pressure on the mobile phase density complicate the understanding of the adsorption behavior of solutes in the supercritical region [93]. How the retention factors of selected compounds vary with temperature and pressure is often reported [80,16] but few papers give their isobaric or isothermal adsorption equilibrium constants in a wide enough range of temperatures or pressures [16]. Fig. 8 (see Section 3.4 shows that the retention factor of naphthalene in carbon dioxide decreases rapidly with increasing pressure in the critical region (pressures between 65 and 90 bar) but far more slowly in the supercritical range, particularly at low temperature [7]. Figs. 33a–c (see Section 7.3) show the consistent, uniform decreases of the retention factor of phenanthrene with increasing mass flow rate of the mobile phase, hence average column pressure, and with increasing concentration of the organic modifier in the mobile phase, in the supercritical region [224].

Fig. 24 shows the retention factors of a few linear C_{10} hydrocarbons and of fluorene on two conventional GC stationary phases as a function of the pressure of carbon dioxide, the mobile phase, at 40 °C. At low pressures, the retention factors of n-decane, trans-decene, and 1-decyne decrease linearly with increasing pressure. At higher pressures, however, the curves exhibit a negative curvature, due to the rapid increase of their solubility in carbon dioxide with increasing pressure, which is consistent with the dependence of the retention factor on the mobile phase density (see later, Section 7.1.2 and Eq. (114)). The behaviors of the linear hydrocarbons and that of fluorene in Fig. 24 are quite different but they are consistent with the data for fluorene having been obtained in the supercritical region, where solubility increases quite slowly with increasing fluid density, while those for the linear hydrocarbons were acquired in the subcritical region, where solubility increases rapidly with increasing fluid density. The assumption that the behavior of fluorene might have been related to the phase diagram of the carbon dioxide - fluorene system not being a type 1 diagram (see Sections 2.1.3, 3.1, and 4.1) was not strongly supported [16].

Sandra, on the other hand, showed that the retention times and separation factor of a pair of enantiomers hardly changed when, at 40 ° C and constant flow rate (1 ml/min), the inlet pressure was increased from 100 to 200 bar (with a correspondingly increasing hydraulic resistance of the downstream restrictor needed to keep the flow rate constant) [64]. Similarly, the elution order of a mixture of caffeine, ibuprofen, theophylline, fenoprofen, flurbiprofen, cortisone, hydrocortisone, and prednisolone remained unchanged and the separation factors of these components were hardly affected when the flow rate of an analysis made on Zorbax RX SIL eluted with supercritical carbon dioxide and a 5.8–33% gradient of methanol was increased from 2 to 5 ml/min, with a fixed restrictor [64]. As pointed out by Sandra, this behavior is similar to that observed in NPLC.

7.1.2. Influence of the mobile phase density on the retention factor

Actually, the critical parameter that controls retention in SFC is the mobile phase density, which increases with increasing pressure and decreases with increasing temperature [199]. An inference of retention factor variation with temperature and pressure, without a reference to the density variation, may lead to contradictory views. When the pressure drop along the column increases significantly above a few bars, retention factors depend on the fluid density, whether the mobile phase is a dense gas or a critical fluid [66]. In SFC, the mass flow rate is constant along the column, as in gas and liquid chromatography, but the volumetric flow rate, and so the mobile phase velocity, vary along the column. Since retention factors increase with decreasing mobile phase density, they also increase with the migration distance [174]. The range of variations of retention factors in the critical region may exceed an order of magnitude, which is why SFC should better be conducted somewhat away from the critical region. As a consequence of the retention factor dependence on the migration distance, separation factors also vary. For small relative variations of the pressure, a linear variation can be assumed and a first order expansion written [255]

$$\rho = \rho_0(1 - \lambda_\rho \frac{d\rho}{dP}\Delta P) \quad (108)$$

where ρ_0 is the mobile phase density at the column inlet and λ_ρ a coefficient depending on the experimental conditions used. The influence of the mobile phase density on the retention and separation factors is given by

$$\ln k_i = \ln k_{i,0}(1 - \lambda_k \frac{d\rho}{dP}\Delta P) \quad (109)$$

$$\ln \alpha = \ln \alpha_0(1 - \lambda_\alpha \frac{d\rho}{dP}\Delta P) \quad (110)$$

To increase the flow rate, the pressure gradient along the column must be increased. This increases the amplitude of the gradient of mobile phase density, changing the average mobile phase density in the column and affecting the retention factors. Based on equation (109), Peaden and Lee [255] showed that if the inlet pressure, hence the inlet mobile phase density, is kept constant, the average mobile phase density in the column decreases because the outlet pressure must be decreased when the mobile phase velocity is increased. This decrease causes an increase in the average retention factors of all analytes and a larger increase in their separation factors [255]. To keep constant the retention factors or the separation factors of certain compounds, the average density of the mobile phase in the column must be kept constant, hence its density at the column inlet,

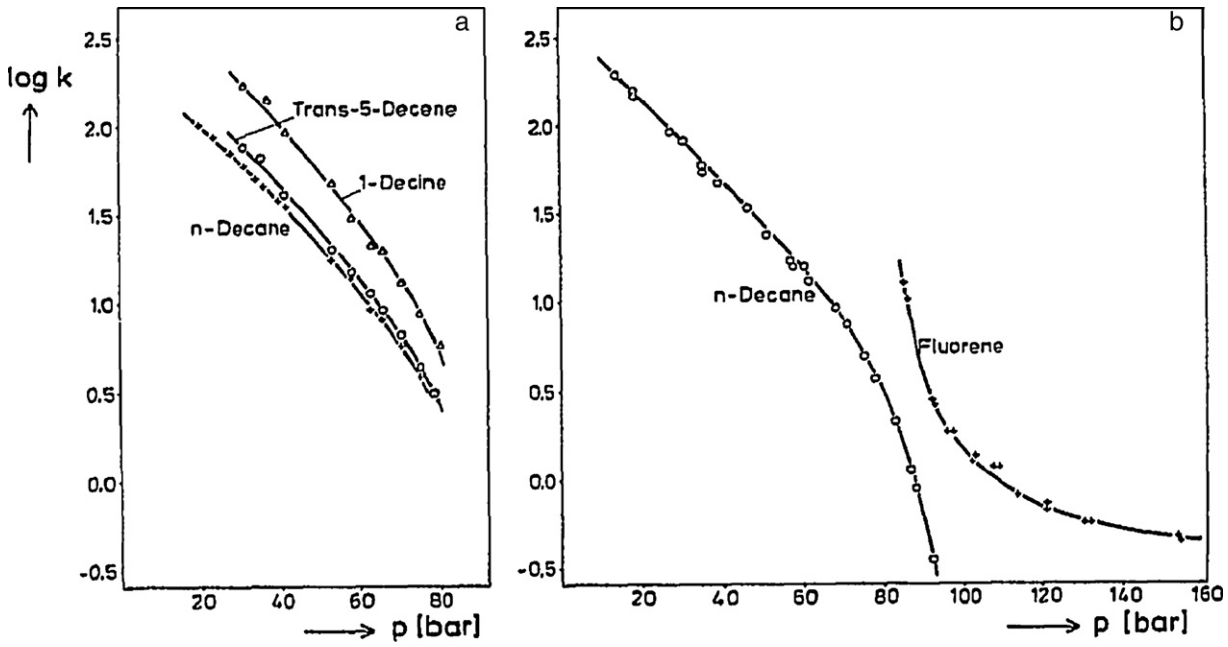

Fig. 24. Plot of the retention factor of some hydrocarbons as a function of the pressure [16]. Instead of decine, read decyne.

must be increased to compensate for its decrease at the column outlet. This will affect the column efficiency (see Eq. (130)). The intensity of these effects depends on the viscosity of the mobile phase and on the column permeability.

Based on the assumption of thermodynamic equilibrium between the two phases of a solute at infinite dilution, van Wasen and Schneider [256] demonstrated that [42,257]:

$$\left(\frac{\partial \ln \rho k_i}{\partial P}\right)_T = \frac{V_{i,ads} - V_{i,sol}}{RT} \tag{111}$$

where k_i is the retention factor of component i, $V_{i,ads}$ and $V_{i,sol}$ its partial molar volumes in the adsorbed phase and in the solution, respectively. Experiment and theory [97,256] agree to show that V_{sol} is proportional to the isothermal compression coefficient in the supercritical region, with

$$\frac{V_{i,sol}}{RT} = -\lambda\left(\frac{\partial \ln \rho}{\partial P}\right)_T \tag{112}$$

where λ is a coefficient depending on experimental condition. Now, if we assume that the molar volume in the mobile phase is much larger than the molar volume in the stationary phase, which is certainly true at moderate pressures but might become merely approximate at high pressures, Eq. (111) reduces to

$$\left(\frac{\partial \ln \rho k_i}{\partial P}\right)_T = -\lambda_i\left(\frac{\partial \ln \rho}{\partial P}\right)_T \tag{113}$$

which can be integrated to

$$k_i' = \rho^{-(\lambda_i+1)} f_i(T) \tag{114}$$

This equation shows that, at constant temperature, the retention factor decreases as a power of the increasing mobile phase density [42]. The applicability of such relation is explained in the next paragraph.

The isothermal variations of the retention factor for four hydrocarbons, as functions of the pressure, are shown in Fig. 25[256]. The experiments were carried out with conventional GC stationary phase and pure CO_2 as the mobile phase. The figure shows the retention factor decreasing by an order of magnitude with increasing pressure, mainly because of the rapidly increasing solubility of the samples in CO_2. It also shows an interesting temperature dependence of the retention factor. The amplitude of its variations increases substantially with increasing temperature, at the same operating pressure, indicating a decreasing solubility. The counteracting, and strongly nonlinear, effects of temperature and pressure variations on the solute retention can result into intriguing process conditions, mentioned earlier in this section. For example, the retention factor of decane is the same at two fairly different temperatures (30 and 40 °C) but at the same pressure (60 bar). Much simpler correlations can be derived when the same data is plotted against the mobile phase density (Fig. 26). Now the variations are mostly linear, and the slight nonlinear behavior can be predicted by Eq. (114).

More interestingly, retention factors decrease with increasing temperature at constant density, which possibly indicates a more familiar variation of the equilibrium constant, when the density variation is not playing any role. Similarly, Fig. 8 shows plots of the retention factor of naphthalene versus the pressure of carbon dioxide at three different temperatures, calculated using Eq. 123, with experimental data points in excellent agreement. The retention factor decreases steeply around the critical pressure, the closer the temperature to the critical temperature, the steeper this decrease (see Fig. 8). The dependence of the retention factor on the mobile phase density, however, is smoother [7]. The calculated curve is consistent with the experimental data of van Wasen et al. [13] (see data in the figure). Such considerations are particularly important in the context of the design of SFC operations. The possibility of a rapidly decreasing mobile phase temperature along and across the column due to mobile phase decompression, and at the same time, the possibility of an increasing mobile phase temperature due to flow frictions (see Sections 5.7.1 and 5.7.2), along with changing pressures and such complex relationships of the retention factor with the operating conditions, can offer both challenge and opportunities for process designers.

Kautz et al. measured the retention factor of benzene, and three symmetrical hexasubstituted benzenes, C_6F_6, C_6Cl_6, $C_6(CH_3)_6$ as a function of the density of the mobile phase (CO_2), at temperatures between 32 and 57 °C. They used three columns, a Nucleosil 100-5 porous silica and the same material bonded with C_{18} alkyl and 1-nitro-4-propyl-benzyl ligands [258]. They calculated the density of

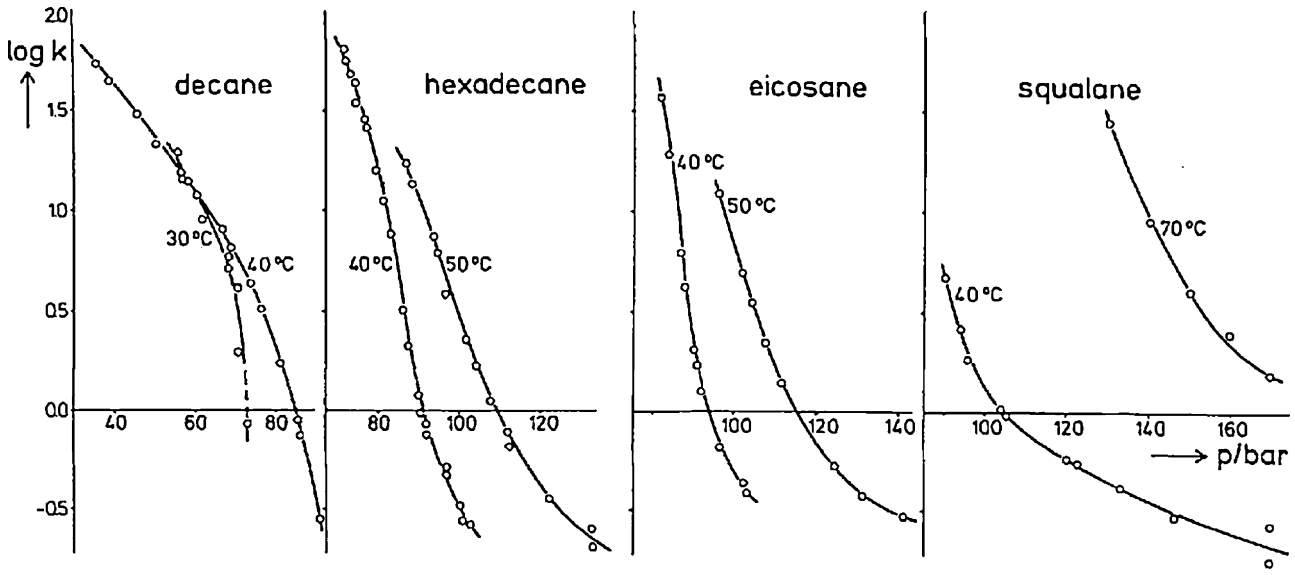

Fig. 25. Temperature and pressure dependence of the retention factors of alkanes [256].

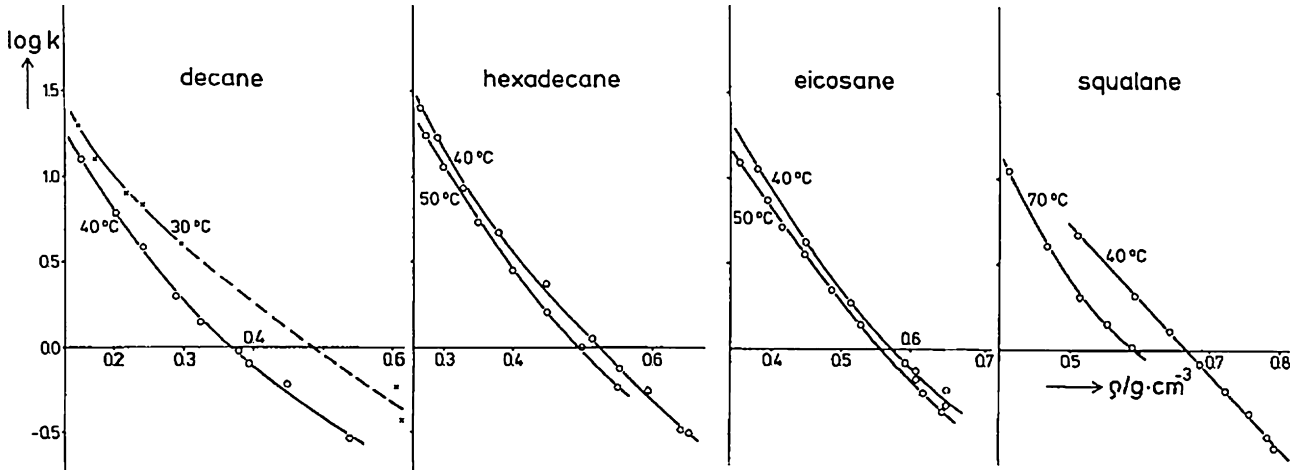

Fig. 26. Temperature and density dependence of the retention factors of alkanes [256].

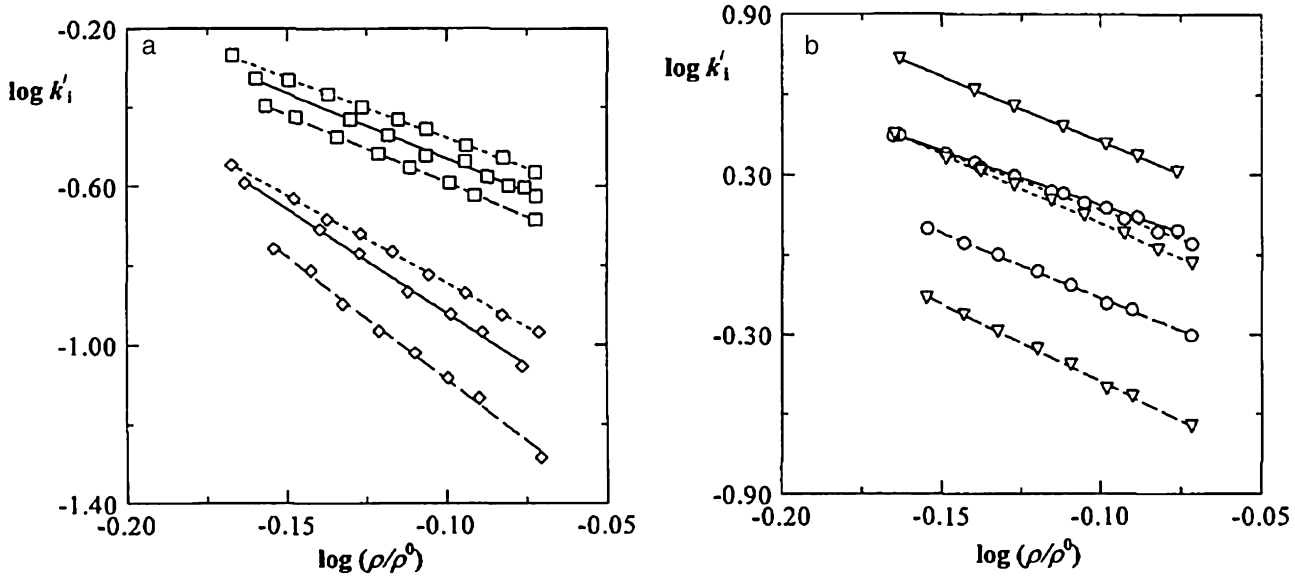

Fig. 27. Isothermal plot of log k versus log ρ/ρ_0 for ◊, hexafluorobenze; □, benzene; ○, hexamethylbenzene; ▼ [258]. Stationary phases: Nucleosil 100-5 (——), same material bonded with C_{18} alkyl (- - - -) and 1-nitro-4-propyl-benzyl-bonded silica (. . . .).

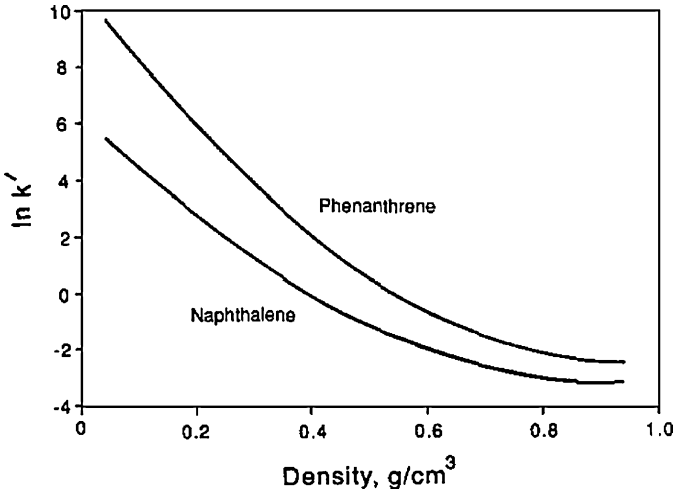

Fig. 28. Effect of the mobile phase density on the capacity factors of naphthalene and phenanthrene on a reversed-phase (octyl) silica at 40 °C. Data for naphthalene from van Wasen et al. [13] Data for phenanthrene predicted using Martire–Boehm equation [66].

carbon dioxide using the Span–Wagner equation of state (Section 6.6.1). The logarithm of the retention factors of all the compounds decrease linearly with increasing logarithm of the mobile phase density (see Fig. 27). The slopes are marginally affected by the nature of the substituents and by the stationary phase. The elution order of hexamethylbenzene and hexachlorobenzene on Nucleosil 100-5 NO_2 is reversed when the density of carbon dioxide (no additive) increases from 0.493 to 0.792 g/ml at 320 K [258].

Fig. 23 illustrates the dependence of the Henry constant of adsorption (proportional to the retention factor) on the density of the mobile phase (supercritical carbon dioxide and ethanol at 65 °C) and the concentration of organic modifier (ethanol) [201]. Fig. 28 illustrates the influence of the density of pure carbon dioxide on the retention factors of naphthalene and phenanthrene on a C_8-silica bonded phase [13].

There are reports that retention factors in SFC fit to a quadratic function of the mobile phase density much in the same way as in HPLC, where it depends on the volume fraction of the organic modifier in the mobile phase [7]. Van Wasen et al. [256] showed that retention factors can be fitted to the relationship

$$\ln k = 6.34 - 9.49\rho_r + 2.35\rho_r^2 \quad (115)$$

with ρ_r is the reduced density of carbon dioxide. This equation is consistent with the general relationship demonstrated by Martire et al. [259].

Finally, the dependence of the retention factor on the mobile phase density makes its local value most sensitive to the intense variations of this density with relatively small changes in the pressure and the temperature that are observed in the critical region. Fig. 16 illustrates these effects at a column temperature (50 °C) such that $T_r = 1.07$; with two mobile phase densities, 0.47 and 0.71 g/ml ($\rho_r = 1.0$ and 1.50). Due to the high compressibility of the mobile phase and its expansion along the column, the intensity of the cooling increases with increasing flow rate, causing a decrease of the apparent retention factor with increasing mobile phase flow velocity. Berger [260] measured the retention factors of several polynuclear aromatic hydrocarbons on neat silica, in a wide range of density of pure carbon dioxide (0.15–0.85) and showed that the variation of log k versus ρ is not linear; two quasi-linear plots are obtained below and above a density of ca. 0.4, with a significant difference between the slopes of the two plots. They suggested the formation of an adsorbed layer of carbon dioxide on the silica surface, the thickness of which increases progressively with increasing density.

Recently, Berger and Fogelman [261] showed how the retention pattern of a 22- compound mixture eluted with a two-ramp gradient varies at constant flow rate and column back pressure (150 bar) when the column temperature is increased from 20 to 70 °C. Numerous elution reversals take place. The authors stress the convenience of adjusting selectivity by setting the column temperature.

7.1.3. Retention factor and the mobile phase composition

Modern SFC is carried out with a complex mobile phase made of carbon dioxide, an organic or primary modifier and, frequently, an additive or secondary modifier. The relative concentrations of the secondary and the primary additives is often as large as one order of magnitude. Most second additives are too polar to be miscible to carbon dioxide in sufficiently large proportion but are soluble in the primary modifier and the ternary solution obtained by mixing carbon dioxide and the solution of primary and secondary modifier is stable. The additives affect the retention and the separation of sample components in several different possible ways: (1) being adsorbed on the stronger adsorption sites of the adsorbent surface, additives compete with sample components and reduce the polarity of the stationary phase; in so doing, they reduce the retention factors of the sample components; (2) additives are polar compounds that increase the polarity of the mobile phase, affect its solvating power, and increase the solubility of the sample compounds in the mobile phase; (3) additives may affect the degree of ionization of analytes and form ion-pair with them. It is often difficult to distinguish between these different modes of action and to tell which one is the most important. Carbon dioxide adsorbs strongly onto column packing materials, with a maximum near the critical conditions [250]. Parcher et al. have even suggested that the thick layer so formed may be part of the stationary phase and may dissolve the additives [250]. The amounts of additives adsorbed on different packing materials was measured by Berger and Deye [262]. Changes made in the nature or in the concentration of the additive in the mobile phase stream that percolates the column may not have immediate effects. The elution of the breakthrough may take a significant time before dynamic equilibrium in the column is restored [263].

Dependence of the retention factor in SFC on the mobile phase composition has been reported quite extensively. Strubinger et al. measured the retention factors of n-hexane and benzene on silica and on C_{18}-bonded silica in relatively wide ranges of temperatures, pressures, and methanol concentrations. These factors decrease with increasing mobile phase density and temperature, and increase with increasing methanol concentration [251]. The values of the partial molar enthalpies of these solutes at constant density (4.7– 5.7 kcal/mole) suggest a partition-like rather than an adsorption retention mechanism for nonpolar compounds. Rajendran et al. [201] reported the nature of variation of the Henry constant of phenanthrene with increasing concentration of ethanol in carbon dioxide. Lesellier et al. [264] tested sixteen solvents as modifiers in separating carotenes in sub-critical fluid chromatography. They found that correlations between the solubility parameters and the dielectric constants account for the elution strengths of these modifiers. West and Lesellier reported that the addition of a small amount of modifier to CO_2 decreases sharply the retention factors of solutes on nonpolar stationary phases [265]. The modifier is adsorbed on the stationary phase and deactivates it partly, changing its surface chemistry. For larger modifier concentrations, the retention factors decrease more gradually, reflecting the influence of the mobile phase composition.

7.1.4. Retention factor and the solubility

The solubility in a particular solvent strongly affects the retention characteristics of chromatographic systems. The importance of this parameter is much higher in SFC than in HPLC because solubility depends on the solvent density, which may vary considerably in SFC systems. Supercritical fluids are powerful solvents, with some unusual properties, particularly a high diffusivity, a low density, and a low viscosity [42]. For these reasons, they have great potential for many separation processes. Unfortunately, reliable and versatile mathematical models of the phase equilibrium thermodynamics are not yet available, making their use in process design and economic feasibility studies difficult.

Chrastil suggested a simple and reliable [42] correlation for the solubility of compounds in supercritical fluids [266]

$$C_i = \rho^{\alpha_i} e^{\frac{a}{T}+b} \tag{116}$$

where C_i is the solubility of solute i and a b, and α are empirical constants. This correlation accounts for the variation of the solubility with the pressure (through its effect on ρ) and the temperature. The equilibrium of a solid solute with a solvent is expressed by

$$\left(\frac{\partial a_{i,sat}^{mob}}{\partial P}\right)_T = \frac{V_{i,pure}^{solid} - V_{i,sat}^{mob}}{RT} \tag{117}$$

where $a_{i,sat}^{mob}$ is the activity of the solute in the saturated mobile phase $V_{i,pure}^{solid}$ and $V_{i,sat}^{mob}$ are the partial molar volumes of the pure solid and of the solute in the saturated mobile phase, respectively (see 3.4). This equation is very similar to Eq. (111) (see Section 7.1). If we assume that Henry's law is valid up to the saturation concentration of a solid solute, we may write [256]

$$\left(\frac{\partial \ln x_{i,sat}}{\partial P}\right)_T = \frac{V_{i,pure}^{solid} - V_{i,sat}^{mob}}{RT} \tag{118}$$

Combining this equation and Eq. (111) and using Chrastil correlation (Eq. 116) to determine $x_{i,sat}$ gives

$$\left(\frac{\partial \ln k_i'}{\partial P}\right)_T = -\alpha_i \left(\frac{\partial \ln \rho}{\partial P}\right)_T \tag{119}$$

This equation is identical to Eq. (113). The numerical values of the exponent, $-\alpha_i$ and $\lambda_i + 1$ derived from the results of equilibria measurements and from Chrastil equation are in excellent agreement [42], which confirms the validity of Chrastil correlation since we know that retention times are closely related to equilibrium data.

7.1.5. Retention factor and the solubility parameter

The solubility parameters have been more extensively used than solubilities to correlate the retention factors. A fair volume of work was done to extract solubility data in supercritical fluids from retention factors on SFC columns [267]. Conversely, if solubility parameter data are available for certain compounds, these data may be used to predict the retention behavior in SFC. Brauer et al. [268] used this concept to understand the relationship between the solubility parameters and the SFC retention behaviors of four compounds. By modifying an expression developed by Giddings [89] they developed the following relation:

$$\frac{RT}{V} \ln \frac{k}{F} = -(\delta_{sp}^2 - \delta_{sf}^2) - 2(\delta_{sp} - \delta_{sf})\delta_i \tag{120}$$

where R is the universal gas constant (cal mol^{-1} K^{-1}), T the temperature (K), and $\delta_s p$, $\delta_s f$ and δ_i are the solubility parameters of the stationary phase, the supercritical fluid phase, and the solutes, respectively (cal$^{1/2}$ cm$^{-3/2}$). It can be noted that Eq. (120) predicts a linear relationship between δ_i and the group $(RT/V)\ln(k'/F)$. This allows a quantitative means to predict retention factors in SFC from solubility parameters, which may be available either from published sources [269], or can be calculated from relevant equations (Eq. (8) or Eq. (15)) when the heats of vaporization of the solutes are known, or can be estimated following other useful methods [268]. Fig. 29 shows calculated values of the solubility parameter of carbon dioxide as a function of the reduced pressure at different reduced temperatures [7]. At temperatures below the critical temperature, carbon dioxide may exist under two states, gas and liquid; each one has its solubility parameter, both markedly different (see Fig. 29). Plots of the solubility parameter versus the mobile phase density show a smoother dependence, actually a nearly linear relationship in a wide density range [7] and a relatively small influence of the temperature (although the pressure needed to achieve a given mobile phase density increases rapidly with increasing temperature). Brauer et al. [268] demonstrated (Fig. 30) that the retention behavior of four compounds, under different operating conditions, can be linearly correlated according to their solubility parameters. This result was expected since these compounds are homologues.

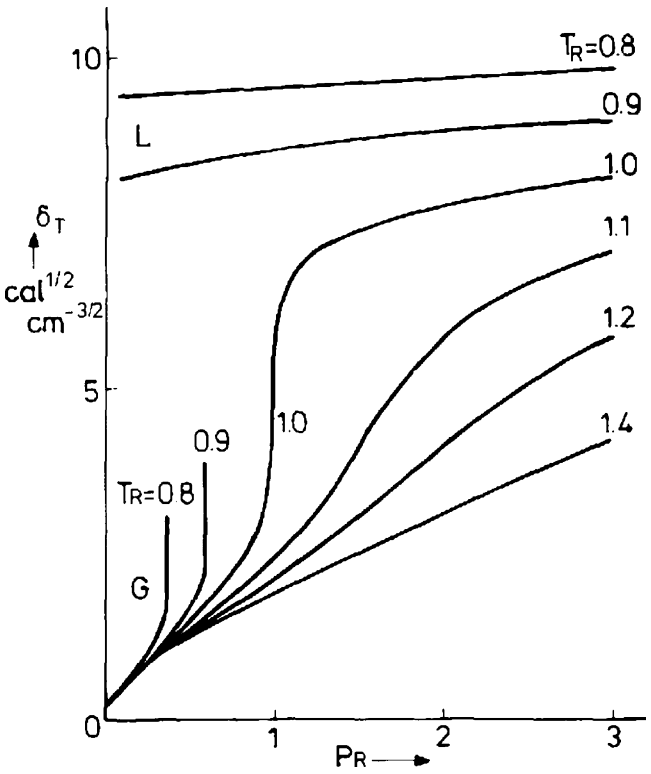

Fig. 29. Solubility parameter of carbon dioxide as a function of the pressure at different temperatures [7].

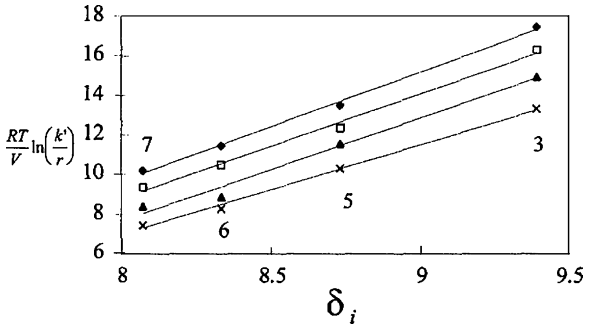

Fig. 30. Relationship between the solubility parameters and $(RT/V_i)\ln(k/r)$ for t-butyl substituted ferrocenes at 100 °C. From top to bottom, pressures 95, 105, 115, and 125 atm. Compounds: (3) t-butyl ferrocene, (5) di-t-butyl ferrocene, (6) tri-t-butyl ferrocene, and (7) tetra-t- butyl ferrocene [268].

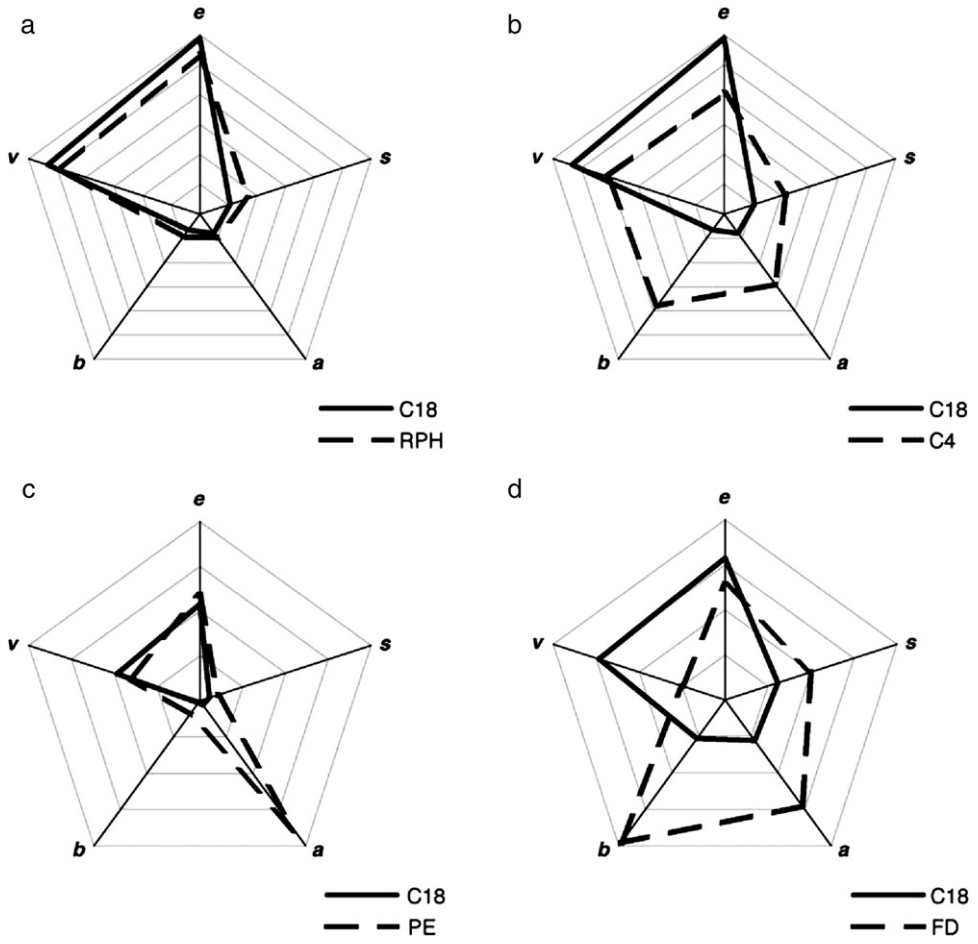

Fig. 31. Diagram illustrating the coefficients e, s, a, b, v of the stationary phases studied. (a) C_{18} dimethylsilane-bonded and C_{18} phenylmethylsilane-bonded silica; (b) C_{18}- and C_4-alkyl-bonded silica; (c) C_{18}- and amide embedded C_{18}- bonded silica; (d) C_{18}- and perfluorodecyl-bonded silica [265], Fig. 7.

Heaton et al. [270] developed a retention model for SFC in order to apply it to predict general retention behavior. This model dissociates the Hildebrand solubility parameter into the contributions of diverse molecular interactions, such as dispersive, dipole–dipole, dipole-induced dipole, and hydrogen bonding with acidity and basicity. This concept has promising capability in predicting the retention of any type of solute. The motivation behind dissociating the solubility parameter into more thermodynamically consistent molecular interaction parameters were inspired by the work of Hansen [88], which was later expanded by Keller et al. [271].

7.1.6. Retention factor and the solvation energy relationships

Few LSER studies have been made in SFC [99]. Weckwerth and Carr studied the effects of pressure and temperature on the retention and the LSER coefficients in a phase system made of carbon dioxide and polydimethylsiloxane [272]. Remarkably, they found that the b coefficient was constantly negative. CO_2 has no hydrogen bond donating ability and act as a strong Lewis acid. It attracts Lewis bases into the mobile phase, lowering their retention. At 100 °C and under a pressure of ca. 93 bar, the coefficients s, a, and e of the LSER are nearly equal to those found in GC on the same stationary phase. In contrast, the coefficient l is much smaller and depends on the pressure, but not on the temperature [99,272]. This confirms that, as expected, dispersive interactions between solutes and CO_2 are stronger in SFC than in GC.

In a long series of papers, West and Lesellier studied the retention mechanisms of many packing materials in SFC [265,273–279]. Their goal was to better understand the actual influence of the stationary phase when the mobile phase is very different from aqueous solutions [265]. Retention in SFC is more closely controlled by the interactions between the solutes and the stationary phase than in RPLC, where the influence of water is dominating. Therefore SFC is more suitable than HPLC to characterize stationary phases. For this purpose, West and Lesellier used quantitative structure–retention relationships (QSRR) and more specifically the linear solvation energy relationship (LSER) derived by Abraham [100]:

$$\log k = c + eE + sS + aA + bB + vV \quad (121)$$

in which the uppercase letters stand for solute properties and the lowercase ones for system properties. Equation 121 limits the number of solute descriptors used in the QSRR and relates them to a few particular interaction properties: c depends essentially on the phase ratio; E is the excess molar refraction, which models the polarizability contributions from the n and π electrons; S is the solute dipolarity/polarizability; A and B are its overall hydrogen-bond acidity and basicity; and V is the McGowan characteristic volume ($cm^3mol^1/100$). The system solute constants (e, s, a, b, v) are obtained through a multilinear regression of the retention data for a sufficiently large number of solutes with known descriptors; they reflect the magnitude of the difference for that particular property between the mobile and the stationary phases. West and Lesellier measured systematically these solvation parameters for a large number of conventional stationary phases. These phases are alkyl-bonded silica [265], polar phases (SiO_2, diol, PEG, NH_2,

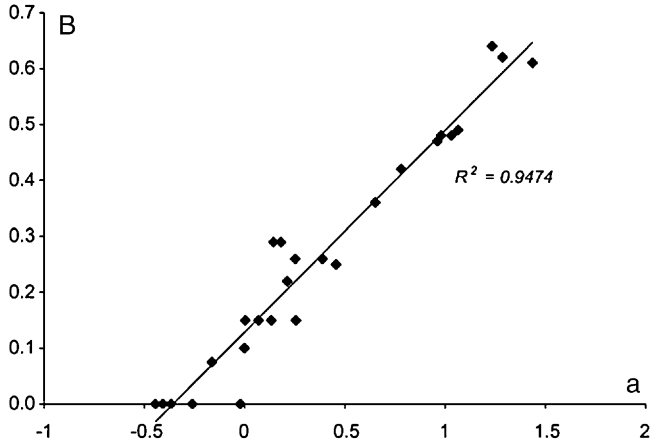

Fig. 32. Plot of the basic character (B) associated with a stationary phase against the basic character of this stationary phase [279]Fig. 3.

CN) [274], aromatic phases [275]. Other papers are dedicated to describe the tools used [273] and to elaborate on the practical applications of the results [276].

The organic modifiers used were methanol and THF, methanol as the modifier (10%), THF mainly as solvent for solutes purely soluble in methanol [265]. The mobile phase flow rate was 3.0 mL/min. The experimental conditions were subcritical, with $T = 25^\circ$ C and a back pressure of 150 bar, with a pressure drop between 25 and 45 bar, depending on the column. A total of 109 solutes were used. Their values of E, S, A, B, V are provided [265,276]. The values of the coefficients for the different stationary phases, e, s, a, b, v are also provided [265]. The analysis of the data, through multiple linear regression analysis was carefully performed. The RSD of the retention factors was always less than 0.3%. Errors on the column hold-up time affect only the value of coefficient c [265,280]. Further analysis of the whole sets of results obtained with the different columns was provided by the use of five-dimensional diagrams, which provide simple comparison between the characteristics of these columns, as illustrated in Fig. 31. Other representation are suggested, offering different compromises between the amount and the detail of the information provided [273],

On classical RPLC phases, the coefficients e and v are positive, the other three negative. Their absolute values are the largest in aqueous mobile phases. In SFC, all the absolute values are smaller than in HPLC, particularly those of e, s, and v, indicating a lower cohesive energy and acidity in SFC than in RPLC. These values increase with increasing length of the bonded alkyl chain, probably because an increase of the chain length enhance dispersive interactions and hinders access to the silica surface. The C_4 chain exhibits a positive b and a near zero a value, which confers to it a different selectivity [265]. The embedding of a bonded amide chain or the bonding of a perfluoroalkyl chain changes completely the distributions of the five LSER parameters. The former gives a very large, positive a coefficient with an increase of all other coefficients, suggesting a strong interaction with acidic solutes. The latter gives much larger values for s (now $s = 0$), a, and b and a negative value for v, confirming the lesser dispersive interactions and the strong polar nature of this ligand. The logarithmic plots of the retention factor on one phase versus those on an other demonstrate the great similarity between the alkyl bonded phases and stronger retentions of the acidic solutes on the embedded amide bonded chain and of the basic compounds on the perfluoroalkyl chain.

West and Lesellier have demonstrated the great practical importance of the coefficients e, s, a, b, v to characterize stationary phases [279]. There is an excellent correlation (see Fig. 32) between these coefficients and the corresponding coefficients E, S, A, B, V of an associated probe solute chosen for each phase as the solute most analogous to the bonded ligand of the stationary phase (e.g., octadecane for ODS silica, propionitrile for the cyanopropyl silica). This result shows that a basic ligand (large B) induces a basic stationary phase (large a). The values of a represents the difference between the hydrogen-bonding characteristics of the solute between the mobile and the stationary phase on the one hand, between the solute and the mobile phase on the other but the mobile phase remained the same in all experiments, leaving variations of a in this study to characterize only the influence of the nature of the stationary phase on the hydrogen bonding interactions between the solute and the stationary phase [279]. Although this does not rule out a possible contribution of the underground silica and the adsorbed modifier, this result suggests that the hydrogen-bonding acceptor character of the stationary phase is mainly due to that of the ligand.

The same approach was used to collect similar data on a series of polar stationary phases, neat porous silica, propanediol-, polyvinylalcohol-, polyethyleneglycol-, aminopropyl- and cyanopropyl-bonded silica [274]. The retention behavior observed in subcritical SFC was found to be close to the one reported in normal-phase LC (NPLC) with hexane. Increases in the hydrogen bond acidity or basicity and in polarity or polarizability of the solute increase retention while increase in its molar volume reduces it [274]. Because water is absent of the mobile phase, the interactions between the solute molecules and the stationary phase have more important and clearer effects on the retention behavior. The work was also extended to a series of aromatic stationary phases, including porous graphitic carbon, PS/DVB and different porous silica bonded to a variety of ligands containing one or two benzyl groups, ethylpyridine, or a pyrenyl group [275]. In all cases, charge transfer interactions contribute to retention, completed by interactions depending on the nature of the aromatic group. Except for silica bonded to ethylpyridine (strongly influenced by the solute acidity) or to pentafluorophenylpropyl (influenced by the solute polarizability), retention depends much on a balance between the effects of e and v, the polarizability and the McGowan characteristic volume of the solute. Note that porous graphitic carbon has much larger values of e and v than other materials and a negligible value of b. Yet, aromatic phases provide a wide range of selectivities [275].

Later, West and Lesellier developed a simple procedure for a rapid and reasonably precise procedure of evaluation of the characteristics of chromatographic systems [276]. Ten key solutes were selected among the hundred previously used by the authors. The separation factors of the 36 pairs of solutes were used to establish new equations and calculate the coefficients of the LSER model [265].

$$\log \alpha = e\Delta E + s\Delta S + a\Delta A + b\Delta B + v\Delta V \quad (122)$$

The calculation of the coefficients of the stationary phase is made easier if a set of compounds differing only by one or two descriptor is available. The parameters s, a, v can be evaluated correctly. So can the parameter b provided that the packing material has no ionic sites under the experimental conditions selected. Estimate of e is uncertain but this coefficient has a weak influence on retention. The implementation of the procedure requires the selection of a reduced set of test solutes adapted to the new problem studied. Examples are provided in a study of mobile phase effects and the comparison of a number of C_{18}-bonded silica columns for the purpose of illustrating the application of the procedure. The method is not accurate enough to predict retention data of other solutes but it forecasts the variations in retention behavior of different chromatographic systems.

7.1.7. Retention factor and the fugacity coefficients

Based on the fugacity coefficient derived from the Lee–Kesler equation of state, Schoenmakers [7] derived an equation for the retention factor

$$\ln k = \ln \phi_2^{\infty} + \ln k_p \frac{P}{\rho} - \frac{v_2^L P}{RT} \quad (123)$$

where ϕ_2^{∞} is the fugacity coefficient of the compound considered at infinite dilution in the stationary phase, v_2^L its liquid molar volume, ρ the mobile phase density, and k_p a constant. However, most stationary phases used in SFC, like in HPLC, are high molecular weight polymers or solid adsorbents not liquids. Then, the fugacity has no physical meaning. So, Eq. (123) merely provides a quantitative relationship between the retention factors, the pressure and the density of the mobile phase.

7.1.8. Retention factor and the dielectric constants

Guillermo et al. [281] reported a thermodynamic model to predict the partition of a solute between stationary and mobile phases in supercritical fluid chromatography with CO_2. The model considered the energy of interaction of a polar molecule with a dielectric continuum, which is the solvent. At constant temperature, the model predicts a linear dependence of the logarithm of the capacity factor on the pressure, with a slope which is a function of the dipole moment of the solute.

7.1.9. Retention factor from thermodynamic constants

By equating the differentials of the logarithm of the fugacity of the compound considered in the two phases in equilibrium, we obtain the following relationship between the adsorption constant or initial slope of the isotherm, K, the temperature and the pressure by [282]:

$$\left(\frac{\partial \ln K}{\partial T}\right)_P = \frac{(h^{IG} - \bar{h}^m) + \Delta H^{ads}}{RT^2} + \alpha^m \quad (124)$$

$$\left(\frac{\partial \ln K}{\partial P}\right)_T = \frac{\bar{v}^m}{RT} - \kappa^m \quad (125)$$

where the superscripts IG and m stand for the ideal gas and the mobile phase, respectively, $\Delta H^{ads} = \bar{h}^s - h^{IG}$ is the heat of adsorption of the compound on the solid adsorbent, $\bar{h}^m$ and h^s are the partial molar enthalpy of the compound at infinite dilution in the mobile and the stationary phases, respectively, h^{IG} its molar enthalpy in the ideal gas, v^m its partial molar volume at infinite dilution in the mobile phase, α^m and κ^m the volume expansivity and isothermal compressibility of the mobile phase, respectively. The partial molar volume of the compound in the stationary phase is neglected in Eq. (125) because its partial molar volume in the mobile phase is large and is negative around the critical point. As α^m and $h^{IG} - \bar{h}^m$ vary rapidly near the critical conditions, a numerical solution of Eq. (124) is required to determine the heat of adsorption [80]. These parameters were calculated using the Peng–Robinson equation of state [81].

7.1.10. Influence of the nature of the modifier

Lessellier et al. investigated the influence of the average pressure, the temperature, and the nature and concentration of the organic modifier in subcritical carbon dioxide, on the retention of homologous alkylbenzenes [283]. Their retention was affected mainly by the organic modifier concentration and by the temperature. Changes in the phase ratio accompanied modifications of the organic modifier concentration and were due to its adsorption. This phenomenon was mostly important for the shorter chain homologs. The methylene selectivity of the stationary phase was different for short- and for long-chain homologues when acetonitrile was the modifier but did not depend on the chain length when methanol was used instead [284].

Following the pioneering work of Guillemin et al. [285], pure, hot but subcritical water has been used to successfully perform a wide variety of separations [118,123,286].

7.2. The sorption effect

The partial molar volume of a solute in a solvent characterizes the molecular interactions between this solute and the solvent [95]. It affects its solubility in subcritical and supercritical fluids (see Section 3.1) and, more particularly, the dependence of its retention on the mobile phase density [96]. Wheeler showed that the partial molar volume of solutes at infinite dilution should diverge toward infinity at the solvent critical point, the values becoming negative if there are attractive interactions between solute and solvent molecules [97]. This prediction was confirmed by experimental results of van Wasen and Schneider who measured the partial molar volumes of naphthalene and fluorene in carbon dioxide in the critical region (see Fig. 9) [23]. At low pressures, in the gas phase, the partial molar volume of compounds decreases with increasing pressure until the pressure nears the critical pressure. At about 10% below the critical pressure of CO_2, the partial molar volume begins to increase rapidly with increasing pressure, in a spike the amplitude of which increases rapidly with decreasing difference between the temperature at which are made the measurements and the critical temperature. This spike corresponds to an approximately six times higher partial molar volume at the critical pressure than under 60 bar at 35 °C, three times higher at 40°, and twice at 50°. The dependence of the retention factor of naphthalene on the pressure were shown earlier in Fig. 8[7], which shows results consistent with those of van Wasen and Schneider. All this suggests that clustering of a large number of solvent molecules takes place around each solute molecule. The partial molar volumes of solutes were also studied by Eckert et al. [98]. Therefore, molecular interactions should be, more than in HPLC, critical to understand the behavior of retention in SFC (see Section 3.4).

The density of the mobile phase in SFC is lower than that of usual fluids, so the partial molar volumes of a solute in the adsorbed and in the mobile phase (see Section 3.4) are markedly different, far more so than in HPLC, although less than in GC. This difference affects the equilibrium constant (see Eq. (111)). Because a given mass of solute occupies more volume in the mobile phase than in the adsorbed phase, the local velocity inside the band is higher than in the pure mobile phase, giving rise to the sorption effect [287–289]. High concentrations tend to move faster than low ones. This renders band profiles unsymmetrical, with the progressive build-up of a front shock layer when the maximum concentration of the band is increased [1,288,289]. The sorption effect was studied in detail in gas chromatography [289] but is negligible in HPLC. In SFC, its importance and its consequences are unknown but may explain difficulties encountered in empirical optimization of SFC. Lochmuller and Mink [253,290] and Yonker and Smith [244,249] suspected that but did not investigate.

7.3. The retention time

The retention time of a compound is the sum of the times that it spends, during its migration along the column, in the mobile and in the stationary phases. Except in size exclusion chromatography, which does not seem to have been used often in SFC, the former time is equal to the column hold-up time (t_0, see Section 5.6). In HPLC, the relationship between the retention time (t_R) and the retention factor (k) is simple ($t_R = (1 + k)t_0$) because the retention factor is practically constant along the column, being the product

of the phase ratio of the column and the equilibrium constant of the solute in the phase system [1]. In contrast, in SFC the equilibrium constant varies along the column, being a function of the density of the mobile phase, which varies along the column. It is given by the following equation [201]

$$t_R = \int_0^L \frac{1}{u(z)}(1 + k(z)dz)\,dz \tag{126}$$

But when the pressure gradient along the column is small, this equation can be simplified to

$$t_R = \frac{L}{u(\bar{\rho})}(1 + k(\rho)) \tag{127}$$

or

$$t_0 = \frac{2L}{u_e + u_i} \tag{128}$$

where u_e and u_i are the mobile phase velocities at the column entrance and exit, respectively. The first equation assumes that the pressure drop is small, which makes the density difference between the inlet and the outlet of the column negligible. the second equation that it is small and that the arithmetic average of the inlet and outlet velocities, ū, can be used instead of their true average, which is given by Eq. (126)[201]. At a constant mass flow rate, Eq. (127) leads to

$$t_R = \frac{L}{u}(1 + k) \tag{129}$$

Eq. (129) is the relationship in HPLC between the retention time and the equilibrium constant between the two phases of the chromatographic system, which is generally valid unless the column is operated with an extremely high inlet pressure, as is done in UHPLC [211]. This is because this equilibrium constant remains unaltered along the column in HPLC while is does vary along the SFC column. Figs. 33 illustrate the dependence of the retention time of phenanthrene on the mass flow rate of the mobile phase and the concentration of the organic modifier (ethanol) in supercritical carbon dioxide (T = 65 °C, pressure as indicated in the graphs) [201]. In SFC, the retention factor depends on the flow rate and the column length, to an extend that depends on the column permeability and on the mobile phase viscosity, since these parameters control the extend of variation of the mobile phase density along the column.

8. Mass transfer processes in chromatographY

Mass transfer kinetics in packed beds control the efficiency of columns in chromatography [1]. The fundamental parameter in this field is the molecular diffusivity or diffusion coefficient of the compounds to be separated. This parameter controls directly the kinetics of all the steps of the mass transfer mechanism in chromatography but one (step 5, below), hence its great importance. These steps are: (1) axial diffusion along the column that tends to relax the axial concentration gradient due to the presence of the component zone; (2) eddy diffusion, which results from the dynamic balance between the unevenness of the distribution of flow velocities along the different stream paths that percolate through the anastomosed network of channels between the particles and the radial diffusion that tends to relax the radial concentration gradients caused by the differences in velocities along these stream paths; (3) external mass transfer through the interface between the flowing mobile phase and the stagnant mobile phase in the particles; (4) diffusion through particles, which results from the combination of pore diffusion, diffusion in the mobile phase that is hindered by the geometrical complexity of the channels and surface diffusion that depends on the adsorption energy; and finally

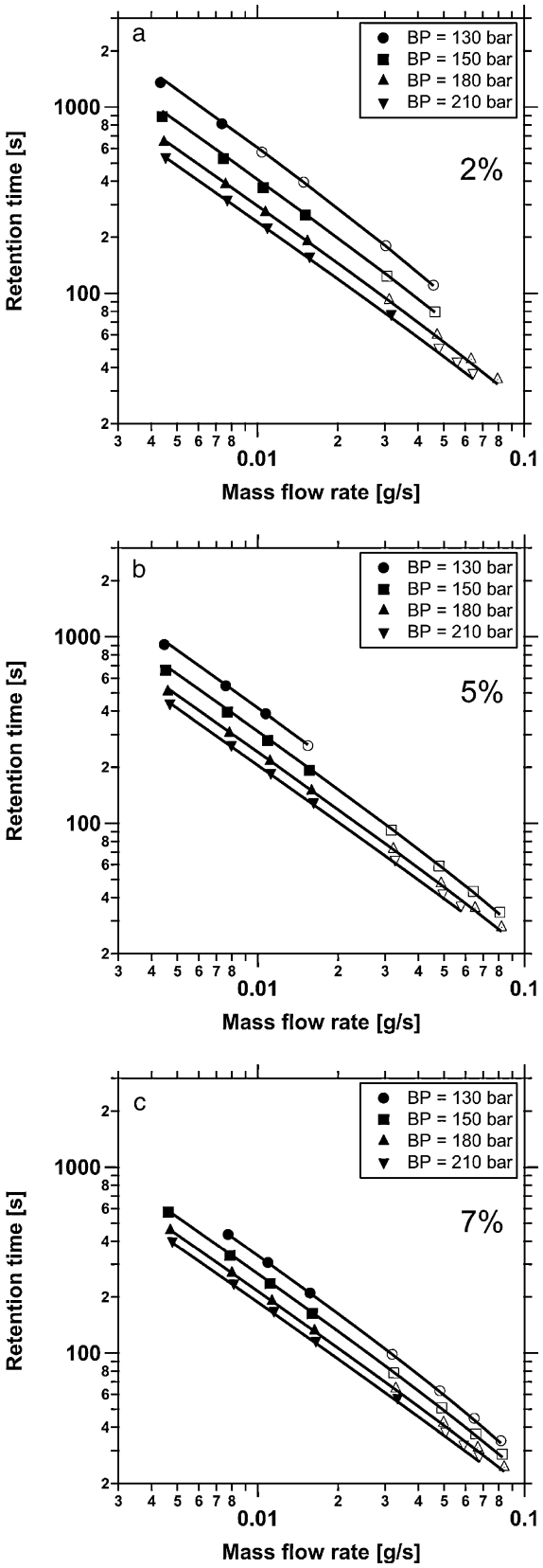

Fig. 33. Experimental (symbols) and calculated (lines) retention times of phenanthrene for different organic modifier concentrations in the mobile phase. (a) 2%; (b) 5%; (c) 7%. The open symbols correspond to the column operated with a density difference between its inlet and outlet of more than 3%, the closed symbols to smaller differences, [201], Fig. 2.

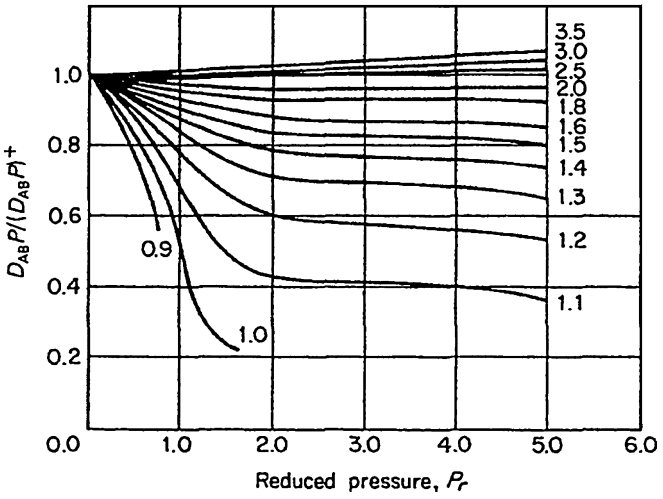

Fig. 34. Correlation for the effects of pressure and temperature on the binary diffusion coefficient [292]. The symbol $^+$ refers to the low pressure data [292]Fig. 1.

(5) the kinetics of adsorption–desorption that is usually fast and rarely controls the rate of the chromatographic process.

8.1. Diffusion coefficients

In chromatography, the diffusion coefficient refers to the diffusion of a solute in a relatively or very dilute solution. The diffusion phenomenon is driven by the gradient of chemical potential in a heterogeneous mixture. Due to the complexity of the relationship between chemical potential and composition, diffusion is affected by more than just the gradient and diffusion fluxes are complex functions of composition, pressure and temperature [6].

The diffusion coefficients in gases are inversely proportional to the pressure. As pressure rises, however, the product $D_m P$ or $D_m \rho$ is no longer constant but decreases with increasing pressure or density. The diffusion coefficients are independent of the concentration at low pressures but deviations take place with increasing pressure.

Giddings showed that the diffusion coefficients of compounds dissolved in critical fluids is related to the fluid density and viscosity through

$$D_m = \frac{D}{\eta\rho} \tag{130}$$

where D is a numerical coefficient. In other words, the product of the diffusion coefficient and the fluid viscosity is inversely proportional to the fluid density in critical fluids (while it depends only on temperature in liquids) [291].

Takahashi [292]suggested a correlation between the value of the product $D_{A,B}P$ and the reduced temperatures and pressures, as shown in Fig. 34. Note that in the figure, $D_{A,B}$ is the binary diffusion coefficient representing the movement of fluid A through fluid B.

Reid et al. plotted (see Fig. 35) a large set of logarithm of the diffusion coefficients measured at near infinite dilution in carbon dioxide, ethylene and sulfur hexafluoride for benzene, propylbenzene, 1,2,3-trimethylbenzene, naphthalene, and benzoic acid versus the logarithm of the reduced pressure of the solvent [6]. The reduced temperature was between 1 and 1.05. Up to a pressure equal to nearly $0.5P_c$, the diffusion coefficient decreases in proportion to the pressure (the product $PD_{A,B}$ is constant). Above that pressure, the product $PD_{A,B}$ decreases sharply, almost vertically in the critical region, then above a reduced pressures of 2, the diffusion coefficient is nearly proportional to $P^{-1/2}$ [6]. In the critical region, the diffusion coefficient is of the order of $2–3 \times 10^{-4}$ cm^2/s, which is about two to three orders of magnitude smaller than in low pressure gases and nearly two orders of magnitude larger than in solutions.

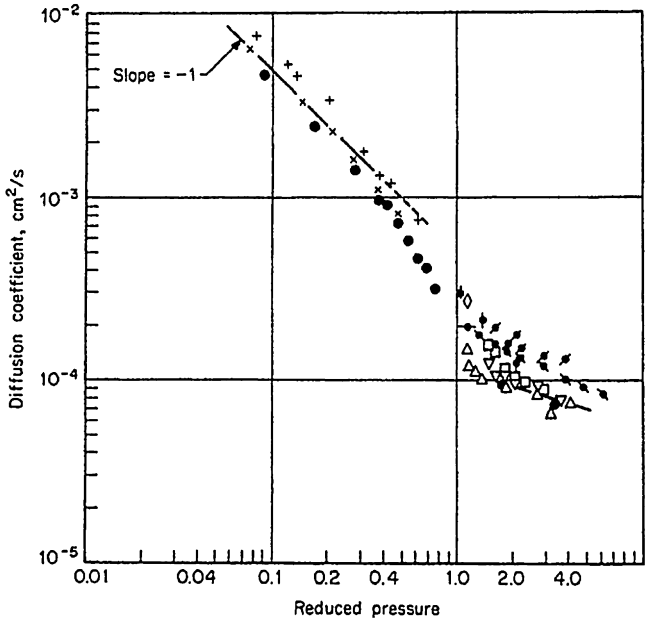

Fig. 35. Diffusion coefficients in supercritical fluids [6]. Solvents: CO_2, C_2H_4, and SF_6, aromatic solutes.

8.1.1. Diffusion in pure carbon dioxide

Using their data and other data found in the literature [293–295], Bartle et al. [296] showed that the product of the mobile phase density of CO_2 and the molecular diffusivity of naphthalene (ρD_m) varies significantly with ρ in the subcritical region, going through a minimum and approaching a limit in the supercritical region. The diffusion coefficient first decreases with increasing solute concentration, going through the minimum value of the product ρD_m at 313 K, under conditions that happen to correspond approximately to half the critical density. Fig. 36 illustrates this result.

The diffusion coefficient of naphthalene in pure carbon dioxide at 40 ° C fits to a second degree polynomial

$$D_m = [3.69 - 2.11\rho_r + 0.361\rho_r^2] \times 10^{-4} \tag{131}$$

where D_m is in cm^2/s and ρ_r is the reduced density of the fluid [203,293].

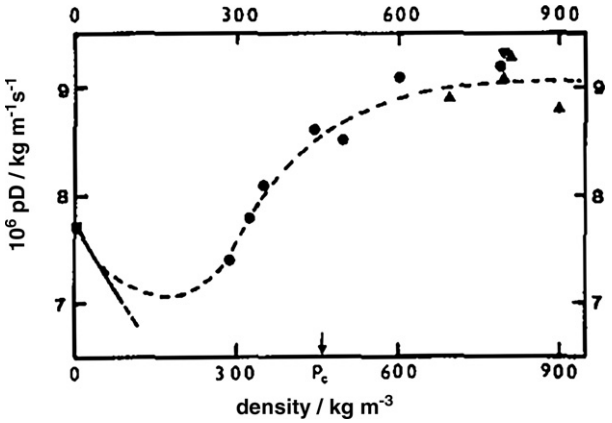

Fig. 36. Plot of the product of the diffusion coefficient of naphthalene in dilute solution and the density of carbon dioxide at 313 K. ■ in air at NTP; ○ [293]; ▲ [294]; ▼ [295]. [296]Fig. 1.

There are several reasons for the minimum of the rate of diffusive transfer in the critical region [296]. The first one is that the diffusive flux is not actually driven by the concentration gradient but by the gradient of the chemical potential of the solute [1,297]. Tyrrell and Harris [297] showed that the diffusion coefficient can be expressed by the equation

$$D_m = \frac{D}{RT}\left(\frac{\partial \mu_2}{\partial \ln x_2}\right)_{p,T} \quad (132)$$

where μ_2 is the chemical potential of the solute and x_2 its mole fraction. This expression tends toward zero at the critical point, except at infinite dilution. At the critical point, however, the fluid would split into two different phases which should be in equilibrium, hence in which the solute must have equal chemical potentials but is at different concentrations, except if these two concentrations are equal to zero, in which case the ratio of these two concentrations (which depends on the equilibrium constant at infinite dilution) may be different from zero. A second reason for a minimum of diffusive transfer is that, in the critical region, the heavier solute molecules strongly attract the lighter solvent molecules that make the solvent, which causes the carbon dioxide density to become higher in the region occupied by the solute band than in the rest of the mobile phase. This increase in local density is important in the critical region. Because the product ρD_m does not vary much with the local density, the diffusion coefficient is lower in the region occupied by the solute band. Finally, diffusion flux is defined with respect to the mass of fluid containing the band, a mass that migrates along the column. Because there is a flux of solvent toward the region of higher solute concentrations (see above), the flux of solute is not the same with respect to fixed coordinates and with respect to the mass center of the band [296,298].

The diffusion coefficient falls sharply around the critical density, to an extent that increases with increasing solute concentration and with increasing proximity to the critical temperature. The decrease in the diffusion coefficient can be as high as 50% at a temperature 1 K higher than the critical temperature for a naphthalene mole fraction of 1×10^{-4} (close to saturation) but only 5% at a temperature 9 K higher [296]. This anomaly is not observed at infinite dilution. Calculations show that the partial molar volume of naphthalene does not depend much on its concentration up to the solubility limit. However, it is very sensitive to the density of carbon dioxide. Addition of naphthalene to CO_2 at its critical density and 1 K above the critical temperature to form a solution with a 1×10^{-4} mole fraction reduces considerably its partial molar volume; the van der Waals equation of state predicts a reduction to half the original value under constant pressure [296]. Because the solute–solvent and solute–solute interactions increase with increasing molecular weight of the solute, the magnitude of the effects just described will increase further with increasing molecular weight of the solute considered. We calculated the diffusion coefficients of naphthalene at infinite dilution in carbon dioxide as a function of the density of CO_2 using the method described by Takahashi [292]. The diffusion coefficient deviates noticeably near the critical temperature, as happened with the thermal conductivity (see Section 5.8 and Fig. 21). The calculated data matches fairly well with the experimental data from Higashi et al. [299]. Both sets of data are shown in Fig. 37. The near independence of the diffusion coefficient from the temperature at higher density should also be noted. The difference near the critical density is expected. Fig. 37 shows also the diffusion coefficients of phenanthrene and hexachlorobenzene as a function of the density of carbon dioxide [300] at three different temperatures. This coefficient is more strongly influenced by the density than by other factors.

This phenomenon may be particularly important in preparative SFC. This phenomenon could explain an unexpected band broadening observed at moderate concentrations even when the equilibrium isotherm is linear. This observation also suggests that the influence of the solute concentration should be assessed when diffusion coefficients are measured. However, no similar effect was ever reported in HPLC. No confirmation of this effect was found in other publications and no report clearly suggesting such a behavior in preparative SFC.

8.1.2. Measurements of diffusion coefficients

Many authors used the Taylor method [301] in the same fashion as it has been used previously in gas [302,303] and in liquid chromatography [304]. The method consists in measuring the broadening of the bands of dilute samples as a function of the linear velocity of the mobile phase. Small samples of the solute are eluted along an empty, long (43 m), narrow (0.409 mm), straight (nearly so, coil radius >0.10 m) tube on the surface of which the compound is not adsorbed. The profiles of the recorded elution band should be Gaussian, with a variance proportional to the diffusion coefficient and related to the tube characteristics [301]. A correction is applied for the radial diffusion contribution due to the tube curvature [1,304].

Weingärtner et al. measured the diffusion coefficients of diphenyl at infinite dilution in carbon dioxide, between 36 and 58 °C, and at pressures between 80 and 200 bar [305], using the Taylor method. The corresponding carbon dioxide densities are between 500 and 850 g/L and the measured diffusion coefficients of diphenyl between 0.9 and 1.8×10^{-4} cm^2 s^{-1}, decreasing linearly with increasing fluid density and slowly with increasing temperature. The density of carbon dioxide being a strong function of the temperature, the diffusion coefficients were measured at constant mobile phase density, as a function of temperature. Then, their variation barely exceeds experimental scatter [305]. Gonzales et al. measured the diffusion coefficients of several solutes in carbon dioxide, using the same method [306].

Miyabe et al. [307] proposed an alternate method that is still simpler than the Aris method [301] and is suitable for easy measurements of accurate diffusion coefficients in compressible fluids. This method is called the peak parking method (PP) and it is a static method.

8.1.3. The peak parking method

In peak parking measurements (PP), a pure compound is injected into a column and the elution of its band is stopped when this band reaches about the middle of the column; the band is left there to diffuse during a certain parking time, t_p, with no eluent flow rate, after which it is eluted. The experiment is repeated at the same flow velocity, with increasing parking times. The plot of the band variance, μ'_2, of the eluted peak *versus* the parking time, t_p, is a straight line with a slope related to the longitudinal diffusion coefficient, $D_{eff}(\nu = 0)$, of the solute in the column [308]:

$$D_{eff}(\nu = 0) = \frac{u_R^2}{2}\frac{\Delta \mu'_2}{\Delta t_p} \quad (133)$$

where $u_R = u_0/(1 + k)$ is the linear velocity of the compound band (not the chromatographic linear velocity u_0) along the column during its migration from the inlet to the middle of the column and from the middle to the outlet of the column. u_R is written as [308]:

$$u_R = \frac{4F_v}{\epsilon_t \pi d_c^2 (1 + k)} \quad (134)$$

where F_v is the flow rate, d_c is the column tube diameter and k the retention factor of the solute.

The peak parking method can provide both the diffusion coefficients in the mobile phase or the dispersion coefficients in the column bed, the latter also a function of the bed tortuosity, of

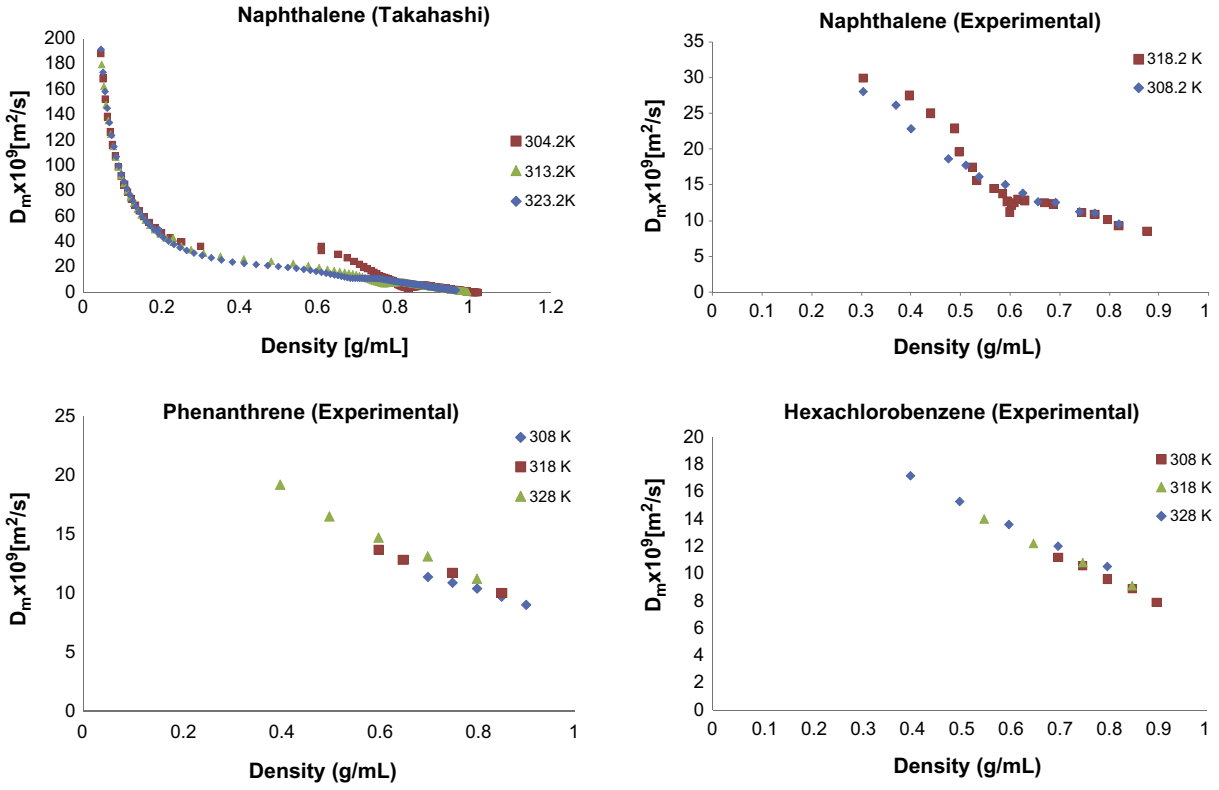

Fig. 37. Top left: Calculated diffusion coefficient of naphthalene at infinite dilution in carbon dioxide [292]. Top right: Experimental values of the same parameter [299]. Bottom left: Experimental diffusion coefficient of phenanthrene at infinite dilution in carbon dioxide. Bottom right: Experimental diffusion coefficient of hexachlorobenzene at infinite dilution in carbon dioxide [300].

pore and surface diffusion. To measure diffusion coefficients in the mobile phase, a column packed with fine, non-porous particles is used. The slope of the plot of the band variance versus the parking time is proportional to the apparent dispersion coefficient (see Eq. (133)), which is itself equal to the product of the diffusion coefficient and the obstructive factor of the bed. To determine the latter a similar measurement is carried out using a long open tube in which the obstructive factor is unity. The comparison of the slopes obtained for a given compound with the tube and the column provides the obstructive factor of the column. This factor is a characteristic of the column, which is thus calibrated [307]. The advantage of using a column rather than an open tube is the markedly higher precision of the results and the shorter time needed [307]. The method provides excellent results in HPLC [307,309].

The same measurement made with a conventional column provides important information on the dispersion coefficients in the bed. The overall longitudinal diffusion of the sample along the column in the absence of any flow rate is a complex combination of solute diffusions in the particle ($D_{eff,part}(\nu = 0)$) and in the inter-particle bulk diffusion coefficient (D_m). Knowing it, we can back-calculate the apparent effective particle diffusivity, provided that a model for solute diffusion in the heterogeneous packed bed is available. Two different models could be used, assuming either (a) the particle and the inter-particle diffusion mechanisms act in parallel [310] or (b) the validity of the effective medium theory of molecular diffusion in heterogeneous media of Davis [311]. These methods provide two estimates of the equivalent effective particle diffusivity and of the reduced C_p term in the van Deemter equation.

Although the PP method works very well in HPLC and can provide accurate values of either the dispersion coefficients of packed beds or of the diffusion coefficients in the mobile phase (provided that a carefully calibrated column packed with solid particles is available [307,309]), its application to perform accurate measurements under SFC conditions is not straightforward. Because the density of the mobile phase varies significantly along the column, the flow rate will not stop immediately when a hard shut-off valve placed at column outlet is actuated. The mobile phase density would adjust progressively to the average density, causing a certain migration of the band at a variable, exponentially decreasing rate, before it stops, hence a further extent of band broadening. To limit the consequences of this effect, two valves switching off the flow rate should be placed upstream and downstream the column and actuated simultaneously. If the flow rate is low and the peak is parked close to the exit of the column to minimize its migration, the perturbation could be made small enough and its effect negligible provided that the experimental conditions (inlet and outlet pressures, flow rate, temperature) are reproducible during the series of experiments needed, so the extra band broadening due to density relaxation along the column be the same during each parking step. Because diffusion coefficients are large in SFC, such a series will be shorter than in HPLC, which may affect accuracy or require the use of long columns.

8.1.4. Equations and correlations providing diffusion coefficients

Using the equation of Vesovic et al. [159] to calculate the viscosity of carbon dioxide, Weingärtner et al. [305] studied the relationship between the diffusion coefficient, the temperature and the density of the eluent. They determined the coefficient C_{SE} of the Stokes–Einstein equation

$$D^{\infty}_{A,B} = \frac{k_B T}{C_{SE} \pi \rho r} \tag{135}$$

where k_B is the Boltzman constant and r the hydrodynamic radius of the solute molecule (π is the mathematical constant). For slip boundary conditions between the diffusing sphere and the continuum, $C_{SE} = 4$. For stick boundary conditions, it is 6. Provided that

the data used are sufficiently remote from the critical point where the viscosity is anomalous, the data for diphenyl give a coefficient between 4.7 and 6.2, which is consistent with the hydrodynamic theory [305]. The values of C_{SE} decrease slowly with increasing mobile phase density and temperature. This result is consistent with that of Lamb et al. [312] who measured the diffusion coefficient of naphthalene in carbon dioxide in the same temperature range by NMR. The comments of Vesovic on the inconsistencies between the various sources of experimental data on CO_2 viscosity should be kept in mind when pondering the comments by Weingärtner et al. on the deviations of the coefficient C_{SE} from a constant value [305].

Suárez et al. have compiled extensive tables of experimental measurements of the diffusion coefficients of numerous compounds in various supercritical fluids used as solvents, particularly in supercritical carbon dioxide. They summarized methods for graphical correlations of these data [313].

The diffusion coefficient of solutes in solvents are usually calculated using the Wilke and Chang correlation [314] or some other useful correlation [1,172,315]. The Wilke and Chang correlation gives a satisfactory approximation for molecules having a moderate molecular weight:

$$D_{A,B} = 7.4 \times 10^{-8} \frac{\sqrt{\psi_B M_B} T}{\eta_B V_A^{0.6}} \tag{136}$$

where V_A is the molar volume ($cm^3\ mol^{-1}$) of the liquid solute at its normal boiling point, M_B the molecular weight of the solvent (g), η_B its viscosity (cP), and ψ_B is a constant which accounts for solute–solvent interactions. Recommended values of ψ_B are 1 for all nonassociated solvents, 1.5 for ethanol, 1.9 for methanol, and 2.6 for water [314]. In Eq. (136), $D_{A,B}$ is in cm^2/s. V_A can be calculated from group contributions [6,316]. The errors made when using Eq. (136) vary greatly from compound to compound, and this equation is not always accurate [1]. Diffusion coefficients can be predicted to within 10% when water is the solvent and 25% for organic solvents, but errors as high as 200% are possible when water is the solute [316]. A more accurate correlation method has been proposed, but it requires the use of the parachor, a parameter known for only a few hundred chemicals and which can be calculated from group contributions available for only a limited number of chemical groups [6].

Other valuable classical correlations include those of Scheibel [317], King et al. [318], Reddy–Doraiswamy [319], Lusis–Ratcliff [320], Hayduk–Laudie [321], and the Young correlation for proteins [322].

Zhu et al. predicted diffusion coefficients in various fluids, using a molecular dynamics method [323]. They used a Lennard–Jones model based on the molecular dynamics simulation data found in the literature and derived an equation allowing the prediction of binary diffusion coefficients at infinite dilution. This equation has no adjustable parameter and uses only the critical constants. The calculated diffusion coefficients were compared to the experimental coefficients available for 55 solutes in 6 solvents, where the prediction accuracy was reported to be about 17%.

Kraska et al. derived correlations between the diffusion coefficients of solutes at infinite dilution and the viscosity of the solvent [324]. These correlations are based on the use of the friction theory [325,326], of an equation of state, and of the Stokes–Einstein equation that relates diffusion coefficients, viscosity and temperature ($D_{1,2}^{\infty} = \alpha T \eta_{solvent}^{\beta}$, with α and β numerical coefficients depending on the solute). Results with the Peng–Robinson equation, which is simple and of wide application, and the Span–Wagner equation, which is very accurate, are provided. The two equations provide results that are in excellent agreement, in spite of the great differences between these equations.

8.1.5. Diffusion in mixed mobile phases

The diffusion coefficient of a solute i in a mobile phase composed of supercritical carbon dioxide and an organic modifier can be calculated using the following equation (see Eq. 11.7.4 in Ref. [6])

$$\frac{1}{D_{m,i}} = \frac{x_{CO_2}}{D_{m,i,CO_2}} + \frac{x_{mod}}{D_{m,i,mod}} \tag{137}$$

where $D_{m,i}$ is the diffusion coefficient of the solute considered in the mixed mobile phase, D_{m,i,CO_2} its diffusion coefficient in pure carbon dioxide, and $D_{m,i,mod}$ its diffusion coefficient in the pure modifier.

8.2. Column efficiency and band broadening in SFC

As in all chromatographic methods, it is important to distinguish between the different phenomena that cause band broadening and between these sources of band spreading in the column and the instrument contributions to band broadening [201]. Admittedly, in analytical applications, this distinction is formal and may even seem needlessly esoteric to analysts. Their main concern is to separate the components of mixtures. Yet, even for them, it is important to find out what are the actual causes of band broadening if they want to perform any meaningful remediation.

Using a system allowing the measurements of the elution profiles of bands in successive points along the column by Raman spectrometry and the local density of carbon dioxide, Baker et al. [178] have measured the variations along a column of the local efficiency. They showed that the HETP profile exhibits important variations, with regions near the inlet and outlet of the column where H is markedly larger than it its middle. The primary cause of band broadening would be the acceleration of the mobile phase near the column exit. However, significant band broadening also takes place near the column inlet.

8.2.1. Column efficiency and instrument contribution to band broadening

The classical solution consists in determining the contributions of the extra column volumes of the instrument (see Section 5.6) by measuring the first and second moments of the elution band of a sample plug of a compound that is not retained but that gives a signal when flowing through the detector. The peak area, the first absolute moment and the second central moment of the recorded band are obtained by calculating the following functions of the signal response

$$A = \int_0^{\infty} C(t, L)\, dt \tag{138}$$

$$\bar{\mu_1} = \frac{\int_0^{\infty} C(t, L) t\, dt}{\int_0^{\infty} C(t, L)\, dt} \tag{139}$$

$$\bar{\mu_2} = \frac{\int_0^{\infty} C(t, L)(t - \bar{\mu_1})^2\, dt}{\int_0^{\infty} C(t, L)\, dt} \tag{140}$$

The same measurements are repeated after replacing the column with a *zero-volume connector*, a short piece of narrow tubing with a flow resistance comparable to that of the column. These new measurements provide estimates of the extra-column hold-up volume and the band broadening contribution of the instrument. The differences between the corresponding first and second moments provided by these equations are the true hold-up volume and band broadening contribution of the column alone. The first equation (138) should give an area proportional to the amount of sample injected. Significant deviations warn against errors made in the results of the other two due to a nonlinear behavior of the detector.

Since the instrument and the column hold-up volumes on the one hand, the variance contributions due to these two volumes on the other are additive [327], the true column HETP can be derived as.

$$H = \frac{\overline{\mu_{2,meas}} - \overline{\mu_{2,0V}}}{(\overline{\mu_{1.meas}} - \overline{\mu_{1,0V}})^2} L \quad (141)$$

where $\overline{\mu_{2,meas}}$ and $\overline{\mu_{2,0V}}$ are the contributions to band broadening measured when the column is attached to the instrument and replaced by the zero-hold-up volume connector, respectively. while $\overline{\mu_{1,meas}}$ and $\overline{\mu_{1,0V}}$ are the corresponding hold-up volumes, respectively. Eqs. (138) and (141) are valid irrespective of the shape of the band profile. Its numerical result, however, is different from the more common but much less informative calculation procedure of using the retention time of the peak apex and the width of the profile at half-height or at any other fractional height, which presumes that the profile is Gaussian [328]. The former values of the hold-up time and the band variance due to the instrument derived from Eq. (138) are more accurate but often less precise than the latter. The HETP defined by Eq. (141) includes the contributions of all sources of band broadening, as long as the column operates under linear conditions [329] because these contributions to both moments are additive. By measuring successively the moments of the peaks of samples eluted with a column fitted to an instrument and without the column but a zero-hold-up volume connector and subtracting the second value from the first, one can determine the contribution of the column alone. Obviously if the second value is not markedly smaller than the first, the analytical results are inferior to those that the column could potentially deliver and something should be done with the instrument [330].

8.2.2. *Influence of the mobile phase velocity on the column efficiency – empirical approach*

The column efficiency depends much on the mobile phase velocity and its temperature in all fields of chromatography. To increase the mobile phase velocity, one needs to increase the pressure gradient along the column (in the process, thermal effects arise and their magnitude increases, heat is generated by viscous friction and absorbed by mobile phase expansion, with partial compensation, see Section 5.7). Since the compressibility of the mobile phases used in SFC is much higher than those used in HPLC, the mobile phase density, hence its velocity, may significantly vary along the column, in spite of the often relatively small pressure gradient. The mass flow rate of the mobile phase, however, remains constant all along the column at steady-state. So, it might be better and more informative to plot the column HETP versus the mass flow rate of the eluent rather than versus its velocity. Actually, the two plots should be equivalent. This practice reminisces of the one used in GC where the HETP is plotted against the average column mobile phase velocity, $\bar{u}$. As an example, Rajendran et al. have measured the HETP of phenanthrene eluted on the same column with supercritical carbon dioxide and ethanol in increasing concentrations and plotted these HETP versus the mass flow rate [201]. They determined the HETP using the classical Gaussian approximation of the band profile, the peaks being nearly symmetrical with an asymmetry factor less than 1.1, except at high flow rates. Fig. 38 illustrates the results of these measurements, after correction for the instrument contribution (see above). Most of the curves in Fig. 38 look very much like those obtained in HPLC. However, there is a significant, systematic difference between the results with a back pressure of 130 bar and the average of those obtained at 150, 180, and 210 bar, particularly at low organic modifier concentration (see Fig. 38a). This trend is similar to the one observed earlier with pure carbon dioxide as the mobile phase [174] and could be explained by the high compressibility of the supercritical mobile phase at moderate pressures (see Fig. 39). The expansion of the mobile phase along the column

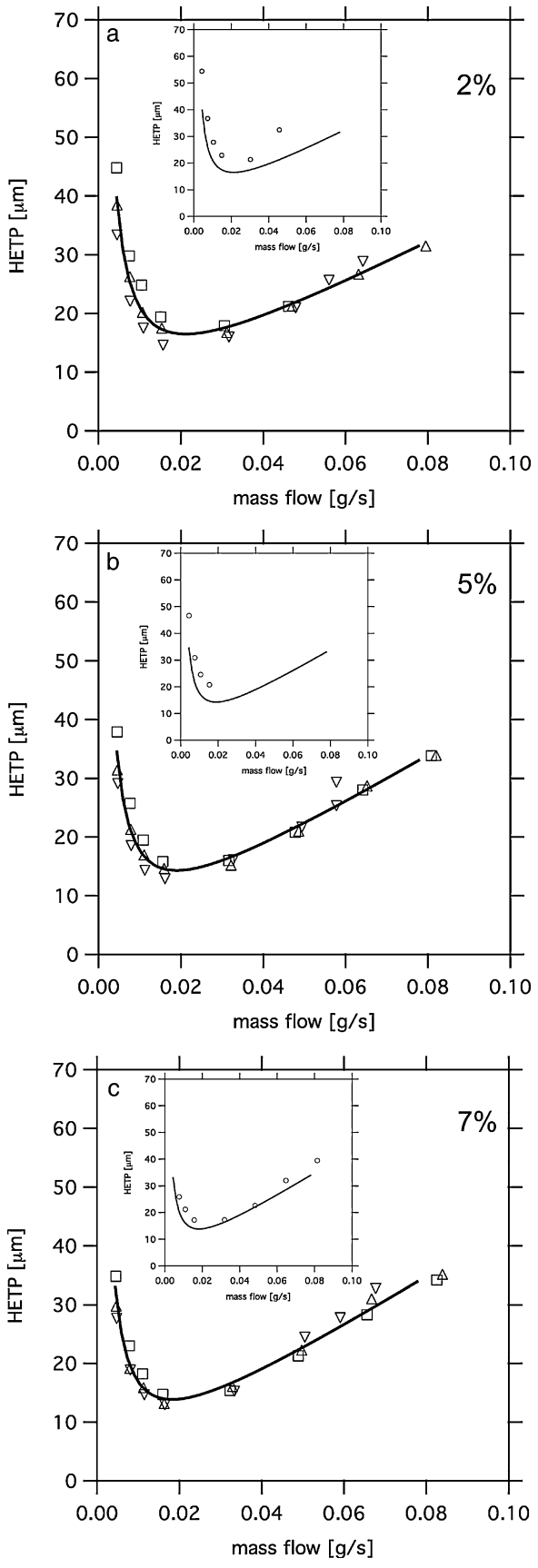

Fig. 38. Experimental values of the column HETP at different organic modifier concentrations. (a) 2%; (b) 5%; (c) 7%. Inlet pressure: □ 150 bar; △ 180 bar; ▽ 210 bar. The solid lines correspond to the average HETP at back pressures of 150, 180, and 210 bar. This average curve is compared to the data at 130 bar in the insets [201], Fig. 4.

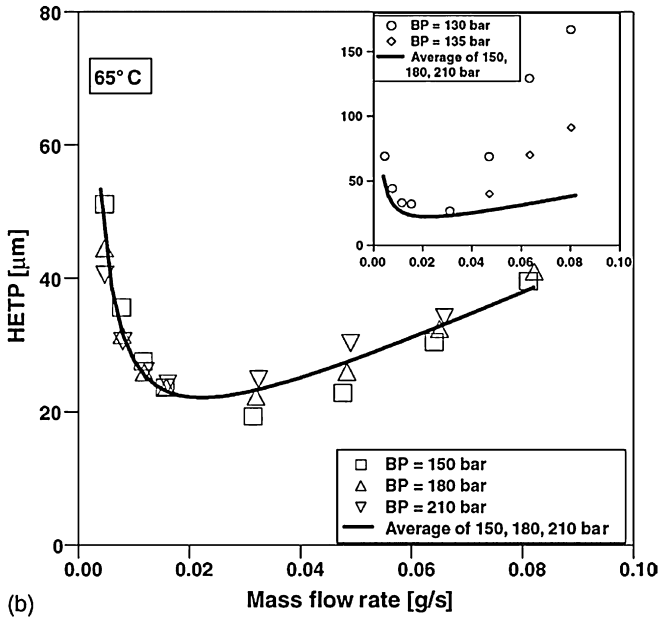

Fig. 39. HETP curves in pure carbon dioxide at 65 °C, at different back pressures. The solid line is the average HETP at back pressures of 150, 180, and 210 bar. The inset compares these average values and the HETP at a back pressure of 130 bar [200].

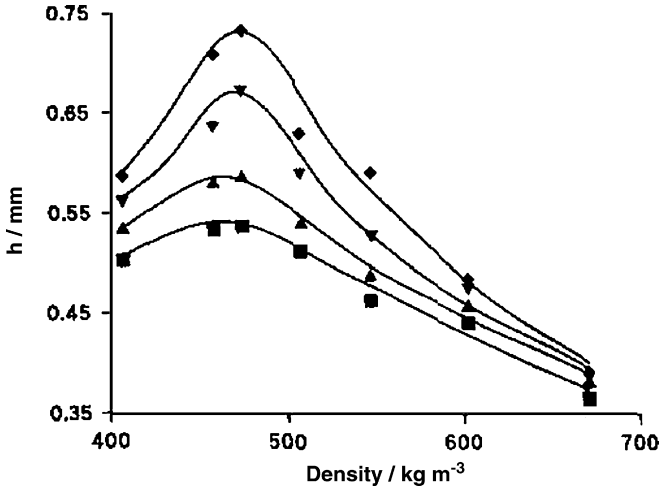

Fig. 40. Plots of the plate height, h, versus the mobile phase density, ρ, at constant mobile phase velocity. Constant naphthalene mole fraction, x_2: ■, $x_2 = 1 \times 10^{-4}$; ▲, $x_2 = 2 \times 10^{-4}$; ▼, $x_2 = 3 \times 10^{-4}$; ◊, $x_2 = 4 \times 10^{-4}$. Temperature 35.0 ° C [296].

causes its cooling, resulting in axial and radial temperature gradients that affect negatively the column efficiency [169,213]. This explanation is consistent with the behavior of the curve at a back pressure of 130 bar with 7% ethanol, since the compressibility of the mobile phase decreases with increasing organic modifier concentration and is much reduced with 7% ethanol. As the back pressure increases beyond 130 bar, its influence on the column efficiency decreases rapidly [201].

The average HETP of a column operated under a given set of experimental conditions can be calculated by numerical integration of the following equation [201]

$$H = L\left\langle \frac{\sigma^2}{t_R^2} \right\rangle = \frac{L}{t_R^2}\int_0^L \frac{H(z)}{v(z)^2}\,dz \tag{142}$$

The van Deemter or another empirical equation can be used for further calculations [1]. Rajendran et al. made this calculation for phenanthrene eluted with solutions of carbon dioxide and ethanol on a column packed with C_{18}-silica particles [201]. The results obtained are in reasonably good agreement with the measured values, although the experimental data suggest a mass transfer resistance term (C term of the van Deemter equation) that is larger than the one calculated. Also, there is a significant deviation between calculated and measured values of the HETP at low mobile phase velocities. Part of this difference may be explained by errors made in the calculation of the diffusion coefficient (for which Eq. (137) was used).

Bartle et al. have shown that the HETP of a column operated under experimental conditions that are close to the critical region increases when the density approaches the critical density [296]. The HETP also increases markedly with increasing solute concentration. This effect decreases with increasing carbon dioxide density beyond the critical density. Fig. 40 shows how the HETP varies with the mobile phase density and with increasing sample size at a temperature ca. 4 ° C above the critical temperature and at constant mobile phase velocity (this velocity was about 10 times the optimum velocity for maximum efficiency at infinite dilution). When columns are operated in the critical region, their HETP is particularly high. At temperatures and pressures beyond the critical region, on the other hand these effects become negligible under analytical conditions. Under preparative conditions, however, even with similar experimental conditions, the effect is more prominent since the diffusion coefficients in SFC fluids decrease rapidly with increasing solute concentrations.

Great progress was recently made in the understanding of the different contributions that combine to cause band broadening in HPLC columns and in the experimental determination of the parameters that control them [150–153,331–334]. These concepts and methods needs to be extended to SFC as well (see Section 8.3).

8.2.3. Influence of the mobile phase velocity on the column efficiency – plate height theory for compressible fluids

Poe and Martire developed a general theory that relates the apparent efficiency of a column, which is provided by a simple analysis of the recorded elution peaks, the local values of the incremental efficiency, and the velocity profile along the column, which is related to the pressure gradient [203]. These authors observed that, since the product of the density and the diffusion coefficients in supercritical fluids is approximately constant, so is the reduced velocity ($\nu = ud_p/D_m$). It is true even when the compressibility of the fluid is significant and the pressure, density, and velocity of the mobile phase vary markedly [6,293,335,336].

There are several different definitions of the column HETP (a parameter that is characteristic both of the column and of the probe solute used). The following ones have proven physical chemistry value, in contrast with the IUPAC definition, which is empirical and would be useless here:

1. The apparent plate height (not local) at any point in the column, measured from the profile of the peak during its passage through the column

$$\hat{H} = z\frac{\tau^2}{t_R^2} \tag{143}$$

where z is the distance travelled, τ is the standard deviation of the peak eluted at distance z in time unit, and t_R the elution time at distance z.

2. If the column is divided into an infinite number of infinitesimally small segments of length l_i, with t_i the time spent by the solute in segment i, and τ_i^2 the incremental increase of the variance during that time, the local plate height at distance z is

$$\tilde{H} = l_i\frac{\tau_i^2}{t_i} \tag{144}$$

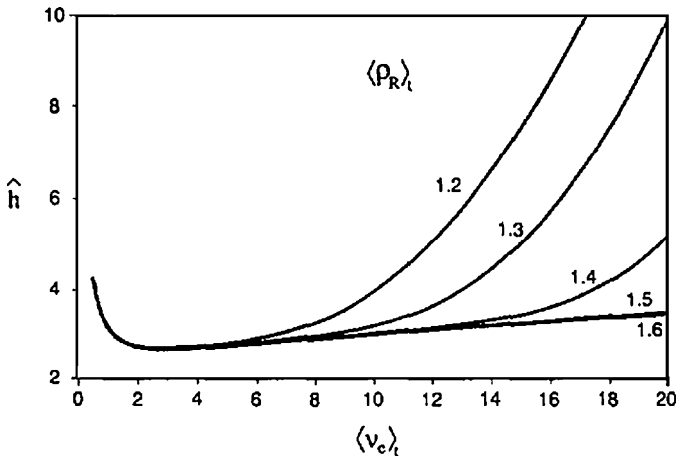

Fig. 41. Predicted effect of the reduced velocity on the efficiency at various mobile phase densities for the elution of naphthalene on a reversed-phase (Perisorb RP-8) silica at 40 °C at different average mobile phase density, $\langle\rho_R\rangle_t$. Column 150 mm × 4.6 mm, packed with 5 μm particles. [203].

3. Giddings showed that $\hat{H}$ is related to the function of local plate heights through [328]

$$\hat{H} = L\frac{\int_0^L(\tilde{H}_i/u_s^2)\,dz}{\left[\int_0^L(dz/u_s)\right]^2} \tag{145}$$

with $dz = l_i$ and u_s the solute zone velocity, $u_s = u_0/(1+k)$. The evaluation of $\hat{H}$ is different in GC, where k is practically independent of the local pressure, and hence is constant, in SFC, where k and u_0 depend significantly on the local pressure, and in HPLC, where the dependence of k on the pressure is linear if not negligible [257].

The column is assumed to be axially and radially homogeneous. Yet, due to the flow of mobile phase and to its compressibility, there are pressure, hence density gradients along the column. The mobile phase flow velocity, the zone migration velocity, its retention factor, and the local efficiency depend on the mobile phase density. So we need to write Eq. (145) in terms of density. Poe and Martire [203] showed that the apparent reduced plate height should be written as

$$\hat{h} = \frac{\hat{H}}{d_p} = \frac{\langle h(1+k)^2\rho\rangle_t}{(1+k)>_t^2\langle\rho\rangle_z} \tag{146}$$

where the brackets $\langle\rangle_z$ and $\langle\rangle_t$ represent the spatial or time average of the enclosed terms, respectively. Although this general equation was applied to GC, SFC, and HPLC, its most important area of application is SFC. In most cases, the carrier gas used in GC behaves as an ideal gas and the result obtained is the same as the one initially derived by Giddings [328]. For HPLC, on the other hand, in most practical situations, the compressibility and the retention factors are small, if not negligible, and the apparent plate height is given by the local plate height equation [203]. Even though HPLC is conducted under increasingly larger pressure drops and it has been shown that the retention factors may vary significantly along the column under such conditions, the consequences are still small and may need minimum corrections.

Based on results from the Schneider group [13] providing the dependence of the retention factors of naphthalene and phenanthrene on the density of carbon dioxide (see Fig. 28) and their diffusion coefficients (see Eq. (131), [293]), Poe and Martire [203] calculated the apparent HETP of a Perisorb RP-8 column as a function of the mobile phase velocity, at different average mobile phase densities for naphthalene (see Fig. 41). The data calculated by them show that the effects of the pressure drop are more severe at low average mobile phase density (see Fig. 41). The effects of a variable density on the apparent column efficiency, on the other hand, would increase with decreasing average particle size. Unfortunately, the paper provided no data to validate these conclusions.

8.3. Detailed procedure of determination of the various contributions to band broadening in SFC

Band broadening in chromatography is caused by the combination of the different contributions due to axial diffusion, eddy dispersion and the mass transfer resistances. Each of these three sources of band broadening contributions is complex; it has been the topic of recent detailed investigations that have resulted in much clarification [1,333,334].

8.3.1. Axial diffusion

Axial dispersion occurs in the stream of mobile phase that percolates through the external porosity of the column bed. It is generally considered as expressed by the classical term $B = 2\gamma_e D_m$, where γ_e is the obstruction factor of the packed bed and D_m the molecular diffusivity of the compound considered. Axial dispersion is driven by the concentration gradient of the solute along the axial profile of its zone. However, axial dispersion can also take place inside the particles (through pore and surface diffusion) since a similar gradient of concentration propagates in both phases along the column axis. The possible influence of diffusion phenomena taking place inside the particles in the axial direction of the column has not been much studied yet, probably because chromatographers have been, until recently, more interested in operating the columns at higher flow rates, i.e. under conditions where axial dispersion contribution to band broadening is insignificant. This issue needs revisiting since modern columns, packed with fine or very fine particles are increasingly used in a velocity range that is moderately higher than the optimum velocity, for achieving maximum efficiency.

The composition of the mobile phase at the interface between the mobile phase that is stagnant in the particle mesopores and the mobile phase that is percolating the external volume, depends on the fluxes of two mass transfer processes, convection around the particle due to the mobile phase stream and particle diffusion due to pore and surface diffusion through the particle. At very high mobile phase velocity, the influence of the former exceeds that of the latter. So the concentration gradient between the particle surface and its center is the same in all directions and the axial diffusion term is given by the classical B term above. At very low mobile phase velocity, in contrast, the concentration gradients between the particle surface and its center depend on the relative orientation of the particle diameter and the stream velocity. This is because the convection flux to the solute in the external mobile phase, at the particle surface, is slower than the diffusion flux across the particle; accordingly, axial diffusion along the particles in the direction of the column axis does contribute significantly to overall axial dispersion. This results in a complex expression [333]. The axial displacements of the band center caused by diffusion and by convection in time Δt are respectively

$$\sigma^2 = 2D_m\Delta t \tag{147}$$

$$\Delta x = u\Delta t \tag{148}$$

The ratio of these displacements is equal to $\sqrt{2D_m/ud_p}$. Since the reduced velocity is given by $\nu = ud_p/D_m$, convection dominates when $\nu > 2$ and diffusion when $\nu < 2$. So, the transition region, in which the contribution of internal diffusion to the HETP is significant, includes most of the region around the minimum of the HETP curve.

8.3.2. Eddy dispersion

Eddy diffusion takes place only in the mobile phase. It is the direct consequence of the uneven distribution of the mobile phase velocity in the immense number of anastomosed channels[2] in the packed bed, with the velocity being maximum in between the particles and zero at their surface, due to viscous drag. Velocity biases are found everywhere in the bed, and at all scales. The anastomosis of the stream lines and molecular diffusion in the radial direction combine to allow the rapid and frequent exchange from rapid to slow pathways and back. Giddings listed up to five groups of contributions to these velocity biases, the trans-channel, short-range inter-channel, long-range inter-channel, trans-particle, and trans-column velocity biases [89,328]. His coupling theory of eddy diffusion is the most rigorous approach available to handle eddy diffusion. However, this division of the column on the basis of the average size of a few selected sub-domains is empirical. It is unclear which of these biases should be omitted depending on the experimental conditions or in which case the contribution of eddy diffusion can be reduced to one single term. Van Deemter proposed a constant term, $A = 2\lambda d_p$. Knox showed that the five contributions proposed by Giddings can be pooled empirically into one, leading to the empirical Knox equation [337] that uses a function of u but provides no clear physical understanding of the function parameters.

The trans-column velocity bias effects may be important. They depend on the packing quality of the column and are hardly affected by diffusion, which cannot operate effectively over long distances. The trans-particle effect, although listed by Giddings as a source of velocity bias, is actually the strict equivalence of the pore diffusion mechanism, discussed later as one of the mass transfer resistances. The flow mechanism does not affect pore diffusion because the intraparticle liquid velocity is zero (stagnant mobile phase) and transfer by diffusion only allows the sample molecules to penetrate into or to leave the particles. This effect should not be taken into account as an eddy diffusion term, otherwise, it would be counted twice in the overall HETP equation. As a result, the overall eddy diffusion reduces to the sum of only three terms (with $i = 1$, 2, and 3) that describe the erratic transfer of the solute by flow and diffusion from different inter-particle fluid channels (trans-channel, short-range inter-channel, and long-range inter-channel):

$$H_{eddy} = \sum_{i=1}^{i=3} \frac{1}{(1/2\lambda_i d_p) + (D_m/\omega_i u d_p^2)} \tag{149}$$

where λ_i and ω_i are parameters that depend on the length of persistence over which the velocity of a channel is affected by anastomosis and its composition by radial diffusion [333].

8.3.3. Mass transfer resistances

The resistances to mass transfer across the column involve several contributions: (1) the resistance across the stationary film of mobile phase surrounding the particles (external mass transfer); (2) the resistance through the porous solid particles, which combines pore and surface diffusion; and (3) the resistance due to the finite rate of adsorption–desorption. Obviously, the classical C term of the van Deemter [338] and of Knox [337] equations is empirical and the different contributions listed should be assessed separately in a more rigorous theoretical approach. The third contribution is generally neglected because, on the surface of the adsorbents used in chromatography, the rate of physical adsorption and desorption is sufficiently fast.

[2] A system of collateral channels providing multiple pathways from a point of the bed to any other one.

Considerable work has been done investigating the mass transfer resistances. All important fundamental work uses the general rate model of chromatography [1]. This model assumes the existence of two different liquid phases, one percolating between the particles of the bed, the other stagnant inside the particles. It assumes a spherical symmetry for each silica particle and includes all relevant contributions of kinetic origin to band broadening in the case considered. There is no general algebraic solution to this model in the time domain but one can be easily derived in the Laplace domain. While this solution cannot be inverted, the various moments of the solution can be derived conveniently. Thus, the measurements of band broadening and the interpretation of the experimental results are based on the moment method [1].

After the pioneering work of Lapidus and Amundson [339] whose results were later simplified by Van Deemter et al. [338] for the rather general case of high efficiency columns, leading to the classical Van Deemter equation, Kubin [340] and Kučera [341] derived the relationships giving the expression of the first few moments of the elution bands under linear conditions. Later, numerous other HETP equations were derived by Giddings et al. [90], Huber [342], Horváth and Lin [343,344], Miyabe and Guiochon [345–347], and Gritti and Guiochon [333]. All these authors used the same approach and derived similar equations that differ by the details of the treatment of the mass transfer resistances. These equations have been reviewed and compared elsewhere [1,348].

The sum of these two contributions is

$$H_{MT} = \frac{1}{3.27} \frac{\epsilon_e^{5/3}}{1-\epsilon_e} \left(\frac{\delta_0}{1+\delta_0} \right)^2 \frac{d_p^{5./3}}{D_m^{2/3}} u^{2/3} + \frac{1}{30} \frac{\epsilon_e}{1-\epsilon_e} \left(\frac{\delta_0}{1+\delta_0} \right)^2 \frac{d_p^2}{D_e} u \tag{150}$$

with

$$\delta_0 = \frac{\epsilon_e}{1-\epsilon_e} [\epsilon_p + (1-\epsilon_p)K] \tag{151}$$

where ϵ_e and ϵ_p are the external porosity of the column and the internal porosity of the particles, respectively, and K is the Henry constant of adsorption of the solute.

Other physical methods, particularly Pulse Field Gradient NMR provide detailed information on the origin, nature and rate coefficients of the various contributions to mass transfer in packed beds of porous particles [150,331,332,349,350].

8.3.4. HETP equation in HPLC

Applications of the HETP equation in liquid chromatography as well as practical methods for the experimental determination of its parameters have been discussed in detail [333,334]. Among the methods of importance are the peak parking method and the pore blocking method. The former permits the accurate measurements of diffusion and dispersion coefficients of solutes and of the obstruction factors of packed beds [307]. The latter involves filling the pores of the particles of an RPLC column with nonane and eluting it with water [351,352]. The combination of the peak parking method, the total pore blocking method, and moment analysis permits the unambiguous measurement of the successive steps of the mass transfer of solutes (axial diffusion, eddy dispersion, film mass transfer resistance, and trans-particle mass transfer resistance), in a wide range of reduced linear velocities.

8.3.5. Current status of HETP studies in SFC

As in HPLC, we assume that the kinetics of adsorption–desorption on the surface of the adsorbent used as the stationary phase is sufficiently fast to make negligible the corresponding contribution to the mass transfer resistances. We also assume that the HETP of the column is given by a van Deemter equation. Bartmann and Schneider [16] showed that, in SFC, this

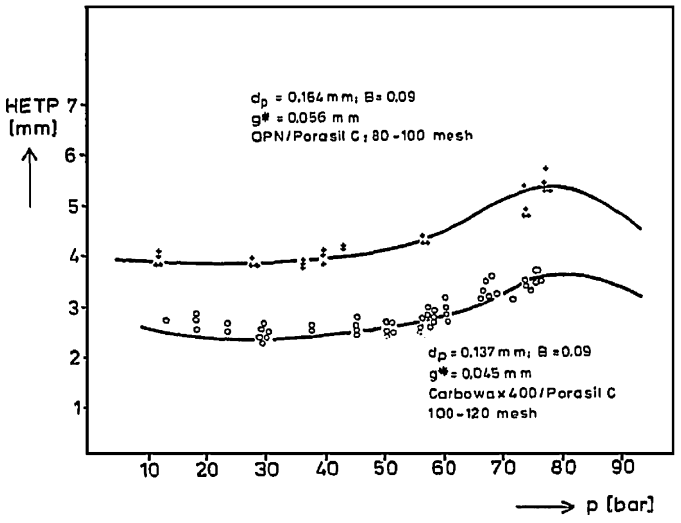

Fig. 42. Plot of a column HETP versus the pressure at constant outlet mobile phase flow velocity [16].

equation could be written as follows

$$H = \lambda \frac{\bar{u} d_p \rho}{\eta} + \frac{1.3 D_m}{\bar{u}} + \frac{1.5k}{(1+k)^2} \frac{\bar{u} d_p}{D_m} F \tag{152}$$

$$H = \left(\frac{B d_p}{Sc} + 1.5k(1+k)^2 F \right) Pe \tag{153}$$

where λ is a numerical coefficient estimated at ca. 0.1, $\bar{u} = L/t_0$ is the average linear velocity of the mobile phase (with L column length and t_0 hold-up time) and D_m is the diffusion coefficient of the solute in the mobile phase. In passing from the first to the second equation, the second term in the RHS of the first one (the axial diffusion term) was neglected. The dimensionless numbers, $Sc = Pe/Re$ or Schmidt number of mass transfer at pressure P, Re or Reynolds number (see Eq. (25)), and $Pe = (ud_p)/D_m$ or Peclet number are all reported to the particle size, as usual. Assuming that the viscosity and the product $D_m \rho$ vary little with the pressure and using values of k previously measured, Bartmann and Schneider calculated the dependency of the HETP on the pressure at constant mobile phase velocity. At low pressures, the first term in Eq. (153) prevails. Under higher pressures, the retention factor decreases and the second term becomes more important. These results are illustrated in Fig. 42. Note the consequences of using large particles: the column pressure drop is small and the HETP large. Modern columns will certainly give different, markedly better results.

8.4. Mass transfer kinetics

The rates of all the mass transfer processes depend on the diffusion coefficients of the compounds involved in the fluid within which they move. For this reason, it is important to know this parameter. A strategy for the determination of the main parameters of the different steps in the mass transfer of solutes in chromatographic columns was recently developed by Gritti et al. [334]. This strategy involves the determination of experimental data using three series of measurements, the HETP of the column in a wide range of mobile phase flow velocity, the peak parking method, and the pore blocking method. These methods are very effective and useful in HPLC and should be easy to apply in SFC but not been, yet.

8.4.1. Determination of the HETP curves

The HETP curves are obtained by measuring the column efficiency in a wide range of mobile phase flow rates. Because peaks always tail to some extent, accurate efficiency data should be derived from measurements of the first and second moments of the recorded peaks [1,346], not from the more conventional peak width at half-height [353]. These data are then fitted to a modified van Deemter HETP model, in which the A term accounts only for the trans-channel [354] and the short-range inter-channel velocity biases [328]. In first approximation, the contributions of the long-range inter-channel and the trans-column velocity biases can be assumed to be negligible for retained compounds. The following modified van Deemter equation is used [333]:

$$H = \frac{2[\gamma_e + ((1-\epsilon_e)/\epsilon_e)\Omega]}{\nu} + \frac{0.01\nu}{1+0.03\nu} + \frac{1}{(1/2\lambda_2) + (1/\omega_2\nu)} + C\nu \tag{154}$$

The first, second, third, and the last terms in the right-handside of Eq. (154) are the longitudinal diffusion term (B), the trans-channel eddy diffusion term ($A_{trans\text{-}channel}$), the short-range inter-channel eddy diffusion term ($A_{SRinter\text{-}channel}$), and the overall solid-liquid mass transfer resistance term (C), respectively. The coefficient Ω is typically around unity for weakly retained molecules [333]. The $A_{trans\text{-}channel}$ term is assumed to be close to that caused by the eddies measured through an ideal ordered pillar array [354]. According to Giddings' estimates, the short-range interchannel coefficients, ω_2 and λ_2, are similar, so we assume $\omega_2 = \lambda_2$ in Eq. (154). This term can be extracted from the fit of the HETP data of low molecular weight compounds to Eq. (154). Note that λ_2 is typically around 0.5 in packed beds of conventional porous particles [333]. The reduced C term is usually in the range 0.02–0.05, provided that frictional heating is negligible [212,352].

The total reduced eddy diffusion term, A, depends on the retention factor of the solutes. The relative importance of the trans-column velocity biases decreases with increasing retention factor because the trans-column concentration gradients, due to the radial heterogeneity of the mobile phase velocity, are relaxed more efficiently with increasing retention time in the column. The ratio, Ω, of the diffusivity of small molecules in the particles to the molecular diffusivity in the bulk phase depends on the particle porosity. The overall C term of small molecules is essentially controlled by the external film mass transfer resistance between the moving eluent in the inter-particle void and the stagnant eluent inside the mesopores (see next section).

As pointed out by Poe and Schroden, there are several ways of measuring HETP curves [183]. The most classical approach, which is used in all the chromatographic methods, GC, HPLC, and SFC, involves raising progressively the inlet pressure while keeping the outlet pressure constant. This has the consequence that the inlet pressure has to be progressively raised, increasing the average density of the mobile phase. This increase is negligible in HPLC and the pressure increase has no effect on retention. This has no more consequences in GC as well, provided that the outlet of the column is at atmospheric pressure; special problems may arise in GC–MS. However, in SFC, retention factors are considerably affected by the mobile phase density and decrease rapidly with its increase. This markedly affects the column efficiency and the experimental data depend much on the variations of the retention factors than on the mobile phase velocity. Keeping the average density of the mobile phase constant while increasing its velocity (i.e., raising the inlet pressure and, in the same time, decreasing the outlet pressure) provides efficiency data that depend only on the mobile phase velocity, making them easier to account for. This approach provides what is called isopycnic (i.e., constant density) plate height data [183].

Fig. 17 compares the efficiencies measured and predicted for a column operated under conditions nearly critical or supercritical. When the column is operated under supercritical conditions, with an average reduced density of 1.5, there is an excellent agreement between the measured and the predicted efficiencies, as usually observed in HPLC, although the column was thermostatted. When

the column is operated under critical conditions, with an average reduced density close to 1.0, the efficiency plot exhibits the same parabolic shape, which is observed for HPLC columns packed with fine particles and operated at high velocities [196–198]. This effect is due to the consequences of the heat adsorbed by the expansion of the mobile phase and to the radial thermal gradient due to this cooling. It disappears when the column is thermally insulated, confirming that the efficiency loss is due to radial temperature gradients caused by the cooling of the mobile phase associated with its expansion [205].

8.4.2. Determination of the dispersion coefficients

The overall longitudinal diffusion of the sample along the column in the absence of any flow rate is a complex combination of solute diffusions in the particle ($D_{eff,part}(\nu = 0)$) and in the inter-particle bulk (D_m). The peak parking method (see Section 8.1.3) provides both coefficients. Knowing them, we can back-calculate the apparent effective particle diffusivity, provided that a model for solute diffusion in the heterogeneous packed bed is available. Two different models could be used, assuming either (a) the particle and the inter-particle diffusion mechanisms act in parallel [310] or (b) the validity of the effective medium theory of molecular diffusion in heterogeneous media of Davis [311]. These methods provide two estimates of the equivalent effective particle diffusivity and of the reduced C_p term in the van Deemter equation.

8.4.3. Pore blocking method

These experiments involve filling the mesopores of a column bed with liquid n-nonane and eluting the peak of a hydrophilic solute with water [351,352,355]. The solute is excluded from the mesoporous volume of the particles and spends the minimum possible time inside the column, the same time as a completely excluded polymer.

Experimental results have shown that the eddy diffusion coefficient does depend on the retention factor of analytes [355]. For example, the A term of a column packed with 5 μm Luna(2)-C_{18} particles for a strongly retained compounds ($k \simeq 16$) was 2.5 while that of an excluded compound ($k \simeq -0.4$) measured after the pores had been blocked was 7.5, three times larger [355]. A similar relative difference was observed for a 5 μm Gemini-C_{18} column [352].

When the mesopores of the particles are blocked, the apparent effective particle diffusivity is zero and the radial dispersion coefficient is minimum. The incremental rate at which the peak variance increases during its migration is maximum. The reduced radial plate height, h_r, across the column diameter is the sum of two contributions, a molecular diffusion term and an eddy diffusion term [356] with:

$$h_r = \frac{2\gamma_e}{\nu} + \gamma_r \tag{155}$$

where $\gamma_e = 0.60$ and $\gamma_r = 0.32$ [356]. The average column radial dispersion coefficient is by definition:

$$\overline{D_r} = D_m \frac{h_r \nu}{2} \tag{156}$$

so,

$$\overline{D_r} = \gamma_e D_m + \frac{1}{2}\gamma_r \nu D_m \tag{157}$$

Under such conditions, the axial solute dispersion through the cylindrical packed column is maximum because the radial concentration gradients that are caused by a heterogeneous radial flow profile distribution (often a quartic flow distribution profile is observed in packed columns [357]) cannot be relaxed rapidly. The difference between the HETP of the column measured for a very weakly retained or unretained compound under pore blocked and unblocked conditions, considering corrections for the instrument variance contribution and for axial diffusion, informs on the importance of the trans-column velocity biases, i.e., on the quality of its packing.

The limiting A term of a packed bed, e.g. the effect of eddy dispersion at infinite linear velocity should not be estimated from the HETP curve of retained solutes because these results are biased by the solute diffusivity across the porous particles. Under retained conditions, surface diffusion contributes significantly to increase the intra-particle diffusivity, speeds up radial mass transfer of the solute from one flow stream-path to the next across the column. In contrast, when access to the mesopore volume is blocked by n-nonane and an unretained solute like nitrate anion is excluded from this volume, neither solute adsorption on the external surface of particles nor diffusion through the particle takes place.

Further measurements of the HETP curves for different compounds permits the assessment of the importance of the contributions of long- and short-range interchannel velocity biases. All these parameters characterize the packing homogeneity of a column. They should have the same values for a given column whether it is operated in SFC or in HPLC. The same methods could be used to measure these HETP contributions in either mode of implementation.

8.5. Coefficients of mass transfer kinetics

The study of band broadening in SFC has so far been based essentially on the use of the simple models of nonlinear chromatography, the kinetic model and the equilibrium-dispersive model, either of which requires the determination of only one parameter, the apparent dispersion coefficient or the rate factor [1]. A first estimate of the former coefficient is easily obtained from the plot of the column HETP versus the mobile phase velocity ($D_L = HL/2t_0$). Compared to HPLC modeling, SFC modeling is more complicated due to the dependence of all the parameters involved, retention factors, mobile phase density and velocity, diffusion coefficients, and column efficiency on both the mobile phase velocity and its average pressure. Like in GC, mass transfer resistances in SFC depend on both the local pressure that controls the diffusion coefficients and the velocity that controls the residence times of molecules in the adsorbed state. In GC these two factors are related through the simple equation of state of the mobile phase, practically that of an ideal gas. In SFC, the equation of state is far more complex (see Section 6) and the details of the mass transfer resistances are still poorly understood. If a kinetic model [1] is modified to account for the dependence of the retention factors on the local pressure (hence on the position along the column), the rate coefficients can be derived from chromatograms recorded under linear conditions (with very small sample sizes) [1]. Alternately, the shock layer theory can provide a procedure applicable to overloaded band profiles that yields average estimates of the apparent dispersion coefficient which are valid at high concentrations [1,358]. Finally, Pulsed Field Gradient NMR may provide estimates of the axial dispersion coefficient [349] and of the rate coefficient of exchange between the mobile phase stream and the solvent stagnant in the particle pores [350]. This method can provide coefficients of mass transfer kinetics in SFC for methanol and other compounds which have NMR signals sufficiently well resolved from that of carbon dioxide.

Although the column efficiency is reported in many papers on analytical and preparative applications of SFC, there are few reports on meaningful measurements of the mass transfer kinetics. Bartmann and Schneider reported that the column HETP depends weakly on the pressure at constant mobile phase velocity [16]. Rajendran et al. showed that the HETP at constant mobile phase velocity decreases with increasing pressure while the rate of the mass transfer kinetics increases under the same condition

[201,223]. Lucas et al. [359] proposed a model for band profiles in nonlinear SFC that is a version of the Thomas model [360], solved by Goldstein [361]. They used the Laplace transform to solve the equations of their model and parameter identification to derive estimates of the model parameters. They applied this model to the extraction of oil from pine resins. Rajendran used the same kinetic model to account for overloaded band profiles of 1-phenyl-1-propanol in SFC [200,362].

Ottiger et al. [223] measured the mass transfer coefficients of 1-phenyl-1-propanol on a cellulose derived chiral stationary phase using a form of the inverse method of isotherm determination and a first-order kinetic equation and lumping all the contributions to mass transfer kinetics into one mass transfer coefficient, k [223]. These authors found that this coefficient increases steadily with increasing modifier concentration but that its dependence on the pressure and the temperature exhibited less clear trends.

9. Nonlinear chromatography

Considerable progress have been made during the last 20 years in the understanding of nonlinear liquid chromatography [1]. A similar albeit less comprehensive level of understanding has been reached in nonlinear gas chromatography [289,363,364]. A comparable level of development of the tools needed to understand, explain, and economically use the phenomena governing SFC is now required. The understanding of nonlinear GC and HPLC which has been accumulated over the years will facilitate investigations of the influences of the various experimental factors involved in the production rate and the yield of separations and purifications performed by nonlinear SFC and the optimization of the instrument design and the experimental parameters. The practical applications of these theoretical results will require a deep understanding of the thermodynamics and kinetics of phase equilibria in SFC. This endeavor should encompass three major areas:

1. The study of the equilibrium isotherms and the mass transfer kinetics in SFC. It is critically important to determine correct values of the parameters controlling the phase equilibria and the rates of equilibration to predict chromatographic band profiles. The practical usefulness of our fundamental results will depend on the possibility to minimize the amount of work necessary to collect the data required for the calculation of practical solutions for new SFC separations.
2. A systematic, quantitative comparison between experimental results and the theoretical predictions derived from different models of nonlinear chromatography, mainly the equilibrium-dispersive [365], the simple kinetic model [360,361], and the general rate models [1]. This comparison should lead to the selection of the models most suitable for the study of important practical problems.
3. Optimization of the experimental conditions for maximum production rate by the various modes of preparative chromatography or for the optimization of any other relevant objective function.

The development of new analytical and numerical solutions to the classical problems of non-linear liquid chromatography is one of the most significant progress made in chromatography during the last 20 years [1]. These results open two lines of work in SFC that should be pursued simultaneously, the thermodynamics of phase equilibration and the kinetics of mass transfer. Theoretical predictions should be checked with experimental results to validate the models, approaches, and methods. Numerous useful applications of these results could then be made.

9.1. Equilibrium isotherms of pure compounds

Accurate knowledge of the multicomponent equilibrium isotherms of the sample components, or at least of those which interfere significantly during their elution and separation, is critical for understanding, interpreting, and predicting nonlinear chromatographic phenomena. Experimental determinations of these isotherms, however, can be extremely difficult because they involve numerous measurements and often consume considerable amounts of products, labor, and time [1,366]. Fortunately, there are proven methods that can, in many cases, predict satisfactory approximations of multicomponent isotherms from the corresponding set of single-component isotherms [1]. This makes the study of single or pure component isotherms important, even in the context of multicomponent separation.

9.1.1. Methods of isotherm determination in SFC

The characteristic of supercritical fluids, of being intermediate between gases and liquids offers the unique opportunity to use measurement techniques typical of those using in either gas or liquid adsorption. The possibility of operating an SFC setup in either a gas or a liquid mode besides from the SFC mode (or unified chromatography) generates scopes of investigation which are otherwise not possible solely in the gas or in the liquid mode. As the possibilities are immense, the present study will highlight only those methods which have been successfully applied to measure adsorption isotherms in the supercritical or near critical state or were applied in the determination of gas/solid or liquid/solid adsorption and have the potential to be applied in any such future endeavor.

From the equilibrium point of view, methods of isotherm determinations can be divided into two categories, static and dynamic methods. Static methods always end with an equilibrium distribution of the solute between the solvent and the stationary phase. In contrast, although local equilibrium is reached in dynamic methods, the entire system may not reach equilibrium. Isotherms are still often measured by static method but to save time and chemicals, single-component isotherms are now preferably measured by dynamic methods that need smaller sample amounts, are faster, and are more accurate than static methods [1]. Broad lists of methods of determination of competitive or single-component isotherms are available [1,367–369].

9.1.2. Static methods

1. *The static methods* measure the isotherm at different solute concentrations by allowing the sample to reach equilibrium with an accurately measured amount of solid phase, in a well stirred container. Although static methods are no longer commonly used in LC, there are reports of their use in SFC, mainly for their greater accuracy under the experimental conditions prevalent in SFC. Su et al. [370] used the static method as a convenient way to measure isotherms of ethyl esters on C18 bonded silica at concentrations beyond the scope of the Langmuir isotherm, something which they could not achieve with the ECP method ("elution by characteristics peaks" [1]) a known but moderately accurate dynamic method), and fitted their data with a BET [371] isotherm (see Fig. 43).
2. *Gravimetric methods* have been employed to measure isotherms under supercritical condition, particularly for precise measurements of the excess isotherms of several species. Rajendran measured adsorption isotherm of CO_2 on polymethyl methacrylate [362]. The method allowed precise measurements of both the adsorption of carbon dioxide and the swelling of the solid phase resulting from the adsorption. Humayun et al. [372] used a gravimetric method to determine the adsorption behavior of carbon dioxide under near-critical conditions. They produced high precision data in the near-critical region and showed that

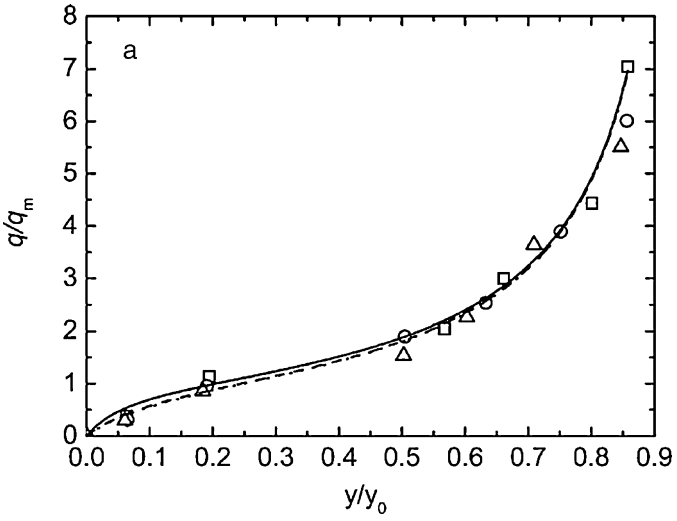

Fig. 43. Adsorption data of DHA-EE atCO_2 density of 0.497 g/mL fitted by the BET equation. □, 318.15 K; ○, 328.15 K; △, 338.15 K; lines – BET equation [370].

the adsorbed phase undergoes a reversible transition very near to the carbon dioxide critical point. They also showed that at high densities the adsorbed phase volume and density become constant and relatively insensitive to temperature. The excess adsorption isotherms of CO_2 on silica and on 13X zeolite in a wide range of temperature and pressure in the subcritical region were measured using a gravimetric apparatus [373,374]. The density of the carbon dioxide was measured simultaneously. The results showed that the most meaningful variable to characterize adsorption is the mobile phase density [66,362,373,374]. The data were interpreted using a model based on the lattice density functional theory and used to analyze the effect of geometric confinement on excess adsorption isotherms under supercritical conditions. Such precise measurements can be critical for developing insight into the adsorption process in SFC.

3. *Other measurement methods* have been frequently used to acquire isotherm data [362] under high pressures, for example piezometry [375,376], volumetry [377,378] and IR spectroscopy [379].

9.1.3. Chromatographic methods

Dynamic methods are more accepted in HPLC for their speed and accuracy over static methods [1], a trend which will likely continue with SFC. In the following paragraphs we list the most important of these methods.

1. *The inverse chromatography method* (IM) has been used in GC, SFC and HPLC. This method has been widely studied in HPLC [380–385]. It consists in minimizing the difference between the experimental band profiles recorded for a compound or a mixture and the profiles calculated for this compound, using an assumed isotherm model and a model of chromatography, usually, the equilibrium-dispersive model. Fast and accurate algorithms are preferred for these calculations, like orthogonal collocation on finite elements (OCFE), the Rouchon model [386], or the Martin-Craig method [385,387,388]. The more efficient the column used, the better the results obtained. Frequently, the shapes of the overloaded band profiles give clear clues suggesting the probably best isotherm model but serious errors might be made if this assumption is erroneous [389]. This method has been used in numerous cases for the determination of liquid–solid equilibrium isotherms in HPLC but less frequently so far in SFC. This method was used by Wenda and Rajendran to measure the isotherms of flurbiprofen on Chiralpak AD-H [225].
2. *The elution by characteristic points* (ECP) method is based on a result of the ideal model of chromatography, that the diffuse boundary of an overloaded band profile is related to the differential of the isotherm, $q(C)$, through the relationship [390,391]

$$t = t_p + \frac{L}{u}\left[1 + F\frac{dq}{dC}\right] \quad (158)$$

where t_p is the width of the injected plug of sample and F the phase ratio. This equation is inaccurate due to a model error, since actual band profiles are more diffuse than those predicted by the ideal model which assumes the column efficiency to be infinite. The error made is not important for small sample sizes but may become large if the column is strongly overloaded. Another error is due to the post-loop dispersion; in a recent publication, a new injection strategy, called CUT-ECP, was proposed to eliminate it [392]. Han et al. [393] used the ECP method to study the adsorption of ethyl esters on silica gel from supercritical carbon dioxide and Peper et al. [394] to determine the equilibrium isotherms of each pure enantiomer of ibuprofen on a chiral stationary phase and predict the band profiles of large size samples.
3. *The FACP method* [395] is similar to ECP, with the difference that the diffuse boundary is the complement to a breakthrough curve instead of being that of a pulse injection. The advantage of this method is that the high concentration range of the isotherm data is less affected by the finite efficiency of the column than the one provided by FA (frontal analysis). Although this method is quite reliable, no application in SFC has been found.
4. *The pulse or perturbation method* (PM) [396–398] in which an isotherm model is postulated, based on the shape of the elution profiles of large samples, and best estimates of the numerical coefficients of this isotherm model are derived from the retention times of a series of small pulses of solutions of the compounds studied eluted on series of successive plateaus of known, increasing concentrations of this compound.

   This method was found to be useful in GC and in HPLC, but a correction for the compressibility of the mobile phase is needed. This correction was neglected by Brunner et al. on the ground that the pressure drop along the column could be assumed to be negligible [399]. On the other hand, it was shown that, for accurate measurements in nonlinear gas chromatography, it is necessary to take this compressibility into account [400]. The method necessary to take the compressibility of a mobile gas phase into account in GC developed long ago [401,402]. It is based on the use of the equation of state of ideal gases. It should be adapted for use in SFC for the same purpose, using an appropriate equation of state. Also, when the plateau concentration increases, the signal noise increases and the perturbation becomes more difficult to detect accurately, especially when the isotherm is anti-Langmuirian, in which case the retention time of the perturbation increases. The technical problems encountered with this method were cogently discussed by Fornstedt et al. [398,403,404].

   The perturbation method was used by Lübbert et al. to measure the equilibrium isotherms of α- and δ-tocopherol between neat silica and a solution of 2-propanol in carbon dioxide [180].
5. *The frontal analysis method* (FA) [395,405–407] uses isotherm data derived from the elution time of the breakthrough fronts of solutions of the studied compound in the mobile phase at known concentrations. This method may be implemented in two different ways. In staircase FA, a solution of the studied component is continuously sent to the column and its concentration is periodically raised in successive steps. Alternately, in plug FA, plugs of solution of finite width are sent to the column, then eluted, and

when the eluent concentration has returned to zero, the operation is repeated, successively increasing the plug concentration. The FA method gives accurate data [408–410], independent of the column efficiency [1,406,407,409]. The technical problems encountered in the application of this method and their solutions were discussed by Gritti [407].

Possibly because of its reliability, the FA method was used by many researchers for isotherm measurements under supercritical conditions. The influence of pressure and temperature on the adsorption of salicylic acid [411] and that of ethyl benzene [412] on activated charcoal were studied with the FA method. The adsorption equilibria from carbon dioxide of pentachlorophenol and hexachlorobenzene on natural clay was investigated with this method. The solubilities of these compounds and their mass transfer coefficients were also measured [413]. Subra et al. [414] studied the adsorption of a mixture of 13 terpenes from supercritical carbon dioxide on silanized silica. Depta et al. [415] measured the adsorption isotherms of cis- and trans-phytol on Lichrospher Si-30 (15 μ m particles), in carbon dioxide with 1.8% of isopropyl alcohol at 313 K, under a pressure of 230 atm.

6. *Mass isotope tracer pulse chromatography*. This method consists in injecting small pulses of an isotopically labeled tracer on a concentration plateau of the same compound and monitoring the elution of these tracer pulses by GC/MS [246,247,250,251]. The tracer pulse method with HPLC/MS detection was recently extended to the more complex measurement of competitive isotherms [416]. The use of this method requires samples of the studied compound that are isotopically labeled. It might be expensive when the synthesis of this compound is difficult. ^{13}C and ^{15}N are the most commonly used stable isotopes. Radioactive isotopes also have been used. When available, pure opposite enantiomers may be used in a similar fashion, provided that a chiral detector is available [417,418].
7. *Empirical or approximate methods*. In 1980, De Jong et al. [419] suggested a simple, approximate method that consists in deriving the coefficient of the second term of the two-term Taylor expansion of the isotherm from the elution time of the concentration C_M, which is given by

$$t_R(C_M) = t_0\left(1 + F\frac{dq}{dC}\right) \tag{159}$$

with F the phase ratio of the column, q and C the concentrations in the stationary and the mobile phase at equilibrium, and C_M the maximum concentration of the elution peak of a narrow rectangular plug injection [1]. This equation is borrowed from the ideal model. If the isotherm were to be parabolic, the peak obtained would be a rectangular triangle. For a Langmuir isotherm ($q = aC/[1 + bC]$), the approximate parabolic isotherm would be $q = aC(1 - bC)$ and the elution profile a rectangular triangle, the profile of which can be used to determine the value of b. Alternately, plotting $(dq/dC) = (1/F)((t_R(C_M)/t_0) - 1)$ versus C for increasing sample size and integrating this curve provides the isotherm in a range of concentrations. This method is similar to the peak maxima method [419,420] but less sophisticated since it affords a simplified isotherm valid only at relatively low concentrations.
8. *Mass spectrometric tracer pulse chromatography*. Strubinger et al. have used mass spectrometric tracer pulse chromatography to measure the equilibrium isotherms of carbon dioxide with different stationary phases as a function of the pressure [250]. They showed that a most accurate determination of the column void volume is critical for the determination of these isotherms but is sometimes difficult to achieve. The adsorption or absorption of the mobile phase itself on the stationary phase makes it difficult to determine the exact volume and composition of the stationary phase. These parameters depend critically on the temperature, the pressure, and the composition of the fluid pumped into the column. The major disadvantages of this method are (1) the need of labeled isotopic probes; and (2) the need of a mass specific detection system. In this context, it is worth mentioning that it was recently demonstrated that underestimating the column void volume in any chromatographic determination of equilibrium isotherms may lead to the assumption of too heterogeneous an isotherm model while overestimating this volume can lead to other erroneous conclusions like assuming multi-layer adsorption processes or solute–solute interactions [421,422].

Due to differences in the practical constraints encountered in GC, HPLC, and SFC and to the dearth of literature on isotherm determination in SFC, it is difficult to predict which method should be recommended. Of all methods discussed here, the inverse method seems to be the most practical, the fastest and most economical of samples, chemicals, and time. It might not be the most accurate, however.

9.1.4. Models of single-component equilibrium isotherms

As in GC and HPLC, we use the experimental not the excess isotherms. The four types of single-component equilibrium isotherms found in chromatography are presented briefly [1,66,366,423–432].

1. Type 1 isotherms characterize ideal adsorption on homogeneous surfaces. These isotherms are the Langmuir [423,424] (Eq. (160)) and the Jovanović [433] models. They are rarely encountered in HPLC or GC because most adsorbents have surfaces that are more or less heterogeneous. The Langmuir isotherm is

$$\Theta = \frac{q}{q_s} = \frac{bC}{1 + bC} \tag{160}$$

where b is the equilibrium constant of the compound considered between the two phases of the chromatographic system and $\Theta = q/q_s$ is the surface coverage. The Scatchard plot is a simple method to determine whether isotherm data fit well to a Langmuir model. The isotherm plot can be linearized by rearranging Eq. (160) as:

$$\frac{C}{q} = \frac{1}{bq_s} + \frac{C}{q_s} \tag{161}$$

If the plot of C/q versus C is linear, the isotherm data should fit well to a Langmuir model, with a slope $1/q_s$ and an ordinate $1/bq_s$.
2. Type 2 isotherms characterize ideal adsorption on heterogeneous surfaces: many such models are available [1,367,368,425]. Many systems of interest in RPLC are satisfactorily accounted for by a bi-Langmuir model [426,427] (Eq. (162)) or a more complex combination of simpler isotherm models that reflects the quilt nature of a surface made of silica and of hydrophobic patches [428]. Note also that the activity coefficients of solutes in both the solution and the adsorbed state vary slowly with the concentration, as proved by Carr et al. [429] and confirmed by calculations [366] based on the UNIFAC model [430]. This complicates isotherm adsorption behavior, particularly for highly soluble compounds for which the accessible concentration range is wide.

   The typical bi-Langmuir isotherm model is

$$q = \frac{a_1 C}{1 + b_1 C} + \frac{a_2 C}{1 + b_2 C} \tag{162}$$

   where a_1, a_2, b_1, and b_2 are numerical parameters.

   Other useful isotherms are the Toth [434], the Freundlich [435], and the Langmuir–Freundlich isotherms [1].
3. Type 3 isotherms characterize nonideal adsorption on homogeneous surfaces. Depending on the intensity of the

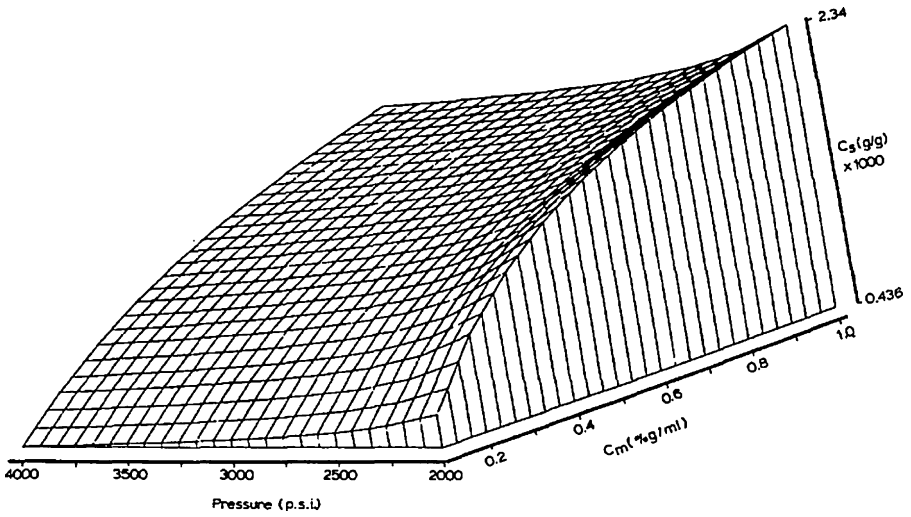

Fig. 44. Equilibrium isotherm of ethyl acetate on Partisil-10, as a function of the pressure of carbon dioxide [290]. Plots of the equilibrium concentration of ethyl acetate in the adsorbed phase (z) versus its concentration in the mobile phase (x) and the pressure of CO_2 (y).

adsorbate–adsorbate interactions, the isotherm is convex upward or S-shaped. Common isotherm models are the quadratic (Eq. (162)), the extended BET, and the Moreau isotherm [1]. The quadratic isotherm [431], suggested by simple statistical thermodynamics, is useful to account for isotherms having an inflection point [432].

$$\Theta = \frac{q}{q_s} = \frac{C(b_1 + 2b_2C)}{1 + b_1C + b_2C^2} \tag{163}$$

The Moreau isotherm is another form of the quadratic isotherm [436].

The third degree Hill isotherm [180] also belongs to this type of isotherm. It corresponds to more complex interactions between the adsorbent surface and the molecules of the component considered:

$$q = \frac{q_s}{3}\frac{b_1C + b_2C^2 + b_3C^3}{1 + b_1C + b_2C^2 + b_3C^3} \tag{164}$$

4. Type 4: Nonideal adsorption on heterogeneous surfaces: Among the many complex models, the best known are the Martire [66] and the bi-Moreau isotherms [1]. High accuracy data are required to obtain reasonably precise estimates of the numerous parameters of these models.

9.1.5. Single-component equilibrium isotherms in SFC

There are few references in the literature that are relevant to preparative SFC. The few that are available use the same isotherm models and the same methods of measurements as those used in HPLC.

In order to investigate the reasons for the significant reduction of the retention factors in SFC which is observed when increasing the concentration of an organic modifier, Lochmüller and Mink measured the adsorption isotherms of dry ethyl acetate on a 200 mm × 4.6 mm column packed with Partisil-10 silica, in supercritical CO_2 at 60 ° C and under pressures between 2000 and 4000 psi (flow rate, 3 ml/min) [290]. They used for this purpose the method suggested by De Jong et al. [419] (see Section 9.1.1). The isotherms obtained for ethyl acetate follow Langmuir behavior. The concentration of ethyl acetate in the stationary phase at equilibrium with a given mobile phase concentration decreases with increasing pressure of carbon dioxide [290]. The monolayer capacity is about a third of what is measured for ethyl acetate in the system made of the same silica and n-hexane. The stationary phase is nearly saturated for a mobile phase concentration of 1% (see Fig. 44). Using the same method, Lochmüller and Mink measured also the adsorption isotherms of methanol and 1-hexanol on the same silica column in supercritical CO_2 at 40, 60, 80, and 100 °C, and at different densities [253]. The isotherms also follow Langmuir behavior. The molar saturation capacity of methanol is larger than that of 1-hexanol but the maximum surface area covered by 1-hexanol is larger than that covered by methanol. As a consequence of the increase in the saturation capacity, the retention factors of solutes interacting with silanol groups decrease with increasing concentration of methanol in carbon dioxide.

The isotherms of some pure compounds were measured and used to calculate band profiles in mobile phases made of supercritical CO_2 modified with methanol, ethanol, or 2-propanol. These measurements were made assuming that the solutes do not compete with the organic modifier contained in the mobile phase, although the latter are significantly adsorbed under the experimental conditions of SMB [80,223,399]. Actually, competition for adsorption on the stationary phase of the organic modifier with the sample components is the mechanism through which these modifiers reduce the retention of the sample components and permit the achievement of elution of these compounds and their separation within a reasonable time. In HPLC, it had been shown that the influence of the adsorption of the organic modifier on that of the solutes can be neglected only if the strong solvent is much less strongly adsorbed than the solutes [437]. The same rule probably applies to nonlinear SFC but its validity has not yet been established nor have the retention factors of most organic modifiers when eluted with carbon dioxide on conventional stationary phases been measured.

Depta et al. [415] measured adsorption data of cis- and trans-phytol on Lichrospher Si-30 (15 μ m particles), in carbon dioxide with 1.8% of isopropyl alcohol at 313 K, under a pressure of 230 atm, modeled these data with a quadratic isotherm. They obtained good agreement between calculated and measured elution band profiles for SFC separations carried out either on a single column or in an SMB. Lübbert et al. used the perturbation method to measure the adsorption isotherms of α- and δ-tocopherol on neat silica, from a 5% solution of 2-propanol in CO_2 at between 160 and 260 atm. They found convex downward isotherms and modeled them with a third degree Hill isotherm [180] (see Eq. (164)). The amount of tocopherol adsorbed at equilibrium with a given mobile phase concentration decreases with increasing pressure, which is explained

by the increasing density of the mobile phase, hence its increasing solubility.

Brunner and Johanssen used the same model to account for the isotherms of caffeine, ibuproprofen, phytol, and vitamin D_3 on various adsorbents, at pressures between 130 and 260 atm, at 313 K [399]. Jha and Madras [80] modeled the adsorption isotherms of naphthalene, biphenyl, 2,6-dimethylnaphthalene, anthracene, hexachlorobenzene, pentachlorophenol, salicyclic acid, and DDT on soil, ODS (C_{18}-bonded silica), activated charcoal, and a zeolite in a range of pressures and temperatures in the supercritical region. They found that the data fitted well to a Langmuir model (see Eqs. (160) and (161)). They also found that the heat of adsorption was independent of the structure of the solute molecule, because it is governed by weak van der Waals interactions [80]. Accordingly, only one experimental value of the equilibrium constant of a compound on any adsorbent at a known temperature and pressure should be sufficient to predict this constant in a wide range of pressures and temperatures. This would be a remarkable result, should it be confirmed.

Strubinger et al. [250] measured the partition equilibrium isotherms of carbon dioxide on silica, on C_{18}-bonded silica (packed in conventional HPLC columns) and in SE-30 poly(dimethylsiloxane) coated in an open tubular column, which is not consistent with the observation of Wasen et al. regarding the long term stability of open tubular columns used in SFC [13] as a function of the temperature and the pressure in the sub- and supercritical regions [250]. The isotherm of CO_2 on SE-30 has a maximum close to the critical pressure, then decreases toward a concentration of ca. 25% above 100 bar. The adsorption isotherms on the two surfaces also have maxima close to the critical pressure. However, the amplitude of these maxima decrease with increasing temperature above the critical temperature and the corresponding pressure increases. The adsorption follows Langmuir behavior in the subcritical region. In the supercritical region, the isotherms plotted as a function of the carbon dioxide density exhibit a normal temperature dependence but an inverse pressure dependence.

9.2. Equilibrium isotherms for mixtures

The simultaneous presence of several compounds dissolved in the mobile phase modifies the adsorption behavior of each one. The volume of the adsorbed layer on the surface of the stationary phase is limited and compounds that are simultaneously present in the mobile phase can either compete for access to this layer or interact together and possibly associate. Usually the simultaneous adsorption of two or several compounds is competitive. Most often, molecular interactions between adsorbates are small and the dominant effect is the limited surface area of the adsorbent surface, resulting in the crowding out of each compound by the other ones; the intensity of this effect increases with increasing retention and increasing concentration of the compounds considered in the solution. However, in a few rare cases, the adsorption of two compounds may be cooperative [438,439].

The study of separation problems requires the use of competitive isotherms [1]. Simple models of single-component isotherms are easily extended to competitive isotherms but these must be consistent with the Gibbs isotherm equation [440]. If a competitive Langmuir isotherm is derived from the single-component isotherms, this requires that the components have the same column saturation capacities [358]. Otherwise, a correction must be made. Radke and Prausnitz [440] extended the ideal adsorbed solution (IAS) theory of Myers and Prausnitz [441] for gas–solid equilibria to liquid–solid equilibria. The extension is valid for SFC. The adsorbate–adsorbate interactions are neglected and the extend of adsorption of each compound is limited by the availability of adsorption sites. The spreading pressure of all the adsorbed compounds must be the same [399,441].

Understanding retention mechanisms in SFC begins with understanding the adsorption of organic modifiers. Strubinger et al. measured the adsorption isotherms of mixture of carbon dioxide and methanol (2–4%) on silica and C_{18}-bonded silica at different temperatures in the pressure range up to 150 bar [251]. The amounts of CO_2 and methanol adsorbed at equilibrium decrease with increasing pressure and can be extremely large around the critical conditions of the mobile phase. Under the conventional experimental conditions used in SFC, the amounts of both carbon dioxide and methanol adsorbed are significant, so these compounds become important parts of the stationary phase.

9.2.1. Methods of determination of competitive isotherms

The most important methods are

- *The inverse method* (IM) [380–385], which is conceptually the same as that described in the section on pure component isotherms (see Section 9.1.1). The elution band profile of the multi-component sample calculated with an assumed set of competitive isotherms is compared with the experimental band profile and the isotherm coefficients are adjusted to minimize the difference.

  Using the inverse method, Ottiger et al. estimated the competitive equilibrium isotherms of the 1-phenyl-1-propanol enantiomers [223]. They modeled them using a binary competitive Langmuir isotherm with independent saturation capacities for the two enantiomers [1]

$$q_i = \frac{H_i C_i}{1 + K_R C_R + K_S C_S} \tag{165}$$

  where R and S stand for the corresponding enantiomers, H_i is the Henry constant of enantiomer i, K_i is its equilibrium constant, and i is either R or S. This isotherm model assumes that only the two enantiomers compete for adsorption. The adsorption of the modifier and carbon dioxide are implicitly involved through the dependence of the isotherm coefficients on the pressure of carbon dioxide and on the concentration of the modifier. The band profiles of the pure compounds calculated using the isotherm model agree well with those recorded. However, the agreement for binary mixtures, although still fair, is not as good between the experimental band profiles and those calculated from the competitive isotherms. It seems that the Henry constants were overestimated. At a constant modifier concentration, the Henry constants of the enantiomers decrease with increasing pressure or density of the mobile phase. At low or moderate pressures, the decrease is nearly linear. At constant mobile phase density, the Henry constant increases with increasing organic modifier concentration [223]. The isotherms tend to deviate less from linear behavior in a given concentration range when the concentration of the organic modifier increases. The saturation capacity clearly increases with increasing concentration of the organic modifier.

  A better isotherm model for the adsorption of enantiomers on chiral selective phases is the model developed by Fornstedt and Guiochon [442].

$$q = \frac{q_n^\star b_n C}{1 + b_n C} + \frac{q_s^\star b_s C}{1 + b_s C} \tag{166}$$

$$q = \frac{q_n^\star b_n C}{1 + b_n C} + \frac{q_r^\star b_r C}{1 + b_r C} \tag{167}$$

  where $q^\star$ is the saturation capacity of the corresponding type of sites, nonselective for the S or selective for the R enantiomers and the indices n, s, and r correspond to the nonselective adsorption sites and to the adsorption sites selective for the S and the R

enantiomers, respectively. It is obvious that for the enantiomers (R) and (S), the following conditions are true:

$$b_{ns,R} = b_{ns,S} = b_{ns} \quad \text{and} \quad b_{s,S} \neq b_{s,R} \tag{168}$$

Further information can be found in the literature on nonlinear or preparative chromatography of enantiomers [1].

- *Breakthrough curves* [1]. The column being in equilibrium with the pure mobile phase, a stream of the mobile phase containing known concentrations of the compounds studied is substituted to the eluent and the composition of the mobile phase exiting the column is monitored. The procedure is repeated to construct the isotherms [1]. The interpretation of the results is complicated because the different components do not elute simultaneously and the composition of the eluent exiting the column is the same as that of the inlet only when the experiment is finished, but it remains different during the elution of the intermediate plateaus.
- *Perturbation method* [1,180,438]. The adsorbent is equilibrated with a solution of the compounds considered at known concentrations. Small samples of pure carbon dioxide or of the compounds studied are injected and isotherm data are derived from their retention times.
- *Gravimetric method*. Ottiger et al. [443] have measured binary and ternary adsorption of carbon dioxide, methane and nitrogen on coal using a gravimetric–chromatographic technique.

9.2.2. Applications

The influence of pressure and temperature on the adsorption of salicylic acid [411] and that of ethyl benzene [412] on activated charcoal were studied with the breakthrough method. The adsorption equilibria from carbon dioxide of pentachlorophenol and hexachlorobenzene on natural clay were investigated with the same method. The solubilities of these compounds and their mass transfer coefficients were also measured [413]. Peper et al. determined the equilibrium isotherms of each pure enantiomer of ibuprofen on a chiral stationary phase using the ECP method and band profiles of large size samples. The data were fitted to a cubic Hill-isotherm [394].

Using the pulse method, Ottiger et al. estimated the competitive equilibrium isotherms of the 1-phenyl-1-propanol enantiomers [223]. They confirmed their results obtained with the inverse method (see earlier, Inverse Method).

Lübbert et al. successfully built the competitive isotherms of α- and δ-tocopherol (see above) using the single-component isotherms that they had determined by the perturbation method and applying the IAS theory [180]. These authors prepared a few binary mixtures of different relative composition; they determined the amount of each component that is adsorbed as a function of its concentration in the mobile phase; and they compared these isotherms to those calculated from the competitive isotherm. The excellent agreement observed validates the approach and the application of the IAS theory in the case considered [180].

9.3. Mass balance in SFC

The theory of HPLC at finite concentrations, its applications, the relationships between band profiles, multi-component equilibrium isotherms, and mass transfer resistances are well known [1]. The calculation of elution band profiles requires the solution of the differential mass balance of each component of the sample. This equation is a partial differential equation of the second order which has algebraic solution only in simplest cases. Algorithms for the calculation of numerical solutions are available. Their use requires that all the values of the coefficients involved be known.

Understanding the migration of bands and the progressive evolution of their shape is more complex in SFC than in HPLC because (1) the mobile phase used in SFC is highly compressible; (2) all its properties depend on the pressure, particularly its viscosity and density; and (3) a significant inlet pressure is required to force the stream of mobile phase through the column. So, a satisfactory model of SFC must include mass balance equations for the mobile phase components, which are needed to account for the variations along the column of (1) the mobile phase velocity; (2) the retention factors; and (3) the diffusion coefficients. Numerical solutions of this model require accurate equilibrium isotherms and mass transfer data for the components involved in a wide range of pressure, temperature, and mobile phase composition. Finally, an equation of state for the supercritical fluid is needed.

How the retention factors of selected compounds vary with temperature and pressure is often reported [80,16] but often separately, as they are generally in HPLC. In this latter method, in contrast with SFC, the pressure has minimum influence on the retention factors, due to the low compressibility of the mobile phase. Few papers give the isobaric or isothermal adsorption equilibrium constants of the probes studied [16]. Even fewer papers give the competitive adsorption isotherms of separated compounds [59,174,200,201,223].

Cretier et al. reported unusual band profiles for large size samples of vanillin, which they attributed to an anti-Langmuirian isotherm. However, the possibility of a sorption effect (see Section 7.2) was not examined [444]. The possible influence of the large concentration of sample (vanillin) on the local density of the mobile phase was also ignored, probably because the experiments were carried out far from the critical region.

9.3.1. Comparison of the Mass Balances in HPLC, GC and SFC

Some of the basic assumptions made in HPLC to write the mass balance equation [1] are invalid in GC and SFC because, in both these cases, the mobile phase is compressible and, due to the significant pressure gradient along the column, the density and many other characteristics of the mobile phase vary markedly along the column; so does the equilibrium constants of the solutes between the two phases, the coefficients of their equilibrium isotherms, and the partial molar volume of the solute in the mobile phase, which is strongly (GC) or significantly (SFC) larger than its partial molar volume in the stationary phase. The same difference is negligible for low molecular weight compounds in HPLC and still small for proteins [257]. All these effects make the problem more complex and more difficult to solve in GC and SFC than in HPLC.

First, due to the compressibility of the mobile phase, which causes its density to decrease monotonically along the column, two mass balance equations are needed in SFC, the first one for the solute, the second one for the mobile phase. Depending on its nature, the mobile phase may be adsorbed on the stationary phase, in which case its equilibrium constant between stationary and mobile phase is a function of the local pressure. If the mobile phase is a mixture, a mass balance equation is needed for each of its components and competitive equilibrium may have to be considered, involving these components and the solute. An equation of state is needed to determine the pressure profile along the column at constant mass flow rate of each compound involved (the presence of solutes at finite concentration might affect the local density of the mobile phase). Finally, we need proper equations to account for the influence of the pressure on the partial molar volumes of the solute in both phases and on the mobile phase viscosity.

The pressure gradient along modern columns packed with fine ($d_p \simeq 5\ \mu$m) or very fine ($d_p < 2\ \mu$m) particles is important along SFC columns, in spite of the low viscosity of the mobile phase used. This mobile phase is essentially made of carbon dioxide, which is highly compressible, so its decompression absorbs heat. The cooling effect of the expansion of the supercritical fluid along the column [362,183] increases the complexity of the modeling of SFC separations. It causes the formation of axial and radial temperature

gradients that can dramatically affect band profiles and column efficiency [169,181–183,187,188,190,213]. The results of Rajendran show small but significant differences between the recorded profiles and the profiles calculated with a transport-dispersive model assuming a high rate of mass transfer [200,362]. However, this model assumes an isothermal column, neglects the thermal effects of the mobile phase expansion, and the fact that the isochoric heat capacity of supercritical fluid varies widely across the critical region of the phase diagram. The consequences of this property have not yet been elucidated [362]. The mass balance for SFC must take these contributions into account.

9.4. The mass balances models in chromatography

For simple models of band propagation, the differential mass balance equation is written for a slice of length *dz* of the whole column. For complex and more accurate models, it is written separately for the mobile phase that percolates through the column bed and for the packing material, including the stagnant mobile phase impregnating the pores and the adsorbed layer of mobile phase and solutes [1]. The simple models include the ideal model, the equilibrium-dispersive model, and the transport model. The complex models are the different versions of the general rate models that include different rate equations, depending on the particularities of the studied problem.

9.4.1. The ideal model in SFC

The ideal model assumes that the mobile and the stationary phases are constantly in equilibrium, hence that the rate of mass transfer in the column is infinite, but axial dispersion is zero. Consequently, the column efficiency in infinite. This model is not realistic because actual columns have a finite efficiency. It is useful only because it isolates the effects of thermodynamics on band profiles and facilitates their understanding. The mass transfer kinetics and axial dispersion blur and smooth the band profiles predicted by the ideal model.

9.4.2. The equilibrium-dispersive model in SFC

This model is the simplest realistic model of chromatography. It assumes that the mobile and the stationary phases are constantly in equilibrium but that all the contributions of the mass transfer resistances to band broadening can be lumped into an apparent axial dispersion term, with a coefficient, $D_L = HL/2t_0$, where H is the column plate height, L its length, and t_0 its hold-up time [1,445–447]. This apparent dispersion coefficient accounts for the finite column efficiency. This coefficient is determined empirically.

The ED model provides excellent results in the study of many practical problems encountered in HPLC [1]. It is well suited for studies of nonlinear SFC because mass transfer kinetics in supercritical fluids are fast (the column efficiency in analytical SFC is as high as or higher than in HPLC) [362]. In contrast with HPLC, a mass balance equation is needed for each mobile phase component, whether retained or not: since the mobile phase density depends on the local pressure and temperature, their local concentrations vary along the column and their migration velocities increase.

9.4.3. The transport-dispersive model in SFC

This model assumes a linear relationship between the rate of change of the concentration of solute adsorbed on the stationary phase and the difference between the concentrations of this solute in the stationary and the mobile phase [1]. Several equations are possible. The mass balance equation of the transport-dispersive model has an algebraic solution in the linear case [339], which eventually leads to the van Deemter equation relating the column characteristics, the mobile phase flow velocity, and the column efficiency [338]. The transport-dispersive model was used in SFC by Rajendran et al. to calculate the overloaded band profiles of the enantiomers of 1-phenyl-1-propanol on Chiralcel-OD in overloaded elution and the eluent composition profiles in an SFC-SMB [200,201,362]. This model was also used by Lucas et al. [359].

9.4.4. The general rate model in SFC

This model is the only rigorous one. It consists of a family of models sharing a few common features [1]. Mostly developed for liquid-solid adsorption processes, the general rate models account for all significant contributions to band broadening of kinetic origin: axial dispersion, mass transfer between the stream of mobile phase percolating through the bed and the eluent stagnant inside the porous particles or external mass transfer [448,449], diffusion across this stagnant fluid or pore diffusion, surface diffusion, adsorption/desorption kinetics. Practical applications of the general rate models raise large difficulties due to the number of its parameters, most of which are difficult to measure accurately. For this reason, the more simple *equilibrium-dispersive* or *transport-dispersive* models (ED) are preferred.

9.5. Practical modeling of SFC

The modeling of preparative separations by SFC requires the calculation of the profiles of the mobile phase properties along the column, the determination of the equilibrium isotherms of the components of the mixture studied, the derivation of estimates of the parameters of the mass transfer kinetics, the calculation of elution band profiles, the optimization of the experimental conditions of the separation, and the validation of these results.

9.5.1. Calculations of the mobile phase properties along the column

First, a combination of: (1) the continuity equation expressing the constancy of the mass flow rate of eluent along the column; (2) the equation of state of the eluent; (3) the Ergun equation that relates the flow rate along a column slice, the pressure gradient and the local characteristics of the column and the mobile phase; and (4) the pressure dependence of the eluent viscosity, provides a relationship between the mass flow rate and the pressure gradient, which varies along the column. Integration of this equation relates the flow rate and the difference between the inlet and the outlet pressures of the column. It also yields the profiles along the column of: (1) the local pressure; (2) the local density of the mobile phase; (3) its velocity; and (4) its viscosity. Calculations using different state equations should be performed for carbon dioxide with different modifiers (methanol, ethanol, 1- and 2-propanol, n-pentane), on packing materials with different average particle sizes and on monolithic columns. Comparisons between the results of these calculations and experimental values of the measured dependence of the hold-up volume of the column on the flow rate and the pressure difference between the column ends may provide effective tests of the reliability of the various state equations. Such a study would provide a sound basis for the selection of equation of state most suitable for use in SFC.

Knowing the profile of the local density of the mobile phase along the column permits also the calculation of the profiles of the local equilibrium constants between the two phases (hence, providing the profiles of the Henry constants and the retention factors along the columns). Integration of the retention factor profiles provides the experimental retention factors. Systematic measurements of the dependence of the retention factors on the pressure difference between the column ends, for a number of compounds on different packing materials made of neat silica and C_{18}-bonded silica of different average particle sizes packed in columns of dif-

ferent lengths could provide further tests of the reliability of the equation of state and of the other models used.

9.5.2. Calculation of band profiles in SFC

The mass balance of a compound in the equilibrium-dispersive model for SFC is analogous to that used in HPLC, the main difference being that the equilibrium constant, the mobile phase velocity, and the apparent dispersion coefficient all vary along the column. Due to the important variation of the local density of the mobile phase, a mass balance for the mobile phase is also needed. A mass balance for the organic modifier is also necessary if the retention of this additive on the stationary phase is not small compared to that of the compound studied. Programs must be written to solve the system of mass balance equation and calculate the profiles of elution bands. The results of these programs must be validated by comparing the elution band profiles of pure compounds, then of multi-component samples and those calculated for the same experimental conditions, using the equilibrium isotherms and mass transfer kinetics data measured independently. In principle, this work is similar to the one that we recently did in nonlinear, non-ideal HPLC, but with the difference that the physico-chemical properties of the mobile phase vary considerably along the column.

In many cases, however, the variation of the mobile phase density along the column is small or moderate. This is particularly true under supercritical conditions. Typical examples are provided by Ottiger et al. [223], who operated their column with $\Delta\rho < 0.2\%$, and Rajendran et al. [201], who operated their columns under such conditions that $\Delta\rho < 1.6\%$ or 0.9%. Then, it is possible to use with a small but acceptable error a simplified equation in which it is assumed that the variation of the pressure and the density along the column are

$$\frac{\partial C_i}{\partial t} + F\frac{\partial q_i}{\partial t} + \frac{\partial (uC_i)}{\partial z} = \frac{\partial}{\partial z}\left(D_{a,i}(\rho)\frac{\partial C_i}{\partial z}\right) \quad (169)$$

9.5.3. Validation of the Calculated Elution Profiles

Systematic measurements of the retention factors, column efficiencies, and resolutions of pairs of compounds eluted with various solutions from columns packed with different materials, involving several retention mechanisms, should provide most valuable information on SFC. Equilibrium isotherm data of single-components and binary mixtures under a wide range of experimental conditions and at different temperatures and pressures, and the modeling of these data will inform on retention mechanisms. Comparison between isotherms measured in HPLC and in SFC with the same columns would provide new, useful clues on the differences between the retention mechanisms involved in these two modes of chromatography. The following systems could be suggested: the enantiomers of propranolol, alprenolol, and metoprolol on the cellulase protein CBH I immobilized on porous silica [407,417,442,450]; 1-phenyl-1-propanol and 1-indanol on cellulose tribenzoate coated on porous silica [408–410,451]; Tröger's base on amylose tri-(3,5-dimethyl-phenyl carbamate) coated on porous silica [452,453]. Previously published data could provide a basis for quantitative comparisons of the performance of preparative SFC and HPLC. Finally, the comparison of band profiles recorded in overloaded elution of these binary mixtures at different compositions will provide useful validation of the postulated retention mechanisms and of the model of nonlinear SFC.

A theory of optimization of the experimental parameters of a preparative SFC separation could then be developed. The production rate of a component of interest, its degree of purity, its recovery yield and the concentration of the collected fractions are the major criteria that characterize the performance of a preparative separation. The main operational parameters of a preparative unit are the column length, the particle size of the packing material, the mobile phase composition, its velocity, the inlet and outlet pressures, the temperature, and the sample size (with the column diameter affecting only the production rate).

10. The important questions that remain unsolved

The literature reviewed here shows that the phenomena involved in SFC are qualitatively well understood and that many implementations of SFC separations have been successfully made, particularly in the analytical realm. The behavior of columns used in SFC under nonlinear conditions still raises a number of questions which have not been solved, if ever understood and raised. It is not possible to predict the results of significant changes in the experimental parameters nor to calculate the optimum values of the set of parameters that maximize the production rate and/or the recovery yield or minimize the consumption of mobile phase.

A list of the important unsolved questions follows

1. Which is, among the many possible equations of state that are available, the one that best accounts for the experimental values of the column hold-up times and the retention times measured in a wide range of temperatures, pressures, and mobile phase compositions. What is the one that is the most practical to use?
2. What are, among the many methods available for the determination of equilibrium isotherms for single-components and for multi-component mixtures, those that provide the most accurate data? the fastest results? What are the main sources of errors and what is the reproducibility of common methods?
3. How do the isotherm coefficients depend on the pressure, the temperature, and the concentration of organic modifiers?
4. Is it possible to apply present theories (e.g., IAS, RAS) to calculate competitive isotherms for pairs of compounds, mostly enantiomers? What precision can be expected depending on the type of isotherms that account for the behavior of the pure compounds and the similarity between the isotherm models of the compounds involved?
5. Do the simple equilibrium-dispersive and kinetic models of chromatography provide numerical solutions that are consistent with experimental band profiles in SFC? What precision can be expected? Should the general rate model be used instead?
6. Could band profiles be calculated with only an equation system accounting only for the equation of state of the mobile phase and the equilibrium isotherms? Or would a system of equations accounting also for the adsorption of the organic modifier be necessary and sufficient?
7. Would it be necessary to include also the influence of the changes of partial molar volumes of the components and the modifiers with the local pressure? What is the actual importance of the sorption effect?
8. Is it possible to calculate the values of the optimum experimental conditions for maximum production rate, with or without constraints (e.g., a specified recovery yield) for a given compound, as a function of the characteristics of the mixture (feed) and of the chromatographic system, knowing all what we know?
9. Are there significant thermal effects in SFC? Under which sets of experimental conditions can columns be considered as radially and axially isothermal? How far from the critical conditions should they be operated? Can the cooling effect due to the expansion of the mobile phase compensate the heating effect due to the friction of the eluent against the bed? A detailed study of the potential heat effects in SFC columns packed with

fine particles and of their possible partial compensation is needed.

10. What effects could the possible thermal effects have on the column efficiency?

11. Experimental issues

Numerous descriptions of instruments can be found in the literature. Some of them are devoted to analytical applications, others to more specific tasks such as the determination of equilibrium isotherms, implementing the frontal analysis (FA), perturbation (PM), and/or profile analysis (aka ECP) [399]. The latter designs involve two columns operated independently but coupled, so that the second column can be used to analyze fractions of the eluent of the first one, e.g., for calibration purposes in the determination of competitive isotherms with the FA or PM methods. Instrumental problems involved in preparative chromatography were discussed by Perrut [42] and by Cox [454].

11.1. Safety

Although conventional HPLC instruments are operated under higher pressures than SFC instruments, the risks generated by the latter are much higher than those due to the former. The risks caused by handling fluids under high pressures does not actually originate from the pressure reached itself but it does essentially come from the energy stored in the compressed fluid. This energy is proportional to the compressibility of the fluid, so it is much higher with gases than with liquids. A considerable energy is stored in a large SFC vessel (e.g., storage tanks, columns, fraction recovery tanks) so particular attention should be paid to the quality of the design and construction of preparative SFC units and to their maintenance. In certain countries, vessels for SFC or SFE fell under formal pressure regulations and require frequent maintenance and testing. Operators must be shielded from the pumps, tubings, and valves used in SFC instruments to limit the risks associated with the brutal rupture of these containers (improperly called explosion in common language). Leaks involving scalding water, suffocating carbon dioxide, and burning acidic or corrosive fluids may not be much more probable in SFC than in HPLC but they are potentially far more dangerous.

Carbon dioxide is not a chronic poison but breathing air containing more than **1** % may be dangerous in an industrial surrounding because it may cause drowsiness or anxiety and discomfort [455]. The intensity of these effects increase with increasing concentration. Other contaminants may increase discomfort. The US OSHA states that the average exposure for healthy adults during an 8-h work day should not exceed 5000 ppm (0.5%). For short-term (under 10 min) exposures, NIOSH recommends a limit of 30,000 ppm (3%). NIOSH also states that carbon dioxide concentrations exceeding 4% are immediately dangerous to life and lethal if the concentration exceeds 10% as this stops breathing almost immediately. For this reason, the rooms where SFC instruments are operated should be well ventilated and there should be warning devices wherever carbon dioxide is stored or used in significant amounts. People should never be alone close to an SFC instrument.

Careful, detailed attention should be paid to the proper cleaning and maintenance of the SFC instruments [456]. This is particularly true for the large-scale instruments used in preparative chromatography but applies to analytical instruments as well. Consideration of these operations, their procedures and constraints must be involved in the design of instruments. Dead-ends and other zones difficult to clean up, wash or swipe should be avoided. Draining of the solvents used for periodic clean-ups must be rapidly completed. Preventive maintenance should be planned and done carefully. The operation of high-pressure equipment requires a high level of reliability and the fulfillment of drastic safety requirements. All sensors should be calibrated periodically and safety sensors continuously logged. Certain critical parts must be changed periodically, e.g., the check-valves and membranes of pumps, the autoclave closure systems, the gaskets, the sintered disks, which may get plugged and deform, then break, the automatic valves that control the process operation.

11.2. Control of the experimental conditions

11.2.1. Temperature regulation

It is most important to be able to accurately set and control the column temperature. The closer the column temperature to the critical temperature of the mobile phase, the smaller should be the fluctuations or drifts of the column temperature, due to their large influence on the density of fluids near their critical point [13]. The column oven should hold a thermal exchanger located upstream the sampling device and the loop of the sampling valve. Temperature gradients along the column should be checked and monitored by placing temperature sensors along the column. Sufficient time must be allowed for thermal equilibration before using the column for meaningful chromatographic work. Radial temperature equilibration is slow. During this time, radial thermal gradients exist and they affect the radial distribution of the viscosity and the velocity of the mobile phase, with deleterious effects on the column efficiency.

11.2.2. Pressure and flow rate regulation

The convection of the mobile phase in chromatography is characterized by two important parameters, the mobile phase velocity and its density. The first one affects the column efficiency and the separations achieved; the second, the equilibrium constants and the separation factors. They need to be regulated separately. Three parameters are relevant to discuss mobile phase flow rates in chromatography, the inlet and the outlet pressures and the flow rate. Due to the finite compressibility of all fluids, only the mass flow rate, not the volume flow rate is constant along a column. This flow rate can be suitably regulated by using a metering pump kept at constant temperature. It can also be regulated by combining regulators for two of the following three parameters, the inlet pressure, the outlet pressure, and the flow rate. These different approaches have been studied.

In liquid chromatography, the compressibility of the mobile phase is neglected, so only the flow rate needs to be regulated, which is done by the pump of the instrument. The inlet pressure depends on the flow rate. The outlet pressure is usually atmospheric but it can easily be set at values far exceeding the atmospheric pressure when needed. It suffices for that to connect a long piece of a narrow tube at the detector exit, providing that the detector cell can stand the increased pressure achieved there. This method has long been used in liquid chromatography to determine the influence of the local pressure on retention factors and equilibrium constants [457]. It permits the easy operation of columns with outlet pressures up to 200 atm. In gas chromatography, either the inlet pressure or the flow rate is regulated while the outlet pressure is atmospheric. Since columns are often operated in temperature programming, the flow rate regulation is preferred but may be difficult to achieve properly for open tubular columns.

In SFC, the outlet pressure must be kept well above atmospheric pressure to obtain a sufficiently large average mobile phase density in the column and a moderate variation of this density along the column. Two solutions have been used, a flow rate regulation upstream and an outlet pressure regulation or a flow rate regulation upstream, and a flow rate resistance placed downstream the column, with its outlet at the atmospheric pressure. The flow rate regulator is usually a pump.

The drawback of flow rate regulation without back-pressure control is that both the column inlet and the outlet pressures increase with increasing flow rate. The column average pressure can be set independently of the flow rate but only provided that the inlet and outlet pressures be properly adjusted. Because retention factors depend on the local pressure, this somewhat hinders the flexibility of the instrument and makes difficult conventional measurements of the column efficiency which should be done at constant retention factor. The importance of this drawback depends on the viscosity of the mobile phase and on the column permeability. The problem is very different for analytical applications and for physico-chemical investigations. In the former case, once a method has been developed – and that will be longer and more difficult than in HPLC – the flow rate is kept constant and the reproducibility of the acquired data is easily achieved, provided that the pump is stable, its setting is reproducible, and that neither the column nor any connection or tubing can become obstructed, e.g., by packing material or particles in suspension in the feed or the eluent. Then, accurate measurements of the inlet and outlet column pressure will suffice. In the latter case, the measurements should be made at constant average mobile phase density along the column when varying progressively the mobile phase flow rate.

Sandra et al. [64] recently showed that the simple combination of flow rate regulation upstream and a flow rate resistance downstream could be applied in SFC chromatography. These authors carried out impressive separations, using as the mobile phase mixtures of liquid carbon dioxide, methanol or water, and possibly other additives, which were obtained by merely regulating the mobile phase flow rate. They combined a metering pump and a mixer to supply a constant volume flow rate of the mobile phase to the column. This arrangement is quite satisfactory when the detector operates at the column outlet pressure. Two detectors that are important in SFC, however, must be operated under pressures much lower than the column outlet pressure, the mass spectrometer and the evaporative light scattering detector. The flow rate is no longer regulated in the downstream connecting tube between the column and the detector, the expansion of carbon dioxide may result into phase separation taking place in this tube and resulting in signal instabilities [458]. Chester and Pinkston [458] proposed the use of a stream of a make-up fluid of regulated composition and pressure, provided by an auxiliary pump. This stream is mixed with the column eluent and sent to the detector. The experimental conditions are set at such values that the T-mixer is at a constant pressure and that phase separation does not take place in either the T-mixer or the downstream connecting tube. The schematics of these different solutions are illustrated in Fig. 45. Because the behavior of ternary mixtures is mostly unknown, it is advisable to use the mobile phase modifier as the solvent in the stream of make-up fluid [458].

Accurate flow rate or pressure programming might require a pressure regulator at the column outlet or, better, at both ends of the column, with all the difficulties associated with the use of outlet flow rate regulation. Finally, the expansion of the mobile phase at the column (or detector) outlet and the release of carbon dioxide should be made in a proper container, allowing separation of the modifiers and additives from carbon dioxide and the safe exhaust of this gas to a hood, avoiding its accumulation in the laboratory (see Section 11.1).

11.2.3. Programming

The retention factors in SFC depend much on the temperature and the pressure, essentially through the influence of these parameters on the density of the mobile phase. The most important changes in the retention factors take place in the inflection region of the isotherms, i.e., in the vicinity of the critical point. For practical reasons, it is easier to operate at a temperature about 10 °C higher than the critical temperature, particularly for separations carried out using pressure or flow rate programming or done in gradient elution with programming of the concentration of organic modifiers; also, raising linearly the pressure at a moderate speed is recommended [13]. What is required is a gradual increase in the solubility of the sample components in the mobile phase.

When the inlet pressure or the column temperature is increased, the mobile phase density varies. Under steady-state conditions, the mass flow of the mobile phase is constant along the column, so the product of the local mobile phase density and the local velocity remains constant. At constant temperature, the density of the mobile phase increases with increasing local pressure. The purpose of programming, in contrast to steady-state, aims at accelerating the elution of the most retained components of the analyzed sample. For this purpose, the temperature may be increased at constant mass flow rate of mobile phase, which, under certain circumstances may increase the retention by decreasing the mobile phase density. Alternate solutions consist in increasing the mobile phase velocity at constant average density of this mobile phase or in increasing the density of the mobile phase, in order to decrease the retention factors. The latter option is the most effective by far.

To increase the flow rate, the pressure difference between the inlet and the outlet pressures must be increased, which may be done at constant inlet pressure, in which case the average column pressure decreases and retention factors increase, or at constant outlet pressure, in which case the average column pressure hence the density increase and the retention factors decrease, or at constant average column pressure, hence average density of the mobile phase, leaving the retention factors nearly constant. Keeping constant either the inlet or the outlet pressures of the column being easier than keeping constant the average column pressure, one of the first two options is usually preferred. Constant mass flow rate of the carrier gas has become the favorite implementation of gas chromatography in temperature programming. The same technical approach could probably be adopted in SFC but it is not practical with packed columns since only slow increases in the temperature are consistent with a nearly homogeneous radial temperature, hence with keeping a reasonable value of the column efficiency.

11.3. Sampling and sample introduction

Conventional HPLC sampling valves are recommended. Syringe injection as was done in GC would be too dangerous, if ever possible, given the high inlet pressure used in SFC and the fragility of glass syringes. Coym and Chester have traced a major source of inaccuracy in SFC to the evaporation of the mobile phase from the injection loop [459]. The loop is then filled with gas instead of liquid, as it is in HPLC, where the same injection system is used. This is a major source of loading problems and of imprecision, explaining the lack of reproducibility of peak areas [459]. Taking proper steps to make sure that all gas is purged before injection of the sample usually result in a precision comparable to that achieved in HPLC.

To increase the sample loading capacity in SFC when the sample solubility in the mobile phase is limited, Yamauchi et al. suggested a combination of sample injection and solvent extraction followed by SFC analysis [460]. They recommended injecting the sample in a small vessel packed with solid (non porous) particles and extracting the sample components by stepwise increase of the pressure in the vessel. The sample can also be mixed with these particles, avoiding the use of a solvent. The solubility of heavy components increasing with the pressure of the SFC mobile phase, the progressive extraction of most components is possible. The residual, insoluble components can be recovered, extracted and analyzed by HPLC.

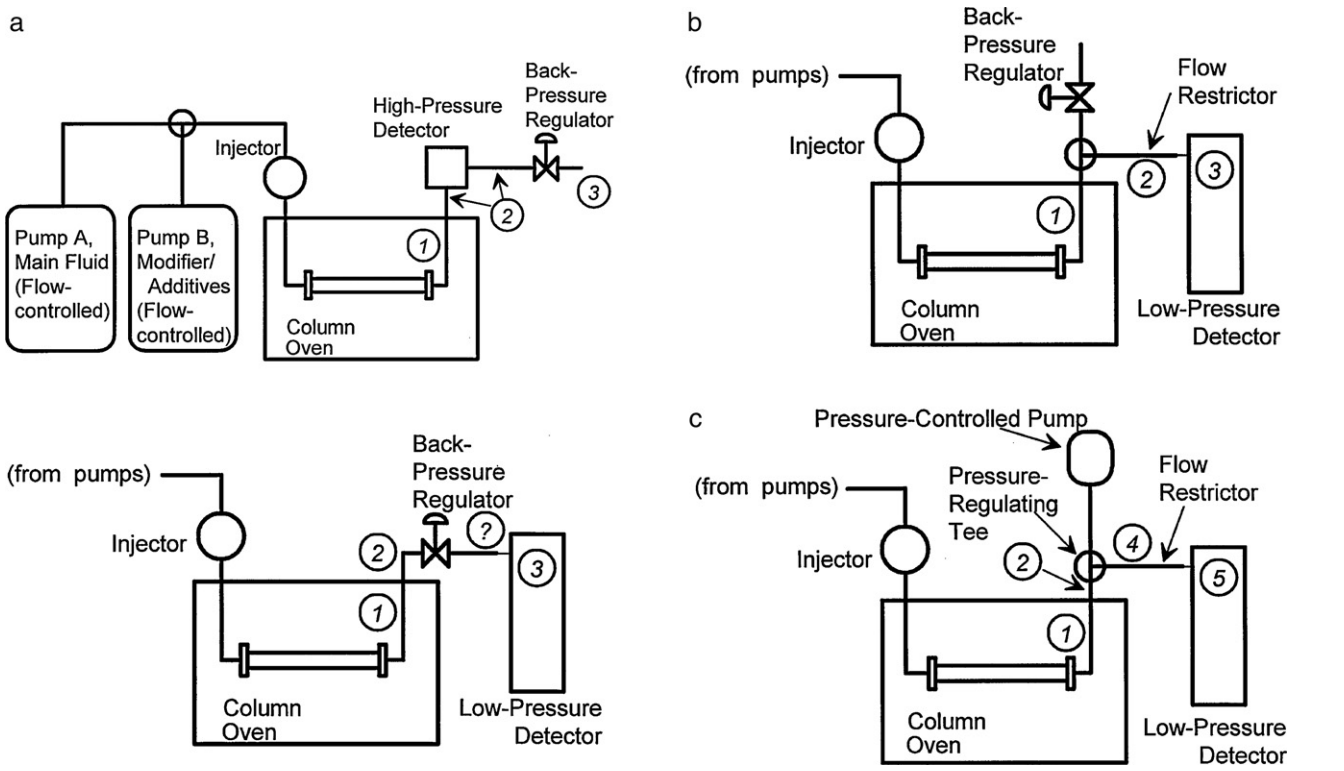

Fig. 45. Regulation of the mass flux of mobile phase in SFC. Left, Top: Schematics of conventional regulation of the flow stream. Left, Bottom: Schematics of conventional flow rate regulation with low-pressure detectors. Right, Top: This instrument uses a pressure-regulated vent; the tee below the pressure regulator operates as a flow splitter. Right, Bottom: The instrument uses a pressure-regulated make-up flow (provided by a pressure-regulated pump) working with the stream from the column into a restrictor leading to the detector inlet. The pressure in the T-mixer is regulated by the make-up pump [458].

11.4. Detection

Several detectors have been used in SFC. Most conventional detectors of HPLC are convenient. Optical detectors such as the UV–vis spectrophotometric detector, the diode-array UV detector, infra-red spectrophotometric detectors or the refractive index detector require the availability of a cell able to operate under pressures of at least 200 bar. These cells are usually available. The mass spectrometric detector requires a suitable expansion chamber. These detectors can be used with most mixtures of sub- or supercritical fluids and organic modifiers. In contrast, the flame ionization detector (FID), which has been used in SFC by numerous authors [461–463] does not give useful signals in the presence of large concentrations of organics. It is a useful detector when the mobile phase contains only carbon dioxide, water, argon, or even nitrous oxide (the most dangerous mobile phase, which should be used only when absolutely needed and with great caution [10]).

The response of the UV-detectors is usually not linear, particularly in the measurements of isotherm data and in SFC, when sample concentrations tend to be large. So, calibration curves are necessary and different methods have been developed for this purpose, particularly in HPLC [394,464–466]. The same methods can be used in SFC. Ottinger et al. [223] suggested the following equation to correlate concentration and detector signal (s)

$$C = b_1 \ln \frac{b_2}{b_2 - s} \tag{170}$$

where b_1 and b_2 are numerical coefficients. This simple equation involves only two positive coefficients. When working with expensive compounds, it is worthwhile to minimize the amounts needed, hence to derive the calibration curve from the profiles of overloaded injections performed when determining equilibrium isotherms using the inverse method. This can be conveniently done by minimizing the sum of square of errors defined as

$$J = \sum_{k=1}^{N} \left(\frac{C_k^0 V^0 - Q \int C_k(t)\,dt}{C_k^0 V^0} \right)^2 \tag{171}$$

where C_k^0 is the concentration of the sample of rank k injected in the loop of volume V^0, Q is the amount of sample in the loop, and $C_k(t)$ is the corresponding elution profile. Minimization of J provides the best values of b_1 and b_2. Obviously these coefficients are functions of the experimental conditions. If the value of J is too large, a different, possible more complex equation should be used instead of Eq. (170).

As recently pointed out by Berger and Fogleman [467], it is most difficult to perform trace analyses in SFC, at least when using the UV or another spectrophotometric detector. The main reason for which SFC provides less sensitive detection is the relatively large noise of the signal. The response of spectrophotometric detectors is sensitive to changes in the refractive index of the mobile phase, because fluctuations of this index affects the refraction angles hence the amount of light reaching the light detector at the exit of the detector cell. Refractive index is most sensitive to the density of carbon dioxide, and also to the pressure and temperature [468]. This sensitivity is such that fluctuations of the pressure at the exit of the conventional pumps used in SFC are the source of the noise observed, much larger in SFC than in HPLC because the same relative pressure fluctuations affect much less the refractive index of a conventional liquid than that of a fluid in the critical region [467]. Sun et al. provided extensive data on the refractive index of carbon dioxide and its mixtures with ethanol in a range of concentrations from 0 to 0.35 mole fraction, as a function of temperature and pressure, as tables and figures [468]. Berger and Fogleman [467] showed that the noise can be dramatically reduced by separating the two func-

tions of the pump, using a typical compression pump as used in SFC equipments to feed an HPLC pump used merely as a metric pump to transfer a constant flow rate of eluent to the column head, with minimum pressure noise.

Most manufacturers of SFC units used to have kits that allow the FID to replace the standard UV/vis detector. This option seems to have disappeared since the use of organic modifiers has become nearly universal. The critical issue is the decompression of the high pressure water and/or carbon dioxide stream when it must be switched from the SFC condition to those necessary for the FID. The CO_2 evaporates during this exchange as the pressure is reduced and the temperature increases. Corrosion by hot concentrated solutions of carbon dioxide in water may be a problem and may render necessary the use of titanium. Fogwill et al. described a system that can overcome these obstacles [286]. These modification can be carried out in the following way. The outlet of the column will be connected to a dead volume stainless steel tee union. If a large flow rate is expected, this tee may be fitted with different diameter fused silica tubing. One side of the fitting will be attached to the FID while the other is attached to a waste container designed to accept high pressure and temperature water/CO_2. Usually these containers are designed as cyclone separators as described by Zhou et al. [461]. By choosing the proper ratio of tube diameters the control of the flow into the FID can be maintained. Initial optimization of the FID would have to be carried out. Miller recommends setting the initial flow rates of hydrogen gas and air to the routine flows of 30–40 mL/min and 300–400 mL/min, respectively [469]. Yet both the inlet flow of hydrogen and air should be checked and optimized periodically, as recommended by Buser et al. [470]. The response factors would also require investigation. Even though the FID response factors has been extensively researched by both Dietz [471] and Ettre [472], the experimental conditions under which SFC could be run to make practical the use of a FID, using water modified by CO_2, or conversely, should be carefully tested to ensure its maximum accuracy.

The evaporative light scattering detector (ELSD) should be easier to use in SFC than in HPLC due to the ease of vaporization of the mobile phase after its nebulization. Numerous applications of the ELSD have been reported [123]. Deschamps et al. separated a series of ceramides under subcritical conditions and reported that the response of the ELSD was improved by addition of equimolecular amounts of triethylamine and formic acid to the eluent [473]. Lesellier et al. separated skin lipids on a column that was not compatible with these additives, so they added them downstream from the column [474]. Carbohydrates and various lipids separated by SFC were also detected with ELSD. The major problem encountered in the use of the ELSD in SFC is phase separation of the eluent in the tube connecting the column and the detector, in which considerable expansion of the eluent takes place [458]. The use of a stream of make-up fluid of properly selected and regulated composition and flow rate permits avoiding the instabilities of the detector signal that phase separation may cause (see Section 11.2.2).

A variety of mass spectrometers have been used as detectors in SFC, e.g., quadrupole and time of flight instruments. The ability to carry out fast data acquisition is important. Because the outlet pressure of an SFC column is not always constant, particularly in the cases of pressure or flow rate programming, the split ratio of the mobile phase does not remain constant when the eluent is split and sent to two different detectors. This might cause difficulties with mass-flow sensitive detectors, like the FID and the MS.

11.5. Fraction collection and product recovery

The problems raised by the recovery of the purified or separated products are very different depending on the scale of the production considered. This is related to the characteristics of carbon dioxide, which is highly toxic in large concentrations and practically not at low concentrations, which is not very expensive and can be vented to the atmosphere for low flow rates but should be recycled for economic and toxicity reasons for large flow rates [475]. They also depend on whether the eluent is pure CO_2 or contains a significant amount of a modifier.

The recovery of the purified compounds from the fractions collected at the end of an SFC column is not straightforward. The fractions could be collected and stored under pressure, then gradually depressurized, in which case collection could be complete if the decompression is made slowly enough [37], which is time consuming, but difficult to avoid because flash vaporization of liquid carbon dioxide is endothermal and generates aerosol mists that carry away part of the products and are difficult to collect. Rapid depressurization leads to the freezing of a large fraction of the eluent or rather of its content, although losses of up to 25% were observed by Heaton et al. when they directed the separated fractions of a mixture of benzoic, phthalic, tri- and tetra-carboxylic benzene separated by SFC to a trap [476]. They attributed these losses to the formation of aerosol mists escaping the traps. A similar problem arose in preparative gas chromatography, a separation process that has been nearly abandoned [477]. The slow cooling of the stream of purified fractions in a tube arranged as a heat exchanger provided recovery yields in excess of 95%. Centrifugation of the mist could also provide excellent recovery. Heaton et al. [476] could achieve high recovery yields of 95% or more by bubbling the rapidly decompressed eluent through a small volume of methanol. The presence of an organic modifier in the eluent may also helps in increasing recovery yields. Warming up the trap could also be an option but has to be done carefully to avoid losses of the vapor.

The feed components need to be separated from the eluent once collected at the column exit. One of several different processes or a combination of several can be used [399]. These include pressure and/or temperature changes, adsorption, membrane separation, or, when the mobile phase contains an organic modifier, a reduction of its concentration. Generally, a decrease of temperature alone is insufficient to recover a sufficient proportion of the product but it can increase much the yield afforded by other means. A drastic pressure reduction separates the carbon dioxide from the organics that it contains. However, this process wastes much energy as the fluid must be recompressed; furthermore, it would deliver the product in solution in the organic modifier, which may be acceptable only for the production of small amounts, in laboratory applications or in many pilot development studies. An adsorption process during which the carbon dioxide remains supercritical is much more economical [478]. However, the product must be recovered from the adsorbent and this delicate operation must be carefully considered and well thought out.

11.6. Columns

Although open tubular columns similar to those used in gas chromatography have been successfully used in SFC and have permitted the achievement of numerous difficult analyses [40,479,480], this approach is now abandoned and there are now many more similarities between SFC and HPLC than between SFC and GC. The considerable advantages of open tubular columns in GC do not convey well to HPLC nor to SFC. Packed columns used in HPLC give excellent results in SFC [45]. Fluids used in SFC dissolve the films of nonvolatile polymers that are used in GC, so the conventional packed or open tubular columns of GC are impractical, unless the film is cross-linked to a moderate degree, to make it really insoluble [13]. Adsorbents such as porous silica, alumina, titania, carbon, or molecular sieves have been used with success. The most common packing materials are those used in HPLC, chemically bonded

porous silica. Because the viscosity of mobile phases are low, fine particles can easily be used without requiring high inlet pressures [35].

Sie and Rijnders noted that increasing the polarity of the stationary phase in SFC (e.g., with carbon dioxide as eluent or as largest eluent component) increases the separation of sample components by functional groups [481]. This was long considered as consistent with SFC being primarily a sophisticated version of normal phase HPLC, when analysts were reluctant to add modifiers to the mobile phase. It is clear now that mixed mobile phases, with moderate concentrations of an organic modifier, provide excellent separations of a wide range of polar compounds. Berger and Berger reviewed recently the wide range of columns and stationary phases used in SFC, most borrowed from HPLC, and of the few specifically made for SFC separations [35].

Practical applications of chromatography often require the simultaneous separation of several components, particularly of enantiomers from each other and from numerous other components of a synthetic mixture. Also, it is often difficult to predict which chiral stationary phase will provide a satisfactory resolution for an unfamiliar pair of enantiomers, in which case it is convenient to check rapidly the separations provided by different columns. Welch et al. modified a commercial instrument with addition of a system of six-position high-pressure connecting valves each controlling a bank of five different columns and a pass through line [482]. This system permits the rapid screening of 10 different columns and of 15 different combinations of columns, providing easy, rapid screening of column arrangements for the separation of complex mixtures.

In preparative SFC as in preparative HPLC, axial compression columns are preferred because the bed homogeneity and stability is easier to achieve and maintain [42].

11.7. Mobile phases

High-density gases (in their subcritical state), mixtures of such gases and organic solvents (modifiers), mixtures of supercritical fluids and organic solvents, or of supercritical fluids have been used as mobile phases in SFC. The most popular fluid by far is carbon dioxide. Other compounds like nitrous oxide (N_2O) and ammonia have also been used. Unfortunately, they are both dangerous to handle, gaseous ammonia being a violent toxic and nitrous oxide an unstable, strong oxidant [10], which should be avoided for this reason. At first glance, nitrous oxide seems to be quite an attractive SFC fluid because its critical properties are similar to those of CO_2 and it has a dipole moment and is a much better solvent of organic compounds. However, its mixtures with organic compounds are potentially explosives and serious accidents are reported in the literature [10,9]. Organic modifiers should **never** be used with nitrous oxide, only small samples of organic compounds, at low concentrations could ever be considered and used only with extreme caution. Nitrous oxide should never be used as a mobile phase in preparative SFC. Argon and xenon have been used as supercritical fluids and have shown advantage when infra-red absorption is used for detection, since they are monoatomic.

Most commonly used modifiers are hydrocarbons (propane, cyclohexane, and benzene); low polarity organic solvents like dichloromethane [140], ethyl acetate, acetone, tetrahydrofuran, and diisopropyl ether; and polar solvents commonly used in HPLC, like methanol, 2-propanol, and acetonitrile. The use of mixtures of ethanol and carbon dioxide (50–75% carbon dioxide) has been recommended by Dos Santos [129,483] to replace aqueous solutions of acetonitrile for the separation of e.g., nucleobases. All these solvents can be used at temperatures up to ca. 100 °C or higher but thermal stability limits the use of many of them at higher temperatures.

Water mixed with carbon dioxide is used at high temperature. The surface tension of water decreases rapidly with increasing temperature beyond 150 °C, causing a much higher solubility of organics in water.

11.7.1. Enhanced fluidity mobile phases

Numerous authors use as the mobile phase mixtures of carbon dioxide and of solvents conventional in HPLC. The concentration of the organic solvent is usually higher than 50%, which is why the approach has been given a different name to underline the fact that the essential role of carbon dioxide in this case is to enhance the fluidity of the eluent and increase the diffusion coefficients. The use of enhanced-fluidity chromatography has been particularly studied by the groups of Sandra and of Olesik [60,129,141,484]. Lee and Olesik used mobile phases made of n-hexane for the analysis of low-polarity compounds in normal phase chromatography. The addition of carbon dioxide increases the column permeability and its efficiency. It also increases the polarity of the mobile phase, decreasing the retention factors. The π^* Taft coefficient of the mobile phase increases with increasing mole fraction in CO_2 and reaches the asymptotic limit at ca. 0.70. Yuan and Olesik [138] have used this approach to perform size exclusion separations of polystyrenes. They reported that an increase of the carbon dioxide concentration in the mobile phase affect the separations in much the same way as a temperature increase, up to ca. 30% CO_2. The column efficiency increases, particularly at high flow velocities, the optimum velocity becomes higher, and the peak asymmetry decreases. However, for concentrations exceeding 50%, the mobile phase strength decreases and selective adsorption takes place. An increase in the pressure can restore the solvent strength.

Using fluoroform (CF_3H) as co-solvent, Zhao and Olesik [485] investigated the separation of mixtures of antidepressants (amitriptyline, nortriptyline and related compounds). The mobile phase was a mixture of methanol, CF_3, and a 20 mM phosphate buffer. The addition of CF_3H improved the performance, increasing the column efficiency and decreasing the retention times. Fluoroform has important advantages over carbon dioxide, with a critical pressure of 48 atm and a critical temperature of 299 K. It is inert, nonflammable, polar and polarizable, and has a low toxicity. Sun and Olesik [486] compared the separations obtained for eight pairs of enantiomers on vancomycin, in normal phase chromatography, using SFC, HPLC and enhanced-fluidity liquid chromatography, this last method being defined as using a mixture of conventional HPLC eluent and no more than 50 mol% of carbon dioxide. They reported that the reduced viscosity of the eluent and the increased diffusion coefficient permit operation of the column at higher flow velocities, leading to faster separations. The resolution and selectivity were generally greater than in SFC. Results tend to be better when CF_3H is used instead of CO_2.

Recently, Santos Pereira et al. [129] demonstrated the use of mixtures of ethanol, an aqueous buffer of ammonium formate at pH = 3, and carbon dioxide as the mobile phase used for HILIC separations at 40 °C, on bare silica of samples of nucleic bases, caffeine, theophylline, cortisol and flurbiprofen. The addition of a stream of carbon dioxide at increasing flow rate from 0 to 1 mL/min to a stream of ethanol/buffer at the constant flow rate of 0.5 mL/min results in increasing retention and a much improved resolution up to 0.75 mL/min of carbon dioxide. The separation achieved is nearly the same as with a solution of the same buffer in acetonitrile but the elution orders are different (inversion between T and U).

From the literature [60,129,141,484], it seems that the advantages of enhanced-fluidity chromatography are as follows

1. The eluent viscosity is at least one order of magnitude lower than that of common HPLC solvents, permitting elution at higher mobile phase velocities, the use of longer columns, and/or of columns packed with finer particles [60,141].
2. The diffusion coefficients are larger, intermediate between those found in HPLC and in SFC, resulting in a markedly higher optimum velocity and lower mass transfer resistances than in HPLC. The optimum velocity for maximum efficiency is higher.
3. The separations performed are generally better and always faster, particularly in chiral chromatography and in normal phase chromatography.
4. The easily adjusted composition of the mobile phase achieved by selecting the nature of the fluid (CF_3H or CO_2) and its concentration (often between 30 and 70 mol%) permits a great flexibility in modulating the separation factors.
5. Interactions of ionogenic compounds with CO_2 affect their retention. Adjusting the concentration of CO_2 has effects similar to those of adjusting the pH and make it possible to affect the elution order without using a buffer. The detrimental effect of buffers on the long-term stability of the stationary phase and on the response of mass spectrometry are thus avoided.

11.7.2. Switchable solvents

Jessop et al. [487–489] have developed an attractive concept, that of switchable solvents that can exist in two different states, being miscible under one and immiscible under the other. Most such pairs involve changes in the concentration of carbon dioxide in the system. Examples of switchable pairs of solvents are (1) the pair of water and an organic solvent containing R–C(=NR)–NR_2 with R = C_4 H_9, which are immiscible but become miscible in the presence of a large concentration of CO_2, the amine group in =NR becoming a quaternary ammonium; and (2) an aqueous solution of tetrahydrofuran and bis-dimethyldiaza[1,6]hexane, which separates into an aqueous solution of bicarbonate and the quaternary ammonium of the base and an aqueous solution of tetrahydrofuran. The advantages of these pairs of solvents is the ease with which a diphasic system can be turned into a monophasic one by changing the concentration of carbon dioxide in the system. The use of similar pairs could facilitate the separation of the eluent and the components purified by SFC.

11.8. Classification of stationary phases

After having developed a new method of characterization the stationary phases used in SFC (see Section 7.1.6), a method based on the use of the linear solvation energy relationship (LSER) [265,274–276], West and Lesellier suggested an original unified classification of stationary phases, which they developed after this large set of results [279]. HPLC can be implemented as either a reversed-phase or a normal-phase implementation of liquid chromatography, using as the mobile phase one of two widely different types of mobile phases, the first one being an aqueous solution of an organic solvent, the other one a dry organic solvent or a dry mixture of organic solvents. Conversely, a nonpolar or a polar packing material is used as the stationary phase. In SFC, in contrast, the same mobile phase can be used and SFC be implemented as either a RPLC or a NPLC method, depending only on the polarity of the stationary phase. Then, the role of the organic solvent used as the modifier is essentially to enhance the solubility of the polar components of the sample and to modify the polarity of the stationary phase by adsorbing on its active sites [279].

The classification developed by West and Lesellier is a five-dimensional classification that is based on the five coefficients of the LSER model that the authors had calculated for a hundred solutes and 28 stationary phases, divided into three groups, nonpolar [265], polar [274], and aromatic [275] (see Section 7.1.6).

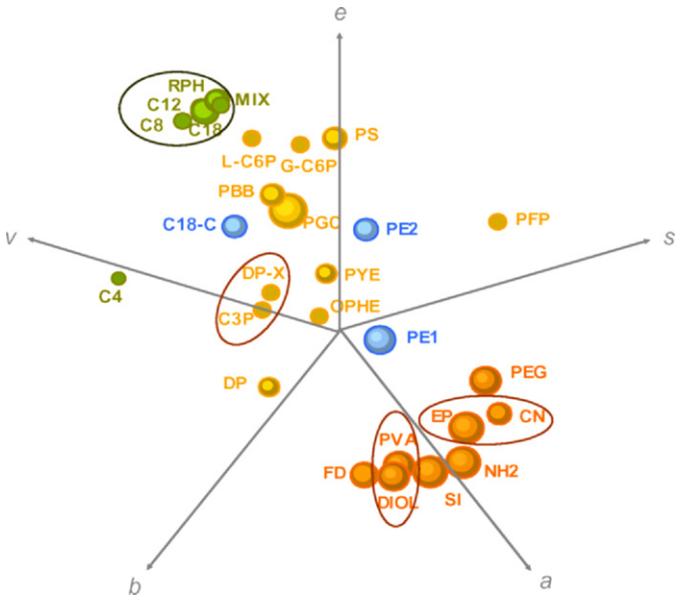

Fig. 46. Five-dimensional representation of the solvation parameter models for 28 stationary phases. Green points, nonpolar phases; blue points, polar alkyl phases; yellow points, moderately polar aromatic phases; orange points, polar phases. Conditions: 25 °C, outlet pressure 150 bar, mobile phase, CO_2, 3 mL/min. [279], Fig. 5.

This nearly exhaustive classification helps in choosing the stationary phase best suited to perform a new separation. To present the classification, the authors use the similarity factors between the different chromatographic systems studied.

A detailed analysis of the results obtained shows that SFC is not really a purely normal phase chromatographic method. The retention factors measured in SFC on neat silica and on ODS silica correlate reasonably well with $\log P$ where P is the octanol/water partition coefficient, similar to the retention behavior observed in NPLC and in RPLC, respectively. On many other stationary phases, however, there is no correlation at all [279]. Furthermore, the addition of methanol as a modifier does not uniformly decrease the retention of polar compounds, retention decreases first, then goes through a minimum and increases with increasing modifier concentration, with $\log k = aC^2 - bC + c$. It has also been reported that the use of hexane as the organic modifier has an effect on retention similar to that of methanol.

The results of the classification of the stationary phases are illustrated by a diagram (Fig. 46). The solvation vectors are those defined by Ishihama and Asakawa [490]. Each stationary phase i is represented by a vector of length

$$u_i = \sqrt{e_i^2 + s_i^2 + a_i^2 + b_i^2 + v_i^2} \quad (172)$$

The diameter of the circle representing this stationary phase in the figure is proportional to u_i. The vector is the sum of the five components projecting on the five axis as e_i/u_i, s_i/u_i, a_i/u_i, b_i/u_i, and v_i/u_i. The angle between two vectors, θ_i, can be calculated according to the rules provided by Ishihama and Asakawa. There are three major groups of phases, nonpolar ones, which have no polar groups (in the circle in the top left of the figure), polar ones (the group at the bottom right of Fig. 46, in a wider arc than the previous group), and the intermediate phases, which are more widely scattered, between n-butyl-bonded silica (C4) and pentafluorophenyl-propyl-bonded silica (PFP) and between amide-embedded hexadecylsiloxane-bonded silica (PE1) and phenylhexyl-bonded silica (L-C6P), almost all of which contain aromatic groups. The angle between the vectors are related to the informational equivalence, similarity or difference between the retention patterns provided by the corresponding

stationary phases. The phases contained in a circle in Fig. 46 should be considered as practically equivalent. All polar phases should not be considered as equivalent even when their representative bubbles are close because they may exhibit similar interactions but with significantly different intensities. Nevertheless, it would be improbable that two compounds that coelute on one phase could be resolved on another phase having an image close to that of the first one in Fig. 46.

The methods developed by West and Lesellier were used to compare the retention characteristics of a series of columns packed with various C_{18}-bonded silica particles [277] and to select a set of nearly orthogonal systems for the separation of a number of components of sunscreen products. The phases selected were n-butyl-bonded silica (i), octadecyl- and phenylpropyl-bonded silica (ii), phenyloxypropyl-bonded silica (iii), and 2-ethylpyridine-bonded silica (iv). All four phases provide markedly different elution order. The latter three phases all provide nearly complete resolution of the 7-component mixture but phases i and iv afford markedly different elution order [278].

12. Applications

SFC being used mostly with a low polarity eluent (CO_2 modified by a polar organic solvent) and a polar stationary phase (porous silica or polar ligands bonded to porous silica) is often rightly considered as an implementation of normal phase liquid chromatography. This implementation complements effectively classical RPLC, which uses a polar eluent (H_2O, modified by an organic solvent) and a nonpolar stationary phase (alkyl ligands bonded to porous silica). Currently, its applications in preparative chromatography are more varied, more numerous, and more important than its applications in actual analysis.

12.1. Analytical applications

As happened also in the beginning of GC, then of HPLC, the separation of alkanes, of cyclic and aromatic hydrocarbons was investigated by many [16,40,44,236,479,491–493]. The initial development of SFC was hampered by the use of pure carbon dioxide as the mobile phase. This fluid has limited solubility for polar compounds which resulted in large retention factors, long analysis times, low sensitivity since the sample sizes were limited and the peaks were wide and short due to their long retention times, hence the need to implement programming of the mobile phase density, i.e., of the inlet and/or the outlet pressure, causing difficulties with the regulation of the flow rates. With the recent advent of sophisticated instruments SFC has matured today to a major separation method, which can provide analyses offering performance comparable to those of HPLC in terms of resolution power, speed of analysis, reproducibility of the data supplied. Modern SFC is often carried out with a complex mobile phase made of carbon dioxide, an organic or primary modifier and, frequently, an additive or secondary modifier (see Section 7.1.3).

In summary, under the experimental conditions currently available, SFC can be run with one of many columns packed with particles of a chemically bonded phase having polar ligands and eluted with a carbon dioxide based mobile phase with some polar additives. So, this chromatographic method appears to be a separation method far closer to HPLC than to GC, because retention factors can be modulated in a wide range. Actually, as explained above, SFC is close to NPLC, over which it has the advantages of using a far less viscous mobile phase, with much higher diffusivities, and of using a phase system in which the equilibrium constants are much less sensitive to the presence of small concentrations of highly polar compounds, e.g., water. This makes SFC a separation method with a mechanism that can be nearly orthogonal to that of RPLC, a great potential advantage for two-dimensional chromatography [494].

If the pressure at the column outlet is set at a relatively high level, in practice larger than 60 bar and the column is operated at a temperature slightly above ambient, the two methods have similar behavior and complementary applications [123]. Not only polar compounds but now ionogenic compounds and ions can be separated, using proper additives, e.g., ammonium salts, compatible with LC/MS coupling, like ammonium formate or acetate as secondary modifiers [495]. The critical effect of the salt may arise either from the formation of ion-pairs between the additive and the analytes and/or from the adsorption of the salt on certain sites of the packing material (deactivation). For example, without secondary modifiers, there is no elution of p-toluenesulfonate even in the presence of a high methanol concentration, while elution of symmetrical peaks with retention factors of the order of 6 takes place with tetrabutyl ammonium (2.5 mM) as the additive. A memory effect persistent for several hours suggests that the cause of the salt additive effect is due to strong chemisorption of the salt additive on the adsorbent surface [496].

SFC is used in the pharmaceutical and the specialty chemicals industries. It has been used to separate numerous pairs of enantiomers and even to separate medium size peptides (angiotensin I, II, and III, urotensin II, and sauvagine; the last one, with 40 amino acid residues, including 4 basic and 7 acidic ones, has a molecular weight of 4500) [497]. One of the most important advantages of SFC in the drug discovery process is the great speed with which the purified components derived by organic synthesis can be separated from the mobile phase, once the corresponding fractions have been collected at column outlet. A large number of drugs and other compounds of clinical interest have been analyzed by SFC. Actually, Sandra advocates the use of HPLC instruments with injection of liquid carbon dioxide at a regulated flow rate into the stream of a conventional HPLC mobile phase, with careful degassing of the eluate and venting of the carbon dioxide [64]. SFC complements excellently RPLC, particularly for the analysis of highly hydrophobic compounds [134].

A wide variety of applications of SFC to the analysis of foods (e.g., lipids, sterols, polyphenolic compounds or traces of pesticides), of natural products, of fossil fuels, of monomers, oligomers, polymers and polymer additives (e.g., plasticizers), of pharmaceutical intermediates, achiral or chiral [123] have been reported. Sandra et al. [60] demonstrated the determination of pesticides in fruit juices, of polycyclic aromatic hydrocarbons, triazines, chlorophenols, and phenoxy acids in water samples by a coupling on- or off-line of supercritical fluid extraction, SFC, and mass spectrometry. The convenient sample preparation, including addition of internal standards and derivatization of acidic solutes after extraction and before separation allowed trace detection below the ppb level.

12.1.1. Chiral separations

Since the first chiral separations by SFC [498], almost all chiral separation phases (CSPs) used in gas or liquid chromatography have also been successfully used in some implementation of SFC [43,52]. Perrut demonstrated preparative separation of enantiomers with significant production rate and high enantiomeric purity [42]. The two enantiomers of 2,2,2-trifluoro-1-(9-anthryl)ethanol were separated and purified on a 76 mm × 60 mm (S)-thio DNB Tyr A-bonded silica column eluted with a 96/4% solution of ethanol in CO_2 at 293 K, with an average pressure of 20 MPa. The enantiomeric purities of the two enantiomers were 96 and 94%. Medvedovici et al. studied the separation of 44 pairs of enantiomers (β-blockers, β-agonists, benzodiazepines, non-steroidal anti-inflammatory drugs, barbiturates, free and derivatized amino acids) on common chiral stationary phases (Chiralcel OD and AD, Chirobiotic V and T)

under the same subcritical conditions, pressure 200 bar, flow rate 2 ml/min., carbon dioxide modified with a 5 min gradient of 5–30% methanol, with 0.1% of TFA and 0.1% triethylamine (TEA) [61]. Under these conditions, over 70% of the enantiomers were resolved on Chiralcel AD with a resolution exceeding 0.4. Baseline separation could then be obtained almost always by fine-tuning the parameters of the separation. Later, this procedure was improved by running the separations under a set of different standard conditions, with an outlet pressure of 110 bar, a temperature of 35 °C, a methanol concentration gradient, 0.2% TEA and a flow rate of 2.5 ml/min for the first 20 min, then ramped up to 4.5 ml/min and hold until total elution of the sample [62]. The use of SFC/MS permits the rapid and accurate determination of the enantiomeric excess [42].

Gasparrini et al. [499] separated successfully stereolabile enantiomers on a chiral stationary phase, between −50 and −30 °C, in solutions of 2-propanol (5%) or methanol (20%) in carbon dioxide. Wolf and Pirkle [500] demonstrated chiral separations at very low temperatures. on Whelk-O type stationary phases, with a solution of 10% MeOH in CO_2. The enantiomeric resolution, the retention, and the column efficiency increase with decreasing temperature, down to −41 °C. The separations are therefore subcritical, actually made in HPLC with liquid carbon dioxide as the main component of the mobile phase. The authors attributed the increase in the column efficiency to the fact that they used a chemically bonded chiral stationary phase rather than a polymeric one and the silica surface and the bonded ligands are easily accessible. Numerous racemic mixtures, which could not be separated at ambient temperature were easily resolved at −10 °C. Atropisomeric arylnaphthalenes, which interconvert too rapidly at ambient temperature to be separated were resolved between −29.5 and −42.0 °C.

Liu et al. illustrated the chiral separation power of the macrocyclic glycopeptide teicoplanin and of some of its common derivatives [501]. Using 250 mm × 4.6 mm columns, operated at a flow rate of 4 ml/min with a 100 atm outlet pressure, at 31 °C, they were able to separate completely or partially 92% of a set of 111 pairs of enantiomers, including heterocycles, analgesics, β-blockers, sulfoxides, N-protected amino acids, and native amino acids. The organic modifier was methanol, with concentrations between 7 and 67%, with the occasional additions of 0.1 to 0.5% of triethylamine or trifluoroacetic acid. All separations were performed in less than 15 min and over two third of them in less than 4 min. The main advantage of SFC is in its speed of analysis, faster than that of HPLC.

Garcia-Martinez et al. determined the enantiomeric composition of samples of (−)-(R)-2-*tert*-butyltetrahydroimizalodinin-4-one by polarometry, ^{1}H NMR, and chiral SFC, with an excellent agreement between the results of the three methods [502]. Ottiger et al. studied the separation of the enantiomers of 1-phenyl-1-propanol on Chiralcel-OD under overloaded, nonlinear conditions [223]. They measured their equilibrium isotherms and their mass transfer kinetics. The measurements were carried out at a temperature slightly below the critical temperature (30 °C) and under a pressure much above the critical pressure (125–185 bar), using methanol as the modifier. The Henry constants of adsorption decrease with increasing mobile phase density and with increasing methanol concentration. The saturation capacity is independent of the mobile phase density but increases with increasing modifier concentration.

Welch et al. modified a commercial instrument by adding column-connecting valves, for the rapid selection of any combination of two columns that can be selected from two banks of five different columns [482]. The five columns in each of the two banks could be the same, or one bank could contain chiral columns, the other bank achiral columns, or the 10 columns in the two banks could be all different chiral columns (see Section 11.6). The authors preferred this last combination on the ground of the ability of chiral columns to separate mixtures of diastereoisomers or positional isomers being far better than that of achiral columns.

Brunelli developed a method for the analysis of a broad spectrum of pharmaceuticals, using a series of five 250 mm × 4.6 mm columns (Zorbax SB-CN, Agilent) packed with 5 μm particles of cyanopropyl-bonded silica, eluted carbon dioxide (outlet pressure 100 bar, flow rate 2.0 ml/min, temperature 40 °C, organic modifier methanol/acetonitrile (3/1) and 0.5% TFA and diisopropylamine [63]. This series of columns had an efficiency in excess of 100,000 plates; its selectivity was tuned by changing the concentration of the modifier and the pressure. The advantages of the method is the high efficiency achieved, the short analysis time, the tunable selectivity and the convenience of using a wide range of detectors. The analytes were steroids, xanthines, and nucleotides.

12.1.2. Analysis of peptides

It is becoming critical to perform targeted determinations of bioactive peptides in complex matrices [134]. The conventional approach is separation by RPLC. In the case of hydrophobic peptides, however, many impurities are difficult to elute or resolve, due to solubility problems in the mobile phase. This may severely hamper the determination of the purity of the studied peptides. Heavier peptides may have to be digested, the digestion products separated, identified, and quantified, involving lengthy procedures. SFC may provide improved and faster analyses of these peptides. Solubility problems may be alleviated because carbon dioxide is compatible not only with methanol but also with chloroform, and many other organic solvents. Typical flow rates are faster than in RPLC and efficiency often better.

Numerous peptides have been separated under a variety of experimental conditions [134]. Cyclosporin, a cyclic hydrophobic undecapeptide, seems to have been the first peptide analyzed with SFC. A 100 mm × 1 mm column packed with 5 μm particles of C_{18} bonded silica was eluted with a mobile phase made of a 2% solution of methanol in carbon dioxide, at 140 °C, under an average pressure of 400 bar [503]. Detection was done by mass spectrometry. Preparative SFC was later used for the extraction of cyclosporin A from a fermentation broth containing a large number (ca. 25) of similar peptides [504]. The two-step process involved an extraction followed with a purification made on a column packed with silica eluted with a mobile phase made of carbon dioxide with 20% 2-propanol. It provided a 98.5% pure product with a yield of ca. 80% and a production in excess of 2000 pounds.

Among the other peptides separated, analyzed, or purified by SFC we found actinomycin D and vancomycin [134], gramycidin A, B, and C [505], their monomeric and dimeric species [506], angiotensin I, angiotensin II, angiotensin III, urotensin II, sauvagine [497], bacteriorhodopsin and cytochrome C tryptic digest [507]. Common stationary phases are amine or cyanopropyl bonded silica or copolymers of styrene and divinylbenzene. Common mobile phases are mixtures of supercritical carbon dioxide in dominant proportion, with haloalkanes (e.g., chlorodifluoromethane), and methanol, ethanol, or 2-methoxyethanol. 0.5% of trifluoroacetic acid or of a surface-active agent has some times been added to the mobile phase but other acidic additives (e.g., heptadecafluorooctanesulfonic acid) are more successful at improving the peak profiles of peptides and at decreasing their retention [134].

12.1.3. Comprehensive SFC × HPLC two-dimensional chromatography

François and Sandra developed a two-dimensional combination of an SFC separation on a cation-exchange column loaded with Ag^+ ions followed by a RPLC separation on a series of a cyanopropyl- and a C_{18}-bonded silica columns for the separation of complex mixtures of triglycerides [65]. The first, SFC separation was performed

at 40 ° C on a series of two Nucleosil 100-5 SA, 250 mm × 4.6 mm columns which had been loaded with Ag^+ following the procedure of Sandra et al. [508]. It was eluted with carbon dioxide and a 6:4 mixture of acetonitrile and isopropanol. A combined pressure and composition gradient was applied. The eluent was trapped on a 7.5 mm × 4.6 mm guard column packed with 5 μm particles of ODS. The period of the sampling was 1 min. The second dimension column was a 50 mm × 4.6 mm Zorbax SB C18 column packed with 3.5 μm particles, eluted at 30 ° C and 5 ml/min, with an aqueous solution of acetonitrile under gradient elution. Great care was taken properly to mix the transferred fractions and the second eluent before their injection into the second dimension column and to reduce the CO_2 concentration in the second eluent.

The two separations are nearly orthogonal. The former separates triglycerides after their number of double bonds and provided a peak capacity of approximately 28. The latter separates the sample components after the number of their carbon atoms. It gives a peak capacity of nearly 26. The actual peak capacity achieved was 550, the loss resulting mainly from undersampling but also from incomplete orthogonality of the retention mechanisms.

12.1.4. Comparison between SFC and HPLC

The relative advantages of the two methods have been abundantly discussed. It is striking that few authors have bothered to develop lengthy description of the advantages of HPLC over SFC, which are taken for granted by a large fraction of the analytical community. In contrast, proponents of SFC have written long pamphlets attempting to vindicate this latter method. Actually, SFC offers important advantages and a balance of problems which complement them; one of its major drawbacks is still related to the lack of practical, advanced instruments. Others are related to the lack of any alternative to carbon dioxide as the major component of the mobile phase. This compound is most useful because it has a low density and a low viscosity but it is hydrophobic and no suitable hydrophilic supercritical fluid is available. Furthermore, carbon dioxide should be stored and transported in closed, heavy cylinders, which makes it far less convenient to handle than the common organic solvents used in HPLC.

An important study comparing the performance of HPLC and SFC for the separation of many compounds of pharmaceutical interest was conducted by Pinkston et al. [509]. This study showed very little difference in the overall scope of RPLC vs. SFC for a large library of compounds and cited several benefits of using SFC (vs. HPLC) in connection with the use of APCI-MS for identification of unknowns.

12.2. Physico-chemical applications

SFC provides a fast, accurate, and convenient method of measurements of many important properties of critical and supercritical fluids as was explained in many of the sections of this review. It provides determinations of (1) the viscosities of carbon dioxide, methanol and many other fluids, including their solutions is a wide range of pressures (from a few to ca. 1000 bar), temperatures (from −40 ° C to 300 °C), and compositions, covering vast domains of subcritical, near-critical and supercritical conditions; (2) the diffusion coefficients of as many compounds as needed in these fluids; and (3) the equilibrium isotherms of these compounds on any available stationary phase or adsorbent. Besides equilibrium constants between adsorbents and dense gases or critical fluids that are derived from retention factors, SFC was used for the determination of the partial molar volumes of different compounds (see Fig. 9) and of second virial coefficients.

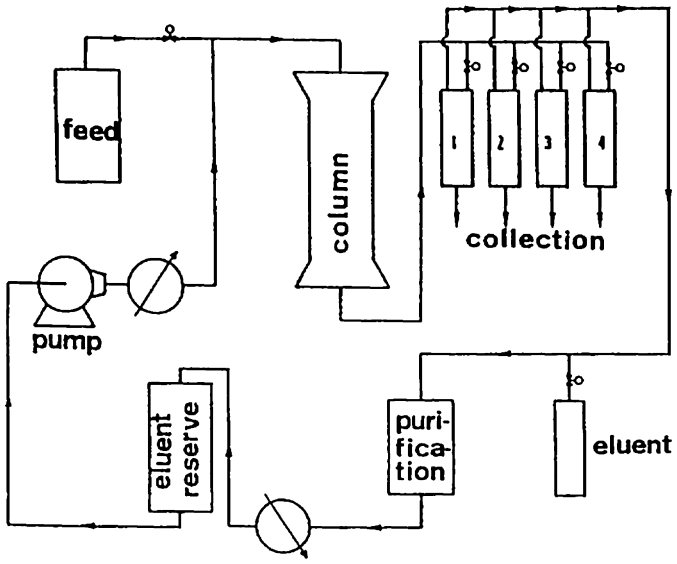

Fig. 47. Flow sheet of a preparative SFC instrument [42].

12.3. Preparative applications

For a long time, considerable interest has been devoted in the pharmaceutical industry to SFC separations. Perrut developed and parented a preparative recycle SFC instrument with cyclone separators [48]. This is in part due to the development of extraction procedures using SFC and to the considerable knowledge developed in chemical engineering of the handling of these processes and of the equipments necessary to handle these fluids. Fig. 47 shows the flow-sheet of a preparative SFC instrument.

One of the main features distinguishing preparative SFC from preparative HPLC instruments is the on-line recycling of the mobile phase. The column efficiencies obtained with short beds are relatively high, with reduced plate heights as low as 3 but it is critical to achieve a high radial homogeneity of the bed, otherwise the column plate height increases with increasing column length [42]. The main advantages of preparative SFC over HPLC seem to be (1) the higher molecular diffusivity of most compounds in the mobile phase, hence the faster optimum velocity for maximum efficiency and the higher productivity; (2) the low viscosity of carbon dioxide that permits operating the columns at high velocity without needing excessively high inlet pressure; and (3) the probably wider concentration range within which equilibrium isotherms follow a linear or quasi-linear behavior. Furthermore, retention is easily and rapidly controlled by adjusting the average column pressure [510]. It can also be adjusted by changing the column temperature but it might be difficult to achieve the isothermicity of the packed bed throughout large size preparative columns.

Several reviews have addressed the capabilities of the method and numerous applications [42,72,123,454,475,511,512] but few applications have been described in the scientific literature. Perrut gave lists of compounds separated, purified, or extracted by SFC [475]. He pioneered the use of organic modifiers to purify polar compounds. Cox separated the isomers of flurbiprofen [513]. Shimata et al. isolated individual oligomers of poly(ethylene glycol) with degrees of polymerization between 6 and 40 [514]. Bartle et al. [72] made suggestions for the optimization of the experimental conditions of preparative SFC separations that are most similar to the conclusions generally reached in preparative HPLC [1]. These authors noted that the two main problems encountered in preparative SFC were the safety and the achievement of high yields in the recovery of the purified fractions. Cox [454] emphasized the

importance of the solubility of the feed in the mobile phase. Many organic compounds are poorly soluble in carbon dioxide at all densities. The use of a modifier is practically needed in all applications of preparative chromatography [140,454]. Methanol is often used for this purpose but numerous organic compounds are only moderately soluble in methanol, in which case good results have been obtained with chloroform.

The separation of α- and δ-tocopherol (vitamins E) and of vitamin D_3 was discussed in great details by Brunner and Johannsen [399]. It was performed by preparative chromatography and by simulated moving bed. The isotherms of these compounds were determined at 313 K under a pressure of 13.7 MPa of carbon dioxide with less than 1% ethanol, on a Zorbax Pro 10/60 CN column. The overloaded band profiles calculated agreed well with those recorded. The SMB experimental conditions were optimized using the triangular diagram method of Morbidelli et al. [515].

White and Burnett [55] developed a procedure to extract and purify selected fractions from a synthetic product by running analytical scale separations on 50 mm × 4.6 mm columns, packed with 5 μm particles of an ethyl-pyridyl stationary phase, operated at 5 ml/min, with an outlet pressure of 100 bar, at 40 °C. The analyses last 2 min. The separation is easily scaled up to a 8.5 min separation made on a 150 mm × 21.2 mm column packed with the same stationary phase and operated at 55 ml/min, at the same temperature and outlet pressure. The use of an empirical correlation involving five different compounds permits the rapid scale-up without the need of running a slow method development process. Considerable productivity gains were achieved over HPLC, due to the faster flow velocity and to the much faster evaporation time needed to recover the products from the collected fractions.

Although this is actually not a preparative chromatographic separation, it is worth mentioning here the extraction of caffeine from green coffee beans or black tea leaves [516]. The solubility of caffeine in carbon dioxide decreases from 1 to 0.1 g/kg when the fluid density decreases from 800 to 450 kg/m^3[517]. In a recycling process, however, this solubility decrease is insufficient to permit reaching the specification for decaffeinated coffee beans. So, the stream of carbon dioxide is percolated through a bed of charcoal [399]. A similar process is used for the extraction and purification of tocopherols from sterols [399].

12.3.1. Industrial and economic issues

Basic chemical engineering material for the design of supercritical fluid equipments and installations is provided by the book of Brunner [516].

The cost of SFC instruments, particularly of simulated moving beds units, increases markedly less with increasing size than most people might be afraid of. The cost of similar units increases as the power 0.24 of the product of their volume and the flow rate under standard operation. So, in practice, the unit cost increases as the square root of the production rate [456]. This suggests that, whenever possible, capital amortization will be markedly less for a large-capacity multi-product unit used in time-sharing than for a series of small-capacity units each dedicated to a single product. Admittedly, the specific purpose of the unit also affects its cost, a unit built according to cGMP requirements will cost 30–100% more than a similar food-grade unit.

The operating costs may also be reduced for a large capacity unit. Energy for heating may be supplied by steam available on the site or by hot water heated by fuel or gas. Carbon dioxide is recycled during SMB operations but when the instrument is purged for clean up or maintenance, it may be recompressed instead of being vented, which would cause the significant mass loss of 150 kg per cubic meter of instrument hold-up volume.

12.3.2. Production of purified enantiomers

Terfloth gave a list of the CSPs available in 1999 [518] and listed the enantiomeric separations performed by preparative chromatography in 2001. Later, Berger and Berger reviewed the columns and packing materials used in modern SFC, with special attention for those used in preparative enantioselective separations [35].

White [54] developed a rapid screening process for the selection of the best separation conditions of a racemate. They use short columns (10 cm long) packed with 5 μm particles, high flow rates (5 ml/min for 0.46 cm i.d. columns); and rapid gradient programs (2.5 min). Four columns were used in the screening, Chiralpak AD-H, AS-H and Chiralcel OD-H and OJ-H. The organic modifier was methanol. When there is even partial resolution of the racemate, the elution times observed under gradient conditions provide a suitable estimate of the best modifier concentration for an isocratic preparative separation on a 25 cm × 2.1 cm column. Due to the rapid elution observed in SFC and the small amount of methanol required, productions of up to 60 g purified enantiomers was systematically possible, a considerable progress over preparative HPLC.

A similar approach was described by Maftouh et al. [56] who showed how the method complements NPLC and RPLC and increases the rate of development of successful separations at the semi-preparative level. To separate the enantiomers of omeprazol, an inhibitor of gastric acid secretion, Toribio et al. preferred an SFC separation on Chiralpak AD at 35 °C, under a 20 MPa average column pressure, with 25% of ethanol or 2-propanol as the organic modifier [519]. They found that S-omeprazol elutes first when the modifier is ethanol, last when it is 2-propanol; in this last case, however, the resolution was less, slightly below 1. The analytical separation was done at a flow rate of 2 ml/min, the preparative separation at the same flow velocity. The maximum production rates were obtained by injecting reasonable amounts of concentrated feed solution.

Rajendran et al. modeled the equilibrium isotherms of 1-phenyl-1-propanol between Chiralcel OD and a mobile phase made of carbon dioxide modified with methanol [200]. They used a competitive Langmuir isotherm model. The calculated band profiles agree with those recorded. The separation was carried out using a SMB operated under the pressure gradient mode, under nonlinear conditions [520]. At low concentrations, the purities of the extract and the raffinate were 99.5 and 98.4%, respectively.

Peper et al. compared the performance of batch preparative chromatography and simulated moving bed in SFC [58]. They investigated three pairs of enantiomers, tocochromanol (α = 1.18), a component of vitamin E, ibuprofen (α = 1.23), an unnamed pair (α = 2.03), and the pair of α- and δ-tocopherol (α = 1.75). The equilibrium isotherms of the first three compounds were modeled with the competitive Langmuir model, those of the fourth pair with an anti-Langmuir isotherm. For three of these four pairs, the production rate of the SMB system was better than that of conventional batch preparative chromatography. However, the batch process was found to be more profitable.

Yan and Orihuela [57] compared the performance of batch preparative SFC and of SFC used in the steady state recycling (SSR) mode [521]. The productivity increased more than four times when the batch mode was replaced by the SSR mode and the solvent consumption decreased four times. The same purification done by batch SFC had a higher production rate and needed less solvent than the same purification done by HPLC. The SSR mode permits the achievement of preparative purifications of enantiomers when their separation factor is relatively low [521].

Although they did not discuss preparative applications, Ottiger et al. [223] measured the equilibrium isotherms of 1-phenyl-1propanol on Chiralcel-OD and modeled their elution band profiles

(see Section 12.1.1). Wenda and Rajendran studied the separation of the enantiomers of flurbiprofen on Chiralpak AD-H at 30 °C, with the use of methanol modifier (7%) [225]. They measured the equilibrium isotherms, modeled them with the Langmuir and the bi-Langmuir models, measured their parameters using the inverse method, and modeled the elution band profiles. They also measured the mass transfer coefficients and found that the resistance to mass transfer is generally very low, which explains this attractive feature of SFC. Miyabe and Guiochon suggested that the low mass transfer resistance in RPLC is due to the rapid surface diffusion of adsorbates. The same rational might apply in SFC.

12.3.3. Optimization of separation processes

Jiang et al. determined the influence of the average pressure, the temperature, and the concentration of ethanol, used as the organic modifier in carbon dioxide, on the retention of tocopherol and the resolution of its isomers under supercritical conditions [522]. They showed that the resolution increases with increasing temperature and with decreasing pressure. The retention factors can be predicted using a five parameter model.

Ventura et al. developed a sophisticated, computer regulated instrument for the rapid analyses of long series of samples prepared by parallel synthesis in 96-well trays [523]. Samples are analyzed and, based on a computer analysis of these data, they are automatically channeled to the most appropriate of three preparative chromatographs, two HPLC ones, one with UV- the other with MS-triggered fraction collection, and an SFC chromatograph with UV-triggered fraction collection. Samples not directed toward the SFC unit include those that are insoluble in methanol, contain highly polar compounds or compounds that have no UV chromophores. The advantage of this approach is to increase markedly the purification success rate for sets of structurally different molecules obtained by combinatorial synthesis. Without MS-triggered fraction collection, it is not possible to purify compounds which do not have good chromophores. SFC avoids the production of salts of compounds when their HPLC separation requires the use of buffers.

12.3.4. Simulated moving bed separations

Mazzotti et al. analyzed the operating conditions and the potential separation performance of a SMB system operated with an SFC eluent, under linear conditions [520]. They considered operation under the isocratic mode in which the mobile phase density is practically uniform (provided that the column permeability is high), and the pressure gradient mode, in which the average column pressure decreases stepwise from section to section, which is made possible by the proper setting of throttle valves. This last process results in a stepwise decrease of the mobile phase density, hence in a stepwise increase of the retention factor of the two compounds, which permits the faster regeneration of the stationary phase in the eluate extraction region. Thus, the elution strength is largest in the first section of the SMB, where the more retained compound must be eluted and lowest in the fourth section where the least retained compound must be retained. As a consequence, the application of the triangle theory shows that the production rate of purified compounds is markedly improved, up to several times. This improvement is particularly important for mixtures of components that have a small separation factor. They concluded that the process could exhibit great performance and supply exceptional separation power.

Di Giovanni et al. improved the performance of SMB separations by adjusting the elution strength of the mobile phase and changing its average pressures in the four sections of the apparatus, by using the pressure gradient mode [59]. The results obtained are consistent with the predictions of Mazzotti et al. [520]. The production rate of the system is markedly improved, especially so for low selectivities. Johanssen et al. used a separation of binaphthol enantiomers that they had previously developed to extend it to a SMB process, achieving an excellent production rate [524].

Denet et al. separated the enantiomers of tetralol (hydroxytetraline, $C_{10}H_{11}OH$, with a 2-2-2-2 SMB unit made of 20 cm × 3.3 cm columns packed with Chiralcel OD, operated at 40 °C, in the pressure gradient mode. Due to the use of ethanol as the organic modifier, at a concentration exceeding 5%, the mobile phase is near-critical, not supercritical. The retention factors of both isomers and their separation factor decrease with increasing ethanol concentration and the retention factors only with increasing mobile phase density. The experimental conditions were optimized using the triangle theory. Compared to the isocratic mode, the pressure gradient mode allows an increase in productivity of up to 3 times [525].

Rajendran has used the classical "triangle theory" of simulated moving bed operation [526,527] to determine the experimental conditions for the separation of enantiomers, which have often small separation factors [224]. The application of this theory under linear conditions requires knowledge of only the Henry constants of the feed components, their concentrations in the feed, and the purity requirements. It is easy to implement and supply a reasonable starting point for a scaling up of the production rate, particularly when the required purity of the product is moderate.

13. Conclusion

The use of preparative SFC for the extraction of valuable compounds from complex matrices or for the purification of finished products when purity specifications are demanding is becoming popular. Such are the requirements for the production of most pharmaceuticals. The production of one of the enantiomers of certain intermediates at a high degree of optical purity or that of pure active pharmaceutical ingredients is often necessary. Chromatography is one of the few tools that can be used to satisfy these requirements. As shown in this review, preparative SFC has distinct advantages over the still predominant liquid chromatography, which is why SFC is frequently used. The advantages of SFC over HPLC include (1) a lower viscosity and higher diffusion coefficients of feed components in the mobile phase allowing separations to be performed at a higher velocity; (2) a superior solubility of pharmaceutical feeds in the mobile phases used in SFC; (3) a higher column loadability, which combined with the higher operating velocity, leads to a several times higher productivity; (4) an easier recovery of the purified compounds from the mobile phase; and (5) the use as the main component of the mobile phase of a cheap, non-flammable and environmentally benign solvent, high density CO_2. However, the success that these advantages promise could be achieved only if we can solve the challenges of interpreting more deeply the physical behavior of SFC systems, through a better modeling of SFC separations, a better design of the implementations of the process, and a better, faster optimization of these preparative systems.

The main objective of this review was to identify and discuss the essential topics that need to be clearly understood before a model-based approach can be developed for the design of preparative SFC systems, and, for this purpose, to provide adequate reference to the published literature. The main conclusion is that the goal of future research should be similar to the one previously achieved in earlier approaches at understanding the design and optimization of HPLC systems. The behavior of these systems is simpler than that of SFC systems from the modeling point of view, due to the high compressibility and the low density of the main solvent and to the extensive variation of the mobile phase properties along the column. This is why this review discusses in detail how the retention behavior is modulated by the temperature, the pressure, the solvent properties and those of the feed components like their solubility, solubility

parameters, partial molar volumes in supercritical solvents, and various other properties. The review also discusses the effect of the column permeability on the hydrodynamics of the column and the temperature distribution that may result from the simultaneous exothermic viscous friction and endothermic solvent expansion. The extremely important role of the mobile phase density in controlling almost all relevant physical properties is demonstrated with various examples from the literature The available equations of state that predict the solvent density from physical properties easy to measure like pressure and temperature are reviewed in detail. The choice of the most suitable equation is debated. The simpler but less accurate Lee and Kesler or Peng and Robinson equations seem preferable to the Span and Wagner equation, which does not have any explicit mechanism to handle the EOS of a mixture while the other two do. Given the compulsion of using polar modifier and other additives in SFC, this is a crucial advantage.

Although SFC may offer a high elution rate of solutes, the task of determining the optimum flow rate to ensure the most efficient operation can be extremely complicated because the solvent velocity changes continuously along the column, due to the pressure gradient and the mobile phase compressibility. This means that columns run with varying efficiencies at different points. The review discusses different possibilities of handling these situations and various methods to determine the transport properties. Toward the end, the review discusses in detail experimental issues which pose significant challenges to the growth of SFC and have not been addressed during the last two decades. It identifies areas in which sufficient understanding of SFC systems under non-linear conditions is pending, lists unresolved questions that need to be addressed for the development of preparative SFC and suggests approaches that may be applied to overcome this void. In general, the review observes that although most significant work was done to develop the fundamentals of SFC for analytical applications, much work remains regarding the understanding of nonlinear or preparative applications of SFC. Given the future scope and utility of this method as a sustainable process, this effort will certainly be worthwhile.

Finally, we should bear in mind that what is generally called SFC in the literature is actually an advanced version of liquid chromatography, which has the potentiality to permit combinations of normal-phase (NPLC), reversed-phase (RPLC) and non-aqueous reversed-phase (NARP) chromatography and which is performed with mixtures of liquid carbon dioxide and various organic solvent(s). Due to the extreme compressibility of this mobile phase, SFC has both a wider flexibility and a greater complexity than HPLC, which is otherwise similar. The merging of our understandings of retention and mass transfer in the different forms and implementations of chromatography into a real understanding of unified chromatography remains the ultimate goal of fundamental research in this field, following the pioneering work of Chester [67,19,68], Giddings [328,89], and Martire [66].

Nomenclature

Symbols which are used only in one single section are not included in this nomenclature.

A	Helmholtz energy
A, B, C	numerical coefficients in the Knox and the Van Deemter plate height equations
a, b, c	coefficients in various equations (e.g., the van der Waals equation)
b_i, c_i, d_i	coefficients in the Lee–Kesler equations
C	concentration of the solute in the mobile phase
D_c	column inner diameter
D_L	axial dispersion coefficient
D_m	molecular diffusion coefficient or molecular diffusivity in the mobile phase
d_p	average particle size
F	phase ratio
F_v	volume flow rate of the mobile phase
f_i	fugacity of compound i in the gas phase
H	height equivalent to a theoretical plate (NB. H is also the enthalpy or the Henry constant)
h	reduced plate height, $h = H/d_p$
K	permeability, Kozeny–Carman constant (K is also the equilibrium constant of the solute in the phase system)
k	retention factor, $k = (t_R - t_0)/t_0$
k_B	(or k) Boltzmann constant
k_F	permeability coefficient of a chromatographic bed
k_0	specific column permeability ($K = k_0 d_p^2$)
L	column length
M_i	molecular weight of compound i
$\mathcal{N}$	Avogadro's number
N	column efficiency, number of theoretical plates of a chromatographic system
P	pressure
Pe	Peclet number
P_c	critical pressure
P_r	reduced pressure ($P_r = P/P_c$)
p	pressure; also number of peaks in the chromatogram of a complex mixture
Q	mass flow rate of the mobile phase
q	solute concentration in the stationary phase
q_s	saturation capacity of the column
$\mathcal{R}$	ideal gas constant
Re	Reynolds number
R_s	resolution between two neighbor peaks
s	parameter characteristic of the probe compound in the definition of the polarity parameter
S, S_G	cross-section area of a chromatographic column
Sc	Schmidt number
T	temperature of the chromatographic system
T_c	critical temperature
T_r	reduced temperature ($T_r = T/T_c$)
t	time
t_R	retention time of a peak maximum (under isocratic or gradient conditions)
t_0	holdup time of the column, $t_0 = L/u = V_m/F_v$
u	mobile phase velocity
$\bar{u} = L/t_0$	average linear velocity of the mobile phase
u_F	superficial velocity of the mobile phase
V_G	volume of the column tube
V_i	partial molar volume of compound i
V_M	molar volume
V_m	volume of mobile phase in the column
V_R	retention volume of a compound
V_r	reduced volume ($V_r = (P_c v/RT_c)$)
V_s	volume of stationary phase in the column
V_0	column void volume or holdup volume
w_i	baseline bandwidth of the peak of component i.
X	retention range of interest in the chromatogram of a complex mixture
x	mole fraction
$x_{i,sat}$	mole fraction of compound i at saturation of the solution
Z	compressibility factor of a fluid
z	abscissa along a chromatographic bed

Greek letters

α	separation factor of two components ($\alpha = a_j/a_k = k_i/k_k$)
α_i	numerical coefficient in Chrastil equation
β	Lee–Kesler parameter

γ	activity coefficient, Lee–Kesler parameter
ΔP	difference between the inlet and outlet column pressures
δ	solubility parameter
ϵ_T	total column porosity or void volume fraction
ϵ_e	interstitial, or external porosity, or interparticle void fraction
ϵ_i	dielectric constant of compound i
ϵ_p	internal or intraparticle porosity of the packing particles
η	mobile phase viscosity
κ_T	compressibility of a fluid at temperature T
λ_i	numerical coefficient in Chrastil equation
μ	chemical potential
ν	reduced mobile phase velocity ($\nu = (ud_p)/D_m$)
ν	molar volume V_r a reduced volume
$\bar{\nu}$, $\bar{\nu}_0$	wavenumbers of the absorbance maxima in the fluid studied and in a reference fluid used in the definition of the polarity parameter
ω	numerical coefficient in the definition of the compressibility factor of real fluids. Also acentric factor in the Peng–Robinson equation of state
π^*	polarity parameter
ρ	density of the mobile phase
ρ_c	critical density of the mobile phase
ρ_r	reduced density of the mobile phase ($\rho_r = \rho/\rho_c$)
σ	standard deviation of a Gaussian peak
σ^2	variance of a distribution
Θ	surface coverage ($\Theta = q/q_s$)
ϕ	concentration of the strong solvent or organic modifier in the mobile phase

Acknowledgments

This work was supported in part by the cooperative agreement between the University of Tennessee and the Oak Ridge National Laboratory. The authors acknowledge fruitful, informative discussions with Terry Berger (Aurora, CA), Fabrice Gritti (UTK, Knoxville, TN, USA), Uwe Neue (Waters, Milford, MA), Don Poe (University of Minnesota, Duluth, MN), Pat Sandra (Research Institute on Chromatography, Kortrij, Belgium), and Christopher Welch (Merck, Raleigh, NY, USA). We thank the two anonymous reviewers who invested a considerable amount of time in reading and commenting this manuscript for their helpful and constructive criticisms and suggestions.

References

[1] G. Guiochon, A. Felinger, A.M. Katti, D.G. Shirazi, Fundamentals of Preparative and Nonlinear Chromatography, Elsevier, Amsterdam, The Netherlands, 2006.
[2] L. Jacob, G. Guiochon, Chromatogr. Rev. 14 (1971) 77.
[3] C. de la Tour, Ann. Chim. Phys. 2 (1822) 127.
[4] J.B. Hannay, J. Hogarth, Proc. R. Soc. Lond. 29 (1879) 324.
[5] A. Michels, B. Blaisse, C. Michels, Proc. R. Soc. Lond. A160 (1937) 358.
[6] R.C. Reid, J.M. Prauznitz, B.E. Poling, The Properties of Gases and Liquids, 4th ed. and 5th ed., McGraw Hill, New York, NY, 2001.
[7] P.J. Schoenmakers, J. Chromatogr. 315 (1984) 1.
[8] P.A. Rock, Chemical Thermodynamics, University Science Books, New York, 2003.
[9] R.E. Sievers, B. Hansen, Chem. Eng. News 69 (29) (1991) 2.
[10] D.E. Raynie, Anal. Chem. 65 (1993) 3127.
[11] A.I. Abdulagatov, G.V. Stepanov, I.M. Abdulagatov, High Temp. 45 (2007) 85.
[12] G.M. Schneider, C.B. Kautz, D. Tuma, in: E. Kiran, P.G. Debenedetti, C.J. Peters (Eds.), Supercritical Fluids: Fundamentals and Applications (NATO Science Series E), Springer, New York, NY, 2000, p. 1.
[13] U. van Wasen, I. Swaid, G.M. Schneider, Angew. Chem. Int. 19 (1980) 585.
[14] P.H.V. Konynenburg, Ph.D. thesis, University of California, Los Angeles, CA (1968).
[15] P.H.V. Konynenburg, R.L. Scott, Phil. Trans. R. Soc., Lond. A298 (1980) 495.
[16] D. Bartmann, G.M. Schneider, J. Chromatogr. 83 (1973) 135.
[17] J.M.H. Levelt-Sengers, in: E. Kiran, P.G. Debenedetti, C.J. Peters (Eds.), Supercritical Fluids: Fundamentals and Applications (NATO Science Series E), Springer, New York, NY, 2000, p. 1.
[18] J.S. Rowlinson, Liquids and Liquid Mixtures, Butterworths, London, UK, 1969.
[19] T.L. Chester, Microchem. J. 61 (1999) 12.
[20] J.W. Ziegler, J. Dorsey, T.L. Chester, D.P. Innis, Anal. Chem. 67 (1995) 456.
[21] J.W. Ziegler, T.L. Chester, D.P. Innis, S.H. Page, J.G. Dorsey, Supercritical Fluid Flow Injection Method for Mapping Liquid–Vapor Critical Loci of Binary Mixtures Containing CO_2, ACS Symposium Series, Washington, DC, 1995.
[22] T.L. Chester, B.S. Haynes, J. Supercrit. Fluids 11 (1997) 15.
[23] U. van Wasen, G.M. Schneider, J. Phys. Chem. 84 (1980) 229.
[24] G.M. Schneider, Pure Appl. Chem. 63 (1991) 1313.
[25] L.P. Cailletet, E.O.J. Mathias, Compt. Rend. Acad. Sci. Fr. 102 (1886) 1202.
[26] E.H. Amagat, Compt. Rend. Acad. Sci. Fr. 114 (1892) 1093.
[27] T.L. Chester, D.P. Innis, J. Microcol. Sep. 5 (1993) 261.
[28] E. Klesper, A.H. Corwin, D.A. Turner, J. Org. Chem. 27 (1962) 700.
[29] S.T. Sie, W. van Beersum, G.W.A. Rijnders, Sep. Sci. 1 (4) (1966) 459.
[30] S.T. Sie, G.W.A. Rijnders, Sep. Sci. 2 (6) (1967) 699.
[31] S.T. Sie, G.W.A. Rijnders, Sep. Sci. 2 (6) (1967) 729.
[32] S.T. Sie, G.W.A. Rijnders, Sep. Sci. 2 (6) (1967) 755.
[33] N.K. Karayanni, A.H. Corwin, E.W. Baker, E. Klesper, J.A. Walter, Anal. Chem. 40 (1968) 1736.
[34] C.G. Giddings, M.N. Myers, J.W. King, J. Chromatogr. Sci. 7 (1969) 277.
[35] T. Berger, B. Berger, LC-GC America 28 (5) (2010) 344.
[36] R.E. Jentoft, T.H. Gouw, J. Chromatogr. Sci. 8 (1970) 138.
[37] R.E. Jentoft, T.H. Gouw, Anal. Chem. 44 (1972) 681.
[38] J. Klesper, W. Hartmann, J. Polym. Lett. Ed. 15 (1977) 9.
[39] W. Hartmann, E. Klesper, J. Polym. Lett. Ed. 15 (1977) 713.
[40] M. Novotny, W. Bertsch, A. Zlatkis, J. Chromatogr. 61 (1971) 17.
[41] L.G. Randall, A.L. Wahrhaftig, Anal. Chem. 50 (1978) 1703.
[42] M. Perrut, J. Chromatogr. A 658 (1994) 293.
[43] K. Anton, C. Berger, Supercritical Fluid Chromatography with Packed Columns, Marcel Dekker, New York, NY, 1998.
[44] M. Novotny, S.R. Springston, P.A. Peaden, J. Fjeldsted, M.L. Lee, Anal. Chem. 53 (1981) 407A.
[45] D.R. Gere, R. Board, D. McManigill, Anal. Chem. 54 (1982) 736.
[46] D.R. Gere, Science 21 (1983) 253.
[47] T.A. Berger, Chromatographia 41 (1995) 133.
[48] M. Perrut, Fractionation process for mixtures by elution chromatography with liquid in supercritical state and installation for its operation, US patent 4,478,720 (1984).
[49] M. Perrut, P. Jusforgues, Entropie 132 (1986) 3.
[50] J. Whatley, J. Chromatogr. A 697 (1995) 251.
[51] K.D. Bartle, C.D. Bevan, A.A. Clifford, S.A. Jafar, N. Malak, M.S. Verrall, J. Chromatogr. A 579 (1995) 585.
[52] G. Terfloth, J. Chromatogr. A 906 (2001) 301.
[53] M. Ventura, W. Farrell, C. Aurigemma, K. Tivel, M. Greig, J. Wheatley, A. Yanovsky, K.E. Milgram, D. Dalesandro, R. DeGuzman, P. Tran, L. Nguyen, L. Chung, O. Fron, C.A. Koch, J. Chromatogr. A 1036 (2004) 7.
[54] C. White, J. Chromatogr. A 1074 (2005) 163.
[55] C. White, J. Burnett, J. Chromatogr. A 1074 (2005) 176.
[56] M. Maftouh, C. Granier-Loyaux, E. Chavana, J. Marini, A. Pradines, Y.V. Heyden, C. Picard, J. Chromatogr. A 1088 (2005) 67.
[57] T.Q. Yan, C. Orihuela, J. Chromatogr. A 1156 (2007) 220.
[58] S. Peper, M. Johannsen, G. Brunner, J. Chromatogr. A 1176 (2007) 246.
[59] O.D. Giovanni, M. Mazzotti, M. Morbidelli, F. Denet, W. Hauck, R.M. Nicoud, J. Chromatogr. A 919 (2001) 1.
[60] P. Sandra, A. Kot, A. Medvedovici, F. David, J. Chromatogr. A 703 (1995) 467.
[61] A. Medvedovici, P. Sandra, L. Toribio, F. David, J. Chromatogr. A 785 (1997) 159.
[62] Y. Zhao, G. Woo, S. Thomas, D. Semin, P. Sandra, J. Chromatogr. A 1003 (2003) 157.
[63] C. Brunelli, Y. Zhao, M.-H. Brown, P. Sandra, J. Chromatogr. A 1185 (2008) 263.
[64] P. Sandra, B. Szucs, R. Sandwich, Hanna-Brown, in: HPLC-2009, 2009. pp. Communication L-1.
[65] I. François, P. Sandra, J. Chromatogr. A 1216 (2009) 4005.
[66] D. Martire, R. Boehm, J. Phys. Chem. 91 (1987) 2433.
[67] T.L. Chester, Anal. Chem. 69 (1997) 165A.
[68] T.L. Chester, in: J.F. Parcher, T.L. Chester (Eds.), Unified Chromatography—ACS Symposium Series 748, 2000.
[69] D.H. Desty, A. Goldup, G.R. Luckhurst, W.T. Swanton, in: D.H. Desty (Ed.), Gas Chromatogaphy, Institute of Petroleum, London, UK, 1962, p. 67.
[70] L.S. Ettre, J. High Resol. Chromatogr. C C10 (1987) 636.
[71] E.M. Senchenkova, Michael Tswett—The Creator of Chromatography, Russian Academy of Sciences, Moscow, Russia, 2003.
[72] K.D. Bartle, C.D. Bevan, A.A. Clifford, S.A. Jafar, N. Malak, M.S. Verrall, J. Chromatogr. A 697 (1995) 579.
[73] G. Guiochon, Am. Lab. 30 (18) (1998) 14.
[74] J.F. Brennecke, C.A. Eckert, AIChE J. 35 (1989) 1409.
[75] T. Charoensombut-Amon, R.J. Martin, R. Kobayashi, Fluid Phase Equilib. 31 (1986) 89.
[76] R.A. van Leer, M.E. Paulaitis, J. Chem. Eng. Data 25 (1980) 257.
[77] U. Akman, A.K. Sunol, AIChE J. 37 (1991) 215.
[78] G.M. Schneider, J. Supercrit. Fluids 13 (1998) 5.
[79] G.M. Schneider, A.L. Scheidgen, D. Klante, Ind. Eng. Chem. Res. 39 (2000) 4476.
[80] S.K. Jha, G. Madras, J. Supercrit. Fluids 32 (2004) 161.
[81] D.-Y. Peng, D.B. Robinson, Ind. Eng. Chem. Fund. 15 (1976) 59.
[82] K. Mishima, K. Matsuyama, M. Baba, M. Ohuchi, T. Hakushi, Solvent Extr. Res. Dev. Jpn. 8 (2001) 215.

[83] D. Toma, B. Wagner, G.M. Schneider, D. Tuma, Fluid Phase Equilib. 182 (2001) 133.
[84] M. Roth, K. Maag, G. Schneider, D. Tuma, J. Phys. Chem. B 105 (2001) 10372.
[85] M. Roth, Fluid Phase Equilib. 212 (2003) 1.
[86] A.W. Francis, J. Phys. Chem. 58 (1954) 1099.
[87] J.H. Hildebrand, R.L. Scott, The Solubility of Nonelectrolytes, 3rd ed., Dover, New York, NY, 1964.
[88] C. Hansen, Hansen Solubility Parameters, CRC Press, Boca Raton, FL, 2000.
[89] J.C. Giddings, Unified Separation Science, Wiley Interscience, New York, NY, 1991.
[90] J.C. Giddings, M.N. Myers, L. McLaren, R.A. Keller, Science (1968) 67.
[91] R. Tijssen, H.A.H. Billiet, P.J. Schoenmakers, J. Chromatogr. 122 (1976) 185.
[92] B.I. Lee, M.G. Kessler, AIChE J 21 (1975) 510.
[93] N.R. Foster, G.S. Gurdial, J.S.L. Yun, K.K. Liong, K.D. Tilly, S.S.T. Ting, H. Singh, J.H. Lee, Ind. Eng. Chem. Res. 30 (1991) 1955.
[94] J.M. Prausnitz, The Molecular Thermodynamics of Fluid-phase Equilibria, Prentice Hall, Englewood Cliffs, 1969.
[95] S. Kim, K.P. Johnston, AIChE J. 33 (1987) 1603.
[96] C.R. Yonker, R.D. Smith, J. Phys. Chem. 92 (1988) 1664.
[97] J.C. Wheeler, Ber. Bunsenges. Phys. Chem. 76 (1972) 308.
[98] C.A. Eckert, D.H. Ziger, K.P. Johnston, S. Kim, J. Phys. Chem. 90 (1986) 2738.
[99] M. Vitha, P. Carr, J. Chromatogr. A 1126 (2006) 143.
[100] M.H. Abraham, A. Ibrahim, A.M. Zissimos, J. Chromatogr. A 1037 (2004) 29.
[101] R.R. Krug, W.G. Hunter, R.A. Grieger, J. Phys. Chem. 80 (1976) 2335.
[102] R.R. Krug, W.G. Hunter, R.A. Grieger, J. Phys. Chem. 80 (1976) 2341.
[103] R.R. Krug, Ind. Eng. Chem. Fundam. 19 (1980) 50.
[104] T. Kortvelyesi, M. Gorgenyi, L. Seres, Chromatographia 41 (1995) 282.
[105] M.J. Kamlet, R.W. Taft, J. Am. Chem. Soc. 98 (1976) 377.
[106] R.W. Taft, M.J. Kamlet, J. Am. Chem. Soc. 98 (1976) 2886.
[107] J.-L. Abboud, M.J. Kamlet, R.W. Taft, J. Am. Chem. Soc. 99 (1977) 8325.
[108] M.J. Kamlet, J.-L. Abboud, R.W. Taft, J. Am. Chem. Soc. 99 (1977) 6027.
[109] M.J. Kamlet, M.E. Jones, R.W. Taft, J.-L. Abboud, J. Chem. Soc., Perkin Trans. II (1979) 342.
[110] M.J. Kamlet, J.-L. Abboud, M.H. Abraham, R.W. Taft, J. Org. Chem. 48 (1983) 2877.
[111] M. Abraham, P. Grellier, R. McGill, J. Chem. Soc. Perkin Trans. 2: Phys. Org. Chem. (1987) 797.
[112] A. Jouyban, S. Soltanpour, H. Chan, Int. J. Pharm. 269 (2004) 353.
[113] J.P. Petitet, in: P. Cansell, F. Petitet, J.P. Petitet (Eds.), Fluides Supercritiques et Materiaux, Presence Graphique, Paris, 1995, p. 251.
[114] J.S. Gallagher, Private communication (1998).
[115] I.M. Abdulagatov, V.I. Dvoryanchikov, B.A. Mursalov, A.N. Kamalov, in: W.M. Haynes (Ed.), Proceedings of the 6th International Symposium on Supercritical Fluids, 2003. pp. 150–151, 525–535.
[116] G. Guiochon, L.A. Beaver, Anal. Chim. Acta 524 (2004) 1.
[117] S.B. Hawthorne, Y. Yang, D.J. Miller, Anal. Chem. 1994 (1994) 2912.
[118] T. Greibrokk, T. Andersen, J. Chromatogr. A 1000 (2003) 743.
[119] T. Teutenberg, High Temperature Liquid Chromatography—A User's Guide for Method Development, RSC Chromatography Monographs, The Royal Society of Chemistry, Cambridge, UK, 2010.
[120] C.L. Guillemin, F. Martinez, S. Thiault, J. Chromatogr. Sci. 17 (1979) 677.
[121] C.L. Guillemin, J.L. Millet, E. Hamon, J. Chromatogr. 301 (1984) 11.
[122] Y. Yang, A.D. Jones, J.A. Mathis, M.A. Francis, J. Chromatogr. A 942 (2002) 231.
[123] T.L. Chester, J.D. Pinkston, Anal. Chem. 76 (2004) 4606.
[124] A.R. Bazaev, I.M. Abdulagatov, E.A. Bazaev, A.A. Abdurashidova, A.E. Ramazanova, J. Supercrit. Fluids 41 (2007) 217.
[125] V.N. Zubarev, A.V. Bagdonas, Teploenergetica 4 (1967) 79.
[126] R.S. Finkelstein, L.I. Stiel, Chem. Eng. Prog. Symp. Ser. 66 (1970) 11.
[127] R. Ta'ani, Dr. Ing. Thesis, Karlsruhe, Germany.
[128] G.C. Straty, A.M.F. Palavra, T.J. Bruno, Int. J. Thermophys. 7 (1986) 1077.
[129] A. dos Santos Pereira, A.J. Girõn, E. Admasu, P. Sandra, J. Separat. Sci. 33 (2010) 834.
[130] P.S. Wells, S. Zhou, J.F. Parcher, Anal. Chem. 74 (2002) 2103.
[131] J.F. Parcher, Y. Xiong, J. Chromatogr. A 986 (2003) 129.
[132] Z. Luo, Y. Xiong, J.F. Parcher, Anal. Chem. 75 (2003) 3557.
[133] A.G. Nazmutdinov, E.V. Alekina, T.N. Nesterova, Russ. J. Phys. Chem. A 82 (2008) 1857.
[134] L.T. Taylor, Am. Pharma. Rev. 12 (5) (2009) 48.
[135] P.S. Wells, S. Zhou, J.F. Parcher, Anal. Chem. 75 (2003) 18.
[136] M.F. Vincent, S.G. Kazarian, B.L. West, J.A. Berkner, F.V. Bright, C.L. Liotta, C.A. Eckert, J. Phys. Chem. B 102 (1998) 2176.
[137] B.L. West, D. Bush, N.H. Brantley, M.F. Vincent, S.G. Kazarian, C.A. Eckert, Ind. Eng. Chem. Res. 37 (1998) 3305.
[138] H. Yuan, S.V. Olesik, J. Chromatogr. A 785 (1997) 35.
[139] J. Zhao, S.V. Olesik, Fluid Phase Equilib. 154 (1999) 261.
[140] G.B. Cox, B. Coryell, J. Lee, W. Watts, Symp. Prep. Chromatogr. 25 (2010) 6.
[141] S.V. Olesik, Adv. Chromatogr. 46 (2008) 423.
[142] R.B. Bird, W.E. Stewart, E.N. Lightfoot, Transport Phenomena, Wiley, New York, NY, 1962.
[143] H. Darcy, Les Fontaines Publiques de la Ville de Dijon, Dalmont, Paris, France, 1856.
[144] J.A.I. Halász, R. Endele, J. Chromatogr. 112 (1975) 37.
[145] U. Neue, HPLC Columns. Theory, Technology, and Practice, Wiley-VCH, New York, NY, 1997.
[146] J.H. Knox, M. Saleem, J. Chromatogr. Sci. 7 (1969) 614.
[147] H. Poppe, J. Chromatogr. A 778 (1997) 3.
[148] S.-T. Popovici, P.J. Schoenmakers, J. Chromatogr. A 1073 (2005) 87.
[149] U. Neue, B. Alden, P. Iraneta, M. Savaria, T. Grady, M. Kele, K. Wyndham, in: HPLC-2006, 2006. pp. Communication L-2102.
[150] S. Khirevich, A. Höltzel, D. Hlushkou, U. Tallarek, Anal. Chem. 79 (2007) 9340.
[151] M.R. Schure, R.S. Maier, D.M. Kroll, H.T. Davis, J. Chromatogr. A 1031 (2004) 79.
[152] M.R. Schure, R.S. Maier, J. Chromatogr. A 1126 (2006) 58.
[153] R.S. Maier, M.R. Schure, J.P. Gage, Water Resour. Res. 44 (2008) W06S03.
[154] H. Landolt, R. Börstein, Physikochemische Tabellen, Berlin, Germany, 1918.
[155] R.A. Alberty, Physical Chemistry, Wiley, New York, NY, 1955.
[156] O.A. Uyehara, K.M. Watson, Nat. Petroleum News, Tech. Section 36 (1944) 764.
[157] N.L. Carr, R. Kobayashi, D.B. Burroughs, Am. Inst. Min. Met. Engrs. Petroleum Tech. 6 (1954) 47.
[158] H. Colin, J.C. Diez-Masa, T. Czaychowska, I. Miedziak, G. Guiochon, J. Chromatogr. 167 (1978) 41.
[159] V. Vesovic, W.A. Wakeham, G.A. Olchowy, J.V. Sengers, J.T.R. Watson, J. Millat, J. Phys. Chem. Ref. Data 19 (1990) 763.
[160] J.A. Jossi, L.I. Stiel, G. Thodos, AIChE. J. 8 (1962) 59.
[161] Z. Al-Syabi, A. Danesh, B. Tohidi, A.C. Todd, D.H. Tehrani, Chem. Eng. Sci. 56 (2001) 6997.
[162] E.W. Lemmon, M.O. McLinden, D.G. Friend, NIST Chemistry WebBook, NIST Standard Reference 39.
[163] H. Iwasaki, M. Takahashi, J. Chem. Phys. 74 (1981) 1930.
[164] A.S. Pensado, A.A.H. Paduá, M.J.P. Comuñas, J. Fernández, J. Supercrit. Fluids 44 (2008) 172.
[165] L.I. Stiel, G. Thodos, AIChE J. 10 (1964) 275.
[166] S.K. Kim, J. Ross, J. Chem. Phys. 46 (1967) 818.
[167] K. Stephan, K. Lucas, Viscosity of Dense Fluids, Plenum, New York, NY, 1979.
[168] F. Gritti, M. Martin, G. Guiochon, J. Chromatogr. A 1070 (2005) 13.
[169] K. Kaczmarski, J. Kostka, W. Zapala, G. Guiochon, J. Chromatogr. A 1216 (2009) 6560.
[170] M. Martin, G. Blu, G. Guiochon, J. Chromatogr. Sci. 11 (1973) 641.
[171] L. Grunberg, A.H. Nissan, Nature 164 (1949) 799.
[172] J.W. Li, P.W. Carr, Anal. Chem. 69 (1997) 2530.
[173] J.H. Park, A.J. Dallas, P. Chau, P.W. Carr, J. Phys. Org. Chem. 7 (1994) 757.
[174] A. Rajendran, O. Kräuchi, M. Mazzotti, M. Morbidelli, J. Chromatogr. A 1092 (2005) 149.
[175] R. Span, W. Wagner, J. Phys. Chem. Ref. Data 25 (1996) 1509.
[176] A. Fenghour, W.A. Wakeham, W. Vesovic, J. Phys. Chem. Ref. Data 27 (1998) 31.
[177] L.R. Baker, M.A. Stark, A.W. Orton, B.A. Horn, S.R. Goates, J. Chromatogr. A 1216 (2009) 5588.
[178] L.R. Baker, A.W. Orton, M.A. Stark, S.R. Goates, J. Chromatogr. A 1216 (2009) 5594.
[179] F. Gritti, G. Guiochon, J. Chromatogr. A 1075 (2005) 117.
[180] M. Lübbert, G. Brunner, M. Johanssen, J. Supercrit. Fluids 42 (2007) 180.
[181] D.P. Poe, J. Chromatogr. A 785 (1997) 129.
[182] D.P. Poe, J. Chromatogr. A 785 (1997) 135.
[183] D.P. Poe, J.J. Schroden, J. Chromatogr. A 1216 (2009) 7915.
[184] F. Gritti, G. Guiochon, Anal. Chem. 80 (2008) 6488.
[185] F. Gritti, G. Guiochon, Anal. Chem. (2008) 5009.
[186] F. Gritti, G. Guiochon, J. Chromatogr. A 1187 (2008) 165.
[187] F. Gritti, G. Guiochon, J. Chromatogr. A 1138 (2007) 141.
[188] K. Kaczmarski, F. Gritti, G. Guiochon, J. Chromatogr. A 1177 (2008) 92.
[189] F. Gritti, G. Guiochon, J. Chromatogr. A 1206 (2008) 113.
[190] F. Gritti, G. Guiochon, J. Chromatogr. A 1166 (2007) 47.
[191] R. Aris, Proc. R. Soc. Lond., Ser. A 252 (1959) 538.
[192] F. Gritti, G. Guiochon, J. Chromatogr. A 1216 (2009) 1353.
[193] F. Gritti, M. Martin, G. Guiochon, Anal. Chem. 81 (2009) 3365.
[194] S.R. Springston, P. David, J. Steger, M. Novotny, Anal. Chem. 58 (1986) 997.
[195] F. Gritti, M. Martin, G. Guiochon, Anal. Chem. 81 (2009) 3365.
[196] K. Kaczmarski, F. Gritti, G. Guiochon, J. Chromatogr. A 1177 (2008) 92.
[197] K. Kaczmarski, J. Kostka, W. Zapala, G. Guiochon, J. Chromatogr. A 1216 (2009) 6560.
[198] K. Kaczmarski, J. Kostka, W. Zapala, G. Guiochon, J. Chromatogr. A 1216 (2009) 6575.
[199] P.J. Schoenmakers, P.E. Rothfusz, F.C.C.J.G. Verhoeven, J. Chromatogr. 395 (1987) 91.
[200] A. Rajendran, S. Peper, M. Johannsen, M. Mazzotti, M. Morbidelli, G. Brunner, J. Chromatogr. A 1092 (2005) 55.
[201] A. Rajendran, T.S. Gilkison, M. Mazzotti, J. Sep. Sci. 31 (2008) 1279.
[202] P.J. Schoenmakers, L.G.M. Uunk, Chromatographia 24 (1987) 51.
[203] D.P. Poe, D.E. Martire, J. Chromatogr. 517 (1990) 3.
[204] K. Kaczmarski, D.P. Poe, G. Guiochon, J. Chromatogr. A 1217 (2010) 6578.
[205] F. Gritti, G. Guiochon, J. Chromatogr. A 1138 (2007) 141.
[206] F. Gritti, G. Guiochon, J. Chromatogr. A 1166 (2007) 47.
[207] F. Gritti, G. Guiochon, Anal. Chem. 80 (2008) 6488.
[208] F. Gritti, G. Guiochon, Anal. Chem. 80 (2008) 5009.
[209] F. Gritti, G. Guiochon, J. Chromatogr. A 1187 (2008) 165.
[210] F. Gritti, G. Guiochon, J. Chromatogr. A 1155 (2007) 85.
[211] F. Gritti, G. Guiochon, J. Chromatogr. A 1206 (2008) 113.
[212] F. Gritti, G. Guiochon, J. Chromatogr. A 1216 (2009) 1353.
[213] K. Kaczmarski, F. Gritti, J. Kostka, G. Guiochon, J. Chromatogr. A 1216 (2009) 6575.

[214] O. Dapremont, G.B. Cox, M. Martin, P. Hilaireau, H. Colin, J. Chromatogr. A 796 (1998) 81.
[215] L.A. Guildner, Proc. Natl. Acad. Sci. 44 (1958) 1149.
[216] Y.P. Zarichnyak, V.V. Novikov, Inzenerno-Fizichezkii Zhurnal 34 (1978) 648.
[217] E.A. Moelwyn-Hughes, Physical Chemistry, Pergamon Press, Oxford, UK, 1961.
[218] M. Martin, G. Guiochon, J. Chromatogr. A 1090 (2005) 16.
[219] M. Martin, G. Blu, C. Eon, G. Guiochon, J. Chromatogr. 112 (1975) 399.
[220] M. Martin, G. Blu, C. Eon, G. Guiochon, J. Chromatogr. 130 (1977) 458.
[221] M. Martin, G. Guiochon, J. Chromatogr. 151 (1978) 267.
[222] J. Sengers, R. Kayser, Equations of State for Fluids and Fluid Mixtures, Elsevier, Amsterdam, 2000.
[223] S. Ottiger, J. Kluge, A. Rajendran, M. Mazzotti, J. Chromatogr. A 1162 (2007) 74.
[224] A. Rajendran, J. Chromatogr. A 1185 (2008) 216.
[225] C. Wenda, A. Rajendran, J. Chromatogr. A 1216 (2009) 8750.
[226] S. Saeki, J. Supercrit. Fluids 8 (1995) 30.
[227] J.F. Brennecke, C.A. Eckert, AIChE J. 35 (1989) 1409.
[228] X.-D. Dou, G.-J. Liu, Q.-L. Chen, S.-J. Zeng, C.-F. Yu, Indian Chem. Engr. A 43 (2001) 263.
[229] A. Michels, C. Michels, Proc. R. Soc. Lond. A160 (1937) 348.
[230] A. Michels, A. Bijl, C. Michels, Proc. R. Soc. Lond. A160 (1937) 376.
[231] D.R. Lide, Handbook of Chemistry and Physics, 88th ed., CRC Press, Boca Raton, FL, 2008.
[232] C. Dieterici, Physikal. Z. 1 (1900) 73.
[233] L. Oellrich, U. Plöcker, J.M. Prausnitz, H. Knapp, Chem. -Ing. -Tech. 49 (1977) 955.
[234] E.B. Bagley, T.P. Nelson, S.-A. Chen, J.W. Barlow, Ind. Eng. Chem. Fundam. 10 (1971) 27.
[235] U. Plöckner, H. Knapp, J.M. Prausnitz, Ind. Eng. Chem. Prod. Res. Develop. 17 (1978) 324.
[236] M. Perrut, J. Chromatogr. 396 (1987) 1.
[237] R. Span, W. Wagner, Intl. J. Thermophys. 44 (2003) 1.
[238] R. Span, W. Wagner, Intl. J. Thermophys. 44 (2003) 41.
[239] R. Span, W. Wagner, Intl. J. Thermophys. 44 (2003) 111.
[240] J.G. Harris, K.H. Yung, J. Phys. Chem. 99 (1995) 12021.
[241] Y. Zhang, J. Yang, Y.-X. Yu, J. Phys. Chem. 109 (2005) 13375.
[242] S.B. Kiselev, J.F. Ely, S.P. Tan, H. Adidharma, M. Radosz, Ind. Eng Chem. Res. 45 (2006) 3981.
[243] S.B. Kiselev, J.F. Ely, J. Phys. Chem. C 111 (2007) 15969.
[244] C.R. Yonker, R.D. Smith, J. Chromatogr. 550 (1991) 775.
[245] J.G.M. Janssen, P.J. Schoenmakers, C.A. Cramers, J. High Resolut. Chromatogr. Chromatogr. Commun. 12 (1989) 645.
[246] M.I. Selim, J.R. Strubinger, Fresenius Z. Anal. Chem. 330 (1988) 246.
[247] J.R. Strubinger, M.I. Selim, J. Chromatogr. Sci. 26 (1988) 579.
[248] P. Menon, Chem. Rev. 68 (1968) 277.
[249] C.R. Yonker, R.D. Smith, J. Chromatogr. 505 (1990) 139.
[250] J.R. Strubinger, H. Song, J.F. Parcher, Anal. Chem. 63 (1991) 98.
[251] J.R. Strubinger, H. Song, J.F. Parcher, Anal. Chem. 63 (1991) 104.
[252] A. Rajendran, B. Bonavoglia, N. Forrer, G. Storti, M. Mazzotti, M. Morbidelli, Ind. Eng. Chem. Res. 44 (2005) 2549.
[253] C.H. Lochmüller, L.P. Mink, J. Chromatogr. 471 (1989) 357.
[254] S.R. Springston, P. David, J. Steger, M. Novotny, Anal. Chem. 58 (1986) 997.
[255] P.A. Peaden, M.L. Lee, J. Chromatogr. 259 (1983) 1.
[256] U. van Wasen, G.M. Schneider, Chromatographia 8 (1975) 274.
[257] P. Szabelski, A. Cavazzini, K. Kaczmarski, X. Liu, G. Guiochon, J. Chromatogr. A 950 (2002) 41.
[258] C.B. Kautz, U.H. Dahlmann, G.M. Schneider, J. Chromatogr. A 776 (1997) 305.
[259] D.E. Martire, J. Chromatogr. 461 (1989) 165.
[260] T.A. Berger, Chromatographia 37 (1993) 645.
[261] T.A. Berger, K. Fogelman, The Peak (LC/GC) (November 2009) 17.
[262] T.A. Berger, J.F. Deye, J. Chromatogr. 547 (1991) 377.
[263] L.T. Taylor, LC–GC N. Am. 27 (2009) 490.
[264] E. Lesellier, A.M. Krstulovic, A. Tchapla, Chromatographia 36 (1993) 275.
[265] C. West, E. Lesellier, J. Chromatogr. A 1110 (2006) 181.
[266] J. Chrastil, J. Phys. Chem. 86 (1982) 3016.
[267] M. Roth, J. Chromatogr. A 1037 (2004) 369.
[268] R. Brauer, T. Bitterwolp, N. Smart, M. Burford, C. Wai, Anal. Chim. Acta 349 (1997) 239.
[269] A.F. Barton, CRC Handbook of Solubility Parameters and Other Cohesion Parameters, second edition, CRC Press, Boca Raton, FL, 1991.
[270] D.M. Heaton, K.D. Bartle, P. Myers, A.A. Clifford, Anal. Chem. 66 (1994) 4253.
[271] Proceedings of the 8th Intl. Symposium on Gas Chromatography, Institute of Petroleum, London, 1971.
[272] J.D. Weckwerth, P.W. Carr, Anal. Chem. 70 (1998) 1404.
[273] C. West, E. Lesellier, J. Chromatogr. A 1110 (2006) 191.
[274] C. West, E. Lesellier, J. Chromatogr. A 1110 (2006) 200.
[275] C. West, E. Lesellier, J. Chromatogr. A 1115 (2006) 233.
[276] C. West, E. Lesellier, J. Chromatogr. A 1169 (2007) 205.
[277] E. Lesellier, C. West, J. Chromatogr. A 1149 (2007) 345.
[278] C. West, E. Lesellier, J. Chromatogr. A 1203 (2008) 105.
[279] C. West, E. Lesellier, J. Chromatogr. A 1191 (2008) 21.
[280] J.A. Blackwell, R.W. Stringham, Chromatographia 46 (1997) 301.
[281] A. Guillermo, A. Alvarez, W. Baumann, Z. Naturforsch. 60a (2004) 61.
[282] M. Modell, R.C. Reid, Thermodynamics and Its Applications, Prentice Hall, Englewood Cliffs, NJ, 1983.
[283] E. Lesellier, K. Gurdale, A. Tchapla, Chromatographia 55 (2002) 555.
[284] E. Lesellier, K. Gurdale, A. Tchapla, J. Chromatogr. A 975 (2002) 335.
[285] C.L. Guillemin, J.L. Millet, J. Dubois, J. High Resolut. Chromatogr. 4 (1981) 280.
[286] M.O. Fogwill, K.B. Thurbide, J. Chromatogr. A 1200 (2008) 49.
[287] C.H. Bosanquet, G.O. Morgan, in: D.H. Desty (Ed.), Vapor Phase Chromatography, Butterworths, London, UK, 1957, pp. 35–50.
[288] L. Jacob, G. Guiochon, Bull. Soc. Chim. France (1970) 1224.
[289] L. Jacob, G. Guiochon, Chromatogr. Rev. 14 (1971) 77.
[290] C.H. Lochmüller, L.P. Mink, J. Chromatogr. 409 (1987) 55.
[291] J.C. Giddings, S.L. Seager, L.R. Stucki, G.H. Stewart, Anal. Chem. 32 (1960) 867.
[292] S. Takahashi, J. Chem. Eng. Jpn. 7 (1974) 417.
[293] R. Feist, G.M. Schneider, Sep. Sci. Technol. 17 (1982) 261.
[294] H.H. Lauer, D. McManigill, R.D. Board, Anal. Chem. 55 (1983) 1370.
[295] T. Funazukuri, S. Hachisu, N. Wakao, Anal. Chem. 61 (1989) 118.
[296] K.D. Bartle, D.L. Baulch, A.A. Clifford, S.E. Coleby, J. Chromatogr. 557 (1991) 69.
[297] H.J.V. Tyrrell, K.R. Harris, Diffusion in Liquids, Butterworths, London, UK, 1984.
[298] A.A. Clifford, S.E. Coleby, Proc. R. Soc. Lond. A433 (1991) 63.
[299] H. Higashi, Y. Iwai, Y. Nakamura, S. Yamamoto, Y. Arai, Fluid Phase Equilib. 166 (1999) 101.
[300] A. Akgerman, C. Erkey, M. Orejuela, Ind. Eng. Chem. 35 (1996) 911.
[301] G. Taylor, Proc. R. Soc. A 219 (1953) 67.
[302] J.C. Giddings, S.L. Seager, J. Chem. Phys. 33 (1960) 1579.
[303] J. Bohemen, J.H. Purnell, J. Chem. Soc. 360 (1961) 2360.
[304] J.G. Atwood, J. Goldstein, J. Phys. Chem. 88 (1984) 1875.
[305] H. Weingärtner, U. Klask, G.M. Schneider, Z. Phys. Chem. 219 (2005) 1261.
[306] K.M. Gonzales, J.L. Bueno, I. Medina, J. Supercrit. Fluids 24 (2002) 219.
[307] K. Miyabe, N. Ando, G. Guiochon, J. Chromatogr. A 1216 (2009) 4377.
[308] F. Gritti, G. Guiochon, Chem. Eng. Sci. 61 (2006) 7636.
[309] K. Miyabe, N. Ando, T. Nakamura, G.G.G. Guiochon, Chem. Eng. Sci. 66 (2011) 5950.
[310] F. Gritti, G. Guiochon, AIChE J. 57 (2011).
[311] H.T. Davis, J. Am. Ceram. Soc. 60 (1977) 499.
[312] D.M. Lamb, S.T. Adamy, K.W. Woo, J. Jonas, J. Phys. Chem. 93 (1989) 5002.
[313] J. Suárez, I. Medina, J.L. Bueno, Fluid Phase Equilib. 153 (1998) 167.
[314] C.R. Wilke, P. Chang, AIChE J. 1 (1955) 264.
[315] J.W. Li, P.W. Carr, Anal. Chem. 69 (1997) 2550.
[316] A.L. Hines, R.N. Maddox, Mass Transfer. Fundamentals and Applications, Prentice-Hall, Englewood Cliffs, NJ, 1985.
[317] E.G. Scheibel, Ind. Eng. Chem. 46 (1954) 2007.
[318] C.J. King, L. Hsuch, K.W. Mao, J. Chem. Eng. Data 10 (1965) 348.
[319] K.A. Reddy, L.K. Doraiswamy, Ind. Eng. Chem. Fundam. 6 (1967) 77.
[320] M.A. Lusis, G.A. Ratcliff, Can. J. Chem. Eng. 46 (1968) 385.
[321] W. Hayduk, H. Laudie, AIChE J. 20 (1974) 611.
[322] M.E. Young, P.A. Carroad, R.L. Bell, Biotechnol. Bioeng. 22 (1980) 947.
[323] Y. Zhu, X.H. Lu, J. Zhou, Y.R. Wang, J. Shi, Fluid Phase Equilib. 194 (2002) 1141.
[324] T. Kraska, S.E. Quiñones-Cisneros, U.K. Deiters, J. Supercrit. Fluids 42 (2007) 212.
[325] S.E. Quiñones-Cisneros, C.K. Zéberg-Mikkelsen, E.H. Stenby, Fluid Phase Equilib. 169 (2000) 249.
[326] S.E. Quiñones-Cisneros, U.K. Deiters, J. Phys. Chem. B 110 (2006) 12820.
[327] J.C. Sternberg, in: J.C. Giddings, R.A. Keller (Eds.), Advances in Chromatography, New York, NY, 1966, p. 205.
[328] J.C. Giddings, Dynamics of Chromatography, Marcel Dekker, New York, NY, 1960.
[329] E.V. Dose, G. Guiochon, Anal. Chem. 62 (1990) 1723.
[330] F. Gritti, G. Guiochon, J. Chromatogr. A 1217 (2010) 3000.
[331] D. Kandhai, H. Hlushkou, A.G. Hoekstra, P.M.A. Sloot, H. van Has, U. Tallarek, Phys. Rev. Lett. 88 (2002) 234501.
[332] D. Kandhai, U. Tallarek, H. Hlushkou, A.G. Hoekstra, P.M.A. Sloot, H. van Has, Phil. Trans. R. Soc. Lond. A 360 (2002) 521.
[333] F. Gritti, G. Guiochon, Anal. Chem. 78 (2006) 5329.
[334] F. Gritti, I. Leonardis, J. Abia, G. Guiochon, J. Chromatogr. A 1217 (2010) 3819–3843.
[335] Z. Balenovic, M.N. Myers, J.C. Giddings, J. Chem. Phys. 52 (1970) 915.
[336] I. Swaid, G.M. Schneider, Ber. Bunsenges. Phys. Chem. 83 (1979) 969.
[337] J.H. Knox, J. Chromatogr. Sci. 15 (1977) 352.
[338] J.J. van Deemter, F.J. Zuiderweg, A. Klinkenberg, Chem. Eng. Sci. 5 (1956) 271.
[339] L. Lapidus, N.R. Amundson, J. Phys. Chem. 56 (1952) 984.
[340] M. Kubin, Coll. Czech Chem. Commun. 30 (1965) 2900.
[341] E. Kučera, J. Chromatogr. 19 (1965) 237.
[342] J.F.K. Huber, Ber. Bunsenges. Phys. Chem. 77 (1973) 179.
[343] Cs. Horváth, H.J. Lin, J. Chromatogr. 126 (1976) 401.
[344] Cs. Horváth, H.J. Lin, J. Chromatogr. 149 (1978) 43.
[345] K. Miyabe, G. Guiochon, J. Phys. Chem. B 103 (1999) 11086.
[346] K. Miyabe, G. Guiochon, Adv. Chromatogr. 40 (2000) 1.
[347] K. Miyabe, G. Guiochon, Anal. Chem. 72 (2000) 1475.
[348] M. Suzuki, Adsorption Engineering, Elsevier, Amsterdam, The Netherlands, 1990.
[349] U. Tallarek, K. Albert, E. Bayer, G. Guiochon, AIChE J. 42 (1996) 3041.
[350] U. Tallarek, D. van Dusschoten, H.V. As, E. Bayer, G. Guiochon, J. Phys. Chem. B 102 (1998) 3486.
[351] D. Cabooter, F. Lynen, P. Sandra, G. Desmet, J. Chromatogr. A 1157 (2007) 131.
[352] F. Gritti, G. Guiochon, AICHE J. 57 (2011) 333–345.
[353] G. Guiochon, J. Chromatogr. A 1126 (2006) 6.
[354] W. de Malsche, H. Gardeniers, G. Desmet, Anal. Chem. 80 (2008) 5391.
[355] F. Gritti, G. Guiochon, AIChE J. 56 (2010) 1495.

[356] U. Tallarek, K. Albert, G. Guiochon, J. Am. Chem. Soc. 120 (1998) 149.
[357] T. Farkas, M.J. Sepaniak, G. Guiochon, AIChE J. 43 (1997) 1964.
[358] B. Lin, T. Yun, G. Zhong, G. Guiochon, J. Chromatogr. A 708 (1995) 1.
[359] S. Lucas, M.P. Calvo, J. Garcia-Serna, C. Palencia, M.J. Cocero, J. Supercrit. Fluids 41 (2007) 257.
[360] H. Thomas, J. Am. Chem. Soc. 66 (1944) 1664.
[361] S. Goldstein, Proc. R. Soc. Lond. A219 (1953) 151.
[362] A. Rajendran, Ph.D. thesis dissertation, Zürich, Switzerland, 2004, pp. 1–230.
[363] L. Jacob, P. Valentin, G. Guiochon, Chromatographia 4 (1971) 6.
[364] L. Jacob, G. Guiochon, J. Chromatogr. 65 (1972) 19.
[365] G. Guiochon, S. Golshan-Shirazi, A. Jaulmes, Anal. Chem. 60 (1988) 1856.
[366] I. Quinones, J.C. Ford, G. Guiochon, Chem. Eng. Sci. 55 (2000) 909.
[367] D.M. Ruthven, Principles of Adsorption and Adsorption Processes, Wiley, New York, NY, 1984.
[368] D.P. Valenzuela, A.L. Myers, Adsorption Equilibrium Data Handbook, Prentice-Hall, Englewood Cliffs, NJ, 1989.
[369] M. Jaroniec, R. Madey, Physical Adsorption on Heterogeneous Solids, Elsevier, Amsterdam, The Netherlands, 1998.
[370] B. Su, H. Xing, Y. Han, Y. Yang, Q. Ren, P. Wu, J. Chem. Eng. Data 54 (2009) 2906.
[371] S. Brunauer, P.H. Emmett, E. Teller, J. Am. Chem. Soc. 60 (1938) 309.
[372] R. Humayun, D.L. Tomasko, AIChE J. 46 (2000) 2065.
[373] O.D. Giovanni, W. Dörfler, M. Mazzotti, M. Morbidelli, Langmuir 17 (2001) 4316.
[374] T. Hocker, A. Rajendran, M. Mazzotti, Langmuir 19 (2003) 1254.
[375] Menon, Chem. Rev. 68 (1967) 277.
[376] I.M. Abdulagatov, A.R. Bazaev, E.A. Bazaev, M.B. Saidakhmedova, A.E. Ramazanova, J. Chem. Eng. Data 3 (1998) 451.
[377] P. Malbrunot, D. Vidal, J. Vermesse, R. Chahine, T.K. Bose, Langmuir 13 (1997) 539.
[378] M. Li, A. Gu, X.S. Lu, R.S. Wang, J. Chem. Eng. Data 49 (2004) 73.
[379] M.S. Schneider, J.D. Grunwaldt, A. Baiker, Langmuir 20 (2004) 2890.
[380] E.V. Dose, S.C. Jacobson, G. Guiochon, Anal. Chem. 63 (1991) 833.
[381] F. James, M. Sépúlvéda, F. Charton, G. Guiochon, in: M. Fay, R. Jeltsch (Eds.), Seventh Intl. Conference of Numerical Mathematics, vol. 129, Zürich (Switzerland), Birkhasër Verlag, 1999, pp. 423–432.
[382] F. James, M. Sépúlvéda, F. Charton, I. Quinones, G. Guiochon, Chem. Eng. Sci. 54 (1999) 1677.
[383] A. Felinger, A. Cavazzini, G. Guiochon, J. Chromatogr. A 986 (2003) 207.
[384] A. Felinger, D. Zhou, G. Guiochon, J. Chromatogr. A 1005 (2003) 35.
[385] K. Kaczmarski, J. Chromatogr. A 1176 (2007) 57.
[386] P. Rouchon, M. Schoenauer, P. Valentin, G. Guiochon, J. Phys. Chem. 89 (1985) 2076.
[387] K. Horváth, J.N. Fairchild, K. Kaczmarski, G. Guiochon, J. Chromatogr. A 1217 (2010) 8127–8135.
[388] P. Forssén, R. Arnell, T. Fornstedt, Comput. Chem. Eng. 30 (2006) 1381.
[389] R. Arnell, P. Forssén, T. Fornstedt, J. Chromatogr. A 1099 (2005) 167.
[390] E. Glueckauf, Trans. Faraday Soc. 52 (1955) 1540.
[391] E. Cremer, H.F. Huber, Angew. Chem. 73 (1961) 461.
[392] J. Samuelsson, T. Fornstedt, Anal. Chem. 80 (2008) 7887.
[393] Y. Han, Y. Yang, P. Wu, J. Chem. Eng. Data 53 (2008) 16.
[394] S. Peper, M. Lübbert, M. Johannsen, G. Brunner, Sep. Sci. Technol. 37 (2002) 2545.
[395] D.H. James, C.S.G. Phillips, J. Chem. Soc. (1954) 1066.
[396] C.N. Reilley, G.P. Hildebrand, J.W. Ashley, Anal. Chem. 34 (1962) 1198.
[397] F.G. Helfferich, D.L. Peterson, J. Chem. Educ. 41 (1964) 410.
[398] J. Lindholm, P. Forssén, T. Fornstedt, Anal. Chem. 76 (2004) 5472.
[399] G. Brunner, M. Johannsen, J. Supercrit. Fluids 38 (2006) 181.
[400] B.J. Stanley, G. Guiochon, Langmuir 11 (1995) 1735.
[401] F. Dondi, M. Gonnord, G. Guiochon, J. Colloid Interface Sci. 62 (1977) 303.
[402] F. Dondi, M. Gonnord, G. Guiochon, J. Colloid Interface Sci. 62 (1977) 316.
[403] J. Samuelsson, P. Forssen, M. Stefansson, T. Fornstedt, Anal. Chem. 76 (2004) 953.
[404] J. Samuelsson, P. Sajonz, T. Fornstedt, J. Chromatogr. A 1189 (2008) 19.
[405] G. Schay, G. Székely, Acta Chim. Hung. 5 (1954) 167.
[406] J. Jacobson, J. Frenz, C. Horváth, Ind. Eng. Chem. Res. 26 (1987) 43.
[407] F. Gritti, G. Guiochon, J. Chromatogr. A 1099 (2005) 1.
[408] F. Gritti, G. Guiochon, J. Chromatogr. A 1097 (2005) 98.
[409] F. Gritti, A. Felinger, G. Guiochon, J. Chromatogr. A 1136 (2006) 57.
[410] F. Gritti, Y.V. Kazakevich, G. Guiochon, J. Chromatogr. A 1161 (2007) 157.
[411] I. Kikic, P. Alessi, A. Cortesi, S.J. Macnaughton, N.R. Foster, B. Spicka, Fluid Phase Equilib. 117 (1996) 304.
[412] R. Harikrishnan, M.P. Srinivasan, C.B. Ching, AIChE J. 44 (1998) 2620.
[413] M. Cross, A. Akgerman, AIChE J. 44 (1998) 1542.
[414] P. Subra, A. Vega-Bancel, E. Reverchon, J. Supercrit. Fluids 12 (1998) 43.
[415] A. Depta, T. Giese, M. Johannsen, G. Brunner, J. Chromatogr. A 865 (1999) 175.
[416] J. Samuelsson, R. Arnell, J.S. Diesen, J. Tibbelin, A. Paptchikhine, T. Fornstedt, P.J.R. Sjöberg, Anal. Chem. 80 (2008) 2105.
[417] J. Lindholm, P. Forssén, T. Fornstedt, Anal. Chem. 76 (2004) 4856.
[418] J. Samuelsson, P. Forsén, M. Stefansson, T. Fornstedt, Anal. Chem. 76 (2004) 953.
[419] A.W.J.D. Jong, J.C. Kraak, H. Poppe, F. Nooitgedacht, J. Chromatogr. 193 (1980) 181.
[420] J.F.K. Huber, R.G. Gerritse, J. Chromatogr. 58 (1971) 137.
[421] J. Samuelsson, P. Sajonz, T. Fornstedt, J. Chromatogr. A 1189 (2008) 19.
[422] J. Samuelsson, J. Zang, A. Murunga, T. Fornstedt, P. Sajonz, J. Chromatogr. A 1194 (2008) 205.
[423] I. Langmuir, J. Am. Chem. Soc. 39 (1917) 1848.
[424] I. Langmuir, J. Am. Chem. Soc. 40 (1918) 1369.
[425] I. Quinones, G. Guiochon, Langmuir 12 (1996) 5433.
[426] D. Graham, J. Phys. Chem. 57 (1953) 665.
[427] R. Laub, ACS Symp. Ser. 297 (1986) 1.
[428] B.J. Stanley, G. Guiochon, Langmuir 11 (1995) 1735.
[429] P.W. Carr, J.W. Li, A.J. Dallas, D.I. Eikens, L.C. Tan, J. Chromatogr. A 656 (1993) 113.
[430] H.K. Hansen, P. Rasmussen, A. Fredenslund, M. Schiller, J. Gmehling, Ind. Eng. Chem. Res. 30 (1991) 2352.
[431] T. Hill, Introduction to Statistical Thermodynamics, Addison-Wesley, Reading, MA, 1960.
[432] M. Diack, G. Guiochon, Anal. Chem. 63 (1991) 2608.
[433] D.S. Jovanović, Colloid Polym. Sci. 235 (1969) 1203.
[434] J. Tóth, Acta Chim. Acad. Sci. Hung. 69 (1971) 311.
[435] C. Boedeker, J. Landw. 7 (1885) 48.
[436] M. Moreau, P. Valentin, C. Vidal-Madjar, B.C. Lin, G. Guiochon, J. Colloid Interface Sci. 141 (1991) 127.
[437] S. Golshan-Shirazi, G. Guiochon, Anal. Chem. 60 (1988) 2626.
[438] K. Mihlbachler, K. Kaczmarski, A. Seidel-Morgenstern, G. Guiochon, J. Chromatogr. A 955 (2002) 35.
[439] M. Mazzotti, A. Tarafder, F. Gritti, G. Guiochon, J. Chromatogr. A 1217 (2010) 2002–2012.
[440] A.L. Myers, J.M. Prausnitz, AIChE J. 11 (1965) 121.
[441] C.J. Radke, J.M. Prausnitz, AIChE J. 18 (1972) 761.
[442] T. Fornstedt, G. Guiochon, Anal. Chem. 73 (2001) 608A.
[443] S. Ottiger, R. Pini, G. Storti, M. Mazzotti, Langmuir 24 (2008) 9531.
[444] G. Cretier, J. Neffati, J.L. Rocca, J. Chromatogr. A 670 (1994) 173.
[445] P. Rouchon, M. Schonauer, P. Valentin, G. Guiochon, Sep. Sci. Technol 22 (1987) 1793.
[446] G. Guiochon, S. Golshan-Shirazi, A. Jaulmes, Anal. Chem. 60 (1988) 1856.
[447] M. Czok, G. Guiochon, Anal. Chem. 62 (1990) 189.
[448] K. Miyabe, M. Ando, N. Ando, G. Guiochon, J. Chromatogr. A 1210 (2008) 60.
[449] K. Miyabe, Y. Kawaguchi, G. Guiochon, J. Chromatogr. A 1217 (2010) 3053.
[450] T. Fornstedt, G. Gotmar, M. Andersson, G. Guiochon, J. Am. Chem. Soc. 121 (1999) 1164.
[451] A. Andrzejewska, K. Kaczmarski, G. Guiochon, J. Chromatogr. A 1216 (2009) 3992.
[452] F. Gritti, G. Guiochon, Anal. Chem. 78 (2006) 5823.
[453] F. Gritti, G. Guiochon, J. Chromatogr. A 1144 (2007) 208.
[454] G.B. Cox, Preparative Enantioselective Chromatography, Blackwell Publishing Co., New York, NY, 2005.
[455] A.E. Ziemann, J.E. Allen, N.S. Dahdale, I.I. Drebot, M.W. Coryell, A.M. Wunsch, C.M. Lynch, F.M. Faraci, M.A. Howard, M.J. Welsh, J.A. Wemmie, Cell 139 (2009) 1012.
[456] M. Perrut, private communication.
[457] X. Liu, D. Zhou, P. Szabelski, G. Guiochon, J. Chromatogr. A 988 (2003) 205.
[458] T.L. Chester, J.D. Pinkston, J. Chromatogr. A 807 (1998) 265.
[459] J.W. Coym, T.L. Chester, J. Sep. Sci. 26 (2003) 609.
[460] Y. Yamauchi, M. Kumajima, M. Saito, J. Chromatogr. 515 (1990) 285.
[461] L.Y. Zhou, L.T. Taylor, J. Chromatogr. A 858 (1999) 209.
[462] N.P. Vela, J.A. Caruso, J. Chromatogr. 641 (1993) 337.
[463] R.M. Smith, R.J. Burgess, J. Chromatogr. A 785 (1997) 49.
[464] L. Asnin, W. Galinada, G. Götmar, G. Guiochon, J. Chromatogr. A 1076 (2005) 141.
[465] L. Asnin, G. Guiochon, J. Chromatogr. A 1089 (2005) 101.
[466] L. Asnin, G. Guiochon, J. Chromatogr. A 1089 (2005) 105.
[467] T.A. Berger, K. Fogelman, The Peak (LC/GC) (September 2009) 17.
[468] Y. Sun, B.Y. Shekunov, P. York, Chem. Eng. Commun. 190 (2003) 1.
[469] J.M. Miller, Chromatography: Concepts and Contrasts, Wiley, New York, NY, 2005.
[470] H.U. Buser, K. Friedrich, K. Grolimund, Chromatographia 9 (1976) 641.
[471] W.A. Dietz, J. Gas Chromatogr. 5 (1967) 68.
[472] L.S. Ettre, J. Chromatogr. 8 (1962) 522.
[473] F.S. Deschamps, K. Gaudin, E. Lesellier, A. Tchapla, D. Ferrier, A. Baillet, P. Chaminade, Chromatographia 54 (2001) 607.
[474] E. Lesellier, K. Gaudin, P. Chaminade, A. Tchapla, A. Baillet, J. Chromatogr. A 1016 (2003) 111.
[475] C. Berger, M. Perrut, J. Chromatogr. 505 (1990) 37.
[476] D.M. Heaton, K.D. Bartle, P. Myers, A.A. Clifford, J. Chromatogr. A 753 (1996) 306.
[477] B. Roz, R. Bonmati, G. Hagenbach, P. Valentin, G. Guiochon, J. Chromatogr. Sci. 14 (1976) 367.
[478] G. Madras, C. Erkey, A. Akgerman, Environ. Progr. 13 (1994) 45.
[479] P.A. Peaden, J.C. Fjeldsted, M.L. Lee, S.R. Springston, M. Novotny, Anal. Chem. 54 (1982) 1090.
[480] J.C. Fjeldsted, M.L. Lee, Anal. Chem. 56 (1984) 619.
[481] S.T. Sie, G.W.A. Rijnders, Anal. Chim. Acta 38 (1967) 31.
[482] C.J. Welch, M. Biba, J.R. Gouker, G. Kath, P. Augustine, P. Hosek, Chirality 19 (2007) 184.
[483] A. dos Santos Pereira, F. David, G. Vanhoenacker, P. Sandra, J. Sep. Sci. 32 (2009) 2001.
[484] S.V. Olesik, Anal. Bioanal. Chem. 378 (2004) 43.
[485] J. Zhao, S.V. Olesik, J. Chromatogr. A 923 (2001) 107.

[486] Q. Sun, S.V. Olesik, Anal. Chem. 71 (1999) 2139.
[487] P.G. Jessop, D.J. Heldebrant, X. Li, C.A. Eckert, C.L. Liotta, Nature 436 (2005) 1102.
[488] P.G. Jessop, L. Phan, A. Carrier, S. Robinson, C.J. Dürr, J.R. Harjani, Green Chem. 12 (2010) 809–814.
[489] S.M. Mercer, P.G. Jessop, ChemSusChem 3 (2010) 467–470.
[490] Y. Ishihama, N. Asakawa, J. Pharm. Soc. 88 (1999) 1305.
[491] D. Bartmann, Ber. Bunseng. Phys. Chem. 76 (1972) 336.
[492] R.E. Jentoft, T.H. Gouw, Anal. Chem. 48 (1976) 2195.
[493] R.P. Simonian, L.B. Rogers, J. Chromatogr. Sci. 16 (1978) 49.
[494] G. Guiochon, N. Marchetti, K. Mriziq, R.A. Shalliker, J. Chromatogr. A 1189 (2008) 109.
[495] J.D. Pinkston, D.T. Stanton, D. Wen, J. Sep. Sci. 27 (2004) 115.
[496] J. Zheng, L. Taylor, J.D. Pinkston, M. Mangels, J. Chromatogr. A 1082 (2005) 220.
[497] J. Zhang, J.D. Pinkston, P.H. Zoutendam, L.T. Taylor, Anal. Chem. 78 (2006) 1535.
[498] P.A. Mourier, E. Eliot, M.H. Caude, P.H. Rosset, Anal. Chem. 57 (1985) 2819.
[499] F. Gasparrini, F. Maggio, D. Misiti, C. Villani, F. Andreolini, G.P. Mapeili, J. High Resol. Chromatogr. 17 (1994) 43.
[500] C. Wolf, W.H. Pirkle, J. Chromatogr. A 785 (1997) 173.
[501] Y. Liu, A. Berthod, C.R. Mitchell, T.L. Jiao, B. Zhang, D.W. Armstrong, J. Chromatogr. A 978 (2002) 185.
[502] C. Garcia-Martinez, G. Hernandez, M. Biba, C.J. Welch, Chirality 17 (2005) 212.
[503] O. Aaltonen, M. Aikio, J. Lundel, S. Ruohonen, L. Parvinen, V. Suoninen, Pharma Tech. Eur. 10 (1998) A42.
[504] A.J. Berry, E.D. Ramsey, M. Newby, D.E. Games, J. Chromatogr. Sci. 34 (1996) 245.
[505] K.B. Thurbide, J. Zhang, Anal. Bioanal. Chem. 382 (2005) 1227.
[506] J. Zhang, K.B. Thurbide, J. Chromatogr. A 1101 (2006) 286.
[507] X. Zhang, M. Scalf, M.S. Westphall, S.M. Smith, Anal. Chem. 80 (2008) 1598.
[508] P. Sandra, A. Medvedovici, Y. Zhao, F. David, J. Chromatogr. A 974 (2002) 231.
[509] J.D. Pinkston, D. Wen, K.L. Morand, D.A. Tirey, D.T. Stanton, Anal. Chem. 78 (2006) 7467.
[510] J. Whatley, J. Chromatogr. A 697 (1995) 251.
[511] L. Hughes, D. Hunter, Curr. Opin. Chem. Biol. 5 (2001) 243.
[512] T.A. Berger, J. Smith, K. Fogelman, K. Kruluts, Am. Lab. 34 (2002) 14.
[513] G. Cox, R. Stringham, A. Matabe, LC–GC, N. Am., August 2002, p. 24.
[514] K. Shimada, R. Nagahata, S. Kawabata, S. Matsuyama, T. Saito, S. Kinugasa, J. Mass Spectrom. 38 (2003) 948.
[515] C. Migliorini, M. Mazzotti, M. Morbidelli, J. Chromatogr. A 827 (1998) 161.
[516] G. Brunner, Gas Extraction. An Introduction to Fundamentals of Supercritical Fluids and the Applications to Separation Processes, Steinkopff/Springer, New York, NY, 1994.
[517] A. Birtigh, G. Brunner, Sep. Sci. Technol. 30 (1995) 3265.
[518] G. Terfloth, LC–GC 17 (1999) 400.
[519] L. Toribio, C. Alonso, M.J. del Nozal, J.L. Bernal, M.T. Martin, J. Chromatogr. A 1137 (2006) 30.
[520] M. Mazzotti, G. Storti, M. Morbidelli, J. Chromatogr. A 786 (1997) 309.
[521] I. Quiñones, C.M. Grill, L. Miller, G. Guiochon, J. Chromatogr. A 867 (2000) 1.
[522] C.W. Jiang, Q.L. Ren, P.D. Wu, J. Chromatogr. A 1005 (2003) 155.
[523] M. Ventura, W. Farrell, C. Aurigemma, K. Tivel, M. Greig, J. Wheatley, A. Yanovsky, K.E. Milgram, D. Dalesandro, R. DeGuzman, P. Tran, L. Nguyen, L. Chung, O. Gron, C.A. Koch, J. Chromatogr. A 1036 (2004) 7.
[524] M. Johanssen, S. Peper, A. Depta, Biochem. Biophys. Methods 54 (2002) 85.
[525] F. Denet, W. Hauck, R.M. Nicoud, O.D. Giovanni, M. Mazzotti, J.N. Jaubert, M. Morbidelli, Ind. Eng. Chem. Res. 40 (2001) 4603.
[526] G. Storti, M. Mazzotti, M. Morbidelli, S. Carra, AIChE J. 39 (1993) 471.
[527] M. Mazzotti, G. Storti, M. Morbidelli, J. Chromatogr. A 769 (1997) 3.